IODP
INTERNATIONAL OCEAN DISCOVERY PROGRAM

icdp

IODP/ICDP

Kolloquium 2016

Institut für Geowissenschaften, Universität Heidelberg

14. – 16. März 2016

DFG Deutsche Forschungsgemeinschaft

GEOW INSTITUT FÜR GEOWISSENSCHAFTEN

HCE HEIDELBERG CENTER FOR THE ENVIRONMENT

UNIVERSITÄT HEIDELBERG ZUKUNFT SEIT 1386

Tagungsort:
DKFZ Kommunikationszentrum, Im Neuenheimer Feld 280, 69120 Heidelberg

Conference Dinner:
Dienstag, 15.03.2016, im Anschluss an das Tagungsprogramm, Kulturbrauerei Heidelberg, Leyergasse 6, 69117 Heidelberg

Geo-Show „Unterirdisch“:
Dienstag, 15.03.2016, 11:00 - 12:30 Uhr, Neue Aula der Universität Heidelberg, Universitätsplatz, 69117 Heidelberg

PROGRAMM:

Montag, 14. März 2016		
10:00	13:00	Registrierung
13:00	13:30	Begrüßung
Neues aus den Programmen		
13:30	13:50	*J. Erbacher/A. Bornemann* IODP Rückblick auf 2015 - Wie geht es weiter?
13:50	14:10	*R. Oberhänsli* ICDP Rückblick auf 2015 - Wie geht es weiter?
Tiefe Biosphäre / Stoffkreisläufe		
14:10	14:30	*A. Schippers* Quantification of Deep Subseafloor Bacteria and Archaea – An Inter-Laboratory Comparison
14:30	14:50	*C. Glombitza* Free and macromolecular-bound formate and acetate as potential substrates for the 2 km deep coalbed-biosphere offshore Shimokita, Japan (IODP Exp. 337)
Paläozeanographie / Paläoklima / Paläoumwelt 1		
14:50	15:10	*R. Tiedemann* DNA-Metabarcoding of phyto- and zooplankton in East African lake sediments as proxies for past environmental perturbation
15:10	16:10	Poster & Kaffeepause
16:10	16:30	*V. Förster* The long HSPDP-Chew Bahir record from southern Ethiopia: Enhancing our environmental record of anatomically modern human origins
16:30	16:50	*B. Wagner* Progress and perspectives of the ICDP SCOPSCO project at Lake Ohrid (Macedonia, Albania)
16:50	17:10	*N. Lübke* Calcareous nannofossil biometry in Upper Aptian to Lower Cenomanian sediments from ODP Site 763B
17:10	17:30	*P. Grunert* Early history of Mediterranean-Atlantic exchange - new insights from IODP Expedition 339
17:30	18:30	Poster & kleiner Umtrunk

Dienstag, 15. März 2016

	Magmatische Petrologie, Metamorphose	
8:30	8:50	*S. Wilke* Magma storage depths of the Yellowstone Supervolcano: New insights from project HOTSPOT
8:50	9:10	*A. Allabar* Quench of bubble bearing magma: The soufflé collapse
9:10	9:30	*M. Regelous* Correlated global variations in abyssal peridotite - mid-ocean ridge basalt composition
9:30	9:50	*L. Steinmann* The shallow structure of the Campi Flegrei caldera: Insights from a semi-3D high-frequency multichannel seismic survey for a combined IODP/ICDP drilling approach
9:50	10:10	*M. Wang* Basalts from the Kimama core (Snake River Plain, Idaho) and experimental study on the link with associated rhyolites
	Gashydrate, Gase, Fluide	
10:10	10:30	*M. Alawi* Impact of geogenic CO_2 on the depth distribution and composition of deep microbial communities in the Hartoušov mofette system in NW Bohemia
10:30	13:00	Poster & Kaffee-/Mittagspause
		parallel stattfindend:
11:00	12:30	Geo-Show „*unterirdisch*“ (Neue Aula, Universitätsplatz)
	Paläozeanographie / Paläoklima / Paläoumwelt 2	
13:00	13:20	*P. Blaser* Mapping the distribution of seawater-derived Nd isotopes across the Atlantic Ocean during the last 30 ka for the reconstruction of water circulation changes
13:20	13:40	*T. Bauersachs* Climate variability controls the formation of cyanobacterial blooms in the Baltic Sea
	IODP Fahrtberichte	
13:40	14:00	*V. Spieß/C. France-Lanord* IODP Expedition 354: Middle Bengal Fan
14:00	14:15	*A. Hahn* IODP Expedition 355: Arabian Sea Monsoon
14:15	14:30	*D. De Vleeschouwer* IODP Expedition 356: Indonesian Throughflow
14:30	14:50	*C. Betzler* IODP Expedition 359: Maldives Monsoon and Sea Level
14:50	16:20	Poster & Kaffeepause
16:20	16:35	*J. Ciazela* IODP Expedition 360: Southwest Indian Ridge Lower Crust and Moho
	Seismogene Zonen, Impaktstrukturen	
16:35	16:55	*M. Ikari* Insights on fault slip behavior from long-term laboratory studies of ICDP/IODP drilling samples
16:55	17:15	*A. Hüpers* Friction properties of rocks in forearcs of accretionary convergent margins
17:15	17:35	*R. Löwe* Analysing the geothermal regime of the scientific COSC-1 well bore, west central Sweden
17:35	17:55	*U. Riller* Mechanics of terrestrial peak-ring crater formation inferred from Expedition 364 (Chicxulub)
ab 19:00		gemeinsames Abendessen (Kulturbrauerei Heidelberg, Leyergasse 6)

Mittwoch, 16. März 2016		
Neue Projekte, Projektvorschläge		
09:00	09:20	*R. Tjallingii* Advanced statistical analyses of XRF core scanner data from the Dead Sea record for an improved and rapid identification of extreme event deposits
09:20	9:40	*E. Hathorne* Indian monsoon development and variability from the radiogenic isotope and clay mineral composition of Bay of Bengal and Andaman Sea sediments
9:40	10:00	*N. Frank* The Climate History of the Mid-Depth Atlantic Deep Water Coral Reefs - Future Needs for IODP?
10:00	10:20	*S. Gilder* Distinguishing detrital versus chemical remanent magnetization in marine sediments
10:20	11:30	Poster & Kaffeepause
11:30	11:50	*K. Panagiotopoulos* New Project: Insights into the origin of a Mediterranean biodiversity hotspot based on palynological and biomarker analyses of Lake Ohrid sediments from Early Pleistocene (> 1.2 Ma)
Berichte/Entwicklungen		
11:50	12:10	*J. Kallmeyer* Report on the ICDP Lake Towuti Drilling Campaign 2015 in Indonesia
12:10	13:00	Posterprämierungen und Schlussworte
13:00		Tagungsende

Mittwoch, 16. März 2016	
Im Anschluss an das IODP/ICDP Kolloquium:	
14:00	**GESEP School 2016** “A course on basics of scientific drilling projects, how drilling and geophysical downhole measurements work, data acquisition and integration and the new ways to publish data and samples”
Ende: Donnerstag, 17. März 2016, 14:00 Uhr	

TEILNEHMERLISTE:

Name	Vorname	Institution und Ort
Adhikari	Rishi R.	MARUM - Zentrum für Marine Umweltwissenschaften, Universität Bremen
Alawi	Mashal	Helmholtz-Zentrum Potsdam, Deutsches GeoForschungsZentrum GFZ, Potsdam
Allabar	Anja	Fachbereich Geowissenschaften, Eberhard Karls Universität, Tübingen
Almeev	Renat	Institut für Mineralogie, Leibniz Universität Hannover
Antz	Benny	Institut für Umweltphysik, Universität Heidelberg
Asmussen	Magnus Ole	Institut für Geosysteme und Bioindikation, Technische Universität Braunschweig
Auer	Gerald	Institut für Erdwissenschaften, Karl-Franzens-Universität, Graz
Bahlburg	Heinrich	Institut für Geologie und Paläontologie, Westfälische Wilhelms-Universität, Münster
Bahr	André	Institut für Geowissenschaften, Universität Heidelberg
Batenburg	Sietske	Institut für Geowissenschaften, Goethe-Universität, Frankfurt
Bauersachs	Thorsten	Institut für Geowissenschaften, Christian-Albrechts-Universität, Kiel
Baumgarten	Henrike	Leibniz-Institut für Angewandte Geophysik (LIAG), Hannover
Behrens	Harald	Institut für Mineralogie, Leibniz Universität Hannover
Bergmann	Fenna	Fachbereich Geowissenschaften, Universität Bremen
Betzler	Christian	Institut für Geologie, Universität Hamburg
Blaser	Patrick	Institut für Umweltphysik, Universität Heidelberg
Böhm	Florian	GEOMAR, Helmholtz-Zentrum für Ozeanforschung, Kiel
Bornemann	André	IODP, Bundesanstalt für Geowissenschaften und Rohstoffe, Hannover
Botcharnikov	Roman	Institut für Mineralogie, Leibniz Universität Hannover
Bouimetarhan	Ilham	MARUM – Zentrum für Marine Umweltwissenschaften, Universität Bremen
Brandl	Philipp	GEOMAR, Helmholtz-Zentrum für Ozeanforschung, Kiel
Brandstätter	Jennifer	Institut für Erdwissenschaften, Karl-Franzens Universität Graz
Bräuer	Karin	Helmholtz-Zentrum für Umweltforschung, UFZ, Halle
Breitkreuz	Christoph	Institut für Geologie und Paläontologie, TU Bergakademie Freiberg
Burschil	Thomas	Leibniz-Institut für Angewandte Geophysik (LIAG), Hannover
Chiang	Oscar	Institut für Chemie und Biologie des Meeres (ICBM), Carl-von-Ossietzky-Universität, Oldenburg
Ciazela	Jakub	Institut für Mineralogie, Leibniz Universität Hannover
Cohuo	Sergio	Institut für Geosysteme und Bioindikation, Technische Universität Braunschweig
Conze	Ronald	Helmholtz-Zentrum Potsdam, Deutsches GeoForschungsZentrum GFZ, Potsdam
Czekay	Laura	Fachbereich Geowissenschaften, Eberhard Karls Universität, Tübingen
De Vleeschouwer	David	MARUM – Zentrum für Marine Umweltwissenschaften, Universität Bremen
Deik	Hanaa	Geologisches Institut, RWTH Aachen
Dersch-Hansmann	Michaela	Hessisches Ministerium der Justiz, für Integration und Europa, Wiesbaden
Deutsch	Alexander	Institut für Planetologie, Westfälische Wilhelms-Universität, Münster
Diester-Haaß	Liselotte	Zentrum für Umweltforschung, Universität des Saarlandes, Saarbrücken
Drath	Gabriela	IODP, Bundesanstalt für Geowissenschaften und Rohstoffe, Hannover
Drewer	Christian	Institut für Geologie und Paläontologie, Westfälische Wilhelms-Universität, Münster
Drury	Anna Joy	MARUM – Zentrum für Marine Umweltwissenschaften, Universität Bremen
Dullo	Christian	GEOMAR, Helmholtz-Zentrum für Ozeanforschung, Kiel
Dultz	Stefan	Institut für Mineralogie, Leibniz Universität Hannover
Dummann	Wolf	Institut für Geologie und Mineralogie, Universität Köln
Dupont	Lydie	MARUM – Zentrum für Marine Umweltwissenschaften, Universität Bremen
Egger	Lisa	Institut für Geowissenschaften, Universität Heidelberg
Engelen	Bert	Institut für Chemie und Biologie des Meeres (ICBM), Carl-von-Ossietzky-Universität, Oldenburg
Engelhardt	Jonathan	Institut für Erd- und Umweltwissenschaften, Universität Potsdam
Engelhardt	Tim	Institut für Chemie und Biologie des Meeres (ICBM), Carl-von-Ossietzky-Universität, Oldenburg
Erbacher	Jochen	IODP, Bundesanstalt für Geowissenschaften und Rohstoffe, Hannover
Erzinger	Jörg	Helmholtz-Zentrum Potsdam, Deutsches GeoForschungsZentrum GFZ, Potsdam
Farber-Pesch	Katja	Institut für Mineralogie & Lagerstättenlehre, RWTH Aachen
Fehr	Annick	Institute for Applied Geophysics and Geothermal Energy, E.ON Energy Research Center, RWTH Aachen
Feldtmann	Mathias	MARUM – Zentrum für Marine Umweltwissenschaften, Universität Bremen
Flögel	Sascha	GEOMAR, Helmholtz-Zentrum für Ozeanforschung, Kiel
Förster	Verena	Institut für Erd- und Umweltwissenschaften, Universität Potsdam
France-Lanord	Christian	Centre de Recherches Pétrographiques et Géochimiques – CRPG CNRS-Université de Lorraine, Nancy
Francke	Alexander	Institut für Geologie und Mineralogie, Universität Köln
Frank	Norbert	Institut für Umweltphysik, Universität Heidelberg
Frank	Martin	GEOMAR, Helmholtz-Zentrum für Ozeanforschung, Kiel
Friedrich	Oliver	Institut für Geowissenschaften, Universität Heidelberg
Friese	André	Helmholtz-Zentrum Potsdam, Deutsches GeoForschungsZentrum GFZ, Potsdam
Gabriel	Gerald	Leibniz-Institut für Angewandte Geophysik (LIAG), Hannover
Garcia-Gallardo	Angela	Institut für Erdwissenschaften, Karl-Franzens-Universität, Graz
Geissler	Wolfram	Alfred-Wegener-Institut, Helmholtz-Zentrum für Polar- und Meeresforschung, Bremerhaven
Gilder	Stuart	Department für Geo- und Umweltwissenschaften, Ludwig-Maximilians-Universität, München
Glombitza	Clemens	Center for Geomicrobiology, Department of Bioscience, Aarhus University
Grimmer	Friederike	MARUM – Zentrum für Marine Umweltwissenschaften, Universität Bremen
Groeneveld	Jeroen	MARUM – Zentrum für Marine Umweltwissenschaften, Universität Bremen
Grunert	Patrick	Institut für Erdwissenschaften, Karl-Franzens-Universität, Graz
Gussone	Nikolaus	Institut für Geologie und Paläontologie, Westfälische Wilhelms-Universität, Münster
Gutjahr	Marcus	GEOMAR, Helmholtz-Zentrum für Ozeanforschung, Kiel
Hahn	Annette	MARUM – Zentrum für Marine Umweltwissenschaften, Universität Bremen
Hasberg	Ascelina	Institut für Mineralogie und Geologie, Universität Köln
Hathorne	Ed	GEOMAR, Helmholtz-Zentrum für Ozeanforschung, Kiel
Heuer	Franziska	Institut für Geologie, TU Bergakademie Freiberg
Himmler	Tobias	MARUM – Zentrum für Marine Umweltwissenschaften, Universität Bremen
Hinderer	Matthias	Institut für Angewandte Geowissenschaften, Technische Universität Darmstadt
Hofmann	Peter	Institut für Geologie und Mineralogie, Universität Köln
Holtz	François	Institut für Mineralogie, Leibniz Universität Hannover
Huang	Huang	GEOMAR, Helmholtz-Zentrum für Ozeanforschung, Kiel

Huber	Barbara	Institut für Geologie und Paläontologie, Westfälische Wilhelms-Universität, Münster
Hüpers	Andre	MARUM – Zentrum für Marine Umweltwissenschaften, Universität Bremen
Ikari	Matt	MARUM – Zentrum für Marine Umweltwissenschaften, Universität Bremen
Iovine	Raffaella	GZG, Abteilung Geochemie, Universität Göttingen
Jakob	Kim	Institut für Geowissenschaften, Universität Heidelberg
Janssen	Christoph	Helmholtz-Zentrum Potsdam, Deutsches GeoForschungsZentrum GFZ, Potsdam
Jonas	Ann-Sophie	Institut für Geowissenschaften, Christian-Albrechts-Universität, Kiel
Kallmeyer	Jens	Helmholtz-Zentrum Potsdam, Deutsches GeoForschungsZentrum GFZ, Potsdam
Kämpf	Horst	Helmholtz-Zentrum Potsdam, Deutsches GeoForschungsZentrum GFZ, Potsdam
Kemner	Fabian	GeoZentrum Nordbayern, Friedrich-Alexander-Universität Erlangen-Nürnberg
Klein	Tina	Institut für Geowissenschaften, Goethe-Universität, Frankfurt
Koepke	Jürgen	Institut für Mineralogie, Leibniz Universität Hannover
Kollaske	Tina	Bundesanstalt für Geowissenschaften und Rohstoffe, Berlin
Kontny	Agnes	Institut für Angewandte Geowissenschaften, Karlsruher Institut für Technologie (KIT), Karlsruhe
Kotthoff	Ulrich	Institut für Geologie, Universität Hamburg
Kousis	Ilias	Institut für Geowissenschaften, Universität Heidelberg
Krastel	Sebastian	ICDP, Institut für Geowissenschaften, Christian-Albrechts-Universität, Kiel
Krauß	Felix	Helmholtz-Zentrum Potsdam, Deutsches GeoForschungsZentrum GFZ, Potsdam
Kudraß	Hermann-Rudolf	MARUM – Zentrum für Marine Umweltwissenschaften, Universität Bremen
Kukowski	Nina	Institut für Geowissenschaften, Friedrich-Schiller-Universität, Jena
Kunze	Sabine	IODP, Bundesanstalt für Geowissenschaften und Rohstoffe, Hannover
Kurz	Walter	Institut für Erdwissenschaften, Karl-Franzens-Universität, Graz
Kurzawski	Robert	GEOMAR, Helmholtz-Zentrum für Ozeanforschung, Kiel
Kutterolf	Steffen	GEOMAR, Helmholtz-Zentrum für Ozeanforschung, Kiel
Lay	Vera	Institut für Geophysik und Geoinformatik, TU Bergakademie Freiberg
Lazarus	David	Museum für Naturkunde, Leibniz-Institut für Evolutions- und Biodiversitätsforschung, Berlin
Lebas	Elodie	Institut für Geowissenschaften, Christian-Albrechts-Universität, Kiel
Lehnert	Oliver	GeoZentrum Nordbayern, Friedrich-Alexander-Universität Erlangen-Nürnberg
Leicher	Niklas	Institut für Geologie und Mineralogie, Universität Köln
Lindhorst	Katja	Institut für Geowissenschaften, Christian-Albrechts-Universität, Kiel
Link	Jasmin	Institut für Umweltphysik, Universität Heidelberg
Linsler	Stefan	Institut für Mineralogie, Leibniz Universität Hannover
Lippold	Jörg	Institut für Geowissenschaften, Universität Bern
Litt	Thomas	Steinmann-Institut für Geologie, Mineralogie und Paläontologie, Rheinische Friedrich-Wilhelms-Universität, Bonn
Liu	Bo	Leibniz-Institut für Ostseeforschung, Warnemünde
Löwe	Richard	GMG Institut, Ruhr-Universität Bochum
Lübke	Nathalie	Ruhr-Universität Bochum
Lückge	Andreas	Bundesanstalt für Geowissenschaften und Rohstoffe, Hannover
Mackensen	Andreas	Alfred-Wegener-Institut, Helmholtz-Zentrum für Polar- und Meeresforschung, Bremerhaven
Mangelsdorf	Kai	Helmholtz-Zentrum Potsdam, Deutsches GeoForschungsZentrum GFZ, Potsdam
Maronde	Dietrich	Institut für Geologie, Mineralogie und Paläontologie, Universität Bonn
März	Christian	School of Civil Engineering and Geosciences (CEGS), Newcastle University
Mäusbacher	Roland	Institut für Geographie, Friedrich-Schiller-Universität, Jena
Meyers	Philip A.	Department of Earth and Environmental Sciences, University of Michigan
Micheuz	Peter	Institut für Erdwissenschaften, Karl-Franzens-Universität, Graz
Namur	Olivier	Institut für Mineralogie, Leibniz Universität Hannover
Neuhaus	Martin	Institut für Geophysik und extraterrestrische Physik, Technische Universität Braunschweig
Nowak	Marcus	Fachbereich Geowissenschaften, Eberhard Karls Universität, Tübingen
Oberhänsli	Roland	ICDP, Universität Potsdam
Orsi	William D.	Department für Geo- und Umweltwissenschaften, Ludwig-Maximilians-Universität, München
Osborne	Anne	GEOMAR, Helmholtz-Zentrum für Ozeanforschung, Kiel
Pälike	Heiko	MARUM – Zentrum für Marine Umweltwissenschaften, Universität Bremen
Panagiotopoulos	Konstantinos	Institut für Geologie und Mineralogie, Universität Köln
Petrick	Benjamin	Max-Planck-Institut für Chemie, Mainz
Pickarski	Nadine	Steinmann-Institut für Geologie, Mineralogie und Paläontologie, Rheinische Friedrich-Wilhelms-Universität, Bonn
Piller	Werner	Institut für Erdwissenschaften, Karl-Franzens-Universität, Graz
Prokopenko	Alexander	Universität Köln
Pross	Jörg	Institut für Geowissenschaften, Universität Heidelberg
Quandt	Dennis	Institut für Erdwissenschaften, Karl-Franzens-Universität, Graz
Regelous	Marcel	GeoZentrum Nordbayern, Friedrich-Alexander-Universität Erlangen-Nürnberg
Reiche	Sönke	Institute for Applied Geophysics and Geothermal Energy, E.ON Energy Research Center, RWTH Aachen
Renaudie	Johan	Museum für Naturkunde, Leibniz-Institut für Evolutions- und Biodiversitätsforschung, Berlin
Reuning	Lars	Geologisches Institut, RWTH Aachen
Reusch	Anna	Geologisches Institut, ETH Zürich
Riller	Ulrich	Institut für Geologie, Universität Hamburg
Röhl	Ulla	MARUM – Zentrum für Marine Umweltwissenschaften, Universität Bremen
Roud	Sophie	Department für Geo- und Umweltwissenschaften, Ludwig-Maximilians-Universität, München
Rüggeberg	Andres	Unit of Earth Sciences, Dept. of Geosciences, University of Fribourg
Sarnthein	Michael	Institut für Geowissenschaften, Christian-Albrechts-Universität, Kiel
Schäbitz	Frank	Universität Köln
Schindlbeck	Julie	GEOMAR, Helmholtz-Zentrum für Ozeanforschung, Kiel
Schippers	Axel	Bundesanstalt für Geowissenschaften und Rohstoffe, Hannover
Schmincke	Hans-Ulrich	GEOMAR, Helmholtz-Zentrum für Ozeanforschung, Kiel
Schneider	Ralph	Institut für Geowissenschaften, Christian-Albrechts-Universität, Kiel
Schuck	Bernhard	Helmholtz-Zentrum Potsdam, Deutsches GeoForschungsZentrum GFZ, Potsdam
Schwab	Markus J.	Helmholtz-Zentrum Potsdam, Deutsches GeoForschungsZentrum GFZ, Potsdam
Schwalb	Antje	Institut für Geosysteme und Bioindikation, Technische Universität Braunschweig
Siebert	Matthias	Institut für Angewandte Geowissenschaften, Karlsruher Institut für Technologie (KIT), Karlsruhe
Spieß	Volkhard	Universität Bremen
Stein	Rüdiger	Alfred-Wegener-Institut, Helmholtz-Zentrum für Polar- und Meeresforschung, Bremerhaven
Steinig	Sebastian	GEOMAR, Helmholtz-Zentrum für Ozeanforschung, Kiel
Steinmann	Lena	Universität Bremen
Stelbrink	Björn	Justus-Liebig-Universität, Giessen
Stipp	Michael	GEOMAR, Helmholtz-Zentrum für Ozeanforschung, Kiel
Strack	Dieter	International Oil & Gas Consultant, Ratingen
Sumita	Mari	GEOMAR, Helmholtz-Zentrum für Ozeanforschung, Kiel

Teichert	Barbara	Institut für Geologie und Paläontologie, Westfälische Wilhelms-Universität, Münster
Tiedemann	Ralph	Institut für Biochemie und Biologie, Universität Potsdam
Timmerman	Martin	ICDP, Institut für Erd- und Umweltwissenschaften, Universität Potsdam
Tjallingii	Rik	Helmholtz-Zentrum Potsdam, Deutsches GeoForschungsZentrum GFZ, Potsdam
Türke	Andreas	Fachbereich Geowissenschaften, Universität Bremen
Uenzelmann-Neben	Gabriele	Alfred-Wegener-Institut, Helmholtz-Zentrum für Polar- und Meeresforschung, Bremerhaven
Voigt	Silke	Institut für Geowissenschaften, Goethe-Universität, Frankfurt
Vuillemin	Aurèle	Helmholtz-Zentrum Potsdam, Deutsches GeoForschungsZentrum GFZ, Potsdam
Wagner	Bernd	Institut für Geologie und Mineralogie, Universität Köln
Wang	Meng	Institut für Mineralogie, Leibniz Universität Hannover
Weber	Michael	Universität Köln
Wefer	Gerold	MARUM - Zentrum für Marine Umweltwissenschaften, Universität Bremen
Westerhold	Thomas	MARUM - Zentrum für Marine Umweltwissenschaften, Universität Bremen
Wiersberg	Thomas	Helmholtz-Zentrum Potsdam, Deutsches GeoForschungsZentrum GFZ, Potsdam
Wiese	Frank	Geowissenschaftliches Zentrum, Universität Göttingen
Wiese	Robert	Institut für Geologische Wissenschaften, Freie Universität Berlin
Wilke	Sören	Institut für Mineralogie, Leibniz Universität Hannover
Wittke	Andreas	Institut für Geologie und Paläontologie, Westfälische Wilhelms-Universität, Münster
Wonik	Thomas	Leibniz-Institut für Angewandte Geophysik (LIAG), Hannover
Wörmer	Lars	MARUM - Zentrum für Marine Umweltwissenschaften, Universität Bremen
Wörner	Gerhard	GZG, Abteilung Geochemie, Universität Göttingen
Zeiß	Jens	Lehrstuhl für Angewandte Geophysik, Montanuniversität Leoben

ABSTRACTS UND FAHRTBERICHTE:

FAHRTBERICHTE:

ABSTRACTS:

A. Bahr, S. Kaboth, D. Hodell	Enhanced Subtropical Gyre circulation feeding ice sheet growth during the Mid-Pleistocene Transition (700 – 1400 ka, Site U1385)	IODP	28
S. J. Batenburg, S. Voigt, O. Friedrich, A. Osborne, T. Klein, C. Neu, M. Frank	Latest Cretaceous- early Paleogene Atlantic deep ocean circulation and connectivity	IODP	29
T. Bauersachs, N. Lorbeer, L. Schwark	Climate variability controls the formation of cyanobacterial blooms in the Baltic Sea	IODP	30
F. Bergmann, V. Spieß, T. Schwenk, C. France-Lanord, A. Klaus, and IODP 354 Scientific Party	Refinement of the Bengal Fan stratigraphy along IODP Expedition 354 drilling transect facilitated by the reprocessing of GI-gun data and integration of high resolution watergun data	IODP	31
P. Blaser, J. Lippold, M. Gutjahr, N. Frank, J. Link, M. Frank	Mapping the distribution of seawater-derived Nd isotopes across the Atlantic Ocean during the last 30 ka for the reconstruction of water circulation changes	IODP	32
F. Böhm, A. Eisenhauer	Calcium and Strontium Isotopes in Low Temperature Alteration Calcites of the Ocean Crust	IODP	123
M. E. Böttcher, B. Liu, I. Schmiedinger, C. Slomp	The Hydrogen and Oxygen Isotope Geochemistry of Interstitial Fluids from IODP Leg 347: A study of Hydrographic Changes in the Baltic Sea since the Late Pleistocene	IODP	33
I. Bouimetarhan	Evolution of the indian summer monsoon and terrestrial vegetation in the Northern Bengal region during the mid-Pleistocene transition (INTERMILAN)	IODP	34
J. Buongiorno, G. Webster, A. Weightman, A. Schumaker, S. Turner, A. Schippers, T. Roy, K. Lloyd	Quantification of Deep Subseafloor Bacteria and Archaea – An Inter-Laboratory Comparison	IODP	34
P. A. Brandl, M. Hamada, R. J. Arculus, C. J. Le Losq	Birth and early life of the Izu-Bonin-Mariana island arc	IODP	35
J. Brandstätter, W. Kurz, K. Krenn, P. Micheuz	Microstructures and fluid inclusion petrography and microthermometry of hydrothermal veins of Site U1414, IODP Expedition 344 (CRISP 2)	IODP	35
H.-T. Brandt, O. Michaelis, U. Kotthoff, Expedition 347 Science Party	Reconstruction of the palaeoecological evolution of the Holocene Bothnian Sea region on the basis of palynomorphs from two IODP Sites (M0061, M0062) from the Ångermanälven estuary	IODP	36
T. Burschil, H. Buness, G. Gabriel	Improved shallow seismic imaging by combining P- and S-waves – Tannwald Basin	ICDP	36
O. E. Chiang, V. Vandieken, B. Engelen	Potential impact of salinity changes on viruses and bacteria in sub-surface sediments from the Baltic Sea	IODP	38

R. Tiedemann, M. H. Trauth, M. Hofreiter	DNA-Metabarcoding of phyto- and zooplankton in East African lake sediments as proxies for past environmental perturbation	ICDP	109
R. Tjallingii, I. Neugebauer, M. Ahlborn, M. J. Schwab, A. Brauer	Advanced statistical analyses of XRF core scanner data from the Dead Sea record for an improved and rapid identification of extreme event deposits	ICDP	109
A. Türke, B. Ménez, W. Bach	Comparing biosignatures from North Pond, Mid-Atlantic Ridge and the Louisville Seamount Chain, off New Zealand	IODP	110
G. Uenzelmann-Neben	Changing sediment provenance in the Atlantic Ocean-Indian Ocean gateway during the Pliocene in relation to current dynamics and variations in continental climate	IODP	111
G. Uenzelmann-Neben, B. Huber, S. Bohaty, J. Geldmacher, K. Hoernle, K. Macleod, C. Poulsen, S. Voigt, T. Wagner, D. Watkins, R. Werner, T. Westerhold	Drilling the Agulhas Plateau and Transkei Basin to reconstruct the Cretaceous - Paleocene Tectonic and Climatic evolution of the Southern Ocean Basin	IODP	111
A. Vuillemin, J. Kallmeyer, D. Wagner, H. Kemnitz, R. Wirth, A. Luecke, C. Mayr, and the ICDP Towuti Drilling Project Science Team	Characterization of diagenetic siderites formed in recent and ancient ferruginous sediments of Lake Towuti, Indonesia	ICDP	111
M. Wang, O. Namur, R. Almeev, B. Charlier, F. Holtz	Basalts from the Kimama core (Snake River Plain, Idaho) and experimental study on the link with associated rhyolites	ICDP	112
M. E. Weber, P. S. Dekens, B. T. Reilly, T. Williams, S. K. Adhikari, P. A. Selkin, H. Lantzsch, L. Meynadier, J. F. Savian, S. K. Das, R. R. Adhikari, B. R. Gyawali, G. Jia, L. R. Fox, J. Ge, Y. Martos Martin, M. C. Manoj, J. Bahk, K. Yoshida, C. Ponton, P. Huyghe, V. Spieß, C. France-Lanord, and IODP Expedition 354 Scientists	Reconstructing the evolution of the Bengal Fan with the aid of physical and optical properties – IODP Expedition 354	IODP	114
T. Westerhold, U. Röhl, B. Donner, J. C. Zachos	New Eocene benthic stable isotope record in the Pacific: completing a 22 Ma single site high-resolution Paleogene section from Shatsky Rise	IODP	115
R. Wiese, J. Renaudie, D. Lazarus	Can genera be used as proxies for species in studies of biodiversity-climate sensitivity? - A test using Cenozoic marine diatoms	IODP	116
S. Wilke, F. Holtz, T. Bolte, P. Nowaczyk, R. Almeev, E. H. Christiansen	Magma storage depths of the Yellowstone Supervolcano: New insights from project HOTSPOT	ICDP	117
A. Wittke, N. Gussone, B. M. A. Teichert	Fractionation of Ca isotopes during transport and recrystallisation processes in marine deep sea sediments	IODP	120

L. Wörmer, R. Adhikari, N. Gajendra, B. Stern, B. Viehweger, T. Meador, K.-U. Hinrichs	Bacterial endospores in the marine subsurface: assessment of their abundance and relevance through culture-independent, biomarker-based quantification	IODP	120
J. Zeiß, M. Paschke, F. Bleibinhaus	Visco-elastic full waveform inversion of controlled seismic data from the San Andreas Fault Observatory at Depth	ICDP	121

Fahrtberichte

IODP Expedition 353 (iMonsoon) Cruise Report: Indian monsoon circulation in the core convective region since the Miocene at tectonic to centennial timescale

W.KUHNT[1], E. HATHORNE[2], O. ROMERO[3] AND THE EXPEDITION 353 SHIPBOARD SCIENTIFIC PARTY

[1]Institut für Geowissenschaften der Christian-Albrechts-Universität zu Kiel, Ludewig-Meynstraße 10-14, 24118 Kiel, Germany
[2]GEOMAR - Helmholtz-Zentrum für Ozeanforschung Kiel, Wischhofstr. 1-3, 24148 Kiel, Germany
[3]MARUM - Center for Marine Environmental Sciences, University of Bremen, 28359 Bremen, Germany

International Ocean Discovery Program (IODP) Expedition 353 (29 November 2014–29 January 2015) drilled six sites in the Bay of Bengal, recovering 4280 m of sediments during 32.9 days of on-site drilling. Recovery averaged 97%, including coring with the advanced piston corer, half-length advanced piston corer, and extended core barrel systems. IODP expedition 353 (iMonsoon) targeted the monsoonal precipitation signal in its core geographic region of influence, the margins of the Bay of Bengal. One of the main objectives is to monitor the variability of the exceptionally low salinity surface water signal that results from both direct summer monsoon precipitation above the Bay of Bengal and runoff from the numerous large rivers that drain into this Bay (Clemens et al., 2014). Changes in rainfall and surface ocean salinity are embedded in a number of chemical, physical, isotopic, and biological proxy indicators within the sedimentary archives at the margins of the Bay of Bengal. Expedition 353 sites were strategically located in key regions where the sedimentary archives are complete and expanded and the paleoceanography proxy signals are particulary strong and well-preserved. Terrigenous runoff and salinity changes at IODP Sites U1445 and U1446 (northeast Indian margin) originate from river basins in peninsular India and the Ganges-Brahmaputra river complex, while salinity changes at IODP Sites U1447 and U1448 (Andaman Sea) record direct precipitation and runoff signals from the Irrawaddy and Salween river basins. IODP Site U1443 (Ninetyeast Ridge) was drilled as an open ocean site with modern surface water salinity very near to the global mean but longterm changes in monsoonal circulation are embedded in isotope, temperature and productivity signals over orbital to tectonic timescales.

The main interest of the German participants on IODP Expedition 353 concentrates on Site U1445 along the northeast Indian margin, the two sites in the vicinity of the Andaman Islands (IODP Sites U1447 and U1448, Andaman Sea) and the the open-ocean Site U1443 which were drilled to address the issues of long-term monsoonal circulation changes in high-resolution sedimentary archives of the Miocene-Pleistocene Indian Monsoon. The new cores from these critical regions will allow us to assess the relative sensitivity of the Indian Monsoon to insolation forcing and climate boundary conditions such as the extent of global ice volume and greenhouse gas concentrations, and the timing and conditions under which monsoonal circulation initiated and evolved. These new records will also allow determination of the temporal and geographical coupling between monsoonal winds (driving upwelling and productivity, in particular the longterm diatom bloom from the early throughout the late Pliocene recorded in Site 1445) .and precipitation (changing salinity and terrigenous runoff). Finally, the new records from the margins of the Bay of Bengal are crucial to test the alternative and partly conflicting hypothesis of linkages between the climatic evolution of South Asia and the tectonic development of the Himalayans and the rising of the Tibetan Plateau.

References:
Clemens, S.C., Kuhnt, W., and LeVay, L.J., 2014. iMonsoon:Indianmonsoon rainfall in the core convective region. International Ocean Discovery Program Scientific Prospectus, 353.

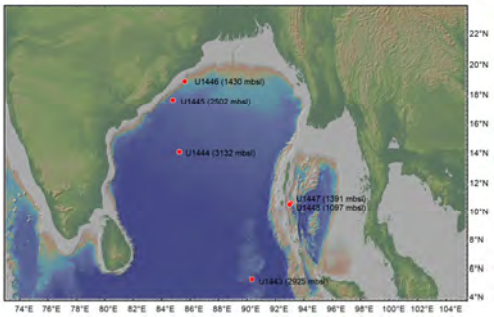

Fig. 1. Location of Expedition 353 sites and seafloor depths. Map was generated using GeoMapApp (http://www.geomapapp.org), using topography and bathymetry from the Global Multi-Resolution Topography synthesis (Ryan et al., 2009).

http://dx.doi.org/10.14379/iodp.sp.353.2014.

IODP Expedition 354 to the Middle Bengal Fan: A Drilling Transect to Reconstruct Oligocene to Recent Himalayan Erosion and Weathering History in a Complex Sedimentary Fan Setting

VOLKHARD SPIESS[1], C. FRANCE-LANORD[2], T. SCHWENK[1], A. KLAUS[3], AND IODP EXPEDITION 354 SCIENTIFIC PARTY

[1] Department of Geosciences, University of Bremen, Klagenfurter Strasse, D-28359 Bremen, Germany
[2] Centre de Recherches Pétrographiques et Géochimiques, CNRS Université de Lorraine, BP 20, 54501 Vandoeuvre les Nancy, France
[3] Texas A & M University College Station, USA

The development of the Himalayan orogenic belt induced a major change in continental distribution, topography and climate that impacted the global biogeochemical cycles. The uprising of the highest mountain range in the world coupled with an intense monsoonal precipitation regime generated an exceptional erosional flux that enhanced both organic carbon burial and silicate weathering. The largest fraction of the sediment flux was exported to the Bengal Fan, accumulating a long-term archive of this erosion. These sediments record the nature of eroded formations in the Himalaya and allow the documentation of weathering as well as organic carbon fluxes.

Consequently, IODP Expedition 354 in the Bay of Bengal February-March 2015 drilled a seven site, 320 km-

long transect across the Bengal Fan at 8°N to investigate interactions between the growth of the Himalaya, the development of the Indian monsoon, and processes affecting the carbon cycle. Three deep penetration and additional four shallow holes provided a spatial overvieof the primarily turbiditic depositional system, comprising the Bengal deep sea fan.

Sediments originate from Himalayan rivers, documenting terrestrial changes of the monsoon evolution and Himalayan erosion and weathering, and are transported through a delta and shelf canyon, supplying turbidity currents loaded with a full spectrum of grain sizes. Mostly following transport channels, sediments deposit on and between levees, while depocenters are laterally shifting over hundreds of kilometers on millennial time scales. Expedition 354 documented these deposits in space and time by identifying, coring and dating numerous stratigraphic marker horizons across the transect, allowing a detailed reconstruction of channel-levee migration, abandonment, reoccupation and overall uniform growth in the late Pleistocene. High resolution records of these growth patterns were acquired in several levee, interlevee and hemipelagic successions (Figure 1).

Miocene through Pliocene fan development was studied at three deeper sites (Figure 2), which document and recovered sand rich facies throughout most of the cores acquired by the half-APC coring technology, intercalated by longer periods of hemipelagic deposition and absence of turbiditic input as the results of major depocenter shifts. Recovered sediments have Himalayan mineralogical and geochemical signatures suitable to reconstruct time series of erosion, weathering and changes in source regions as well as impacts on the global carbon cycle. Miocene shifts in terrestrial vegetation, in sediment budget and in style of sediment transport have been tracked. Expedition 354 has extended the record of early fan deposition by 10 Ma into the Late Oligocene.

Overall, the expedition obtained a comprehensive record of turbiditic deposition since the Late Oligocene, with chemical and mineralogical composition of turbiditic sediments cored across the transect being relatively stable throughout the Neogene. They reveal a weak regime of chemical weathering with no significant variation through time. This differs from the distal fan record of ODP Leg 116, where from ~7 to 1 Ma, weathered and smectite rich sediments dominated. This difference implies that the distal fan record is not related to a direct evolution of the erosion regime but rather is controlled by a change in sediment transport within the fan. Shipboard estimates of organic carbon loading and behavior resemble observations made in the modern Ganga-Brahmaputra river sediments, suggesting efficient terrestrial organic carbon burial in the Bengal Fan. Preliminary observations support the idea that Himalayan erosion has consumed atmospheric CO_2 through the burial of organic carbon, more than by silicate weathering.

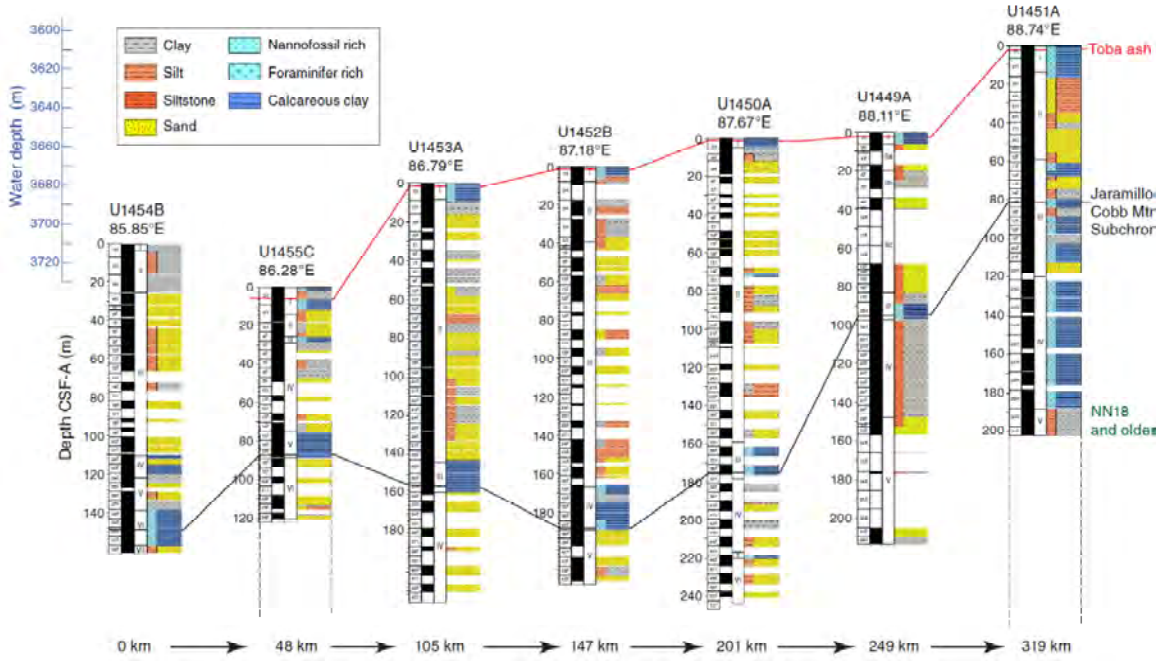

Figure 1: Coring results of IODP Expedition 354 from the middle Bengal Fan drilling transect for the upper 120 to 245 meters. The black line indicates a magneto-stratigraphically confirmed transect-wide marker horizon through the Jaranmillo/Cobb Mountain Subchrons. The lithology column indicates the high sand content recovered through the half-APC coring technology.

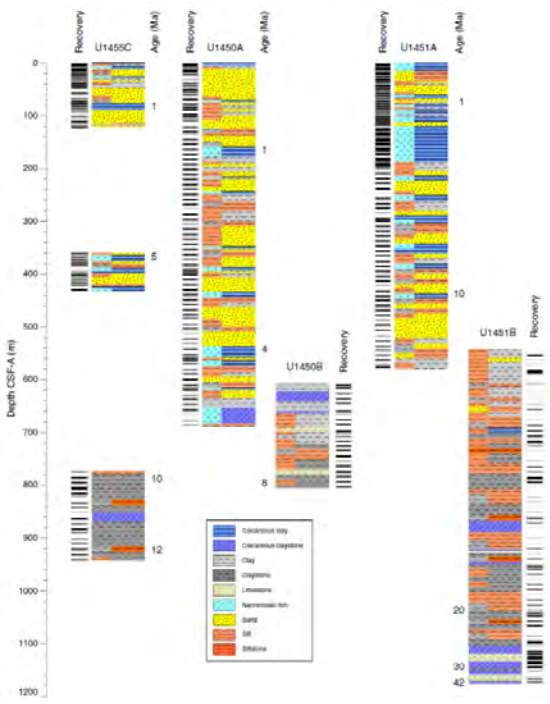

Figure 2: Deep drill sites U1455 (DSDP Site 215), U1450 and U1451, which date back to Miocene (8 Ma, U1450 and 12 Ma, U1455, resp.) and Oligocene/Eocene times (U1451). Sand content drastically drops, when rotary coring has to be used beneath 700 mbsf (U1450) or 580 mbsf (U1451). The absence of sand is thereby not indicative of a change in the sediment distribution system. Penetration rates rather indicate high sand content back to the Oligocene, but overall recovery of coarse material is very low.

IODP Expedition 355 – Arabian Sea Monsoon

D.K. PANDEY[1], P.D. CLIFT[2], D.K. KUHLHANEK[3], A. HAHN[4], S. STEINKE[4], AND THE EXPEDITION 355 SCIENTISTS

[1]Department of Marine Geophysics National Centre for Antarctic and Ocean Research (NCAOR), Vasco da Gama, India
[2]Department of Geology and Geophysics, Louisiana State University, Baton Rouge, LA, USA
[3]International Ocean Discovery Program ,Texas A&M University, College Station, TX, USA
[4]MARUM – Center for Marine Environmental Sciences, University of Bremen, Bremen, Germany

The International Ocean Discovery Program Expedition (IODP) 355 Arabian Sea Monsoon -Deep sea drilling in the Arabian Sea: constraining tectonic-monsoon interactions in South Asia- set sail from Colombo (Sri Lanka) on April 5, 2015 and ended in Mumbai (India) on May 31, 2015. During the IODP Expedition 355, two sites (U1456 and U1457) were drilled in the Laxmi Basin in the eastern Arabian Sea to (a) reconstruct changes in erosion and weathering intensity, including to assess whether any changes occurred at ~23 Ma, 15 Ma, and 10-8 Ma, which are hypothesised to represent times of changes in monsoon intensity, and (b) to decipher the composition of the basement rocks in the Laxmi Basin in order to determine the timing of early rifting processes and its linkage to the development of the Deccan Flood Basalts along the western continental margin of India (Pandey et al., 2015).

A total of ~1722 m of core was recovered and from August 24-28, 2015, the IODP 355 Science Party assembled at the Gulf Coast Repository, Texas A&M University (College Station, TX, USA) to sample the cores for post-cruise research. Drilling operations during IODP Expedition 355 retrieved sediment from Sites U1456 and U1457 in the Laxmi Basin, penetrating 1109.4 m and 1108.6 m below seafloor (mbsf), respectively. The age models for Sites U1456 and U1457 are based on a combination of calcareous nannofossil and planktonic foraminifera bioevents, together with magneto-stratigraphy. The succession of bioevents indicates that Site U1456 spans the late early to early middle Miocene (13.5–17.7 Ma) to recent but is punctuated by several hiatuses of varying duration. Sediments at Site U1457 are dated to the early Paleocene to recent but with a ~50 million year hiatus between lower Paleocene and upper Miocene sediment (~62 to ~10.9 Ma). At both sites, hiatuses span ~8.2-9.2 Ma and ~3.6–5.6 Ma, with a possible condensed section spanning ~2.0–2.6 Ma (Pandey et al., 2015).

The sediments recovered at Site U1456 are divided into four lithologic units. A ~121 m thick Pleistocene sequence (Unit I) consists of nannofossil ooze and foraminifer-rich nannofossil ooze with numerous intercalated clayey, silty, and sandy layers. The sand layers are interpreted as distal basin plain turbidites. Unit II is a massive ~240 m thick sand and silt sequence interbedded with thin nannofossil-rich clay of late Pliocene to early Pleistocene age. The upper Pliocene to lower Pleistocene sandy intervals at Site U1456 were most likely deposited in lower fan sheet lobe settings.

The upper Miocene to upper Pliocene lithologic Unit III is a ~370 m thick light brown to dark green clay/claystone, light brown to dark gray sand/sandstone, light greenish nannofossil chalk, and light to dark greenish gray nannofossil-rich claystone. Sand layers within this unit are interpreted as turbidites, most likely deposited in a sheet lobe. Unit IV consists of ~380 m of interbedded lithologies dominated by dark gray massive claystone, light greenish massive calcarenite and calcilutite, and conglomerate/breccia, with minor amounts of limestone. Biostratigraphy indicates that these rocks range in age from Eocene to early Miocene; however Unit IV is characterized by a variety of deformation structures, such as microfaults, soft-sediment folds, slickensides, and tilted to vertical bedding, indicating that it is a mass transport deposit emplace in the early late Miocene.

The recovered sedimentary sequence at Site U1457 is divided into five lithologic units. The Unit I (~74 m thick) is similar in lithology and age to Unit I at Site U1456, whereas the Unit II (~311 m thick) is also similar in age to Unit II at Site U1456, but the sediment is much finer grained at Site U1457. Upper Pliocene to upper Miocene light brown to dark green silty claystone, light brown to dark gray silty sandstone, light greenish nannofossil chalk, and light to dark greenish gray nannofossil-rich claystone characterize the ~450 m thick Unit III. A ~225 m thick mixture of interbedded lithologies consisting of dark gray to greenish gray massive claystone, light greenish massive calcarenite and calcilutite, breccia, and limestone represent Unit IV.

Similar to Unit IV at Site U1456, deformation structures indicate a mass transport deposit that emplaced Paleogene to lower Neogene sediment in Laxmi Basin

during the early late Miocene. Dark brown to dark greenish gray claystone and dark gray to black volcaniclastic sediment characterize the ~30 m thick Paleocene Unit V, which overlies the basaltic basement.

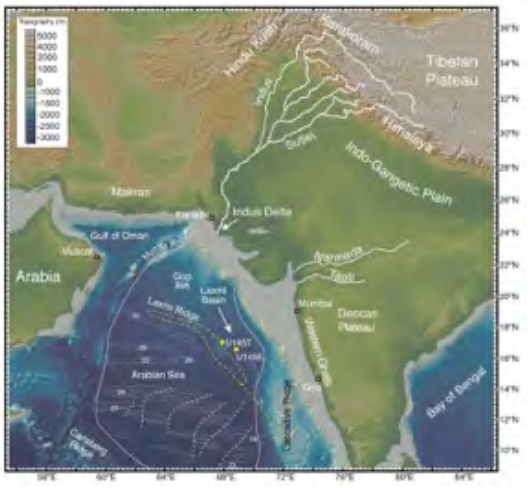

Fig.1
Bathymetric map of the Arabian Sea and surrounding landmasses. Yellow circles = Expedition 355 sites, white lines = major rivers and tributaries, pink line = approximate extent of the Indus fan; yellow dashed lines = speculated location of the continent/ocean boundary, depending on whether Laxmi Basin is oceanic or continental, gray lines with numbers = magnetic anomalies from Royer et al. (2002).

The recovery of 8.72 m massive basalt, classified as clinopyroxene-plagioclase/plagioclase-clinopyroxene-phyric basalt at this site, should us to address key questions related to rifting and volcanism associated with the formation of the Laxmi Basin.

Our first results suggest that a major submarine fan draining the western Himalaya and Karakoram must have been supplying sediment to the eastern Arabian Sea since at least ~17 Ma. Initial shipboard results suggest that most of the sediment was supplied by the Indus River. Pliocene sandy intervals at Site U1456 were deposited in a lower fan "sheet lobe" setting, whereas Site U1457 reflecting a more marginal setting.

No major active lobe appears to have affected the Laxmi Basin since the Middle Pleistocene (~1.2 Ma). The mass transport deposit, measuring ~330 m and ~190 m thick at Sites U1456 and U1457, respectively, represents one of the world's largest mass transport deposits. The recovery of sediments back to ~17 Ma allows us to address major objectives related to changes in monsoon during the Neogene, such as the 10-8 Ma climatic transition. Additionally, a mostly continuous Pleistocene sequence at both Sites enables us to study glacial-interglacial variations in the Indian summer monsoon during much of the Pleistocene.

References:

Pandey, D.K., Clift, P.D., Kulhanek, D.K., Andò, S., Bendle, J.A.P., Bratenkov, S., Griffith, E.M., Gurumurthy, G.P., Hahn, A., Iwai, M., Khim, B.-K., Kumar, A., Kumar, A.G., Liddy, H.M., Lu., H., Lyle, M.W., Mishra, R., Radhakrishna, T., Routledge, C.M., Saraswat, R., Saxena, R., Scardia, G., Sharma, G.K., Singh, A.D., Steinke, S., Suzuki, K., Tauxe, L., Tiwari, M., Xu, Z., and Yu, Z. (2015). Expedition 355 Preliminary Report: Araian Sea Monsoon. InternationalOcean Discovery Program. http://dx.doi.org/10.14379/iodp.pr.355.2015.

International Ocean Discovery Program (IODP) Expedition 356 (Indonesian Throughflow): operations and lithologic characterization

STEPHEN GALLAGHER[1], CRAIG FULTHORPE[2], KARA BOGUS[3], DAVID DE VLEESCHOUWER[4], JEROEN GROENEVELD[4], TOBIAS HIMMLER[4], LARS REUNING[5], AND EXPEDITION 356 SCIENTISTS.

1 School of Earth Sciences, University of Melbourne, Victoria 3010, Australia
2 Institute for Geophysics, Jackson School of Geosciences, The University of Texas at Austin, 10100 Burnet Road, Austin, TX7 8758, USA
3 International Ocean Discovery Program, Texas A&M University, College Station, TX 78845, USA
4 MARUM/Department of Geosciences, University of Bremen, D-28359 Bremen, Germany
5 Geological Institute, RWTH Aachen University, Germany

IODP Expedition 356 aboard the RV JOIDES Resolution began 31 July 2015 in Fremantle (Australia) and ended 30 September 2015 in Darwin (Australia). Seven shelf and upper slope sites (Sites U1458 to U1464) were cored off Western Australia along a 10° latitudinal transect (28°S to 18°S) from the Perth Basin, through the Northern Carnarvon Basin, to the Roebuck Basin (Fig. 1). Water depths of the drill sites ranged from 87 mbsl (U1462) to 264 mbsl (U1464). Drilling operations during Expedition 356 achieved continuously cored sections of 300 m to 1.1 km, accumulating a total of ~5200 m of sediment (total recovery: 67%). Downhole logging was carried out at five drill sites (U1459 and U1461-U1464) in order to better characterize the sedimentary succession where core recovery was incomplete or disturbed, and to complement core data.

U1458 & U1459

The vessel arrived at the first Site **U1458** after <24h of transit. Due to low core recovery (3.72 m), only one Hole (U1458 A) was drilled. The recovered material suggested a hard seafloor, comprising a ~10 cm thick lithified skeletal rudstone layer with a thin soft sediment cover. As a result of the poor recovery and shallow penetration, this site was abandoned in favor of the alternate Site **U1459**, which was located north of U1458. This site consisted of three holes. A total of 224.96 m of core was recovered (46% recovery). Using the half-length advanced piston corer (HLAPC) and extended core barrel (XCB) systems Holes U1459A and U1459B penetrated down to 70 and 233 m CSF-A, respectively. For Hole U1459C, the RCB (Rotary Core Barrel) system was used to core material below 233 m CSF-A down to the final depth of ~400 m CSF-A. Due to increased ship heave during RCB drilling, coring was suspended for almost 24h at this site. Overall, the recovered sediment comprised mainly interbedded lithified and unlithified skeletal packstone, mudstone, and grainstone intervals. Quartz, glauconite, and dolomite content increased with depth. Sediment in the lowermost ~100 m (296.4 to 397.72 m CSF-A) at the site is characterized by abundant chert nodules. Biostratigraphic data reveal that Holes U1459A and U1459B contain Pleistocene to late Miocene sediments, while the lowermost strata in Hole U1459C were early Miocene to early-middle Eocene age. Downhole measurements in Hole U1459C were successful and consisted of runs with the triple combination tool string and the Formation Micro-Scanner and Sonic imager (FMS-sonic).

U1460

After nearly seven days of operations at Site U1459, the vessel moved 85 nmi (nautical miles) north to Site **U1460**. Two Holes were cored using the HLAPC, each to a total depth of 300.1 m CSF-A (Hole 1460A) and 306.6 m CSF-A (Hole U1460B), respectively, and yielded very good recovery (592.2 m; 98%). In the upper ~250 m, the recovered material consisted of unlithified to partially lithified skeletal packstone, wackestone, and grainstone. Several hardground layers were found in this interval. Glauconite and dolomite content increase with depth. Below 250 m, unlithified to partially lithified packstone, mudstone and wackestone alternate. Mass-wasting deposits were observed in the lowermost 50 m, characterized by graded beds and contoured contacts. Biostratigraphic data reveal an early Pliocene age (<4.3 Ma) for the lowermost section of U1460 (Section U1460B-68F-CC, 306.6 m CSF-A).

U1461

After three operational days at site U1460, the ship moved 469 nmi north to Site **U1461** which is located in the Northern Carnarvon Basin. This site consisted of four holes, with the deepest Hole (U1461D) reaching a maximum total penetration of 1095.3 m CSF-A. Total recovery was 83%, yielding 1804.87 m of sediment recorded in 301 cores. After coring was completed, Hole U1461D was logged with the triple combination tool string to a depth of 1030 m WMSF. The FMS-sonic tool failed to pass below 192.7 WMSF, but yielded good-quality sonic velocity measurements. Recovered sediment of the upper ~11 m consisted of unlithified homogeneous olive gray to greenish-gray packstone with abundant foraminifers and occasional bivalves. Sediment below 11 m CSF-A was characterized by alternating beds of unlithified packstone, wackestone, and mudstone down to ~280 m CSF-A (U1461A), ~450 m CSF-A (U1461B and C), and ~460 m CSF-A (U1461D). The degree of lithification increased with depth and well-lithified wackestone with abundant bioturbation traces, pyrite, and various sedimentary features characteristic of gravity flows were observed. Micropaleontology data revealed an early Pleistocene age (<1.93 Ma) for the bottom of Holes U1461A and U1461C. The sediments retrieved from Hole U1461B are of Pliocene-Pleistocene age, with the bottom estimated to be older than >4.07 Ma. In Hole U1461D, the abundance and preservation of calcareous nannofossils and planktonic foraminifera decreased markedly from Section U1461D-52R-CC (1008.3 m CSF-A) downhole, with possible reworking, suggesting a probable unconformity. The bottom of Hole U1461D was dated to the middle to late Miocene.

U1462

After twelve days of operations at Site U1461, the ship sailed 61 nmi to Site **U1462**. Three holes were drilled at Site U1462, with Hole 1462C reaching the maximum depth of 950 m CSF-A. The total length of the cored interval was 1824.3 m, yielding a recovery of 720.82 m (40%) in 286 cores. After coring to 855 m CSF-A, Hole U1462A was successfully logged with the triple combination and FMS-sonic tool strings. The third Hole (U1462C) was drilled with the RCB down to 950.0 m CSF-A and successfully logged with the triple combination, FMS-sonic and Versatile Seismic Imager (VSI) tool strings. In general, the upper ~300 m sediment is characterized by partially to fully lithified, light grayish green to dark greenish gray, non-skeletal packstone with lesser amounts of skeletal pack- to grainstone, including the oldest recovered Quaternary ooid deposits in the Indo-Pacific realm (Hole U1462C; 144.5 m CSF-A). Planar laminations, bioturbation, and sharp to wavy, gradational, and bioturbated contacts were commonly observed. Below 300 m CSF-A, a distinct increase in planktic foraminifers and siliciclastic components was observed, and the sediment comprised mainly of lithified olive gray packstone with some wackestone intervals. Sedimentary structures indicated gravitational flows and other small-scale mass-transport deposits (e.g., laminations, grading, contact surfaces) at about 770 m CSF-A. The quartz content increased downhole and the lowermost sediment was characterized by a major change in the mineralogy from carbonate (packstone and grainstone) to poorly sorted siliciclastic sandstone. The deepest recovered material was composed of dolostone and quartz-rich sandstone. Anhydrite nodules with a chicken wire texture were common. Biostratigraphic data indicated a Pliocene-Pleistocene to late Miocene age for the section.

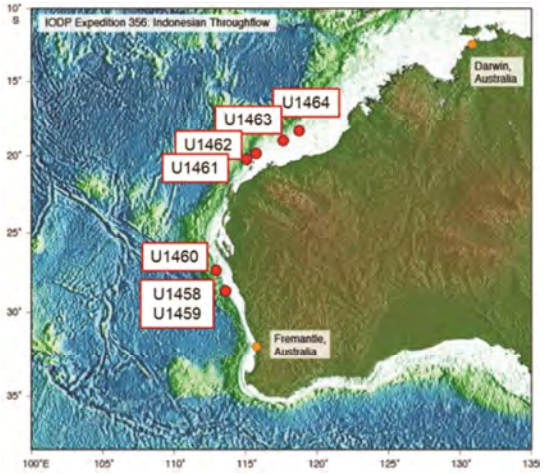

Figure 1: Locations of IODP Expedition 356 sites U1458–U1464. (Gallagher et al., 2016 – Preliminary Report).

U1463

After almost 14 operational days at Site U1462, the vessel moved 131 nmi to Site **U1463**. Four holes were drilled, with the deepest penetration reached at Hole U1463B (530 m CSF-A). The total recovery was 1151.54 m (89%). Site U1463 yielded a complete stratigraphic succession from the early Pleistocene to late Miocene, as indicated by biostratigraphy and corroborated by paleomagnetic data. Five lithostratigraphic units were defined, including: I) unlithified, creamy gray to light greenish gray wackestone and mudstone with abundant peloids; II) wackestone, packstone and mudstone intervals; III) homogeneous mudstone; IV) dolomitic grainstone; and V) dolostone with abundant dissolution features, containing sand-sized grains of pyrite and/or glauconite, and abundant anhydrite nodules. Downhole measurements were successfully conducted in the deepest Hole (U1463B) with the triple combination and FMS-Sonic tool strings. A run with the VSI tool string was attempted, but since marine mammals were commonly seen within the exclusion zone,

operations with the VSI were terminated with measurements carried out only at a single station.

U1464

After six days of operation at Site U1463, the ship headed to the final site of Expedition 356. Site **U1464** was reached after a 79 nmi transit. At this site four holes were drilled. Hole 1464D reached the deepest penetration (529.6 m CSF-A). Total recovery was 687.04 m (49%). At this site a complete stratigraphic succession from the early Pleistocene to late Miocene was recovered. Five lithologic units were defined, including: I) 0 to ~44 m CSF-A, unlithified grainstone to mudstone with silt- to fine sand-sized peloids; II) ~95 m thick, largely unlithified, homogeneous wackestone with high abundance of authigenic glauconite and glauconitized microfossils; III) ~170 m thick, wackestone to mudstone with various amounts of siliciclastic content, grayish-green to greenish-gray homogeneous mudstone with moderate bioturbation and common disseminated pyrite and pyrite concretions; IV) ~215 m thick, dolomitic packstone with abundant gypsum nodules co-occuring with anhydrite nodules in the lower 46 m of the unit; V) ~311.50 m thick, consisting primarily of dolomitic limestone and dolostone. Downhole measurements consisted of a single run with the triple combination tool string in Hole U1464C to a depth of 783 m WMSF.

IODP Expedition 359: Maldives Monsoon and Sea Level

C. BETZLER[1], G. EBERLI[2], C. ALVAREZ-ZARIKIAN[3] AND IODP EXPEDITION 359 SCIENTISTS

[1]Institute of Geology, University of Hamburg, Germany
[2]Rosenstiel School of Marine & Atmospheric Science, University of Miami, USA
[3]International Ocean Discovery Program, Texas A&M University, USA

Drilling the carbonate platforms and drifts in the Maldives aimed to recover the marine tropical record of the Neogene sea-level changes and the onset of the monsoon related current system in the Indian Ocean. To reach this goal, eight sites were drilled along two transects in the Kardiva Channel in the Inner Sea of the Maldives during IODP Expedition 359. The recovered cores and log data retrieved the material to achieve all the objectives set for the expedition. The most arresting accomplishment is the documentation of how the sea level controlled carbonate platform system that was thriving during the Miocene Climate Optimum abruptly transitioned into a current-dominated system in the late Middle Miocene. This transition is linked to the onset of an early intensification of the Indian monsoon and the coeval demise of some of the Maldivian platforms.

Cores and downhole logs allowed producing a solid record and reconstructing the Neogene environmental changes in the central Indian Ocean. Preliminary shipboard analyses allow a precise dating of this major paleoclimatological and paleoceanographical change, as it also applies for the extension of the Oxygen Minimum Zone (OMZ) into this part of the Indian Ocean. Coring produced a solid framework to foster the post-cruise research of these distinct topics. In addition, complete spliced sections and logging at key sites during Expedition 359 provide the potential to assemble a cycle-based astrochronology for the Neogene section in the Maldives. This high-resolution chronology will allow: 1) independent ages to be assigned to key biostratigraphic events in the Maldives for comparison with those from other tropical regions; 2) more precise ages for the major sequence boundaries and unconformities; and 3) evaluation of higher-resolution sedimentation rate variations.

Cruise Report: IODP Expedition 360: Southwest Indian Ridge Lower Crust and Moho

J. CIAZELA[1], J. KOEPKE[2], H.J.B. DICK[3], C.J. MCLEOD[4], P. BLUM[5], AND THE EXPEDITION 360 SCIENTISTS

[1] Jakub Ciazela, Institut fuer Mineralogie Universitaet Hannover, jciazela@mineralogie.uni-hannover.de
[2] Juergen Koepke, Institut fuer Mineralogie,Universitaet Hannover, koepke@mineralogie.uni-hannover.de
[3] Henry J.B. Dick, Department of Geology and Geophysics,Woods Hole Oceanographic Institution, hdick@whoi.edu
[4] Christopher J. McLeod, Department of Earth Sciences, Cardiff University mcleod@cardiff.ac.uk
[5] Peter Blum, International Ocean Discovery Program, Texas A&M University, blum@iodp.tamu.edu

Expedition 360, Atlantis Bank, started at 30.11.2015 in Colombo (Sri Lanka) and ended at 30.01.2015 in Port Louis (Mauritius). Expedition 360 was Leg 1 of the SloMo Project, a Multi-Phase Drilling Program to drill through the Moho at a slow-spreading ocean ridge. The primary objective of the SloMo Project is to test competing hypotheses on the nature of the Moho at the slow-spreading oceanic lithosphere. Based on seismic survey and geologic mapping, the Moho beneath Atlantis Bank is believed to represent a serpentinization front, and not an igneous boundary between gabbros and peridotites as postulated by the Penrose Model. Beside drilling a deep re-entry hole for Leg 1, the primary objective of expedition 360 was exploring the lateral variability of the lower crust by stratigraphic comparison to previous holes and drilling drilling through the magnetic boundary between reverse geomagnetic polarity chron C5r.3r and normal polarity chron C5r.2n projected to lie below the site.

Atlantis Bank is an oceanic core complex located at 32°40′ S and 57°15′ E in the Indian Ocean. The bank consists of a raised dome ~40 km long by ~30 km wide, rising from 5700 m depth at the base of the transform wall to ~700 m on a ~25 km^2 flat-topped platform. The platform is part of a continuous gabbro massif, emplaced ~12 myr ago and exposed throughout the dome. Gabbro overlies granular mantle peridotite that forms the lower slopes of the eastern wall of the Atlantis II Transform. The drilling was carried out in ~710 m water depth, 2.2 km NNE of Hole 735B and 1.4 km N of 158-m deep Hole 1105A in the center of the wave-cut platform. Expedition 360 Hole 1473 was drilled 789.7 m through massive gabbro. It encountered a highly fractured carbonate cemented zone from 170 to 570-m with 44% recovery and highly variable hole diameter, likely representing a late high-angle normal fault. Under 570 m, drilling conditions were excellent, with 96% recovery. This is the deepest single-leg basement hole drilled in ocean crust, and can be re-entered by Leg 2.

Hole U1473A with Hole 735B and 1105A demonstrate a continuity of process reflecting the complex interplay of

magmatic accretion and steady-state detachment faulting over a 128,000 year time period. Preliminary assessment indicates that these sections reflect repeated intrusion represented by chemically upwardly differentiated 100-m scale olivine gabbro cumulates. The bulk of these are too fractionated to be in equilibrium with the MORB hanging wall debris. Fe-Ti rich oxide gabbro and gabbronorite layers and patches occur within the olivine gabbros, and in shear zones cutting them. These appear to have crystallized from late melt compacted out of the olivine gabbro cumulates representing late-stage melt migration through the section. Numerous long intervals of sheared, dominantly porphyroclastic to ultramylonitic, gabbro, representing a 600-m thick shear zone, demonstrate that this occurred in a dynamic environment beginning while the gabbros were partially molten, and continuing as they cooled and were emplaced diapirically and tectonically upward into the zone of diking beneath the rift valley floor. In this context it is likely significant that below 600 mbsf, deformation becomes more discrete and primary subophitic igneous textures are often well preserved.

Hole U1473A gabbros have H_2O contents of 0.3 to 8 wt.%, typical of oceanic gabbros and much higher than expected in pristine cumulate rocks. The abundance of H_2O decreases with depth and reflects deep and pervasive infiltration of seawater through the crustal section. Felsic veins in Hole U1473 often have a high abundance of secondary sulfides and clay minerals, and the emplacement of primary plagioclase by albitic and occasionally secondary quartz, showing that these were pathways for large volumes of hydrothermal fluids, as also found in Hole 735B. Another key similarity to Hole 735B is the occurrence of amphibole veins largely only in the upper few hundred meters of the holes, which also are found in the much shallower Hole 1105A.

The magnetic boundary between reverse geomagnetic polarity chron C5r.3r and normal polarity chron C5r.2n has not been reached. All igneous intervals have positive inclinations, indicating, in the southern hemisphere, a reversed polarity magnetization that places the hole within geomagnetic polarity chron C5r.3r. However, negative inclinations were revealed in some narrow zones of altered gabbro in the lower part of the hole. The presence of these zones within broader intervals with reversed polarity indicates near complete remagnetization of these rocks during a subsequent normal polarity period. The timing of the alteration cannot be uniquely determined from these data, but the presence of these components suggests that the reversal boundary between reverse geomagnetic polarity chron C5r.3r and normal polarity chron C5r.2n may occur in close proximity to the current bottom of the hole.

Expedition 360 Scientific Party: Natsue Abe, Donna K. Blackman, Julie A. Bowles, Michael J. Cheadle, Kyungo Cho, Jeremy R. Deans, Virginia P. Edgcomb, Carlotta Ferrando, Lyderic France, Biswajit Ghosh, Benoit M. Ildefonse, Mark, A. Kendrick, James A.M. Leong, Chuanzhou Liu, Qiang Ma, Tomoaki Morishita, Antony Morris, James H. Natland, Toshi Nozaka, Oliver Pluemper, Alessio Sanfilippo, Jason B. Sylvan, Maurice A. Tivey, Riccardo Tribuzio, Luis G.F. Viegas

Abstracts

IODP

Deep Biosphere in Bengal Fan Sediments (IODP Exp. 354)

R.R. ADHIKARI[1], K.-W. HINRICHS[1], C. FRANCE-LANORD[2], V. SPIESS[3], T. SCHWENK[3], A. KLAUS[4] AND THE EXP. 354 SCIENTISTS

[1]Organic Geochemistry, MARUM, University of Bremen, Leobener Strasse, 28539 Bremen, Germany
[2]Centre de Recherches Pétrographiques et Géochimiques, Centre National de la Recherche Scientifique (CNRS), BP 20, 15 Rue Notre-Dame-des-Pauvres, 54500 Vandoeuvre les Nancy Cedex, France
[3]Department of Geosciences, University of Bremen, Klagenfurter Strasse, 28359 Bremen, Germany
[4]JOIDES Resolution Science Operator, International Ocean Discovery Program, Texas A&M University, 1000 Discovery Drive, College Station TX 77845, USA

Seven Sites were drilled in the Bay of Bengal along 8°N transect during IODP Expedition 354 (February to March 2015; Singapore to Colombo, Sri Lanka) to study interactions between tectonics, climate change and the global carbon cycle in the late Paleogene and Neogene (France-Lanord et al., 2015). In addition to the main objectives, the expedition has provided a great opportunity to investigate deep biopshere in Indian Ocean, which is one of the additional objectives of the expedition. To understand paleoclimate and global carbon cycle, the Expedition explores organic matter preservation/degradation in detail, which is closely linked to the deep biosphere. We succesfully collected samples for our shore-based microbiological investigations, in which we aim to: 1) determine the size of buried biomass by prokaryotic cells and endospores counting, 2) charaterize the biospher by molecualar study, 3) quantify microbial activity, and 4) estimate organic matter turnover by incubation experiments.

Preliminary results of onboard hydrocarbon gas monitoring and porewater geochemistry clearly point to the presence of active biosphere at all sites and depths. A continuous increase in dissolved ammonium, the major end product of organic nitrogen mineralization, confirms metabolically active biosphere at shallow depth. At the deeper depth sulfate reduction followed by methanogenesis is found to be predominant. We observed deep sulfate methane transition zones (SMTZ). High phosphate at SMTZ confirms elevated microbial activity at these depths. However, stable carbon isotopes of hydrocarbon gases has to be determined to confirm microbial methanogenesis. From these observations, we can confirm that there is a large spatial and temporal variation in microbial activity. The spatial variation is due to a dynamic channel levee system of the Bengal fan whereas temporal variation could potentially be linked to the paleoclimatic variations.

References:

France-Lanord, C., Spiess, V., Klaus, A., and the Expedition 354 Scientists, 2015. Bengal Fan: Neogene and late Paleogene record of Himalayan orogeny and climate: a transect across the Middle Bengal Fan. International Ocean Discovery Program Preliminary Report, 354. http://dx.doi.org/10.14379/iodp.pr.354.2015

ICDP

Impact of geogenic CO_2 on the depth distribution and composition of deep microbial communities in the Hartoušov mofette system in NW Bohemia

M. ALAWI[1], K. MANGELSDORF[2], H.-M. SCHULZ[2], QI LIU[1], H. KÄMPF[2], D. WAGNER[1]

GFZ German Research Centre for Geosciences, Helmholtz Centre Potsdam, [1]Sect. 5.3 Geomicrobiology, [2]Sect. 3.2 Organic Geochemistry, Telegrafenberg, 14469 Potsdam, K.Mangelsdorf@gfz-potsdam.de

The Cheb Basin (western Eger Rift, North western Bohemia) is characterised by a network of *Diffuse Degassing Structures* (DDS) in mofette areas along an active fault zone (Kämpf et al., 2013). Further specific characteristics of this area are periodically occurring earthquake swarms and magmatic activities having strong impact on the changes in the composition and dynamics of the outflowing, mantle CO_2-dominated gases (Bräuer et al., 2005). From a biogeochemical and microbiological point of view these CO_2 seeps form an interesting and unique life habitat for microbial communities. The intense geogenic CO_2 fluxes provide a particular carbon and energy source forming the setting for a specific indigenous microbial community being well adapted to these specific environmental conditions. We hypothesize that in active fault zones, due to an intensified substrate support, microbial processes are significantly accelerated compared to other continental Deep Biosphere ecosystems.

Therefore active fault zones could be seen as „Hot Spots" of microbial life in the deep subsurface. Thus, the aim of the current study will be the investigation of the impact of degassing CO_2 on the depth distribution and composition of the indigenous microbial communities and their carbon and energy sources at the Hartoušov mofette area between Nebanice and Milhostov. To address this topic, not only surface but also deeper sediments from a 120 m deep research well, which is planned to be drilled in March 2016, will be investigated, therefore, enabling the examination of the deep microbial ecosystems (deep biosphere) at the degassing site. Two proposal were applied concerning the characterisation of the indigenous microbial communities, one using microbiological and DNA-based methods and a second one using organic-geochemical, isotope geochemical and biogeochemical approaches. These two projects can be seen as pre-examination studies to the proposed ICDP-drilling campaign (Drilling the Eger Rift: Magmatic fluids driving earthquake swarms and the deep biosphere).

In the frame of the microbiological project, which started already this January, we are applying high-throughput DNA sequencing techniques to get insight into the microbial community structure in CO_2 conduits of the rift zone. Additionally, quantitative PCR analyses and cultivation-based methods will provide data on the distribution pattern and activity of bacteria and archaea along the depth profile. The results of the molecular biological approaches, together with a detailed geochemical analyses of the fluid and pore water, expands our knowledge on the complex geo-bio-interactions in fluid-active faults.

In the biogeochemical proposal the depth distribution of present and past microbial communities will be determined using microbial biomarkers, representing living (life markers) and dead microbial biomass. Carbon isotopic compositions of life markers will provide insight into the carbon sources (sedimentary organic matter ca. -25‰ vs. geogenic CO_2 ca. -2‰) and will help to identify geosphere-biosphere interaction processes. Past microbial biomarkers bear the potential to provide information on the history of the degassing site. Compound-specific carbon isotope measurements of the past microbial biomarkers will be applied to test whether changes in the fluxes and/or direction of the degassing CO_2 with depth and, therefore, over time can be recorded. Furthermore, the potential of the sedimentary organic carbon as a carbon source vs. the geogenic CO_2 for the indigenous microbial life will be assessed in this unique environment and mineral matrix investigations will deliver valuable information on the life habitat of the deep microbial ecosystem.

References:
Bräuer, K., Kämpf, H., Faber, E., Koch, U., Nitzsche, H.-M., Strauch, G., 2005. Seismically triggered microbial methane production relating to the Vogtland-NW Bohemia earthquake swarm period 2000, Central Europe. Geochemical Journal 39, 441-450.
Kämpf, H., Bräuer, K., Schumann, J., Hahne, K., Strauch, G., 2013. CO_2 discharge in an active, non-volcanic continental rift area (Czech Republic): Characterisation ($\delta^{13}C$, $^3He/^4He$) and quantification of diffuse and vent CO_2 emissions. Chemical Geology 339, 71-83.

ICDP

Quench of bubble bearing magma: The soufflé collapse

A. ALLABAR, P. BONS, M. NOWAK

Department of Geosciences, Eberhard Karls University Tuebingen, Germany

An important controlling factor of volcanic activity and eruption style is the dynamic degassing of H_2O and CO_2 during ascent of volatile bearing magma. Nucleation and growth of bubbles are recorded in the textures of vesiculated volcanic glasses. The degassing processes during magma ascent can be retraced by bubble number density, size distribution and porosity of these volcanic rocks. In natural subaquatic, subglacial and subaerial glassy volcanic rocks deformed ellipsoidal bubbles are observed. To date, this deformation occurring in low-viscosity basalts to high-viscosity rhyolites is interpreted as a result of collapse of porous magma due to bubble coalescence and open-system degassing or viscous flow during eruption.
Bubbles in experimentally decompressed and rapidly quenched phonolitic melts display similar deformation textures as observed in natural volcanic rocks and additionally some of the bubbles are dented. Flow textures observed in the bubbly glasses of Marxer et al. (2015) indicate bubble deformation at low temperature implying viscous flow. Marxer et al. (2015) suggest that bubble deformation is due to bubble shrinkage that is induced by the decreasing molar volume (V_m) of the exsolved H_2O fluid during quench from the run temperature (T_{melt}) to the glass transition temperature T_g. The corresponding pressure drop in the bubbles relative to the far field pressure P_q (P at which melts are isobarically quenched) is compensated by the reduction of bubble volume by a factor of ~2.5 accompanied by melt transport which stops at T_g.

In a first step, the shrinkage of H_2O bubbles in phonolitic melt quenched isobarically at a P_q of 100 MPa from a temperature of 1323 K to T_g was calculated using the EOS of H_2O (Duan and Zhang, 2006), assuming that during cooling P_q is maintained in the fluid bubble providing the equilibrium volume $V_{eq}(T)$ (Fig. 1). In the second step an explicit finite-difference model was developed to test the suggestions of Marxer et al. (2015). The calculation is based on the analytical solution for the shrinking/expansion of a spherical inclusion in an infinite viscous matrix (Nye, 1953). The change of V_m and viscosity η with temperature ($dV_{m,(volatile)}/dT$ and $d\eta/dT$) as well as the quench rate q (= dT/dt) and a P_q of 100 MPa are considered (Fig. 1). At a fast q of 150 $K \cdot s^{-1}$ T_g is 790 K corresponding to η of $1.3 \cdot 10^9$ Pa·s. However, the shrinkage of a spherical bubble stops at a fictive temperature T_f of 890 K ($\eta = 1.5 \cdot 10^7$ Pa·s). The decrease in bubble volume at T_f reaches 80 % of the V_{eq} reduction expected at T_g. At a moderate q of 1.5 Ks^{-1} the timescale for viscous flow to maintain a spherical bubble shape is increased because T_f and T_g are shifted to 776 K ($\eta = 3 \cdot 10^9$ Pa·s) and 711 K ($\eta = 1.4 \cdot 10^{11}$ Pa·s), respectively. The decrease in bubble volume at T_f reaches 92 % of the V_{eq} reduction expected at T_g.

Considering different cooling scenarios of different volcanic melt and volatile compositions, the numerical calculation has to be expanded. For tholeiite, rhyolite, phonolite and H_2O and CO_2 shrinkage of a spherical bubble at a slow q of 0.15 $K \cdot s^{-1}$ stops at η ranging from 10^7 (P_q = 1 bar) to 10^{10} Pa·s (P_q = 100 MPa) and the decrease in bubble volume at T_f reaches 45 to 90 % of the V_{eq} reduction expected at T_g, respectively. At high q of 150 $K \cdot s^{-1}$, the timescale for viscous flow to maintain spherical bubble shape is limited and bubbles stop to shrink at significantly lower η, ranging from 10^4 (P_q = 0.1 MPa) to 10^7 Pa·s (P_q = 100 MPa) and the decrease in bubble volume at T_f reaches 1 to 80 % of the V_{eq} reduction at T_g.
We suggest that further bubble volume reduction from T_f to T_g can be achieved at minimum viscous flow by bubble collapse from spheres to ellipsoids. Shortening of one sphere axis by 5-50 % is sufficient to achieve the V_{eq} at T_g (Fig.1). This is substantiated by ellipsoidal bubbles in vitrified experimental samples. Spherical bubble shrinkage and subsequent volume reduction by bubble deformation is suggested to occur during cooling of e.g. subglacial/subaquatic erupted rhyolites (e.g. on Iceland), popping rocks (partially degassed CO_2 rich submarine basalts) and subaerial phonolites. Bubble volume shrinkage factors during cooling from T_{melt} to T_g range from 1.5 – 5 depending on melt and volatile composition, P_q and q.

The calculated bubble shrinkage demonstrates that failed soufflé-like magma collapse works during closed-system degassing. The suggested model for bubble shrinkage down to T_g provides a tool to calculate the density of a magma based on the porosity of natural volcanic rocks. The porosity, density and the volatile content of the glass can be measured. P_q, T_{melt} and q have to be estimated. T_g is calculated using the model of Giordano et al. (2008) and Dingwell and Webb (1990) considering the quench rate and bulk composition of the melts. The shrinkage factor for the calculation of the magma porosity and density is determined by using T_{melt}, T_g, P_q and the EOS of Duan et al. (2006). Without correction of the porosity of volcanic rocks, the corresponding magma porosity,

buoyancy and ascent velocity are significantly underestimated. The density of CO_2 rich submarine basaltic melt is 9 % higher than the equivalent values of the quenched rock with a typical porosity of 20 %. The densities of subaerial phonolite and subglacial rhyolite with a porosity of 30 % are 23 % and 30 % smaller than the densities of the corresponding magmas, respectively.

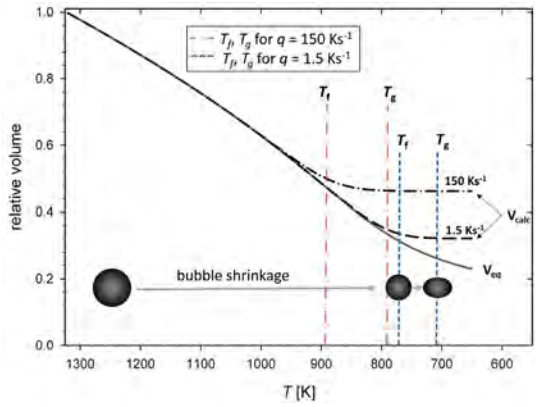

Fig. 1. Relative volume of a H_2O bubble in hydrous phonolitic melt (3 wt% H_2O) during isobaric cooling (P_q = 100 MPa; q = 150 and 1.5 K· s^{-1}) from a T_{melt} of 1323 K to T_q.

References:
Dingwell DB, Webb S (1990) Eur J Mineral 2: 427-449
Duan and Zhang (2006) GCA 70: 2311-2324
Giordano D, Russel JK, Dingwell DB (2008) EPSL 271: 123-134
Marxer H, Bellucci P, Nowak M (2015) J Volc Geotherm Res 297: 109-124
Nye JF (1953) Proc. R. Soc. London, A, Math. Phys. Sci. 219, 477-489

IODP

Origin and evolution of magmas in the course of subduction initiation, Izu-Bonin Mariana arc – new research project from the Leibniz University of Hannover

R. ALMEEV[1], S. LINSLER[1], F. HOLTZ[1], R. BOTCHARNIKOV[1], M. PORTNYAGIN[2]

[1]Institute of Mineralogy, Leibniz University of Hannover, Callinstr. 3, Hannover, 30167, Germany
[2]Helmholtz Centre for Ocean Research (GEOMAR), Division of the Ocean Floor, Wischhofstr. 1-3, Kiel, 24148, Germany

The process of subduction is considered as one of the major manifestations of a dynamic Earth. However, little is known about how subduction starts and proceeds. The so-called supra-subduction zones ophiolites are interpreted to be associated with subduction initiation and are potential rocks suited to understand geological processes occurring at the initiation of a subduction. Another unique example and key locality to study ongoing subduction initiation and arc evolution is the Izu-Bonin-Mariana (IBM) forearc system which demonstrates a similar lava chemostratigraphy as found in many ophiolites. According to one of the first conceptual model of Stern and Bloomer (1992), in the course of subduction initiation, the old and relatively dense oceanic lithosphere begins to sink into the asthenosphere. Lithosphere in the upper plate adjacent to the sinking lithosphere rapidly extends into the gap left as the dense lithosphere sinks. In this setting, mantle flows into the nascent mantle wedge and interacts with a small and variable contribution of fluids from the sinking plate. Melting induced by the fluid augments that resulting from decompression, leading to a higher degree of melting than at mid-ocean ridges. These MORB-like lavas with arc-signatures originating in this setting have been recently termed as *forearc basalts* (*FABs*, Reagan et al. 2010). Combination of rapid decompression melting with fluid enhanced lowering of the solidus leads to more extensive melting of the shallow asthenospheric wedge, creating refractory Mg-rich and Si-rich lavas such as *boninites* and high-Mg andesites and leaving an extremly refractory harzburgitic residue (Shervais, 2001). Thus, in the Stern-Bloomer model, the presence of boninites at the top of a FAB lava sequence is a major indicator of a subduction-initiation setting (Pearce, 2014). *The knowledge on the main changes in magma origin and magma evolution conditions at the transition from FAB to boninite is crucial to understand the general process of subduction initiation, the role of mantle reorganization and specifics of mantle melting regimes.*

In August-September 2014, IODP Expedition 352 (Expedition 352 Scientists, 2015) successfully cored 1.22 km of igneous basement and 0.46 km of overlying sediment, providing stratigraphically controlled suites of FABs and boninites. FABs were recovered at the two deeper water sites U1440 and U1441 and boninites at the two sites U1439 and U1442 drilled upslope to the west. The expected sequence of FABs presented at the base of the Bonin fore-arc volcanic succession followed by boninite-series lavas was not encountered at any of the drill sites. The presence of dikes at the base of the sections at Sites U1439 and U1440 provides new evidence that these lavas are underlained by their own conduit systems and that FAB and boninite group lavas are likely offset more horizontally than vertically. Preliminary on-board geochemical data (Expedition 352 Scientists, 2015) demonstrate that cored basalts from sites U1440 and U1441 are compositionally similar to FABs from Bonin and Mariana forearcs documented during diving expeditions (Reagan et al., 2010). FABs are typically aphyric to sparsely phyric, Plag-pyroxene-phyric basalts and dolerites. The differentiation trends (from basalt to andesite) indicate that all analyzed samples could derive from a similar parent magma composition. The small variations in CaO (and CaO/Al_2O_3) indicate differences in degrees of differentiation and/or pressures of partial crystallization. Overall, the compositions of FAB lavas erupted at Sites U1440 and U1441 are relatively evolved, with most MgO concentrations within the range 5–8 wt%. These lavas could have been fed from magma chambers that persisted throughout the eruptive history of FABs. Boninitic lavas from holes U1439C and U1442A are Ol- and Opx-phyric rocks with a groundmass of pale glass and acicular pyroxene. In contrast to FABs, lavas in both of the boninite sites have compositions that become more primitive (MgO-rich, Si-rich and Ti-poor) upward the holes. The extreme depletion of the mantle sources and/or high degrees of melting for boninitic lavas is reflected in the low TiO_2 concentrations (<0.3 wt%). The changes in composition support a model in which probably a system of persistent magma chambers was present early during genesis of boninite group lavas.

Our new research project (started in 2016) is aimed at understanding the evolution of petrological and geochemical characteristics of magmatic rocks at the

initiation of a subduction process and during early arc development. The working plan of the project includes:

- Systematic petrological and geochemical investigations including microprobe analysis of matrix glasses, glass inclusions and mineral compositions for all representative FAB and boninite magma types. The mineral and glass compositions will be used to apply geothermobarometers to constrain magma storage conditions.
- Determination of crystallization conditions using available thermodynamic models for FABs and high pressure experimental studies of boninites. The experimental work of boninites is necessary considering the lack of high-pressure volatile-bearing experiments in high Si and high Mg systems. Experiments will be conducted up to 700 MPa and may also be useful to interpret the formation of boninitic melts from a harzburgitic source.
- Geochemical analyses of chalcophile and redox-sensitive elements/ratios in glasses. The results will be used to understand the effects of fO_2, partial melting and mantle preconditioning (Pearce and Peate, 1995) on the composition and evolution of magmas during the initiation of subduction processes.

References:
Expedition 352 Scientists. (2015) Izu-Bonin-Mariana Fore Arc: Testing subduction initiation and ophiolite models by drilling the outer Izu-Bonin-Mariana fore arc. IODP Prel. Rept. 352.
Pearce, J.A. (2014) Immobile Element Fingerprinting of Ophiolites. ELEMENTS 10, 101-108.
Reagan, M.K., et al. (2010) Fore-arc basalts and subduction initiation in the Izu-Bonin-Mariana system. Geochemistry, Geophysics, Geosystems 11, Q03X12.
Shervais, J.W. (2001) Birth, death, and resurrection: The life cycle of suprasubduction zone ophiolites. Geochem. Geophys. Geosyst. 2.

IODP

Comparison of Heinrich Stadial 1 & 2 by the Analysis of sedimentary $^{231}Pa/^{230}Th$ from the North Atlantic

B. ANTZ[1], J. LIPPOLD[1,2], N. FRANK[1], H. SCHULZ[3]

[1]Institut für Umweltphysik, Universität Heidelberg, Deutschland
[2]Institut für Geologie, Universität Bern, Schweiz
[3]Fachbereich Geowissenschaften, Universität Tübingen

The Atlantic meridional overturning circulation (AMOC) plays a key role in the distribution of heat, moisture and carbon and affects the gobal climate system [Rahmstorf 2002]. Freshwater-Events of the past, in particular Heinrich-Event I and II [Heinrich 1988; Hemming 2004], are believed to cause a significant reduction of AMOC strength, or in an extrem case, even a total cessation of thermohaline circulation and thus crucial changes in heat and carbon transport to northern Hemisphere. Heinrich-Events are characterised by iceberg discharge of continental ice sheets and their abrupt melting in the open North Atlantic, followed by the supression of deep water formation in the North due to salinity decrease of northern surface water.

This study adresses the reconstruction of the AMOC around Heinrich Stadial I and II (ca. 17 resp. 24 ka BP) in comparison with the Holocene (Hol) and Last Glacial Maximum (LGM) applying the $^{231}Pa/^{230}Th$ ratio as a kinematic proxy measured from deep sea sediments. ^{231}Pa and ^{230}Th are produced in the ocean through radioactive decay of their temporally and spatially uniform distributed parent isotopes ^{235}U and ^{234}U at a constant rate (activity ratio = 0.093). Due to the shorter residence time of ^{230}Th compared to ^{231}Pa, the $^{231}Pa/^{230}Th$ ratio indicates the strength of AMOC in the past [Yu et al. 1996] [Gherardi et al. 2009; McManus et al. 2004; Lippold et al. 2012; Böhm et al. 2014; Bradtmiller et al. 2014]. Here we present new $^{231}Pa/^{230}Th$ measurements combined with published data for the above mentioned time ranges (Hol, LGM, HS1, HS2).

A basin wide feature is the general decrease of $^{231}Pa/^{230}Th$ with water depth as a result of preferential advective export of ^{231}Pa over ^{230}Th [Lippold 2011] witnessing an actice AMOC mode during the Holocene. However, this trend is inverted during Heinrich Stadial 1 and can be interpreted as a substantially weakened overturning of North Atlantic Deep Water (NADW) during HS1 along with a Antarctic Bottom Water seizing much more volume of the Atlantic Ocean than during the Holocene. Comparing the $^{231}Pa/^{230}$ Th from the same sediment core locations between HS1 and HS2 yields mostly higher values for HS1 than for HS2. This finding suggests that there was a measurable reduction of the AMOC strength during HS2 compared to the Holocene, but not as dramatic as during HS1.

References:
Böhm, E., J. Lippold, M. Gutjahr, M. Frank, P. Blaser, B. Antz, J. Fohlmeister, N. Frank, M. B. Andersen & M. Deininger, 2014. Strong and deep Atlantic meridional overturning circulation during the last glacial cycle. Nature 517, 73–76.
Bradtmiller, L. I., McManus, J. F., & Robinson, L. F., 2014. 231Pa/230Th evidence for a weakened but persistent Atlantic meridional overturning circulation during Heinrich Stadial 1. Nature communications, 5.
Gherardi, J.-M., L. Labeyrie, S. Nave, R. Francois, J. F. McManus, *and* E. Cortijo, 2009. Glacial-interglacial circulation changes inferred from 231Pa/230Th sedimentary record in the North Atlantic region, Paleoceanography, 24, PA2204.
Heinrich, H., 1988. Origin and Consequences of Cyclic Ice Rafting in the Northeast Atlantic Ocean during the Past 130,000 Years. Quaternary Research, 29, 142-152.
Hemming, S. R., 2004. Heinrich events: Massive late Pleistocene detritus layers of the North Atlantic and their global climate imprint, Rev. Geophys., 42, RG1005.
Lippold, J., Gherardi, J. M., & Luo, Y., 2011. Testing the 231Pa/230Th paleocirculation proxy: A data versus 2D model comparison. Geophysical Research Letters, 38(20).
Lippold, J., Y. Luo, R. Francois, S. Allen, J. Gherardi, S. Pichat, B. Hickey and H. Schulz, 2012. Strength and Geometry of the glacial Atlantic Meridional Overturning Circulation. Nature Geoscience, 10.1038/NGEO1608.
McManus, J. F., Francois, R., Gherardi, J. M., Keigwin, L. D., & Brown-Leger, S., 2004. Collapse and rapid resumption of Atlantic meridional circulation linked to deglacial climate changes. Nature, 428(6985), 834-837.
Rahmstorf, S., 2002. Ocean circulation and climate during the past 120,000 years. Nature 419, 207-214.

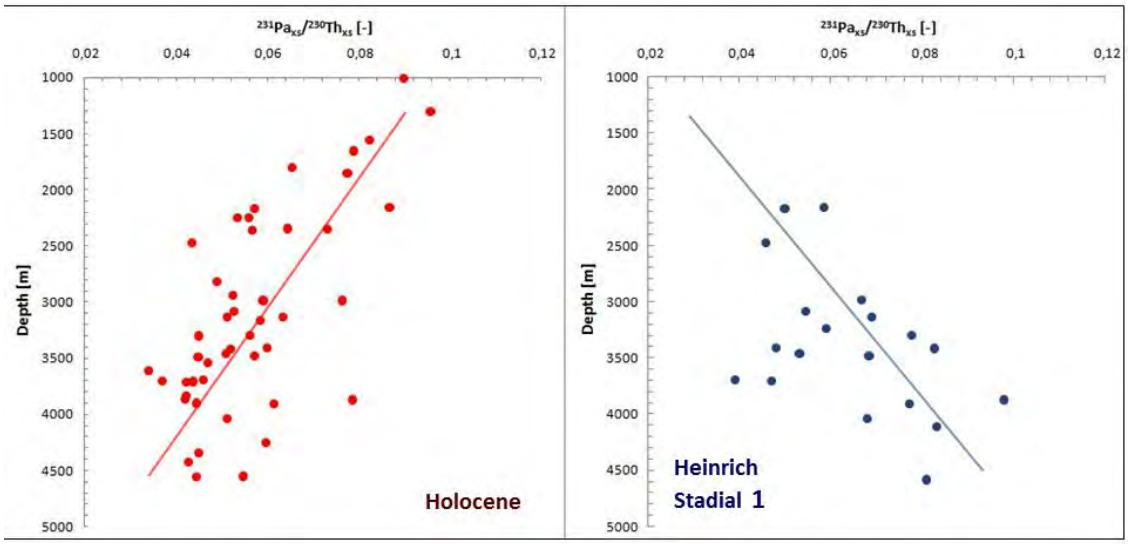

Abb.1: Available Pa/Th data of Holocene (0-9 kyr BP, red) and Heinrich Stadial 1 (HS1: 14,9-18 kyr BP, blue) for cores of the main North-Atlantic basin (Lat. between 5° and 50°). In comparison there are clear opposed trends with increasing depth for both time intervalls.

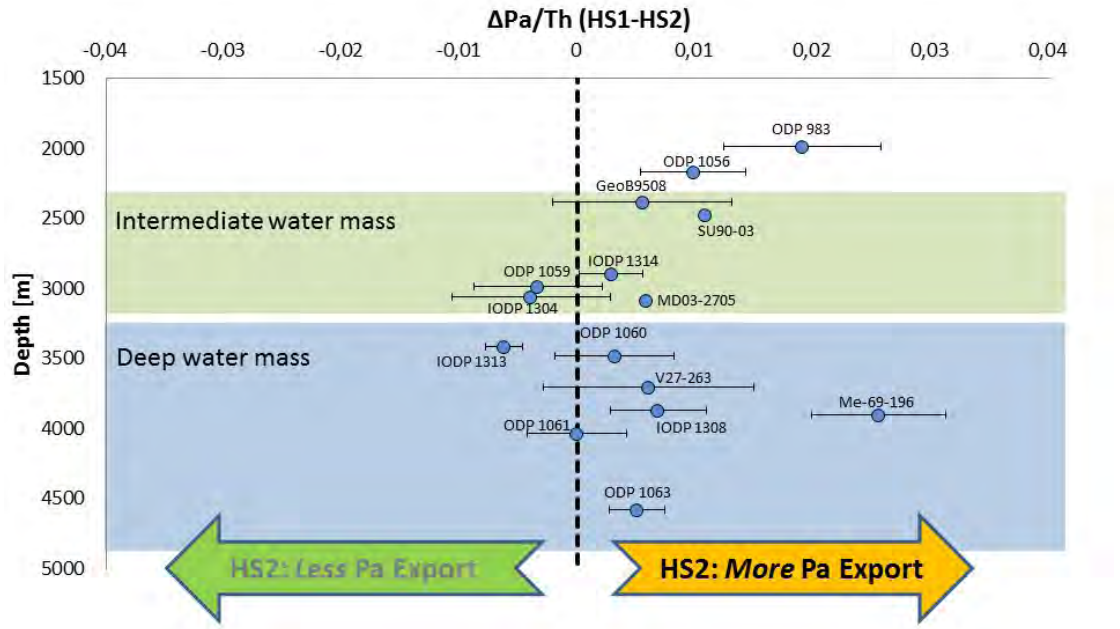

Abb.2: Difference between Pa/Th data of north atlantic cores during HS1 and HS2, if both are available. At almost all water depths there is more Pa Export during HS2, wich indicates a stronger circulation during this time period.

ICDP

Effects of two late Pleistocene volcanic ash deposits on the aquatic ecosystem of Lake Petén Itzá, Guatemala, inferred from geochemical and biological indicators

M. ASMUSSEN[1], S. COHUO[1], L. MACARIO-GONZALEZ[1], A. SCHWARZ[1], F. SYLVESTRE[2], C. PAILLES[2], L. PEREZ[3], S. KUTTEROLF[4], A. SCHWALB[1]

[1]Institut für Geosysteme und Bioindikation, Technische Universität Braunschweig, Germany
[2]CEREGE, Université Aix-Marseille, CNRS, IRD, Europôle méditerranéen de l'Arbois
[3]Instituto de Geología, Universidad Nacional Autónoma de México, Ciudad Universitaria, 04510 México, D.F. Mexico
[4]GEOMAR Helmholtz-Zentrum für Ozeanforschung, Kiel, Wischhofstr. 1-3, 24148 Kiel Germany

Volcanic ash depositions are important drivers of changes in water chemistry and biological assemblages, as shown for marine environments (Hardes et al., 2010; Schacht et al., 2008). There is little information, however, from lacustrine environments. Effects of distal tephras are even less known despite they represent important components of sedimentary sequences and are often used for geochronological analysis (Müller et al., 2010). In addition, most of the volcano-effect studies in the Neotropics focus on sediments from the Holocene because of the scarcity of older sequences. We therefore investigated the effects of two distally originated Pleistocene volcanic ash deposits on ostracode and diatom assemblages of Lake Petén Itzá: the L-Tephra (LFT, 191 ka BP) and the Los Chocoyos (LCY, ca. 85ka BP) tephra layer, deposited during the MIS 6 glacial and MIS 5 interglacial periods, respectively. Geochemical analysis included determination of water content, total organic matter, carbonate content of sediments by Loss on ignition (Heiri, 2001). Ages were calculated using the sedimentation rates from Ansemetti et al. (2007).

Species assemblages from approximately 3 cm (ca. 50 yrs) below to 7 cm (ca. 116 yrs) above the LFT were characterized by the absence of ostracodes and the dominance of the planktonic diatom *Aulacoseira ambigua*. Prior to the ash deposition, the content of organic matter showed an increasing trend (from 2 to 10 %) while carbonate content remained relatively low (ca. 9 %). After tephra deposition, the content in organic matter decreased, and the diatom assemblage composition changed from a dominance of planktonic to a dominance of benthic species. High organic matter content and a dominance of planktonic diatoms were reestablished after some decades, suggesting a relatively short-term effect of the ash input on the Lake Petén Itzá ecosystem during this glacial period.

Prior to the LCY ash fall (from 4 cm below LCY, representing ~ 67 yrs), the ostracode species assemblage was composed of littoral ostracodes Cytheridella ilosvayi, C. peten-ensis, Cypridopsis sp. and Paracythereis opesta. Diatom assemblage was dominated by benthic species E. minuta and D. kuetzengii. Organic matter (9 %) and carbonate contents (7 %) were relatively high. After the LCY ash fall (up to ~116 yrs), C. petenensis was the only ostracode species present, and the diatom assemblage composition switched from a dominance of benthic to a dominance of planktonic species. Organic matter and carbonate content increased. The return to before ash fall lake conditions occurred after several decades, suggesting again a relatively short-term effect of ashes during this interglacial period.

Our results suggest that the deposition of distal volcanic tephras in Lake Petén Itzá exerted strong effects on the geochemical and biological composition of sediments independent from the prevalent climate state.

References:

Hardes, R., Kutterolf, S., Hensen, C., Moerz, T, Bruckmann, W., 2010. Tephra layers: A controlling factor on submarine translational sliding? Geochemesistry, Geophysics,Geosystems, Vol. 11, Number 5, DOI: 10.1029/2009GC002844

Schacht, U., Wallmann, K., Kutterolf, S., Schmidt, M., 2008. Volcanogenic sediment-seawater interactions and the geochemistry of pore waters. Chemical Geology 249, 321-338.

Müller, A.D., Anselmetti, F. S.; Ariztegui, D., Brenner, M., Hodell, D.A., Curtis, J.H., Escobar, J., Gilli, A., Grzesik, D.A., Guilderson, T.P., Kutterolf, S.; Plötze, M., 2010. Late Quaternary paleoenvironment of northern Guatemala: evidence from deep drill cores and seismic stratigraphy of Lake Petén Itzá. Sedimentology 57, 1220-1245, DOI: 10.1111/j.1365-3091.2009.01144.x

Heiri, O., Lotter, A.F., Lemcke, G., 2001. Loss on ignition as a method for estimating organic and carbonate content in sediments: reproducibility and comparability of results. Journal of Paleolimnology 25, 101-110.

IODP

Enhanced Subtropical Gyre circulation feeding ice sheet growth during the Mid-Pleistocene Transition (700 – 1400 ka, Site U1385)

ANDRÉ BAHR[1], STEPHANIE KABOTH[2], DAVID HODELL[3]

[1]Institute of Earth Sciences, Im Neuenheimer Feld 234, 69120 Heidelberg, Germany
[2]Department of Earth Sciences, Faculty of Geosciences, Utrecht University. Heidelberglaan 2, 3584CS, Utrecht, The Netherlands
[3]Department of Earth Sciences, University of Cambridge, Downing Street, Cambridge, Cambridgeshire, CB2 3EQ, UK

During the mid-Pleistocene Transition (MPT), at around ~900 ka, a fundamental shift in the glacial/interglacial cyclicity from a "41 kyr world" into the present-day "100 kyr world" took place accompanied by a distinct growth of glacial ice shields[1]. The growth of ice volume goes along with more pronounced winter cooling in high altitudes, necessary to sustain large ice sheets[2]. In this project we investigate the influence of low and mid-latitude cirulation changes on the observed high-latitude cooling. For this purpose, we study surface and subsurface properties (temperature, salinity) on Site 1385 ("Shackleton Site"), drilled during IODP Exp. 339 at the Iberian Margin. Focus is the time interval of ca. 700 – 1400 kyr (MIS 18 – 44), which captures the major changes during the MPT. Site 1385 is located at the eastern margin of the North Atlantic Subtropical Gyre, an area characterized by the accumulation of warm and saline subsurface waters. These gyre waters are a major source for the salt and heat transported northward by the Gulf Stream and North Atlantic Current and therefore represent a pivotal component of the thermohaline circulation. The extend of the North Atlantic Subtropical Gyre, on the other hand, is directly affected by variations in ice shield expansion: enhanced glacial ice volume should lead to a southward shifts of wind fields accompanied by a strengthening of the surface wind stress due to an increased latitudinal temperature gradient. The direct coupling of ocean-atmosphere processes makes the North Atlantic Subtropical Gyre therefore very sensitive to climate changes. The

present study aims to shed light on the behavior of the North Atlantic Subtropical Gyre during the MPT, in particular regarding its response to ice volume change. For this purpose, combined $\delta^{13}C$, $\delta^{18}O$ and Mg/Ca records on the shallow dwelling foraminifer *Globigerinoides bulloides* and the deep dweller (i.e. ~200-300 m water depth) *Globorotalia inflata* were obtained. The combination of $\delta^{18}O$ and Mg/Ca-derived surface and subsurface temperatures (SST, and Tsub, respectively) allows for the calculation of the ice-volume corrected $\delta^{18}O_{seawater}$ ($\delta^{18}O_{ivc-sw}$) as an approximation of salinity.

SST and subT generally follows the glacial-interglacial pattern. However, we observe that the long-term trend of subT as well as of $\delta^{18}O_{ivf-sw}$ are opposed to that of successively more intensified glacials imprinted into the SST record. Notably, relatively weak glacials such as MIS 38 and 40 are accompanied by persistent and strong subsurface cooling, interpreted as a much reduced or absent influence of gyre waters. Subsequent glacials do not show this degree of subsurface cooling, with the exception of the prominent MIS 22. This unexpected and complex behaviour of the subtropical gyre circulation might be explained by a southward shift and strengthening of the Westerlies during glacials over the course of the MPT. Intensified surface winds cause a deepening of the thermocline at the Iberian Margin, which could on subsurface level at least partly compensate for the stronger surface cooling. An enhanced meridional SST contrast during the MPT also argues in favor of stronger zonal wind fields, in support of our interpretation. A strengthening and southward displacement of the mid-latitude wind fields would have far reaching consequences not only for the ocenanic circulation but alter the moisture distribution over the continent.

References:
Clark, P. U. et al. The middle Pleistocene transition: characteristics, mechanisms, and implications for long-term changes in atmospheric pCO2. Quaternary Science Reviews 25, 3150-3184 (2006).
McClymont, E. L., Sosdian, S. M., Rosell-Melé, A. & Rosenthal, Y. Pleistocene sea-surface temperature evolution: Early cooling, delayed glacial intensification, and implications for the mid-Pleistocene climate transition. Earth-Science Reviews 123, 173-193 (2013).

IODP

Latest Cretaceous-early Paleogene Atlantic deep ocean circulation and connectivity

S. J. BATENBURG[1,2], S. VOIGT[1], O. FRIEDRICH[3], A. OSBORNE[4], T. KLEIN[1], C. NEU[1], M. FRANK[4]

[1]Institut für Geowissenschaften, Goethe-Universität Frankfurt, Altenhöferallee 1, 60438, Frankfurt am Main, Germany
[2]Department of Earth Sciences, University of Oxford, South Parks Road, Oxford OX1 3AN, United Kingdom
[3]Institut für Geowissenschaften, Universität Heidelberg, Im Neuenheimer Feld 234-236, 69120 Heidelberg, Germany
[4]GEOMAR Helmholtz-Zentrum für Ozeanforschung Kiel, Wischhofstr. 1-3, 24148 Kiel, Germany

Different origins have been suggested for deep water masses in the Atlantic Ocean during the Late Cretaceous and early Paleogene. The distribution of deep water was largely controlled by tectonic processes, as the Atlantic Ocean was much narrower than at present day, and submarine highs of volcanic origin restricted the flow of waters at depth. To disentangle tectonic constraints on circulation from climate-driven changes, this study aims to assess the role of submarine barriers and to determine the timing of the establishment of a true deep-water connection between the North and South Atlantic.

Exchange of intermediate and deep waters is suggested to have commenced during distinct time intervals throughout the Late Cretaceous, based on parallel trends in deep water neodymium isotope compositions ($\varepsilon_{Nd}(t)$) obtained from localities across the Atlantic (Moiroud et al., 2015, and references therein). Alternatively, the deep domains of the Atlantic Ocean may have operated as sub-basins with limited connectivity well into the Paleocene, with common trends in $\varepsilon_{Nd}(t)$ stemming from mixing of surface waters.

Here we present neodymium isotope data of ferromanganese sediment coatings from a wide geographical and bathymetric range of ocean drill sites across the Atlantic Ocean for the latest Cretaceous and early Paleogene (Fig. 1). Comparison with existing data enables us to identify distinct deep and intermediate water masses and to follow their development through time. In particular, the new data from Site U1403, Newfoundland, Sites 525 and 1267, Walvis Ridge, Site 369, Canary Islands and Site 516, Rio Grande Rise, resolve the interval spanning and following the K/Pg boundary in detail. To assess whether the Nd isotope signature of bulk sediment coatings represents a genuine sea water signal, accompanying measurements of Nd isotopes are performed on different archives. Overall, the $\varepsilon_{Nd}(t)$ data from the North and South Atlantic display a similar decrease throughout the Maastrichtian and early Paleocene, although marked leads and lags are observed.

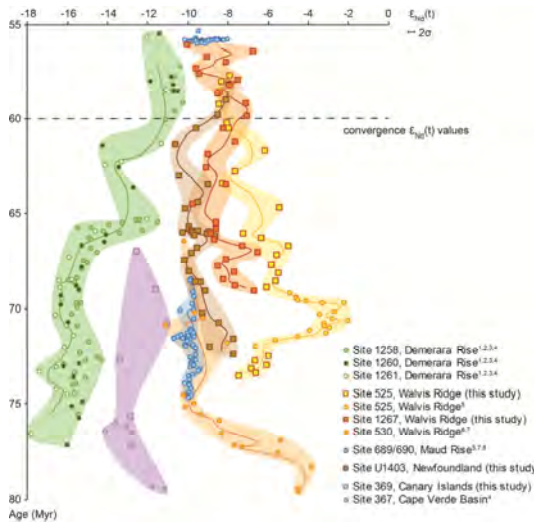

Figure 1. $\varepsilon_{Nd}(t)$ signatures of selected North and South Atlantic DSDP, ODP and IODP Sites. Coloured lines represent two point moving averages of the data series, for Demerara Rise, only the average for Site 1261 is diplayed. 1: MacLeod et al., 2008; 2: Jimenez-Berrocoso et al., 2010; 3: MacLeod et al., 2011; 4: Martin et al. 2012; 5: Voigt et al., 2013, 6: Robinson et al., 2010, 7: Murphy and Thomas, 2013, 8: Thomas et al., 2003.

Parallel trends in Nd isotope signatures throughout the North and South Atlantic have been interpreted to reflect the occurrence of a common deep water mass originating in either the southern high latitudes (Robinson et al, 2010; Robinson and Vance, 2012, Voigt et al., 2013, Murphy and

Thomas, 2013) or in the North Atlantic (MacLeod et al., 2008, 2011; Martin et al., 2012). The progressive opening of the Atlantic Ocean was accompanied by gradual subsidence of the oceanic crust and sills. Potentially, water masses may have by-passed ridge complexes, such as the Rio Grande Rise – Walvis Ridge, across fracture zones and other deep channels (Murphy and Tomas, 2014, Moiroud et al., 2015). The Nd isotope signatures of these deep water masses changed gradually long their flow path due to mixing with other water masses. Since the early Atlantic Ocean was limited in depth and width, the contact area with the margins was large with respect to ocean volume. Regional processes such as boundary exchange could have had a profound effect on water column chemistry. However, detrital $\varepsilon_{Nd}(t)$ values and sea water signatures remain clearly offset, suggesting that deep water Nd isotope values were not strongly influenced by exchange with local detrital material. Instead, the common trend towards less radiogenic values in the Campanian – Maastrichtian may have been caused by an overall decrease in volcanic activity and weathering of subaerially exposed volcanic terrains. In addition, the deeper domains of the Atlantic Ocean were separated into sub-basins, in which different mechanisms of deep-water formation may have operated at the same time. This may explain the disparity in observed Nd isotope signatures at the end of the Cretaceous.

The $\varepsilon_{Nd}(t)$ values of sediment coatings from North and South Atlantic drill sites converge around 60 Ma, suggesting that a common deep water mass filled the deepest reaches of the basin. The Nd isotope data of Sites U1403, 516, 1267 and 525 indicate the occurrence of a common deep-water neodymium isotope signature ($\varepsilon_{Nd}(t)$ -8) in the North and South Atlantic since 60 Ma. At this time, the sub-basins of the deep Atlantic became fully connected through subsidence of the Walvis Ridge - Rio Grande Rise barrier as well as broadening and deepening of the Central Atlantic Gateway. A deepwater mass with a common $\varepsilon_{Nd(t)}$ signature, likely originating in the high southern latitudes, prevailed over a broad range of water depths, indicating vigorous deep ocean circulation. The data suggest that between 62 and 60 Ma, the vertical stratification of the Atlantic Ocean decreased and a global mode of thermohaline circulation commenced.

References:

Jiménez-Berrocoso, Á., MacLeod, K. G., Martin, E. E., Bourbon, E., Londoño, C. I., & Basak, C. (2010). Nutrient trap for Late Cretaceous organic-rich black shales in the tropical North Atlantic. *Geology*, *38*(12), 1111-1114.

MacLeod, K. G., Londoño, C. I., Martin, E. E., Berrocoso, Á. J., & Basak, C. (2011). Changes in North Atlantic circulation at the end of the Cretaceous greenhouse interval. *Nature Geoscience*, *4*(11), 779-782.

MacLeod, K. G., Martin, E. E., & Blair, S. W. (2008). Nd isotopic excursion across Cretaceous ocean anoxic event 2 (Cenomanian-Turonian) in the tropical North Atlantic. *Geology*, *36*(10), 811-814.

Martin, E.E., Blair, S.W., Kamenov, G.D., Scher, H.D., Bourbon, E., Basak, C. and Newkirk, D.N., 2010. Extraction of Nd isotopes from bulk deep sea sediments for paleoceanographic studies on Cenozoic time scales. *Chemical Geology*, *269*(3), pp.414-431.

Martin, E. E., MacLeod, K. G., Jiménez Berrocoso, A., & Bourbon, E. (2012). Water mass circulation on Demerara Rise during the Late Cretaceous based on Nd isotopes. *Earth and Planetary Science Letters*, *327*, 111-120.

Moiroud, M., Pucéat, E., Donnadieu, Y., Bayon, G., Guiraud, M., Voigt, S., Deconinck, J.F. and Monna, F., 2015. Evolution of neodymium isotopic signature of seawater during the Late Cretaceous: Implications for intermediate and deep circulation. Gondwana Research.

Murphy, D.P. and Thomas, D.J., 2013. The evolution of Late Cretaceous deep-ocean circulation in the Atlantic basins: Neodymium isotope evidence from South Atlantic drill sites for tectonic controls. *Geochemistry, Geophysics, Geosystems*, *14*(12), pp.5323-5340.

IODP

Climate variability controls the formation of cyanobacterial blooms in the Baltic Sea

T. BAUERSACHS[1], N. LORBEER[1], L. SCHWARK[1,2]

[1]Christian-Albrechts-University, Institute of Geosciences, Department of Organic Geochemistry, Ludewig-Meyn-Straße 10, 24118 Kiel

[2]Curtin University, WA-OIGC, Department of Chemistry, G.P.O. Box U1987, 6845 Perth, Australia

During late summer, massive cyanobacterial blooms develop in the modern Baltic Sea. Their abundance has intensified significantly within the last 50 years with drastic consequences for the aquatic ecosystem as the massive export of cyanobacterial biomass from the photic zone has resulted in a severe spread of bottom water hypoxia (dissolved oxygen < 2 mg/L) that has increased in area about four times since the second half of the last century (Zillén et al., 2008). As a consequence, the Baltic Sea currently turns into one of the world's largest dead zones that experiences a dramatic loss of benthic faunal and floral communities, the reduction of fish populations and major alterations of biogeochemical cycles (Conley, 2012). Although there is common consensus that the anthropogenic loading of nutrients (in particular of phosphorus) has promoted the formation of N_2-fixing cyanobacterial blooms in the Baltic Sea in the recent past, there is evidence that such blooms may have occurred repeatedly in the Baltic Sea at least since the establishment of the current brackish phase (e.g. the Littorina Sea) about 7000 B.P. ago (Bianchi et al. 2000) and that the formation of cyanobacterial blooms may be triggered by parameters other than nutrient availability.

Sediment cores recovered during IODP Expedition 347: "Baltic Sea Paleoenvironment" represent valuable archives of paleoenvironmental and climate change, which allow reconstructing the history of the Baltic Sea and investigating the role of climate change on the formation of cyanobacterial blooms in a previously unpreceprecended manner. At the Landsort Deep (IODP Site M0063), a ca. 90 m-thick sedimentary sequence consisting of varved to homogeneous glacial clays and organic-rich Holocene muds were collected that span a continous and undisturbed record of paleoenvironmental change from the present-day to the last deglaciation. Total organic carbon values were generally low in the glacial clays (<0.5%) but at a depth of ca. 28 m (representing the transition from the Ancylus Lake to the Littorina Sea) significantly increased to average values of ca. 2-10%. Sediments deposited during the Modern Warm Phase (MWP), the Medieval Climate Anomaly (MCA) and the Holocene Climate Optimum (HCO) are well laminated and evidence a deposition under stratified and oxygen-depleted conditions. Interestingly, these time intervals are characterized by high concentrations of biological markers (so-called heterocyst glycolipids) that are indicative for N_2-fixing heterocystous cyanobacteria (Bauersachs et al. 2009) and by simultaneously high TEX^{L}_{86}-reconstructed sea surface temperatures (SST) that on average exceeded 16 °C. In combination, our data suggests that climate-induced variations of SST largely controlled the formation and extent of cyanobacterial blooms in the Baltic Sea and that once cyanobacterial blooms are established they induces a self-sustaining feedback loop that facilitates and

accelerates the spread of bottom water hypoxia in the Baltic Sea. Our data also suggest that cyanobacterial blooms were more prevelant during the MCA and HCO compared to the MWP and suggest that cyanobacterial blooms may intensify under a scenario of future climate warming.

References:
Bauersachs, T., Compaoré, J., Hopmans, E.C., Stal, L.J., Schouten, S., Sinninghe Damsté, J.S. (2009). Distribution of heterocyst glycolipids in cyanobacteria. Phytochemistry 70: 2034-2039.
Bianchi, T.S., Engelhaupt, E., Westman, P., Andrén, T., Rolff, C., Elmgren, R. (2000). Cyanobacterial blooms in the Baltic Sea: Natural or human-induced? Limnology and Oceanography 45: 716-726.
Conley, D.J. (2012). Save the Baltic Sea. Nature 486: 463-464.
Zillén, L., Conley, D.J., Andrén, T., Andrén, E., Björck, S. (2008). Past occurrence of hypoxia in the Baltic Sea and the role of climate variability, environmetal change and human impact. Earth-Science Reviews 91: 77-92.

IODP

Refinement of the Bengal Fan stratigraphy along IODP Expedition 354 drilling transect facilitated by the reprocessing of GI-gun data and integration of high resolution watergun data

F. BERGMANN[1], V. SPIEß[1], T. SCHWENK[1,] C. FRANCE-LANORD[2], A. KLAUS[3] AND IODP 354 SCIENTIFIC PARTY

[1] Department of Geosciences, University of Bremen, Klagenfurter Strasse, D-28359 Bremen, Germany
[2] Centre de Recherches Pétrographiques et Géochimiques, CNRS Université de Lorraine, BP 20, 54501 Vandoeuvre les Nancy, France
3 Texas A & M University College Station, USA

The Bengal Fan, located in the northern Indian Ocean, is the largest submarine fan on Earth. Fan evolution started in the Early Eocene as a direct response to the collision of India with the Asian continent in Middle Paleocene times (Curray et al., 2003). Subsequently the Himalayan plateau uplift was initiated. Thereby generated interactions with the regional climate caused the evolution of the Indian monsoonal system. Drained by the Rivers Ganges and Brahmaputra, ~ 80% of eroded Himalayan sediments are deposited in the Bengal Fan. Hence, the fan provides the most complete record of the Himalayan history and is well suited to investigate the direct link between the tectonic uplift and the climate evolution of the region.

Sediments are transported onto the deep sea fan by turbidity currents constructing channel-levee systems. These channel-levee systems are the main architectural elements of the Bengal Fan and are suspected to have their onset in Late Miocene times (Schwenk and Spieß 2009). Frequent channel avulsions on the upper fan result in the abandonment of old channels and formation of new channel-levee systems or even in channel-reoccupation. This complex erosional/depositional system involves lateral depocenter migration, probably on millennial timescales. Consequently, investigations of the Himalaya as sediment source begins with a comprehensive understanding of transport, deposition and modification within the Bengal Fan sediment sink.

In February/March 2015 the IODP Expedition 354 'Neogene and late Paleogene record of Himalayan orogeny and climate: a transect across the Middle Bengal Fan' drilled at 7 sites along a ~320 km long E-W transect at 8° N. Aiming at the recovery of pre-fan deposits and deposits of the Pliocene and Upper Miocene Fan evolution, three of these sites reached down to 900 – 1200 mbsf. All seven sites provided high recovery from the shallow section (200-300 mbsf) for a detailed study of the fan deposits of the last 1-2 million years, including the latest known channel activities (Holocene times). Numerous channel-levee systems and inter-channel deposits were drilled, representing fan activity from stacked sequences as well as absence of fan deposition by hemipelagic sedimentation. New stratigraphic markers were identified and will help to refine the so far existing stratigraphy and age model. A thorough correlation of these time markers between the 7 IODP sites requires a careful and high-resolution imaging and seismic reinterpretation.

One major aim of the DFG-funded project "The Bengal Fan stratigraphy as a function of tectonic and climate – Correlation of IODP Expedition 354 results and available seismic data from the Bay of Bengal" is the refinement of the Bengal Fan stratigraphy with respect to its tectonic and climate history. Furthermore, channel-levee system architecture, stacking pattern and life times are investigated to improve the understanding of the complex Bengal Fan depositional system. The project is realized based on IODP Exp. 354 results and a large seismic dataset acquired during extensive (pre-site) seismic and hydroacoustic surveying (cruises SO93 (1994), SO125/126 (1997), SO188 (2006), carried out in cooperation between the University of Bremen and the BGR, Hannover). The acquired dataset contains multichannel seismic (MCS), PARASOUND echosounder as well as swath bathymetry data. MCS data were recorded using simultaneously different seismic sources, namely, two different sized GI-airguns and a small volume watergun. Due to their different operational frequencies, differing subbottom penetration/resolution ratios are achieved. This allows a detailed seismo-stratigraphic analysis with a high vertical resolution of the upper few hundred meters with one dataset as well as with deeper penetration for an optimal imaging of relevant deeper structures with the second dataset.

Although most of the pre-site survey data were already processed for the purpose of site selection between 1997 and 2006, major improvement could be expected by thorough (re)processing using new processing techniques and software developments. First processing results show significantly enhanced S/N ratio, resolution and reflector coherency. This enables the tracing of stratigraphic markers more precisely and over long distances. Additional improvement could be obtained in the imaging of deeper lying reflections and faults. In addition to the GI-gun data, processing of the watergun data was conducted for the first time. This high vertical resolution data will complement the existing database to carry out a more detailed study of the upper few hundred meters of Bengal Fan deposits. First examinations of the watergun data proved them to be beneficial for the crucial borehole – seismic correlation and the imaging of the channel-levee architecture.

For the understanding of the Bengal Fan architecture several advantages were achieved by the recently improved seismic dataset. A study of the latest active channel-levee system, based on watergun as well as borehole data, will allow the development of a comprehensive understanding of channel-levee depositional conditions and timeline of events, as radiocarbon dating will eventually become

available. This in turn may be used to create a general model of channel-levee growth and stacking pattern for the Bengal Fan. Combined with stratigraphic markers, the seismic subbottom information will finally be used to establish a detailed, refined Bengal Fan stratigraphy and to extend it throughout the rest of the study area between the drill sites, allowing to budget sedimentary bodies and fluxes.

References:
Curray, J.R., Emmel, F.J., and Moore, D.G., 2003. The Bengal Fan: morphology, geometry, stratigraphy, history and processes. Marine and Petroleum Geology, 19(10):1191–1223.
France-Lanord, C., Spiess, V., Klaus, A., and the Expedition 354 Scientists, 2015. Bengal Fan: Neogene and late Paleogene record of Himalayan orogeny and climate: a transect across the Middle Bengal Fan. International Ocean Discovery Program Preliminary Report, 354.
Schwenk, T. & Spieß, V., 2009. Architecture and stratigraphy of the Bengal Fan as response to tectonic and climate revealed from high resolution seismic data. In Kneller, B., Martinsen, O.J., and McCaffrey, B., eds., External Controls on Deep-Water Depositional Systems: SEPM Special Publication 92, p. 107–131.

IODP

Mapping the distribution of seawater-derived Nd isotopes across the Atlantic Ocean during the last 30 ka for the reconstruction of water circulation changes

PATRICK BLASER[1]*, JÖRG LIPPOLD[2], MARCUS GUTJAHR[3], NORBERT FRANK[1,4], JASMIN LINK[1,4], MARTIN FRANK[3]

[1]Institute of Environmental Physics, Heidelberg University, 69120 Heidelberg, Germany.
[2]Institute of Geological Sciences and Oeschger Centre for Climate Change Research, University of Bern, 3012 Bern, Switzerland.
[3]GEOMAR Helmholtz Centre for Ocean Research Kiel, 24148 Kiel, Germany.
[4]Institute of Earth Sciences, Heidelberg University, 69120 Heidelberg, Germany.

The ocean circulation is one of the key players in the climate system and the strength of the Atlantic Meridional Overturning Circulation (AMOC) closely correlates to major climatic shifts in Earth's younger past. Reconstructing the AMOC of the past in detail is thus crucial in order to get insight into its interaction with the whole climate system. Depending on the age of the surrounding continents, oceanic water masses adopt a certain radiogenic neodymium isotope composition ($^{143}Nd/^{144}Nd$, expressed as ε_{Nd}), which can be used as a quasi conservative tracer. Nd is adsorbed to deep sea sediments directly from bottom waters and archived in the hydrogenetic sediment fraction [1]. This renders Nd isotopes an ideal proxy for past deep-water provenance. There are several different archives available for the extraction of seawater derived Nd from pelagic sediments. The most important ones are fish debris, corals, foraminifera tests and hydrogenetic ferromanganese accretions, both in the form of nodules and crusts, as well as dispersed in the sediment as cements. However, the extraction of a purely bottom-water derived Nd isotope signature is not trivial, since other fractions containing Nd, like volcanogenic or terrigenic material, can contaminate the sample. Hydrogenetic ferromanganese oxyhydroxides present the ideal archive for authigenic Nd, for they are present in practically all sedimentary environments, take up trace elements in high concentrations, can be used in high temporal resolution and leached off the bulk sediment very efficiently. Several attempts have been made to use weak acids and reducing chemicals in order to selectively leach these accretions off the bulk sediment without releasing non-hydrogenetic Nd. While some of these studies were successful, most could not provide a procedure applicable to all sedimentary environments. Especially sediments containing volcanogenic material (e.g. from Iceland or the Azores [2]) have been shown to be challenging, because these volcanogenic particles are easily leached with commonly used acids and thus contaminate the extracted solution [3]. The most common alternative, namely obtaining seawater ε_{Nd} from authigenic accretions bound to foraminiferal tests has lately become the preferred since most reliable method [4].

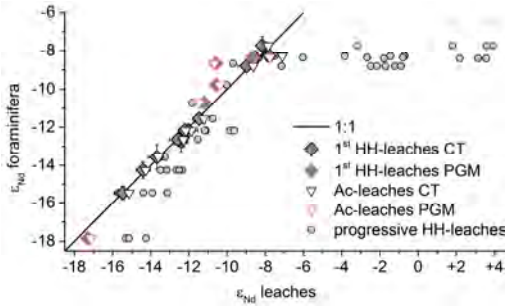

Fig.1: Comparison of Nd isotope signnatures of sediment leaches with those extracted from foraminifera. Radiogenic contamination can be observed under progressive leaching, whereas both Ac and HH-leaches match the signatures of foraminifera at the start of the leaching series. Ac-leaches: buffered acetic acid. HH-leaches: buffered acetic acid combined with reductive reagent and EDTA. CT: core top sediments. PGM: penultimate glacial maximum aged sediments. Error bars mark 2 standard deviations.

In this project, in order to investigate the applicability and reliability of the leaching method, a suite of sediment samples were successively leached with two commonly applied acidic solutions [5]. The leachates were analysed on their elemental and Nd isotope compositions, as well as rare earth element (REE) distributions. By graduating the total leaching procedure into smaller stages the results display which processes take place in the course of sediment leaching in the laboratory. We find that carbonate in the sediment dominates the course of the chemical reactions due to its high reactivity, and seawater Nd isotope signatures are extracted at the beginnning of the weak acid-reductive leaching series. The partial dissolution of volcanogenic detritus during further leaching leads to a strong positive excursion in ε_{Nd} in sediments from the vicinity of Iceland. Furthermore, we show that the Al/Nd ratio, in contrast to other proxies like REE patterns, correlates closely with lithogenic contamination in the leachate, so that this parameter can be used as a verification of the extracted Nd isotope signature. We thus developed an improved and simplified method for the reliable and verifiable extraction of deep water Nd isotope signatures archived in sedimental ferromanganese oxyhydroxides.

We then apply this method to a variety of sites of the Atlantic Ocean in order to reconstruct the deep water mass provenance in high temporal resolution during the last 30 millenia. We focus on reconstructions in the North Atlantic because changes are supposed to be most prominent in this region and to better constrain the

formation and composition of North Atlantic Deep Water (NADW) in the past. We present preliminary together with literature data and assess the differences in the Nd isotope curves across the Atlantic. A gradual shift towards unradiogenic signatures during the deglaciation with different magnitudes dominates the overall trend, indicating a stronger NADW formation in the Holocene. Records in the northern North Atlantic exhibit higher variability on short time scales as well as larger glacial-interglacial shifts. Deposition of ice rafted detrital carbonate off the canadian shelf during glacial times and in the North Atlantic IRD belt during Heinrich Events, however, leads to contamination of the leachate and possibly a relabelling of deep water masses by the introduction of a source of unradiogenic Nd. Further ongoing investigations will close geographic gaps and assess Nd isotope changes in the northeastern Atlantic basin.

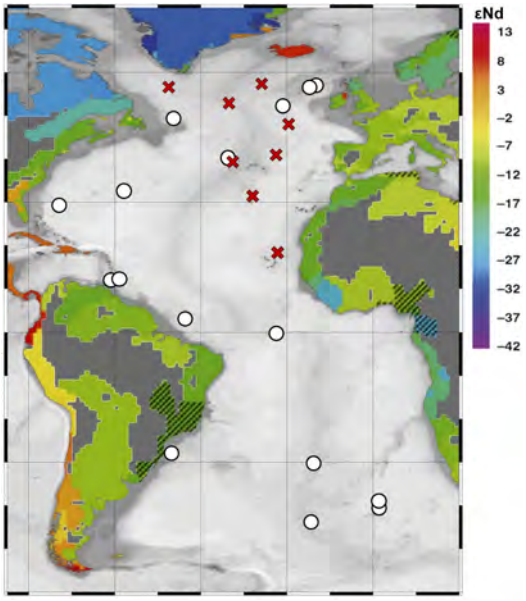

Fig.2:
Map of sites with existing Nd isotope records in the range of 0- 30 thousand years (white circles) and sites with records under work in progress (red crosses). Color core indicates the Nd isotope signature($\varepsilon_{Nd)}$ of the continental crust (6].

References:
[1] Crocket, K., Vance, D., & Gutjahr, M. (2011). Persistent Nordic deep-water overflow to the glacial North Atlantic. Gelology, 39(6), 515–518.
[2] Elmore, A., & Piotrowski, A. (2011). Testing the extraction of past seawater Nd isotopic composition from North Atlantic deep sea sediments and foraminifera. Geochemistry, Geophysics, Geosystems, 12(9), 12.
[3] Wilson, D., Piotrowski, A., Galy, A., & Clegg, J. (2013). Reactivity of neodymium carriers in deep sea sediments: implications for boundary exchange and paleoceanography. Geochimica et Cosmochimica Acta, 109, 197–221.
[4] Tachikawa, K., Piotrowski, A. M., & Bayon, G. (2014). Neodymium associated with foraminiferal carbonate as a recorder of seawater isotopic signatures. Quaternary Science Reviews, 88, 1–13.
[5] Gutjahr, M., Frank, M., & Stirling, C. (2007). Reliable extraction of a deepwater trace metal isotope signal from Fe–Mn oxyhydroxide coatings of marine sediments. Chemical Geology, 242(3-4), 351–370.
[6] Jeandel, C., Arsouze, T., Lacan, F., Téchiné, P., Dutay, J.-C. (2007). Isotopic Nd compositions and concentrations of the lithogenic inputs into the ocean: A compilation, with an emphasis on the margins. Chemical Geology, 239, 156-164.

IODP

The Hydrogen and Oxygen Isotope Geochemistry of Interstitial Fluids from IODP Leg 347: A study of Hydrographic Changes in the Baltic Sea since the Late Pleistocene

BÖTTCHER, M.E. [1], LIU, B. [1], SCHMIEDINGER, I. [1] & SLOMP, C. [2]

[1] Geochemistry & Isotope BioGeoChemistry, Leibniz Institut for Baltic Sea Research (IOW), Warnemuende, Germany.
[2] Marine Biogeochemistry, University of Utrecht, The Netherlands

The stable hydrogen and oxygen isotope ($^2H/^1H$, $^{18}O/^{16}O$) composition of interstitial waters extracted from long sediment cores retrieved during IODP Leg 347 in the Baltic Sea was analysed to constrain the main hydrographic changes of the Baltic Sea from the late Pleistocene to modern time. Prior to its reconnection with the North Sea (through the Skagerrak-Kattegat connection), the Baltic Sea had evolved into a lake, with a brief interruption during the Yoldia stage. Upon reconnection with the open ocean, hydrologic and bottom water compositional changes in the Baltic Sea were dramatic. Current pore water profiles reflect these changes, further impacted by internal transport processes like diffusion and advection. Investgations were carried out at Sites M0059 (Little Belt), M0060 (Kattegat), M0065 (Bornholm Basin), and M0063 (Landsort Deep). Associated with a steep vertical decrease in salinity a strong enrichment of the lighter stable isotopes in water is observed (e.g., Fig.1). The resulting shape of the pore water gradients differ substantially due to different modern and paleo bottom water and sedimentation rates conditions.

In order to reconstruct the temporal evolution of the Baltic Sea hydrograhy since the late Pleistocene, it is planed in a newly proposed project to use an advection-diffusion model considering different scenarios for sedimentation and bottom water changes.

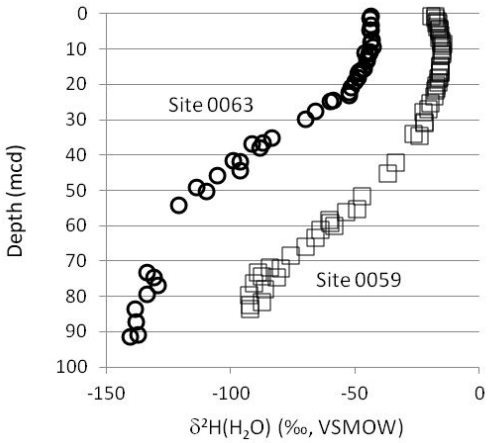

Fig1: H isotope signals at two Leg 347 sites

IODP

Evolution of the indian summer monsoon and terrestrial vegetation in the Northern Bengal region during the mid-Pleistocene transition (INTERMILAN)

I. BOUIMETARHAN

MARUM-Centre for Marine Environmental Sciences. Leobener Str. University of Bremen, Bremen. Germany

The Indian summer monsoon (ISM) is one of the Earth's most dynamic interactions between land, ocean and atmosphere. The aim of the proposed project is to get insights into the past behavior of the ISM system at orbital to suborbital timescales through high resolution records of vegetation change over northeast India and the hydrological history of this region during the last 1.2 million years using samples recovered in the Bay of Bengal during IODP Expedition 353. During this time period, the mid-Pleistocene glacials and interglacials differed from that observed during the late Pleistocene. Between 0.9 and 0.6 Myrs, interglacials were characterized by warm dry conditions and glacials were cool and humid, while during the last 0.2 Myrs, the opposite trend is observed. To get insights into thoses differences, the proposal will focus particularly on two main time windows : 1) the mid-Pleistocene transition (MPT), a very important climatic interval that led to the development of the late Pleistocene ice ages around ~900 kyr BP and 2) the last interglacial/glacial cycle (120 kyrs BP), that consists of well-pronounced late Pleistocene fluctuations involving major re-organizations in the atmiosphere, oceans and biosphere.We assume that, during both time intervals, changes in atmospheric moisture content driven by tropical sea-surface temperatures and the strength of the Indian summer monsoon controlled precipitations and hence large-scale vegetation changes. Fluctuations in the monsoon precipitation regime induced aslo variations in the river discharge that transports large amounts of terrestrial material into the Indian Ocean. To track those changes in marine sediments, I will use marine palynology analysing two independent proxies: 1) terrestrial palynomorphs (pollen and spores) to assess vegetation changes on the adjacent continent and operating trasnport agents and 2) organic-walled dinoflagellate cysts (dinocysts) to investigate quantitatively (transfer functions) and qualitatively (assemblages) past sea-surface conditions mainly salinity, primary productivity, temperature and stratification. The planned palynological study will enable the recognition of simultaneous changes in both oceanic and continental mechanisms allowing for a detailed land-ocean correlation that would offer an important complement to the almost exclusively paleoceanographic (foraminifera and isotopes) multi-proxy studies investigated by expedition scientists of the IODP Indian Monsoon Expedition 353. Despite the fact that marine palynology provide a powerful tool to reconstruct past ISM evolution and its impact on different ecosystems, good datasets of pollen/spores and organic dinocysts assemblages are (as goos as) non-existant for the core convective region of the Indo-Asian monsoon system during this time period. To test if material and methods are appropriate for the proposed project, a palynological pilot study has been carried out in a coarse temporal resolution. It shows significant changes of the terrestrial content in the marine sediments with high concentrations of pollen, spores and organic dinocysts between 1.2 and 0.8 Myrs. The pollen to dinocysts ratios show a greater terrestrial input in the studied site reflecting stronger terrigenous discharge. Throughout the sequence, pollen record shows the dominance of three distinct vegetation types: grassland plants such as Poaceae and Cyperaceae, coastal plant communities such as mangrove (mainly represented by Rhizophora) and Chenopodiaceae/Amaranthaceae, and humid deciduous tropical forest such as Alchornea and Celtis. Mountainous vegetation represented by Podocarpus is also found especially between 1.2 and 0.8 Myrs. The dinocyst assemblages are dominated by cysts produced by heterotrophic dinoflagellates, mainly Brigantedinium spp. This group is present through the entire studied sequence but decrease after 0.8 Myrs in favor of the photoautotrophic dinoflagellates Lingulodinium machaerophorum and other cysts from the Gonyaulacales, mainly Spiniferites species generally found in close vicinity to river mouths where low salinity, high nutrient concentrations in upper waters and considerably stratified surface water conditions prevail. The results of the pilot study justify the expectation that a palynological study is appropriate to investigate variations in the ISM magnitude and frequency and the land-ocean-atmosphere interaction through changes in vegetation and associated hydrologic fluctuations.

IODP

Quantification of Deep Subseafloor Bacteria and Archaea - An Inter-Laboratory Comparison

JOY BUONGIORNO[1], GORDON WEBSTER[2], ANDREW WEIGHTMAN[2], ALEXANDER SCHUMAKER[3], STEPHANIE TURNER[4], AXEL SCHIPPERS[4*], TAYLOR ROY[1], KAREN LLOYD[1]

[1] Department of Microbiology, University of Tennessee, Knoxville, TN, USA
[2]Cardiff School of Biosciences, Cardiff University, Cardiff, UK
[3]Nelson Biology Laboratories, Rutgers University, Piscataway, NJ, USA
[4]Geomicrobiology, Federal Institute for Geosciences and Natural Resources, Hannover, Germany

The marine subsurface biosphere is populated by abundant, diverse, and geographically distinct microorganisms. The two most common methods used for quantifying particular microbial taxa within subseafloor sediments is quantitative PCR (qPCR) and catalyzed reporter deposition fluorescence *in situ* hybridization (CARD-FISH). In this study, qPCR and CARD-FISH were performed on Baltic Sea Basin (IODP Exp. 347) sediment samples down to 85 meters below the seafloor within independent laboratories in three different institutions. Working with similar protocols, we demonstrated reproducibility of qPCR and CARD-FISH quantification data across the laboratories, with total cell counts ranging from $1.39x10^7$ to $1.87x10^9$ cells/mL. The highest yields of qPCR were obtained with the use of an additional sediment slurry preparation step, resulting in $3.88x10^6$ to $2.34x10^9$ copies/cm^3 combined bacterial and archaeal 16s rRNA gene copy numbers. Overall, the qPCR quantification results consistently showed that bacteria are more abundant than archaea in these sub-seafloor sediments, with both

domains above the quantification limit 88% of the time on average across laboratories. Results of qPCR quantification demonstrate no significant difference (p-value > 0.05) in qPCR values when using the same bacterial and archaeal primers to amplify DNA extracted with similar protocols. Although total cell counts from direct counting were all above the quantification limit of $1.3x10^7$ cells/mL (after accounting for the dilution to physically separate cells from sediment), only 45/435 counts (10%) with CARD-FISH were above this quantification limit. Proteinase K permeabilization of archaeal cell walls was not sufficient to bring these samples above the quantification limit. In addition, this study showed that quantification of particular microbial taxa gives inconsistent results when comparing CARD-FISH and qPCR, and that further improvement of methods is required.

Ref: Submitted to Frontiers in Microbiology

IODP

Birth and early life of the Izu-Bonin-Mariana island arc

P.A. BRANDL[1,2], M. HAMADA[3], R.J. ARCULUS[1], C.J. LE LOSQ[1]

[1] Research School of Earth Sciences, The Australian National University, 142 Mills Road, Acton ACT 2601, Australia
[2] GeoZentrum Nordbayern, FAU Erlangen-Nürnberg, Schloßgarten 5, 91054 Erlangen, Germany
[3] Department of Solid Earth Geochemistry, Japan Agency for Marine-Earth Science and Technology (JAMSTEC), 2-15 Natsushima-cho, Yokosuka 237-0061, Japan

In mid-2014, IODP Expedition 351 Izu-Bonin-Mariana (IBM) Arc Origins successfully drilled the geological record of subduction initiation and island arc inception at Site U1438 in the Amami Sankaku Basin, in the northwest Philippine Sea. Whereas the young oceanic igneous basement formed during subduction initiation some 52 Ma ago, the overlying volcaniclastic sediments record the magmatic evolution of the juvenile Kyushu-Palau-Ridge, a remnant part of the presently active Izu-Bonin-Mariana island arc. Fresh magmatic crystals (mainly clinopyroxenes) recovered from this sequence contain numerous pristine glass inclusions that provide important insights into the composition of primitive melts, magmatic differentiation and evolution of island arcs.

Here we present the major element analyses of 340 glass inclusions along with volatile (Cl, S, H_2O) and trace element data of a representative subset of samples. Even though hosted in clinopyroxenes, we can show that the vast majority of these glass inclusions are pristine and our record is thus unique in terms of a consistent suite of samples. U1438 glass inclusions cover the full compositional range from high-Mg (basaltic) andesite and basalt to rhyolite with different suites belonging to either the low-K and high-Fe or medium-K and low-Fe rock series. More interestingly, these chemical differences are not random but systematic with the volcaniclastics shed shortly after arc inception hosting glass inclusions more similar to high-Mg andesites, whereas melts erupted at a later stage of IBM arc evolution are overall more evolved (lower MgO) but also interestingly tend to a tholeiitic composition.

Trace and volatile elements give further insights into the magmatic processes behind these compositional changes and argue for variable contributions from the slab either by fluids or sediments and the mantle wedge itself. Further work is in progress to set qualitative and quantitative constraints on the different components contributing to the parental melt.

IODP

Microstructures and fluid inclusion petrography and microthermometry of hydrothermal veins of Site U1414, IODP Expedition 344 (CRISP 2)

JENNIFER BRANDSTÄTTER[1], WALTER KURZ[1], KURT KRENN[1], PETER MICHEUZ[1]

[1]Institut für Erdwissenschaften, Universität Graz, Heinrichstraße 26, 8010 Graz, (jennifer.brandstaetter@uni-graz.at)

We present new data from microthermometry of fluid inclusions entrapped in hydrothermal veins within the Cocos Ridge basalt and the overlying lithified sediments of Unit III from the IODP Expedition 344 Site U1414. This concerns a primary task of IODP Expedition 344 to evaluate fluid/rock interaction linked with the tectonic evolution of the incoming Cocos Plate from the Early Miocene up to recent times. Aqueous, low saline fluids are concentrated within the veins from both the Cocos Ridge basalt and the overlying lithified sediments. Fluid inclusion analyses show evidence for communication with deeper sourced, high-temperature hydrothermal fluids within the Cocos Plate magmatic basement. Hence, the source of the aqueous low saline fluids may be related to an early carbonic/aqueous fluid where the mobile aqueous phase acted as pore water mixed with invaded seawater. Isochores from primary, modified and secondary fluid inclusions crossed with litho-/hydrostatic pressures indicate an anti-clockwise PT evolution during vein precipitation and modification by isobaric heating and subsequent cooling at pressures between ca. 210 and 350 bar. Internal over- and underpressures in the inclusions enabled decrepitation and re-equilibration of early inclusions but also modification of vein generations in the Cocos Ridge basalt and in the lithified sediments. We propose that lithification of the sediments was accompanied with a first stage of vein development in the Middle Miocene and was a result of the Galapagos hotspot activity. Heat advection, either related to the Cocos-Nazca spreading center and/or the Galapagos hotspot or a further heating event close to the trench, led to subsequent vein modification related to isobaric heating. The latest mineralization within aragonite and calcite veins occurred during crustal cooling up to recent times.

Furthermore we show results of microstructural observations within the vein mineralizations. Mineralization and crosscutting relationships give constraints for different vein generations. Calcite veins within the sedimentary rocks contain twin lamellae with maximum twin width of 120 µm. Mean twin densities indicate differential stress between ca. 30 to 141 MPa. These differential stresses exceed the lithostatic pressures within hole U1414 by a factor of 10 and are therefore assumed to be related to tectonic stresses related to plate convergence and subduction of the Cocos Plate along the Middle American Trench.

IODP

Reconstruction of the palaeoecological evolution of the Holocene Bothnian Sea region on the basis of palynomorphs from two IODP Sites (M0061, M0062) from the Ångermanälven estuary

H.-T. BRANDT[1], O. MICHAELIS[1], U. KOTTHOFF[1], EXP.-347 SCIENCE PARTY[2]

[1]Centrum für Naturkunde und Institut für Geologie, Universität Hamburg, 20146 Hamburg
[2]c/o C. Cotteril, British Geological Survey, Edinburgh, UK

Global climate change has a particularly strong impact on ecosystems in continental shelf seas and enclosed basins. These ecosystems are influenced by oxygen depletion, intensifying stratification, and increasing temperatures, which are partly caused by anthropogenic influence. In order to predict future changes in water mass conditions, it is essential to reconstruct how these conditions have changed in the past and which factors drove the respective changes. The brackish Baltic Sea provides a unique opportunity to analyse such changes because it is one of the largest semi-enclosed basins worldwide. The Baltic Sea region is also of particular interest for the reconstruction of past changes in terrestrial ecosystems, since it is adjacent to different vegetation zones, from cool temperate forest with mixed coniferous and deciduous trees in the South to closed boreal forest with taiga-like conditions in the North. Among other goals, IODP Expedition 347 to the Baltic Sea aims at the reconstruction of ecosystem, climate, and sea level dynamics and the underlying forcing in different settings in the Baltic Sea region from the Marine Isotope Chrone 5 until today. During Expedition 347, a exceptional set of long sediment cores from eight different sites was recovered from the Baltic Sea, which allow new high-resolution reconstructions.

Here, we present an effort to reconstruct the evolution of marine and terrestrial ecosystems in the Bothnian Sea region during the Holocene by analysing palynomorphs extracted from sediment samples from IODP-Exp.-347 Sites M0061 and M0062. In the framework of two BSc-theses (Brandt 2015; Michaelis 2015) and subsequent high-resolution studies (in progress), pollen and dinocysts were extracted from the sediment and prepared for analyses. In several samples from Site M0061, processes of *Operculodinium centrocarpum* ("*Protoceratium*") were measured following approaches used by, e.g., Mertens et al. (2011). The analysis of *O. centrocarpum* revealed low average process lengths, indicating a low sea-surface salinity. During an interval of particular high sea level, *O. centrocarpum* is also present in sediments from Site M0062 (10 km inbound from the Ångermanälven estuary). Pollen-based results in respect of *Picea abies* (spruce) were compared with data published by Gliemeroth (1997), Eriksson (2001), Segerström & Stedingk (2003), and Giesecke (2004). This comparison allows age estimations for both sites. *Picea* firstly occurred in the research area after ca 5500 cal. ^{14}C yr BP (reflected in Site M0061 at ca. 5.5 mcd and in Site M0062 at ca. 7 mcd). *Picea* became abundant in the Bothnian Sea region probably a short time after 3000 cal. ^{14}C yr BP , reflected for Site M0061 at ca. 3.0 mcd and for Site M0062 at ca. 5.5 mcd. The pollen-based age estimations for the examined sites can in a later phase be used to support other dating methods, which are still in progress. Coevally with the interval of particularly high sea-level indicated by the dinoflagellate cysts (between ca. 6.0 and 4.0 mcd for Site M0061), populations of thermophilous deciduous trees like *Alnus* and *Carpinus* were expanding, while *Pinus* (Pine) shows a significant decrease. In the framework of the ongoing high-resolution studies, the focus will be on the upper sections of Site M0062. The palynomorph-based results shall be compared with results based on additional proxies (foraminifers, diatoms); and we will analyzed when cereals were introduced into the Bothnian Sea region.

References:

Brandt, H.-T. (2015): Palynomorphen-basierte Rekonstruktion der holozänen Ökosystementwicklung im nördlichen Ostseegebiet. Bachelorarbeit, Geologisches Institut der Universität Hamburg, Hamburg, 56 S.

Eriksson, B. (2001): Palynology of two postglacial sediment cores from the baltic sea; North Central Basin and Gotland Deep. Report, Research and Development Section, Geological Survey of Finland, Espoo, 1-11.

Giesecke, T. (2004): The holocene Spread of Spruce in Scandinavia. In: Dissertation, Comprehensive Summaries of Uppsala Dissertations from the Faculty of Science and Technology, Uppsala University, Uppsala, 1027, 46 S.

Gliemeroth, A.K. (1997): Holozäne Einwanderungsgeschichte der Baumgattungen *Picea* und *Quercus* unter paläoökologischen Aspekten in Europa. Eiszeitalter und Gegenwart, Quarternary Science Journal 47, 28-41.

Mertens, K.N., Dale, B., Ellegaard, M., Jansson, I.-M., Godhe, A., Kremp, A., Louwye, S. (2011): Process lenth variation in cysts of the dinoflagellate *Protoceratium reticulatum*, from surface sediments of the Baltic-Kattegatt-Skagerrak estuarine system: a regional salinity proxy. Boreas 40, 242-255.

Michaelis, O. (2015): Holozäne Klima- und Umweltentwicklung im Gebiet der heutigen Flussmündung des Ångermanälven (Ostsee) - ein palynologischer Ansatz. Bachelorarbeit, Geologisches Institut der Universität Hamburg, Hamburg, 47 S.

Segerström, U. und von Stedingk, H. (2003): Early-Holocene spruce Picea abies (L.) Karst., in west central Sweden as revealed by pollen analysis. The Holocene, 13, 897-906.

ICDP

Improved shallow seismic imaging by combining P- and S-waves - Tannwald Basin

T. BURSCHIL[1], H. BUNESS[1], G. GABRIEL[1]

[1]Leibniz Institute for Applied Geophysics, Stilleweg 2, 30655 Hannover, Germany

Major valleys and basins mark the prominent settlement area in alpine areas and bear potentially overdeepened structures (Preusser et al., 2010). These valleys and basins were primarily carved out by glaciers and refilled with deposits during Quaternary glaciations. Their sediment succession allows studying erosion and sedimentation processes of glacial cycles, which is the main purpose of the ICDP proposal DOVE (Drilling Overdeepened Alpine Valleys; Anselmetti et al., 2014).

Among various geophysical methods that can be used for the exploration of overdeepened valleys, the seismic method allows the most detailed imaging of sedimentary structures. In the 1990's, the Tannwald Basin has been explored using refraction seismics. However, this methods only revealed the borders of gross geological units, e.g. top Molasse. Shallow reflection seismic method, which is established since the 1990's, can accomplish the imaging and is sporadically used in Alpine valleys. One limitation of the method is the resolution achievable with P-waves, since the elastic wave transmission and typical velocities in a water saturated environment restrict resolution to ca. 5 –

10 m. In addition, the uppermost 20 – 40 m beneath the surface are hard to image with P-wave surveys, leaving a considerable depth gap to, e.g. very high resolution radar measurements. A new development in shallow exploration seismic that may overcome these problems is the utilization of shear waves. Due to the very high Vp/Vs relations in unconsolidated sediments and the insensitivity to the presence to water, they promise a much higher seismic resolution. S-wave recording proved to be very useful in some environments but have never been used for exploration of overdeepened structures.

How far DOVE can benefit from multi-component reflection seismics, is investigated in a DFG-funded project (KR2073/3-1; GA749/5-1). It intends a structural and facies characterization of the sediments in overdeepened structures and the transfer of methodological results to the DOVE drill sites. Test sites are the Tannwald Basin, located about 50 km NE of Lake Constance at the margin of the last glacial maximum (LGM), and the inner-alpine basin of Lienz (Austria) (Fig. 1).

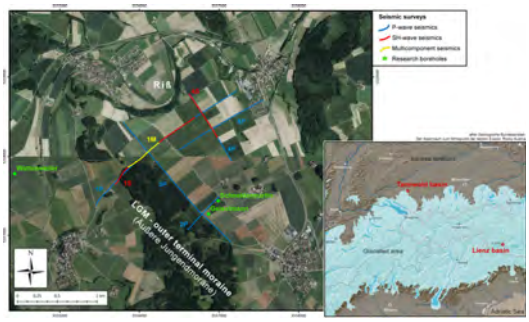

Figure 1: Extent of the last glacial maximum (LGM) in the central part of the Alps (right) and location map of reflection seismic profiles in the Tannwald Basin (left). The Tannwald Basin is located about 50 km north of Lake Constance (Bodensee) at the margin of the LGM. Profiles 1P and 1S cross the outer terminal moraine and are shown in Fig. 2.

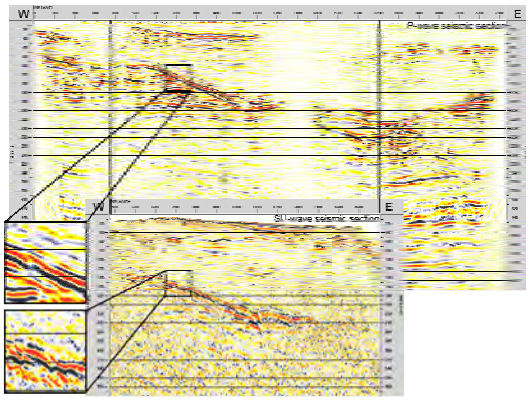

Figure 2: Seismic sections for P-wave (1P in Fig. 1, top) and SH-wave (1S in Fig. 1, bottom) and detailed view of the ramp-like dipping of top Molasse (left). SH-waves do not display all features of conventional P-wave reflection seismics but possess a higher resolution.

In the Tannwald Basin, we have accomplished several reflection seismic surveys using conventional high-resolution P-wave, horizontally polarized SH-wave, and multi-component (SV- and SH-wave source, 3-component receiver) techniques (Fig. 1). In addition, several cross-lines were registered to study 3-D effects and to test 3-D multi-component approach. First results of the P-wave and SH-wave reflection seismic measurements are presented here (Fig. 2).

The P-wave and SH-wave profiles have high quality and exhibit same overall structures. All P-wave profiles delineate strong reflections of the base of the Tannwald Basin, i.e. top Molasse. This preliminary interpretation is supported by nearby, deep boreholes, that were drilled in the 1990's, e.g. for groundwater exploration. Depth of the basement varies from ca. 80 m in the western part of the study area to 220 m at the deepest point in the eastern part of the study area. Further, partially incoherent reflections appear below top Molasse. The sedimentary filling of the basin shows faint reflection segments, which are partially connected. The SH-wave seismic sections contain fewer reflections than conventional P-wave sections and depict only a part of the structures imaged in P-waves, but the resolved structures reveal more details.

The western part of profile 1 (Fig. 2) shows a ramp-like dipping of top Molasse of about 10°, which increases the depth of the basin from 80 m to 160 m. This structure is visible in the P-wave as well as in the SH-wave seismic section, but shear waves provide higher resolution. This manifests in the shorter wave length of the reflection and in a resolved fault (Fig. 2, detailed views). Horizontal reflections below the ramp are bright in the P-wave section but very faint to evanescent depicted with SH-waves. The reflection pattern of top Molasse at the deepest part of the basin (Fig. 2, between 1400 – 1700 m) is difficult to interpret with SH-waves. Reflections in the sedimentary filling resolved with P-waves (Fig. 2, at 50 ms between 500 – 1100 m) are faintly pictured by SH-waves. A possible reason for the difference in data quality between P-waves and SH-waves may be higher damping and scattering of the SH-waves, which causes a lower depth of investigation or the response to different parameters in addition.

In conclusion, combined interpretation of P-wave and SH-wave reflection seismics reveal more details of near-surface overdeepened structures by providing complementary information. P-wave seismics shows a more coherent image with higher penetration depth, but SH-wave seismics resolves partly more details due to their higher resolution. The combination seems to be an enhanced tool to investigate sedimentary succession preparatory to scientific drilling.

Future steps include a revised processing of the P-wave and SH-wave data as well as the processing of the multi-component data. First breaks will be analysed with refraction tomography to gain detailed velocity information for elastic parameters, i.e. Vp/Vs, Poisson ratio, and to investigate anisotropy caused by tectonic and glacial loads. A 3-D processing of the cross-lines for P-waves and multi-component data will estimate the potential and benefit for a complete 3-D multi-component survey. Furthermore, two reflection seismic campaigns are scheduled for 2016 in the Lienz basin (Austria).

References:

Anselmetti et al. (2014). Drilling overdeepened Alpine Valleys (DOVE). In EGU General Assembly Conference Abstracts (Vol. 16, p. 12437).

Preusser et al. (2010). Distribution, geometry, age and origin of overdeepened valleys and basins in the Alps and their foreland. Swiss Journal of Geosciences, 103(3), 407-426.

IODP

Potential impact of salinity changes on viruses and bacteria in sub-surface sediments from the Baltic Sea

O.E. CHIANG, V. VANDIEKEN, B. ENGELEN

Institut für Chemie und Biologie des Meeres, Carl von Ossietzky Universität Oldenburg, Carl-von-Ossietzky Straße 9-11, D-26129 Oldenburg, Germany, www.pmbio.icbm.de

The marine subsurface sediment (>1 meter below seafloor) is an environment with low metabolic activity and bioavailability of organic carbon that still harbors a high abundance and diversity of prokaryotes and viruses (Kallmeyer et al. 2012, Engelhardt et al. 2014).

Exceeding the abundance of prokaryotic cells, viruses have been detected in marine sediments as deep as 320 m. However, their ecological role in the deep biosphere remains largely unknown. In marine surface sediments, viruses impact microbial communities by regulating their composition and diversity. Production of new viruses leads to the death of prokaryotes, but additionally viral lysis releases nutrients to stimulate new microbial growth via the viral shunt (Suttle 2005).

Viruses proliferation is led mainly by two virus' life strategies: the lytic and lysogenic cycle. During the lytic cycle, the virus redirects the host's metabolism towards the production of new viruses. While in the lysogenic cycle, the genome is integrated into the host genome (so called "prophage") and replicates along with the host, until the lytic cycle is induced by an inducing event.

In the laboratory, the production of prophages can be induced by the DNA-damaging agent mitomycin. In nature, increasing evidence suggests that physical and chemical variabilities (e.g., gradients in salinity, oxygen) can have a strong influence on viral dynamics because such factors have a significant effect on host activity (Payet & Suttle 2008). However, the induction of viruses by environmental stress (e.g., osmotic shock) has not been shown for bacteria of the deep biosphere yet. Here, we report the first results of a study conducted on samples from sediments from the Baltic Sea collected during IODP Exp. 347. We hypothesize that changes in salinity (osmotic shock) can act as an induction stimulus of lysogenic phages in new bacterial isolates from these sediments.

Sediments from the Baltic Sea have undergone alterations between limnic, brackish and marine conditions during their geological history due to repeated glaciations. Sediments samples were taken during IODP Exp. 347 from 4 sites (M0059, M0060, M0063, M0065). In an initial stage, cultivation of fresh sediment was carried out in enrichments with three media of different salinities (i.e., freshwater, brackish, marine).

By repeated transfer in anoxic deep agar dilution series, 36 new bacterial strains were isolated into pure cultures from all four microbiology sites. The new strains belong to gammaproteobacterial *Vibrio, Aeromonas* and *Shewanella*, deltaproteobacterial *Desulfovibrio, Actinobacteria* with the genus *Sanguibacter*, *Bacteriodetes* with the genus *Marinifilum* and Gram-positive *Firmicutes* including genera of *Alkaliphilus, Lactococcus, Acetobacterium* and *Desulfosporosinus*. The strains showed considerable differences in their salt tolerance with optimum growth at freshwater, brackish or marine conditions as well as narrow or broad salinity tolerances.

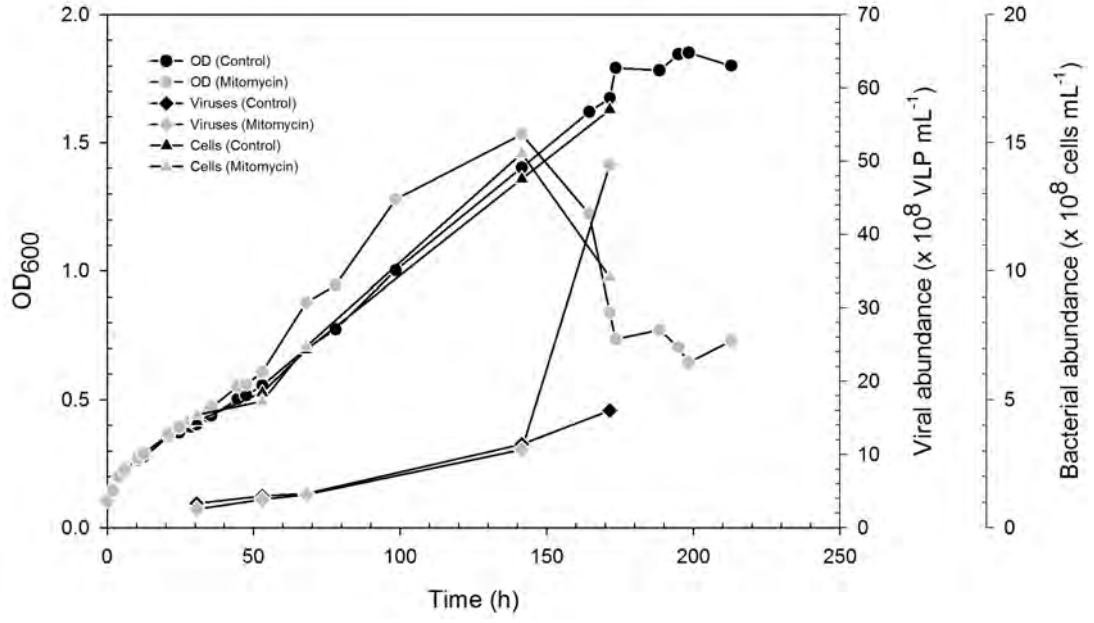

Fig. 1. Induction of prophages of *Shewanella* sp. strain 65.4F. A preculture (400 mL) was grown aerobically. At the beginning of the exponential phase (OD = 0.4) the preculture was divided into 2 sub-cultures: one of them acted as a control, while a second one, was treated with mitomycin. *OD = optical density at 600 nm.* Dots indicate average values.

By now, we have identified 4 strains to posses mitomycin-inducible prophages (Fig. 1), while other strains continuously produce viruses during growth but these viruses cannot be induced by mitomycin. For virus numbers, we have successfully established to count SYBR-Green-stained viruses by flow cytometry besides the regular counting by epifluorescence microscopy. Viruses were detected based on the fluorescence properties and specific scatter signals from the flow cytometer. All the analysis showed a well defined low fluorescence group of

viruses in the cytograms of SYBR-Green I-stained samples. At the moment, we are studying the prophages of three strains *Lactococcus* sp., *Marinifilum* sp. and *Shewanella* sp. (Fig. 2). Induction of prophages from these strains is investigated by osmotic shock experiments. Later on, we will further identify the influence of salinity on respiration rates and carbon turnover of the bacteria.

The overall goal of the project is contribute to understanding the dynamics of viruses in relation to salinity-change events during the paleoenvironmental history of the Baltic Sea.

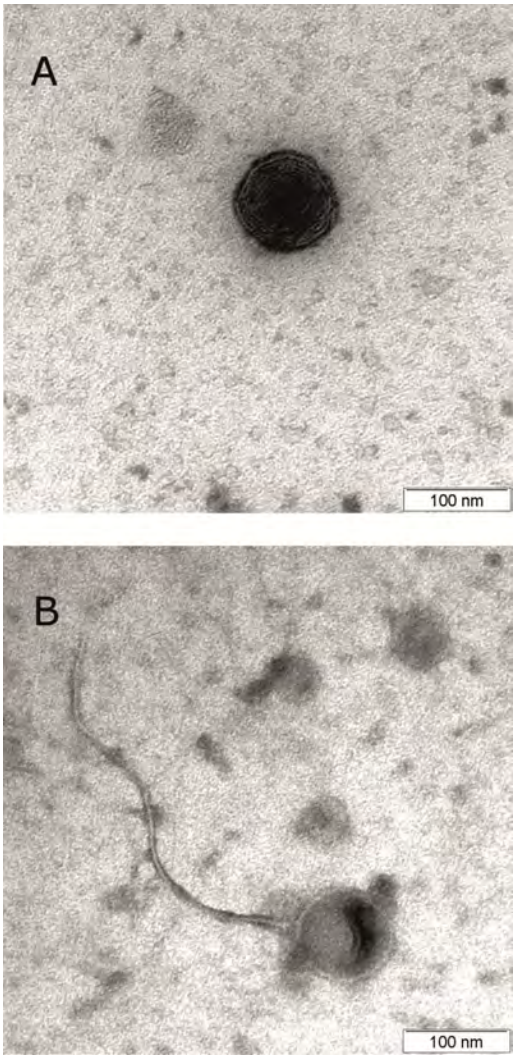

Fig. 2. Electron microscope images of viruses. A) Siphoviridae-like virus induced from *Marinifilum* sp. strain 60.6 M and B) non-tailed virus induced from *Shewanella* sp. strain 65.4F.

In the past, events of high virus production due to salinity changes might have had major impacts for the prokaryotic community and the biogeochemical cycles in Baltic Sea sediments by lysis of certain community members and introduction of nutrients via the viral shunt.

References:
Engelhardt T, Kallmeyer J, Cypionka H, Engelen B (2014) High viruses-to-cell ratios indicate ongoing production of viruses in deep subsurface sediments. ISME J 8: 1503-1509.
Kallmeyer J, Pockalny R, Adhikari RR, Smith DC, D´Hondt S (2012) Global distribution of microbial abundance and biomass in subseafloor sediment. Proc Natl Acad Sci 109: 16213–16216.
Payet J, Suttle CA (2008) Physical and biological correlates of virus dynamics in the southern Beaufort Sea and Amundsen Gulf. J Mar Syst 74: 933-945.
Suttle CA (2005) Viruses in the sea. Nature 437: 356-361.

IODP

Orbital scale variation of primary productivity and sea level in the central equatorial Indian Ocean (Maldives) during the early Pliocene

H. DEIK[1], L. REUNING[1], M. PFEIFFER[1]

[1] RWTH Aachen University, EMR – Energy and Mineral Resources Group, Geological Institute

Orbital scale variations in primary productivity and sea-level change are recorded in early Pliocene sediments recovered at ODP Site 716, Maldives Ridge, central equatorial Indian Ocean. The aragonite content tracks sea-level variations with high values indicating sea-level highstand. It was suggested that chlorin, a degradation product of chlorophyll, is a proxy for primary productivity (Reuning et al., 2006). This was confirmed by quantitative analysis of planktonic foraminiferal abundances that show a positive correlation between chlorin content and the relative abundance of thermocline species. The aragonite content shows precession and eccentricity cycles, whereas the primary productivity proxies show only precessional cycles. The negative correlation between aragonite content and the relative abundance of thermocline species implies that the primary productivity increased during glacial times. This phase coupling between primary productivity and glacial/interglacial cycles is consistent with Quaternary productivity records from the central Indian Ocean that are controlled by orbital induced variations of the Southern Oscillation (Cayre et al., 1999).We therefore propose that a similar mechanism was active in the early Pliocene despite major changes in the global boundary conditions.

References:
Cayre, O., Beaufort, L., & Vincent, E. (1999). Paleoproductivity in the Equatorial Indian Ocean for the last 260,000 yr: a transfer function based on planktonic foraminifera. *Quaternary Science Reviews*, *18*(6), 839-857.
Reuning, L., Reijmer, J. J., & Mattioli, E. (2006). Aragonite cycles: diagenesis caught in the act. *Sedimentology*, *53*(4), 849-866.

IODP

Achieving accurate orbital calibration of the late Miocene (8-6 Ma): a high-resolution chemo- and magnetostratigraphy from IODP Sites U1337 and U1338 (equatorial Pacific)

A.J. DRURY[1], T. WESTERHOLD[1], T. FREDERICHS[2], R.WILKENS[3], J.CHANNELL[4], H.EVANS[5], D.HODELL[6], C.M.JOHN[7], M.LYLE[8], U.RÖHL[1], J.TIAN[9]

[1]MARUM - Center for Marine Environmental Sciences, University of Bremen, Leobener Strasse, 28359 Bremen, Germany
[2]Department of Geosciences, University of Bremen, P.O. Box 330440, D-28334 Bremen, Germany
[3]School of Ocean and Earth Science and Technology (SOEST), University of Hawai`i at Manoa, Honolulu, Hawai'i, USA;
[4]Department of Geological Sciences, University of Florida, Gainesville, FL 32611, USA
[5]International Ocean Discovery Program, Texas A&M University, 1000 Discovery Drive, College Station Texas 77845-9547, USA
[6]Department of Earth Sciences, University of Cambridge, Cambridge CB2 3EQ, UK;
[7]Department of Earth Science and Engineering, Imperial College London, London, SW7 2BP, UK;
[8]College of Earth, Ocean, and Atmospheric Sciences, Oregon State University, USA;
[9]State Key Laboratory of Marine Geology, Tongji University, China;

The late Tortonian to early Messinian (8-6 Ma) is characterised by a long-term reduction in benthic foraminiferal $\delta^{18}O$ and by distinctive short-term $\delta^{18}O$ cycles. Coevally, the late Miocene carbon isotope shift (LMCIS) marks a permanent –1 ‰ shift in oceanic $\delta^{13}C_{DIC}$, which is the largest, long-term marine carbon cycle perturbation since the mid Miocene Monterey excursion. Accurate age control is crucial to ascertain the origin of the $\delta^{18}O$ cyclicity and to determine the precise timing of the LMCIS onset and termination.

The Tortonian-Messinian Geological Time Scale was mainly constructed using astronomically tuned sedimentary cycles in Mediterranean road-cut outcrops (Hilgen et al., 1995; Krijgsman et al., 1999), which were also used to calibrate the $^{40}Ar/^{39}Ar$ 'rock-clock' synchronisation and to adjust the Fish Canyon sanadine (FC) $^{40}Ar/^{39}Ar$ standard age to 28.201 ± 0.046 Ma (Kuiper et al., 2008). Recent studies utilising astronomically tuned deep-sea sedimentary successions challenge the Mediterranean tuning and FC standard age (Channell et al., 2010; Westerhold et al., 2012). Discrepancies in tuning could originate as road-cut outcrops are often more difficult to integrate and interpret than deep-sea sedimentary successions, which benefit from multiple hole sedimentary splices and integration between multiple sites. To test the 'rock-clock', it is crucial to obtain highly accurate ages for magnetic polarity Chrons between 6-8 Ma, particularly C3An.2n, C3.Ar and C3Bn, independent of the Mediterranean calibration. However, beyond the Mediterranean basin, a stand-alone high-resolution chemo-, magneto-, and cyclostratigraphy at a single DSDP/ODP/IODP site does not exist.

The absence of appropriate records changed with the retrieval of adjacent equatorial Pacific IODP Sites U1337 and U1338 (4463 and 4200 m below sea level respectively) (Pälike et al., 2010). Both sites are characterised by sedimentation rates ~2 cm/kyr, high biogenic carbonate content, and cyclic Milankovitch-related variations in colour and lithology (Expedition 320/321 Scientists, 2010a, 2010b; Lyle et al., 2012). Refined composite records generated for both sites ensure complete sedimentary successions were retrieved (Wilkens et al., 2013). In addition, a basic shipboard magnetic polarity stratigraphy was recovered at Site U1337, with great potential for improvement (Expedition 320/321 Scientists, 2010a).

Here we present on-going research to produce a high-quality benthic stable isotope and magnetic polarity record from Sites U1337 and U1338. At Site U1337, ~400 discrete palaeomagnetic cube samples were analysed between 110 and 167 m CCSF-A (core composite depth below seafloor along the Wilkens et al., 2013 splice). Although natural remanent magnetisation is low (1.4E-01 mA/m), the inclination and declination of discrete samples corroborates the shipboard whole-core measurements and we identify 14 polarity reversals at Site U1337 from the top of Chron C3An.1n (6.033 Ma) to the base of Chron C4n.2n (8.1.08 Ma). Eight reversals are identified to ± 2.5 cm precision. An additional set of ~200 discrete samples will enable identification of the remaining six reversals with comparable precision. The final Site U1337 discrete sample palaeomagnetic data will be integrated with those from Site U1338 to generate the first robust deep-sea magnetostratigraphy across 6-8 Ma.

We present a high-resolution correlation of Sites U1337 and U1338 using the Milankovitch-related cycles in core images, physical property and X-ray fluorescence core scanning data. Using this alignment, new high-resolution (<1.5 kyr) stable isotope records generated at Site U1337 correlate highly with published lower resolution (3-4 kyr) stable isotope records from Site U1338 (Drury et al., 2015). Integrating the available chemo- and magnetostratigraphies from Sites U1337 and U1338 enables the construction of a high-resolution stack for the 8-6 Ma interval. Initial orbital tuning shows that the distinct $\delta^{18}O$ cyclicity is obliquity-driven, indicating a high-latitude climate forcing dominates this interval. The benthic $\delta^{13}C$ records show a strong 405-kyr-eccentricity cycle component suggesting that the carbon cycle dynamics in the late Miocene equatorial Pacific are mainly driven by eccentricity, despite the dominance of obliquity in the $\delta^{18}O$ record. Orbital tuning determines the onset of the LMCIS at 7.55 Ma (during Chron C4n.1n) and its termination at 6.70 Ma (during Chron C3An.2n). We are currently analysing the final 200 discrete palaeomagnetic samples to increase the precision of the magnetic reversal positions down to ±2.5 cm. Coupled with the distinct cyclicity in the $\delta^{18}O$ records the final integrated U1337-U1338 chemo-magnetostratigraphy will be ideal to test the 'rock-clock' synchronisation.

References:

Channell, J. E. T., D. A. Hodell, B. S. Singer, and C. Xuan (2010), Reconciling astrochronological and 40Ar/39Ar ages for the Matuyama-Brunhes boundary and late Matuyama Chron, *Geochemistry, Geophys. Geosystems*, *11*, doi:10.1029/2010GC003203.

Drury, A. J., C. M. John, and A. E. Shevenell (2015), Evaluating climatic response to external radiative forcing during the late Miocene to early Pliocene: new perspectives from Eastern Equatorial Pacific (IODP U1338) and North Atlantic (ODP 982) locations, *Paleoceanography*, n/a–n/a, doi:10.1002/2015PA002881.

Expedition 320/321 Scientists (2010a), Site U1337, in *Proceedings of the Integrated Ocean Drilling Program*, vol. 320/321, edited by H. Pälike, M. Lyle, H. Nishi, I. Raffi, K. Gamage, A. Klaus, and E. 320/321 Scientists, pp. 1–146, Tokyo (Integrated Ocean Drilling Program Management International, Inc.).

Expedition 320/321 Scientists (2010b), Site U1338, in Proceedings of the Integrated Ocean Drilling Program, Volume 320/321, vol. 320/321, edited by H. Pälike, M. Lyle, H. Nishi, I. Raffi, K. Gamage, A. Klaus, and E. 320/321 Scientists.

Hilgen, F. J., W. Krijgsman, C. G. Langereis, L. J. Lourens, A. Santarelli, and W. J. Zachariasse (1995), Extending the astronomical (polarity) time scale into the Miocene, *Earth Planet. Sci. Lett.*, *136*, 495–510, doi:10.1016/0012-821X(95)00207-S.

Krijgsman, W., F. J. Hilgen, I. Raffi, F. J. Sierro, and D. S. Wilson (1999), Chronology, causes and progression of the Messinian salinity crisis, *Nature*, *400*, 652–655, doi:10.1038/23231.

Kuiper, K. F., A. Deino, F. J. Hilgen, W. Krijgsman, P. R. Renne, and J. R. Wijbrans (2008), Synchronizing rock clocks of Earth history., *Science*, *320*, 500–504, doi:10.1126/science.1154339.

Lyle, M., A. O. Lyle, T. Gorgas, A. Holbourn, T. Westerhold, E. Hathorne, K. Kimoto, and S. Yamamoto (2012), Data report : raw and normalized elemental data along the Site U1338 splice from X-ray fluorescence scanning 1 X-ray fluorescence analytical technique, in *Proceedings of the Integrated Ocean Drilling Program, Scientific Results*, vol. 320/321, edited by H. Pälike, M. Lyle, H. Nishi, I. Raffi, K. Gamage, A. Klaus, and E. 320/321 Scientists.

Pälike, H., M. Lyle, H. Nishi, I. Raffi, K. Gamage, A. Klaus, E. 320/321 Scientists, and Expedition 320/321 Scientists (2010), Expedition 320/321 Summary, in *Proceedings of the Integrated Ocean Drilling Program*, vol. 320, edited by H. Pälike, M. Lyle, H. Nishi, I. Raffi, K. Gamage, A. Klaus, and E. 320/321 Scientists, pp. 2–141.

Westerhold, T., U. Röhl, and J. Laskar (2012), Time scale controversy: Accurate orbital calibration of the early Paleogene, *Geochemistry, Geophys. …*, *13*, doi:Q06015 10.1029/2012gc004096.

Wilkens, R. H., G. R. Dickens, J. Tian, J. Backman, and E. 320/321 Scientists (2013), Data report: revised composite depth scales for Sites U1336, U1337, and U1338, in *Proceedings of the Integrated Ocean Drilling Program, Scientific Results*, edited by H. Pälike, M. Lyle, H. Nishi, I. Raffi, K. Gamage, A. Klaus, and E. 320/321 Scientists.

IODP

Evolving carbon sinks in the young South Atlantic: Drivers of global climate in the early Cretaceous greenhouse?

W. DUMMANN[1], P. HOFMANN[1], T. WAGNER[2], J.O. HERRLE[3], S. KUSCH[1], J. RETHEMEYER[1], S. FLÖGEL[4], S. STEINIG[4]

[1]Insitute of Geology and Mineralogy, University of Cologne, Zülpicher Str. 49a, D-50674 Cologne, Germany
[2]Sir Charles Lyell Centre, School of Energy, Geoscience, Infrastructure and Society, Heriot-Watt University, Edinburgh, EH14 4AS, UK
[3]Institute of Geosciences, Goethe-University Frankfurt, Altenhöferallee 1, D-60438 Frankfurt am Main, Germany
[4]GEOMAR Helmholtz Centre for Ocean Research Kiel, Wischhofstr. 1-3, D-24148 Kiel, Germany

The Mesozoic Era is punctuated by transient episodes of enhanced deposition of organic-rich sediments in the world‘s oceans representing periods of intensified carbon burial in the marine realm (e.g., Takashima et al., 2006). Although the mechanisms triggering the accumulation of marine organic-rich sediments remain a focal point of research/intense debate, young ocean basins are thought to play a key role as marine carbon sinks (e.g., Trabucho-Alexandre et al., 2012, McAnena et al. 2013, and references therein). Expanding young ocean basins often experience widespread anoxia due to their distinct bathymetry (i.e., high shelf-to-open ocean ratio) and restricted deep water ventilation, which in turn promotes the drawdown of atmospheric carbon. However, the individual role of young ocean basins evolving during the Mesozoic is not well understood.

This project aims to test and quantify the impact of organic carbon burial on global climate perturbations using the opening of the early Cretaceous South Atlantic as a case study. Recent studies have argued that the evolving South Atlantic and Southern Ocean basins have acted as a primary site of organic carbon production, biotransformation, and burial during the mid-Cretaceous (i.e., Aptian-Albian) as manifested by extensive black shale (e.g., Wagner et al., 2013) and prolific hydrocarbon provinces along both continental margins (e.g., Cameron et al., 1999). Modeling results suggest that carbon burial in the South Atlantic and Southern Ocean (representing 5% of the Cretaceous global ocean by area) accounts for 35% of the atmospheric carbon sequestered by the world’s ocean during this time period (McAnena et al., 2013).

We postulate that carbon burial in the South Atlantic is, at least partly, of causal significance for global climate perturbations during the Aptian-Albian and that the dynamics of carbon burial in the South Atlantic are controlled by multiple gateway openings (Falkland Gateway and Walvis Ridge Gateway). We test this hypothesis using a combined approach of multiproxy-based reconstructions derived from South Atlantic and Southern Ocean DSDP drill cores to establish a detailed framework for the dynamics and controls of carbon deposition in this young oceanic basin and by quantifying the effect on the global carbon budget by quantifying carbon accumulation using novel climate and biogeochemical modelling.

In the first phase of the project we focus on the initial opening phase of the South Atlantic during the Aptian, which was closely linked to the history of the Falkland Gateway. We study well preserved sediments from DSDP Site 361 (Cape Basin) and DSDP Site 511 (Falkland Plateau) recording the development of water mass exchange and redox fluctuations between the Southern Ocean and the emerging South Atlantic. In a partner project hosted at GEOMAR Kiel we started to develop a bathymetry model for the South Atlantic, which serves as a base for the modelling approach (see abstract of Steininger et al.).

In order to unravel the history of the Falkland Gateway, we first generate a stratigraphic framework for sites 361 and 511 by combining existing and updated calcareous nannofossil biostratigraphy with new high resolution carbon isotope records of organic matter ($\delta^{13}C_{org}$). This improved chronology allows us to precisely define global carbon burial events, including the oceanic anoxic event 1a (OAE 1a), and correlation between the two study sites.

To assess the carbon burial history, we performed x-ray fluorescence (XRF) and organic geochemical studies. First XRF results from sites 361 and 511 and organic geochemical data from Site 361 indicate permanent anoxic conditions on the sill (Site 511) and in the basin (Site 361) during the beginning of the Aptian including parts of the OAE 1a. Organic geochemical data show short-term events of intense euxinic conditions (e.g., high abundance of 28,30-bisnorhopane) in the Cape basin, accompanied by high accumulation of marine-derived organic carbon (e.g., diacholestene/diasterene ratio).

During OAE 1a redox conditions became dysoxic to oxic on the Falkland sill, whereas anoxic conditions continued to prevail in the Cape Basin. This change in redox conditions on the sill was accompanied by a shift in the sediment source region as indicated by a lower potassium-aluminium and low zirconium-silicium ratios. The sediment signatures prior to the shift in redox conditions are similar at Site 511 and Site 361 suggesting a sediment supply to both sites from the African continent (sediment source includes K-rich igneous rocks of the Cape Province). With the onset of oxygenated sedimentation conditions at Site 511 this “African” sediment signature is not further detectable. We propose that both, the inundation of the Falkland sill with oxygenated bottom waters and the

change in sediment source were linked to the progessive opening of the Falkland Gateway, i.e. the westward drift of South America (including the Falkland Plateau with Site 511) away from the African continent (Site 361).

References:
Cameron, N., Bate, R., Clure, V. and Benton, J. (1999): Oil and gas habitats of the South Atlantic: Introduction, Geological Society, London, Special Publications, Vol. 153(1), pp. 1-9
McAnena, A., Flögel, S., Hofmann, P., Herrle, J., Griesand, A., Pross, J., Talbot, H., Rethemeyer, J., Wallmann, K. and Wagner, T. (2013): Atlantic cooling associated with a marine biotic crisis during the mid-Cretaceous period, Nature Geoscience, Vol. 6(7), pp. 558-561
Takashima, R., Nishi, H., Huber, B. T. and Leckie, R. M. (2006): Greenhouse, Oceanography, Vol. 19(4), pp. 64
Trabucho-Alexandre, J., Hay, W. and De Boer, P. (2012): Phanerozoic environments of black shale deposition and the Wilson Cycle, Solid Earth, Vol. 3(1), pp. 29-42
Wagner, T., Hofmann, P. and Flögel, S. (2013): Marine black shale deposition and Hadley Cell dynamics: A conceptual framework for the Cretaceous Atlantic, Ocean Marine and Petroleum Geology, Vol. 43, pp. 222-23

IODP

Magnetostratigraphically calibrated dinoflagellate cyst bioevents for the uppermost Eocene to lowermost Miocene of the western North Atlantic (IODP Expedition 342, Newfoundland Drift)

L. EGGER[1], K. K. ŚLIWIŃSKA[2], R.D. NORRIS[3], P.A. WILSON[4], O. FRIEDRICH[1], J. PROSS[1]

[1]Institute of Earth Sciences, University of Heidelberg, Im Neuenheimer Feld 234-236, D-69121 Heidelberg, Germany
[2]Geological Survey of Denmark and Greenland (GEUS), Øster Voldgade 10, DK-1350 Copenhagen, Denmark
[3]Scripps Institution of Oceanography, University of California, San Diego, 9500 Gilman Drive, La Jolla, CA92093-0244, United States
[4]Southampton Oceanography Centre, School of Ocean and Earth Sciences, European Way, Southampton SO14 3 ZH, United Kingdom

The Oligocene epoch represents a somewhat neglected chapter in paleoclimate and paleoceanographic research, which is at least partially due to the scarcity of complete Oligocene sedimentary archives.

However, the limited understanding of the Oligocene world can also be ascribed to the yet relatively poor biostratigraphic age control for that time interval. In many biotic events registered during the Oligocene, microfossil faunas show a strongly diachronous pattern across latitudes, which can be assigned to the development of stronger meridional temperature gradients connected to global cooling.

To improve biostratigraphic age control for the Oligocene of the North Atlantic Ocean, we have carried out a high-resolution study of dinoflagellate cysts from Integrated Ocean Drilling Program (IODP) Sites U1405, U1406 and U1411 off Newfoundland.

Besides representing an apparently complete Oligocene sequence, the sites contain excellently preserved palynomorphs and exhibit magnetostratigraphic age control; this allows us to firmly tie the identified dinoflagellate cyst bioevents to the geomagnetic polarity timescale. In the latest Eocene (magnetochron C15n) to the earliest Miocene (magnetochron C6AAr.2n) dinoflagellate cyst assemblages studied from IODP Sites U1405, U1406 and U1411, we have identified and magneto-stratigraphically calibrated 10 first (FAD; e.g., Artemisiocysta cladodichotoma, Chiropteridium lobospinosum, and Spiniferites manumii) and 19 last appearance data (LAD; e.g., Areosphaeridium diktyoplokum, Enneadocysta pectiniformis, and Schematophora speciosa). Notably, the Eocene/Oligocene transition interval is characterized by a number of LADs of typical lower-latitude, Tethyan marker species such as Schematophora speciosa, Hemiplacophora semilunifera, and Cordosphaeridium cf. funiculatum (Fig. 5).

Considering that cyst-forming dinoflagellates are highly sensitive to changes in the shallow surface waters, in particular with regard to temperature, the disappearance of these lower-latitude taxa during the latest Eocene and earliest Oligocene points to surface-water cooling off Newfoundland, possibly due to an enhanced influence of the proto-Labrador Current.

This hypothesis is supported by the first documentation of the cold-water indicator, high-latitude taxon *Svalbardella* spp. in the same interval, which also suggests surface-water cooling and can be explained by the southward expansion of cool surface-water masses from the high northern latitudes. The comparison with the available magnetostratigraphically calibrated dinocyst datums from other regions of the higher-latitude North Atlantic (such as the Norwegian-Greenland and the Labrador Seas), the North Sea, and the western Tethys has allowed quantification of supraregional leads and lags for a number of dinocyst events. Our magnetostratigraphically calibrated dinoflagellate cyst biostratigraphy, which has a temporal resolution of ~200 kyrs, contributes to an improved age framework for future paleoceanographical studies in the higher-latitude North Atlantic.

References:
Egger, L.M., et al., submitted: Magnetostratigraphically calibrated dinoflagellate cyst bioevents for the uppermost Eocene to lowermost Miocene of the western North Atlantic.
Gradstein, F.M., Ogg, J.G., Schmitz, M., Ogg, G., 2012. The Geologic Time Scale 2012. Elsevier, Amsterdam.

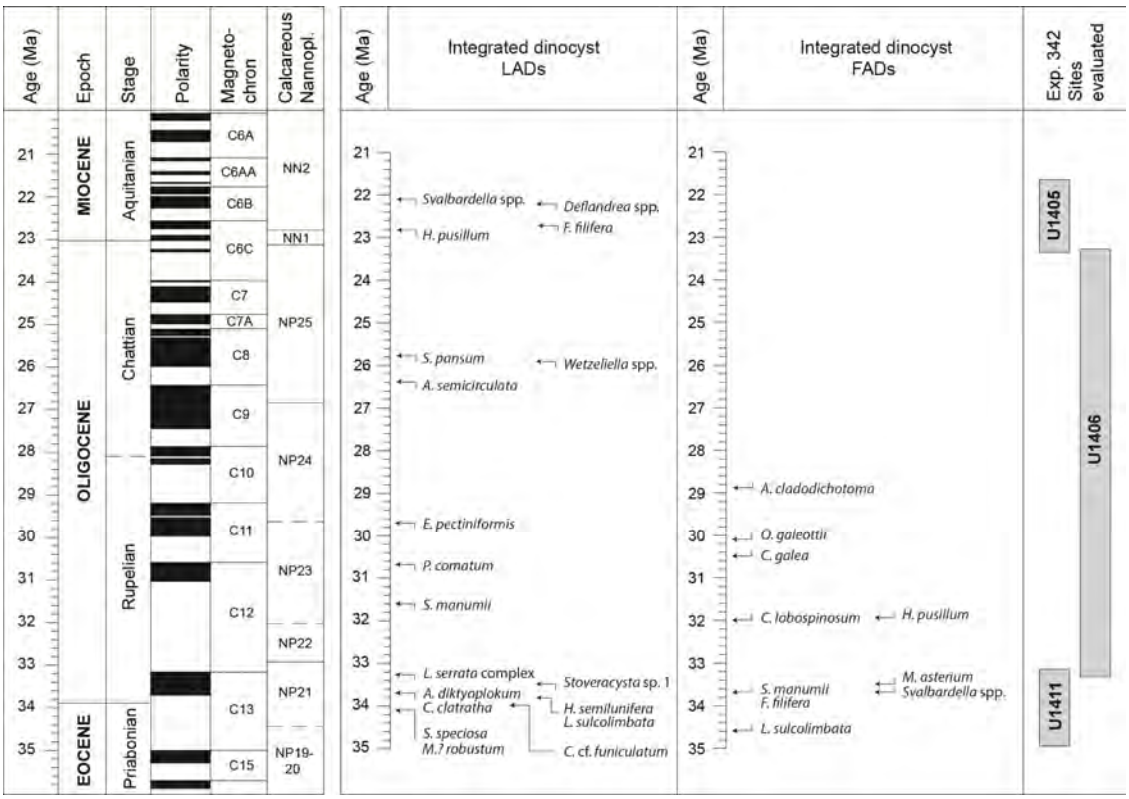

Fig. 1: Integrated scheme of magnetostratigraphically calibrated dinocyst events for the uppermost Eocene to lowermost Miocene of the Newfoundland Margin based on the observations from IODP Sites U1405, U1406 and U1411. Time scale, magnetostratigraphy, and Calcareous Nannoplankton Zones after Gradstein et al. (2012).

ICDP

ICDP PALEOVAN cores troubleshoot 40Ar/39Ar results containing excess 40Ar from ternary feldspar at uniform concentrations

J.ENGELHARDT, M. SUDO, R. OBERHÄNSLI

Institut für Erd- und Umweltwissenschaften, Universität Potsdam

The application of the $^{40}Ar/^{39}Ar$ method on ternary feldspars in the Quaternary is challenged by the presence of extraneous ^{40}Ar at uniform concentrations (Chen et al., 1996), mixed phases (Kelley, 2002) and complex growth histories (Ginibre et al., 2004). Pyroclastic fall deposits in ICDP cores from Lake Van, Turkey contain sodium-rich sanidine and anorthoclase that are tainted with the above-mentioned effects. Stockhecke et al. (2014) defined an age model recording the lake's history based on climato-stratigraphic correlations, tephrostratigraphy, paleomagnetics and $^{40}Ar/^{39}Ar$ analytics for a composite core from drilling site number two at the Ahlat Ridge. Comparing 16 results from total-fusion analyses and three from stepwise-heating experiments with the age model allows systematic monitoring of the methods' feasibility on non-ideal ternary feldspar.

Nine total-fusion and two step-wise heating analyses resulted in inverse isochron ages that overlap with the age model of Stockhecke et al. (2014) within two σ uncertainties. The residual experiments resulted in significantly older isochron ages. Feldspars from deviating analyses have either transparent melt inclusions or distinct textural zoning that indicate complex growth histories. The textural features are visible in cathodoluminescence (CL) or back-scattered electron (BSE) images and can be subdivided following a definition from Ginibre et al. (2004). Pseudo-oscillatory and concentrically zoning has the potential to record resorption processes mostly due to a sensitive alternation of Fe contents and is visible in CL images. Compositional zoning reflects anticorrelated anorthite and orthoclase contents. Contrasting Ba concentrations cause the zone's visibility in BSE images. Deviating samples that are relatively enriched in calcium-derived $^{37}Ar_{Ca}$ are dominated by compositional zoning type feldspar and could therefore reflect variations of the feldspars' anorthite components in their ratios of $^{37}Ar_{Ca}/^{39}Ar_K$. Total fusion analyses that resulted in highest values for $^{37}Ar_{Ca}/^{39}Ar_K$ contain most radiogenic ^{40}Ar relative to $^{39}Ar_K$. As the compositional zoning type feldspars show their anorthite-rich components as resorbed xenocrystic subdomains that are overgrown by an An-poorer component they indicate that the subdomains were not fully degassed and lead to older and deviating ages.

Intensities of blank-, potassium- and atmosphere-corrected ^{38}Ar are commonly interpreted to be derived from chlorine (McDougall and Harrison, 1999) and to have degassing fingerprints of other phases than feldspar. Analyses that reveal a correlation of high $^{38}Ar_{Cl}/^{39}Ar_K$ to high $^{40}Ar^*/^{39}Ar_K$ indicate an excess of ^{40}Ar form either Cl-rich alteration products or from melt- and their appendant fluid-inclusions.

Chlorine and calcium derived isotopic evidence and their corresponding textural compositions explain seven out of eight deviating results. Only four of the deviating results indicate excess ^{40}Ar in their initial $^{40}Ar/^{36}Ar$ ratios. The residual deviating analyses are possibly an effect of extraneous ^{40}Ar at uniform concentrations that adulterates erroneous excess analyses into isotopically reliable ages. Similar investigations of xenocrystic contaminations (Chen et al., 1996; Spell et al., 2001; Renne et al., 2012) caution about samples where age contrasts between xeno- and phenocrysts are less pronounced. ICDP Lake Van cores monitor both a xenocrystic and a melt-inclusion derived contamination that hardly indicates evidence for non-atmospheric initial $^{40}Ar/^{36}Ar$.

References:
Chen, Y.S., Smith, P.E., Evensen, N.M., York, D., Lajoie, K.R., 1996. The edge of time: Dating young volcanic ash layers with the Ar-40-Ar-39 laser probe. Science, 274(5290): 1176-1178.
Ginibre, C., Worner, G., Kronz, A., 2004. Structure and dynamics of the Laacher See magma chamber (Eifel, Germany) from major and trace element zoning in sanidine: A cathodoluminescence and electron microprobe study. Journal of Petrology, 45(11): 2197-2223.
Kelley, S., 2002. Excess argon in K-Ar and Ar-Ar geochronology. Chemical Geology, 188(1-2): 1-22.
McDougall, I., Harrison, T.M., 1999. Geochronology and Thermochronology by the 40Ar/39Ar Method. Oxford University Press, New York, Oxford, 269 pp.
Renne, P.R., Mulcahy, S.R., Cassata, W.S., Morgan, L.E., Kelley, S.P., Hlusko, L.J., Njau, J.K., 2012. Retention of inherited Ar by alkali feldspar xenocrysts in a magma: Kinetic constraints from Ba zoning profiles. Geochimica Et Cosmochimica Acta, 93: 129-142.
Spell, T.L., Smith, E.I., Sanford, A., Zanetti, K.A., 2001. Systematics of xenocrystic contamination: preservation of discrete feldspar populations at McCullough Pass Caldera revealed by Ar-40/Ar-39 dating. Earth and Planetary Science Letters, 190(3-4): 153-165.
Stockhecke, M., Kwiecien, O., Vigliotti, L., Anselmetti, F.S., Beer, J., Çağatay, M.N., Channell, J.E.T., Kipfer, R., Lachner, J., Litt, T., Pickarski, N., Sturm, M., 2014. Chronostratigraphy of the 600,000 year old continental record of Lake Van (Turkey). Quaternary Science Reviews, 104: 8-17.

IODP

Virus-host interaction in autotrophic sulfate-reducing bacteria in subsurface sediments of Juan de Fuca ridge, IODP 301

TIM ENGELHARDT[1], KATJA FICHTEL[1], BERT ENGELEN[1], HERIBERT CYPIONKA[1]

[1]Carl von Ossietzky University Oldenburg, Institut for Cemistry and Biology of the Marine Environment (ICBM), Oldenburg, Germany

The oceanic crust resembles a large interconnected aquifer with intense fluid circulation. Diffusive flow of fluids from the crust aquifer provides nutrients and electron acceptors to the overlaying sediments. This effect is pronounced near oceanic ridges. At Juan de Fuca ridge (IODP 301), a geochemical zonation is established and results in three compartments of an upper and lower sulfate zone and a sulfate-minimum zone that spreads in between. Microbial communities in the upper sediments have access to relatively young sources of organic carbon and sulfate as main electron acceptor. For the lower sulfate zone, the available organic carbon is recalcitrant, however, the introduction of nutrients from the crust fluid has been shown to support microbial activity (Engelen et al., 2008).

Viruses are active parts of deeply buried microbial communities with diverse virus-host interactions (Engelhardt et al., 2015). Viral genomes can be integrated into the host cell genomes (provirus) and may be induced to eventually lyse the host cell. Viral-mediated cell lysis results in a carbon turnover by providing bioavailable organic carbon.

Desulfovibrio indonesiensis strain P23 is an autotrophic sulfate reducer that was isolated from the lower sulfate zone at Juan de Fuca ridge in a depth of 260 meter below seafloor and was shown to be an abundant and viable inhabitant in deeply buried sediments (Fichtel et al., 2012). Whole genome analysis of Dv. indonesiensis has now shown the presence of multiple integrated provirus infections. In addition, detailed analysis of sequence information from clustered regularly interspaced short palindromic repeats (CRISPR) revealed that Dv. indonesiensis has been subjected to multiple viral attacks. First cultivation experiments to characterize the phage-host interaction have shown the proviruses to be still functional and to cause a continuous lysis of the host cells. The burst size as well as the latent period are increased in the absence of organic carbon sources which indicates the dependency of viral proliferation on host cell´s carbon metabolism, e.g. autotrophy or heterotrophy. We further showed that cell debris that is released upon viral lysis of autotrophically grown hosts can be utilized by indigenous heterotrophs to enable cell growth. The release of organic carbon (cell debris) upon lysis of autotrophs, resembles viral-mediated transfer of inorganic carbon to the pool of labile organic carbon. These first results indicate that viruses potentially contribute to the maintenance of a labile organic carbon pool for deeply buried microbial communities.

References:
Engelen B, Ziegelmüller K, Wolf L, Köpke B, Gittel A, Treude T, Nakagawa S, Inagaki F, Lever MA, Steinsbu BO, Cypionka H (2008) Fluids from the oceanic crust support microbial activities within the deep biosphere. Geomicrobiol J 25:56-66
Fichtel K, Mathes F, Könneke M, Cypionka H, Engelen B (2012) Isolation of sulfate-reducing bacteria from sediments above the deep-subseafloor aquifer. Front Microbio 3:65
Engelhardt T, Orsi WD, Jørgensen BB (2015) Viral activities and life cycles in deep subseafloor sediments. EMI Rep 7(6): 868–873

IODP

Fluid inclusion analysis of quartz veins hosted by metamorphosed komatiites of the 3.3 Ga Mendon Formation, BARB4 drillcore, Barberton greenstone belt, South Africa

K. FARBER[1], A. DZIGGEL[1],

[1]Institute of Mineralogy and Economic Geology, Wüllnerstr. 2, 52062 Aachen

The 3.55-3.23 Ga. Barberton greenstone belt (BGB) is a well preserved Palaeoarchaen volcano-sedimentary sequence. As in other Palaeoarchaen greenstone belts, rocks of the BGB show pervasive alteration including widespread silicification and chert and quartz veining. The silicification is generally regarded as a result of fluid-rock interaction in shallow subseafloor convection cells, in which both seawater and hydrothermal fluid interacted with the Archaean crust (Hofmann and Harris, 2008). In an attempt to constrain the composition of the fluid responsible for the silicification, Farber et al. (2015a) analysed fluid inclusions in chert and quartz veins from the Mendon Formation using microthermometry and bulk crush-leach methods. It was found that the fluid inclusions are secondary and reflect a metamorphic overprint. In this study, we used fluid inclusion microthermometry and bulk crush-leach analyses of quartz veins hosted by altered

komatiites and silicified sediments from the BARB4 drill core, with the aim to provide further insight into the composition and evolution of fluids in the Mendon Formation. In contrast to the completely silicified komatiites (>90 wt.% SiO_2) studied by Farber et al. (2015a), those in the drill core are less silicified (≈50 wt.% SiO_2) and are locally characterised by a strong carbonate alteration.

The silicified sedimentary unit at the top of the Mendon Formation in the BARB4 drill core shows different layers of black chert and brownish layers of volcaniclastic detritus. The chert layers consist of carbonaceous matter, microcrystalline quartz and accessory chlorite and carbonate. These layers are brecciated by small quartz veins showing multiple vein generations. Sheet silicates often surround the veins, where they define a well-developed foliation. The ultramafic rock is mostly fine-grained and consists of carbonate, quartz, chlorite, muscovite, biotite, albite, and locally, K-feldspar, stilpnomelane, and anthophyllite. Primary minerals such as olivine or pyroxene have not been found but pseudomorphs and well-preserved spinifex textures are common throughout the core. Abundant veins of quartz, and less commonly carbonate or feldspar occur in the core. Quartz veins often show recrystallization features such as subgrain formation. Dolomite is found in veins and as idiomoprhic crystals in the matrix. Large vein crystals or cores of zoned crystals are more Fe-rich (X_{Fe} = 0.2) than the rims and late-formed idiomorphic grains in the matrix (X_{Fe} = 0.15). Chlorite in the black chert is Si-poor chamosite (Si = 5.3-5.6 a.p.f.u.;.X_{Fe} ≈ 0.6-0.7), whereas chlorite in the ultramafic part is Si-rich clinoclore (Si = 5.8-6.5; X_{Fe} ≈ 0.2). All other minerals are unzoned and have a homogeneous composition throughout the drill core.

General temperature constraints in the central BGB indicate maximum temperatures of 350°C during greenschist facies metamorphism (e.g. Grosch et al., 2012 and references therein). Outcrop samples of the Mendon Formation near the BARB4 drill site gave temperatures of 257 ± 31°C (Farber et al., 2015a). Pressures of 230-400 MPa and temperatures of 250 to 400°C have been calculated for our results of fluid inclusion microthermometry by intersecting the isochores with a 30°C/km-geotherm.

Microthermometry was done on quartz in five samples – one banded chert and four altered ultramafic rocks. Vein minerals contain abundant homogeneous two-phase (L+V) liquid-rich aqueous inclusions. The inclusions are found in trans- and intragranular trails and clusters and interpreted to be of secondary origin. Intragranular and isolated fluid inclusions in the banded chert and in the ultramafic samples have a similar homogenisation temperature (T_h) range of 130 to 200 °C, with most data ranging from 145 to 175 °C (Fig. 1). Salinities cluster in three different groups of high (20-27 wt.% NaCl equiv.), medium (10-15 wt.% NaCl equiv.) and low salinity (0.3-1.5 wt.% NaCl equiv.). The banded chert contains low and high salinity inclusions whereas the ultramafic samples each contain only one group. Fluid inclusion analysis reveals a slight decrease in salinity with increasing depth, which may indicate a progressive change in fluid composition or fluid mixing. The results are similar to the results of fluid inclusion analyses of quartz veins in strongly silicified komatiites of the Mendon Formation, which have salinities ranging from 3 to 11 % NaCl equiv. and T_h of 150 to 200°C (Farber et al., 2015a; Fig. 1).

Bulk crush-leach data plot near the seawater evaporation trend and the Na/Br vs Cl/Br ratios show the development to a highly saline fluid. This trend is not correlated to depth. These results are also similar to the results from crystalline vein cores of silicified komatiites (Farber et al., 2015a). Additionally, Na/K ratios of <10 indicate high fluid-rock ratios.

The composition of the fluid inclusions analysed within the drill core show similarities to those found in quartz veins in silicified komatiites of the Mendon Formation. The variation in T_h seems to be lower in drill core samples, but this may simply be a result of the smaller amount of inclusions analysed. The presence of high salinity inclusions indicates the occurrence of a highly saline fluid that locally mixed with the dominant lower salinity fluids. The high salinity might have been derived from fluid circulation through evaporites. There is no definite evidence for evaporites in the study area, although pseudomorphs after nahcolite or gypsum have been described (e.g. Lowe and Fisher Worrell, 1999). The presence of evaporites may also explain the very low B-isotope values found in hydrothermal tourmaline of the Mendon Formation (Farber et al., 2015b).

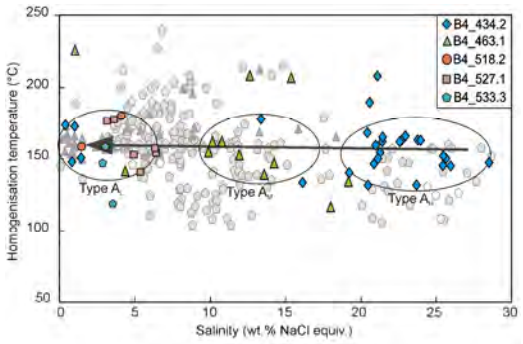

Fig. 1 Results of fluid inclusion microthermometry. Shaded polygons show literature data of inclusions in silicified komatiites (Farber et al., 2015a).

References:

Farber, K., Dziggel, A., Meyer, F.M., Prochaska, W., Hofmann, A., Harris, C., 2015a. Precambrian Research, 266: 150-164

Farber, K., Dziggel, A., Trumbull, R.B., Meyer, F.M., Wiedenbeck, M., 2015b. Chemical Geology, 417: 134-147.

Grosch, E.G., Vidal, O., Abu-Alam, T., McLoughlin, N., 2012.. Journal of Petrology, 53(3): 513-545.

Hofmann A., Harris C., 2008. Chemical Geology, 257(3-4): 221-239.

Lowe, D.R., Fisher Worrell, G., 1999. Special Paper - Geological Society of America, 329: 167-188.

IODP

Studies of groundwater flow at New Jersey Shallow Shelf

A. FEHR[1], F. PATTERSON[1], J. LOFI[2], S. REICHE[1]

[1]RWTH Aachen University, Applied Geophysics and Geothermal Energy, Aachen, Germany
[2]Géosciences Montpellier, Université Montpellier, France

During IODP Expedition 313, three boreholes were drilled in the so-called New Jersey transect to obtain deep sub-seafloor samples and downhole logging measurements in the inner shelf region. Hydrochemical studies revealed the groundwater situation as more complex than expected, characterized by several sharp boundaries between fresh and saline groundwater (Mountain et al., 2010). Two conflicting hypotheses regarding the nature of these freshwater reservoirs are currently debated. One hypothesis is that these reservoirs are connected with onshore aquifers and continuously recharged by seaward-flowing groundwater. The second hypothesis is that fresh groundwater was emplaced during the last glacial period.

From the three boreholes (M0027: 631 m, M0028: 668 m and M0029: 755 m) drilled with ~80 % core recovery during the expedition, a complete set of geophysical data and about 5800 m of downhole logging data are available. In addition to the petrophysical properties measured during IODP 313 expedition, Nuclear Magnetic Resonance (NMR) measurements were performed on samples from boreholes M0027, M0028 and M0029 in order to deduce porosities and permeabilities. These results are compared with data from alternative laboratory measurements and with petrophysical properties inferred from geophysical data and downhole logging data collected during Expedition 313.

We incorporate these results into a 2D numerical model that reflects the shelf architecture as known from drillings and seismic data to perform submarine groundwater flow simulations. In order to account for uncertainties related to the spatial distribution of physical properties, such as porosity and permeability, systematic variation of input parameters was performed during simulation runs.

The target is to test the two conflicting hypotheses of fresh groundwater emplacements offshore New Jersey and to improve the understanding of fluid flow processes at marine passive margins in general.

References:

Mountain G. M., Proust J.-N. and the Expedition 313 Science Party (2010): The New Jersey Margin Scientific Drilling Project (IODP Expedition 313): Untangling the Record of Global and Local Sea-Level Changes, in Scientific Drilling No. 10, September 2010, p. 26-34.
DOI: 10.2204/iodp.sd.10.03.2010

IODP

Climate Patterns of the early middle Eocene High-Resolution Planktonic Stable Isotope Data From IODP Expedition 342, Site 1408, Newfound-land Ridge

M. FELDTMANN, H. PÄLIKE, M. VAHLENKAMP, D. DE VLEESCHOUWER

MARUM – Center for Marine Environmental Sciences, University of Bremen, Leobener Straße, D-28359 Bremen, Germany

The Eocene is characterised by a transition from a virtually ice-free, greenhouse world during the early Eocene Climatic Optimum (EECO) towards an increasingly cooler climate resulting in the onset of Antarctic glaciation near the Eocene/Oligocene-Transition. However, high-resolution stable isotope datasets from critical intervals during the Eocene, particularly planktonic foraminifers, are yet missing, prohibiting further understanding of the detailed evolution of the mid-Eocene climate and resulting in this so-called Eocene Gap.

One of the reasons for this gap is a shallow calcite compensation depth (CCD) during the mid-Eocene that limited the deposition of carbonate-rich sediments (Pälike et al. 2012). IODP Site U1408 (Norris et al. 2014) bears carbonate-rich sediments from sediment drifts offshore of Newfoundland that were deposited above the CCD. High sedimentation rates of up to 3cm/kyr and good preservation of highly abundant planktonic foraminifers allow, for the first-time, the generation and analysis of high-resolution planktonic stable isotope data.

For this study, high-resolution stable isotope datasets ($\delta^{13}C$ and $\delta^{18}O$) of the planktonic foraminifera *Acarinina bullbrooki*, a mixed layer dweller and *Subbotina eocaena*, a thermocline dweller, have been established. The record spans magnetic polarity chron C20r (46.4~43.8 million years before present, Ma) with a resolution of 2.1 kyrs.

Preliminary stable isotope analysis reveals a high variance in the carbon stable isotope time series. *A.bullbooki* shows a variability of ~2.48‰, ranging from 1.07‰ to 3.55. This variability is especially pronounced during two newly described excursions at ~45.3 and 45 Ma. Thermocline dwelling *S. eocaena* shows lower values of 0.72‰ to 1.46‰ with an essentially lower variability of 0.74‰. The variability of the oxygen isotope data is similar for *A. bullbrooki* and *S. eocaena* with 0.9‰ or 1.04‰, respectively with a range of -2.1‰ to -1.2‰ or -1.73‰ to -0.69‰, respectively. *A. bullbrooki* shows a declining trend in the carbon stable isotope ratio, pronounced during intervals between 45.27 and 45.17 Ma as well as 45.02 and 44.68 Ma whereas S. eocaena displays no clear trend.

Initial stable isotope datasets thus reveal prominent carbon excursions in surface dwelling foraminifers and no similar response in thermocline dwelling species, perhaps driven by biological changes like symbiont change or morphological change of mixed layer A. bullbrooki . The stable oxygen isotope record shows a high fluctuation in the gradient between mixed layer and thermocline, but no trend. Possible drivers like preservation or water mass changes will be investigated next.

References:

Pälike, H., Lyle, M.W., Nishi, H., Raffi, I., Ridgwell, A., Gamage, K., Klaus, A., Acton, G., Anderson, L., Backman, J., Baldauf, J., Beltran, C., Bohatz, S. M., Bown, P., Busch, W., Channell, J. E. T., Chun, C.O.J., Delaney, M. Dewangan, P., Dunkley Jones, T. Edgar, K. M., Evans, H., Fitch, P., Foster, G. L., Gussone, N., Hasegawa, H.,

Hathorne, E.C., Hayashi, H., Herrle, J.O., Holbourn, A., Hovan, S., Hyeong, K., Iijima, K., Ito, T., Kamikuri, S.-I., Kimoto, K., Kuroda, J., Leon-Rodriguez, L., Malinverno, A., Moore Jr., T.C., Murphy, B. H., Murphy, D.P., Nakamura, H., Ogane, K., Ohneiser, C., Richter, C., Robinson, R., Rohling, E. J., Romero, O., Sawada, K., Scher, H., Schneider, L., Sluijs, A., Takata, H., Tian, J., Tsujimoto, A., Wade, B.S., Westerhold, T., Wilkens, R., Williams, T., Wilson, P.A., Yamamoto, Y., Yamamoto, S., Yamazaki, T. and Zeebe, R.E. (2012) A Cenozoic record of the equatorial Pacific carbonate compensation depth. Nature 488, 609–614

Norris, R.D., Wilson, P.A., Blum, P., Fehr, A., Agnini, C., Bornemann, A., Boulila, S., Bown, P.R., Cournede, C., Friedrich, O., Ghosh, A.K., Hollis, C.J., Hull, P.M., Jo, K., Junium, C.K., Kaneko, M., Liebrand, D., Lippert, P.C., Liu, Z., Matsui, H., Moriya, K., Nishi, H., Opdyke, B.N., Penman, D., Romans, B., Scher, H.D., Sexton, P., Takagi, H., Turner, S.K., Whiteside, J.H., Yamaguchi, T., and Yamamoto, Y.Scientists, 2014. Site U1408. In Norris, R.D., Wilson, P.A., Blum, P., and the Expedition 342 Scientists, Proc. IODP, 342: College Station, TX (Integrated Ocean Drilling Program).

ICDP

The long HSPDP-Chew Bahir record from southern Ethiopia: Enhancing our environmental record of anatomically modern human origins

V.FOERSTER[1], A. ASRAT[2], A. COHEN[3], R. GROMIG[4], C. GÜNTER[1], A. JUNGINGER[5], H.F. LAMB[6], F. SCHÄBITZ[7], M.H. TRAUTH[1], THE HSPDP SCIENCE TEAM

[1]University of Potsdam, Institute of Earth and Environmental Science; Karl-Liebknecht-Str. 24-25; Germany
[2]Addis Ababa University, School of Earth Sciences; P. O. Box 1176, Addis Ababa; Ethiopia
[3]University of Arizona, Department of Geosciences, Tucson, AZ 85721; USA
[4]University of Cologne, Institute of Geology and Mineralogy; Zülpicher Str. 49a; 50674 Cologne, Germany
[5]Eberhard Karls Universität Tuebingen, Department of Earth Sciences,
Senckenberg Center for Human Evolution and Palaeoenvironment (HEP-Tuebingen); Hölderlinstrasse 12; 72074 Tuebingen; Germany
[5]Aberystwyth University, Department of Geography and Earth Sciences; Aberystwyth SY23 3DB; U.K.
[6]University of Cologne, Seminar for Geography and Education; Gronewaldstrasse 2; 50931 Cologne; Germany

What role did climate dynamics play in human evolution and the dispersal of Homo sapiens within and beyond the African continent? In order to provide an environmental context to this central question, the ICDP-funded Hominin Sites and Paleolakes Drilling Project (HSPDP) has successfully completed coring five fluvio-lacustrine archives of climate change during the last ~3.5 Ma in East Africa. The five high-priority areas in Ethiopia and Kenya are located in close proximity to key paleoanthropological sites covering various steps in evolution. The Chew Bahir basin in southern Ethiopia is one of those sites, located ~90 km east of the Lower Omo River valley -site of the oldest known fossils of anatomically modern humans. Chew Bahir was cored in late 2014, yielding two (278.58 m and 266.38 m, >85% recovery) adjacent cores (HSPDP-CHB14-2A and 2B) from the western margin of the Chew Bahir rift basin. The long Chew Bahir record is expected to provide valuable insights into the pronounced moisture fluctuations during the last > 500 ka BP, a time interval that comprises the transition into the Middle Stone Age as well as the origin and dispersal of Homo sapiens.

We present here our initial results of the long HSPDP Chew Bahir cores, including the correlation of the two parallel sediment cores, the stratigraphy that was developed during the initial core description and several high-resolution multi sensor core logging (MSCL) data sets. The magnetic susceptibility data reveals cycles of ca. 15 m, 30 m, 50 m and 125 m, that can be tentatively linked with orbital cycles controlling wet-dry alternations in the Chew Bahir basin. A first chronology will be based on radiocarbon, OSL, Ar/Ar dating and paleomagnetics as soon as the ages have been determined. The sampling of the nearly continuous (>90%) composite core has been completed at a 32 cm routine sample spacing. The earliest results of the ~4,000 discrete sediment samples for further multi-proxy investigation show that the Chew Bahir deposits seem to have reacted sensitively towards changes in moisture influx, provenance, transport mechanisms and diagenetic processes. Combining our first results from the long cores with the results from a pilot study of short cores taken in 2009/10 along a NW-SE transect across the basin (Foerster et al., 2012, 2015, Trauth et al., 2015), we have developed a hypothesis linking climate forcing and paleoenvironmental signal formation processes in the basin, providing an important prerequisite for understanding the environmental record contained in the long sediment cores. X-ray diffraction on the first sample sets from the long Chew Bahir record show a similar process that has been recognized for the uppermost ~20 m during the pilot-study of the project: the diagenetic illitization of smectites during episodes of higher alkalinity and salinity in the closed-basin lake caused by a drier climate followed by a threshold-type formation of analcime during phases of pronounced aridity.

The good recovery and anticipated excellent time resolution of the cores will give us a continuous record of environmental fluctuations on decadal to orbital timescales, that will allow us to test current hypotheses of the influence of climate on human evolution and dispersal.

References:

Foerster, V., Vogelsang, R., Junginger, A., Asrat, A., Lamb, H.F., Schaebitz, F., Trauth, M.H., 2015. Environmental Change and Human Occupation of Southern Ethiopia and Northern Kenya during the last 20,000 years. Quaternary Science Reviews 129, 333–340.

Trauth, M.H., Bergner, A.G.N., Foerster, V., Junginger, A., Maslin, M.A., Schaebitz, F., 2015. Episodes of Environmental Stability and Instability in Late Cenozoic Lake Records of Eastern Africa. Journal of Human Evolution 87, 21–31.

Foerster, V., Junginger, A., Langkamp, O., Gebru, T., Asrat, A., Umer, M., Lamb, H., Wennrich, V., Rethemeyer, J., Nowaczyk, N., Trauth, M.H., Schäbitz, F., 2012. Climatic change recorded in the sediments of the Chew Bahir basin, southern Ethiopia, during the last 45,000 years, Quaternary International 274, 25–37.

HSPDP: http://hspdp.asu.edu/

ICDP

Progress and perspectives of the ICDP SCOPSCO project at Lake Ohrid (Macedonia, Albania)

A. FRANCKE[1], B. WAGNER[1], J. JUST[1], L. SADORI[2], H. VOGEL[3], K. LINDHORST[4], S. KRASTEL[4], N. LEICHER[1], R. GROMIG[1], G. ZANCHETTA[5], B. GIACCO[6], R. SULPIZIO[7,8], J. LACEY[9,10], M.J. LENG[9,10], A. DOSSETO[11], L. ROTHACKER[11], T. WILKE[12]

[1] University of Cologne, Cologne, Germany
[2] Sapienza University of Rome, Rome, Italy
[3] University of Bern, Bern, Switzerland
[4] Christian-Albrechts-Universität zu Kiel, Kiel, Germany
[5] University of Pisa, Pisa, Italy
[6] CNR, Rome, Italy
[7] University of Bari, Bari, Italy
[8] CNR, Milan, Italy
[9] University of Nottingham, Nottingham, UK
[10] British Geological Survey, Keyworth, Nottingham, UK
[11] University of Wollongong, Wollongong, Australia
[12] Justus-Liebig-University, Giessen, Germany

Lake Ohrid is located at the border of Macedonia and Albania (40°70′ N, 20°42 E, 698 m asl) is situated in a tectonic active, N-S trending graben and is considered to be the oldest lake in Europe. The lake is about 30 km long, 15 km wide and covers a surface area of about 358 km^2. The tub-shaped bathymetry of the lake basin is relatively simple with a maximum water depth of 293 m and a mean water depth of 150 m. To date, more than 300 endemic species are described in Lake Ohrid (Föller et al., 2015), which makes it the most diverse lake in the world when the surface area is taken into account. The catchment area of Lake Ohrid comprises about 2393 km^2 and also includes Lake Prespa, which drains into Lake Ohrid via the intensively karstified rocks of the Galicica Mountain range. Up to 50% of the inflow into Lake Ohrid originates from karstic inflow, with the remainder coming from direct precipitation and river and surface runoff from the up to 2200 m a.s.l. high surrounding mountains. The lake level of Lake Ohrid is balanced by evaporation (40%) and by surface outflow of the Crn Drim River to the North (60%).

Recent studies, encompassing the chronostratigraphic interpretation of prominent cyclic patterns of hydro-acoustic data (Lindhorst et al., 2015) and molecular clock analyses of DNA data (summarized by Wagner and Wilke, 2011), imply that the lake is around 2 Ma old. In order to obtain more information about the history of Lake Ohrid, more than 2100 m of sediment were recovered from 5 different drill sites between 2011 and 2013 within the scope of the ICDP SCOPSCO (Scientific Collaboration On Past Speciation Conditions in Lake Ohrid) project. The analytical work of the sediment cores is still in progress but results obtained so far already imply that the recovered sediments have the potential to substantially improve the understanding of the geological, biological, and environmental history of Lake Ohrid and the central Mediterranean region, and to address the main targets of the SCOPSCO project. The main targets are (1) to reveal the precise age and origin of Lake Ohrid, (2) to unravel the seismotectonic history of the lake area including effects of major earthquakes and associated mass wasting events, (3) to obtain a continuous record containing information on volcanic activities and climate changes in the central northern Mediterranean region, and (4) to better understand the impact of major geological/environmental events on general evolutionary patterns and shaping an extraordinary degree of endemic biodiversity as a matter of global significance.

During the first drilling campaign in 2011, a 10 m long sediment core using UWITEC platform and corers was retrieved from the LINI drill site from the western part of Lake Ohrid. On the basis of 3 tephra markers and 6 radiocarbon ages, a robust chronology was established, indicating that the sediment succession covers the Late Glacial and Holocene period. Lacey et al. (2015) conducted a high-resolution study of isotope and geochemical data, which improved the understanding of organic matter and calcite formation and preservation in the sediments of Lake Ohrid, and helped to understand proxy data response to environmental variability in the long cores. Wagner et al. (2012) could show on the same sediment sequence that an earthquake during the early 6th century likely triggered a massive, subaquatic mass-wasting event, which resulted in the sedimentation of a 2 m thick mass wasting deposit in the upper part of the succession.

The deep drilling campaign in 2013 was operated by DOSECC (Drilling, Observation and Sampling of the Earth´s Continental Crust) using the DLDS (Deep Lake Drilling System). Overall, more than 2100 m of sediments were recovered from four different drill sites. Three of these sites are located along the eastern and southeastern shoreline of the lake (CERAVA, GRADISTE, PESTANI). The aims of these three drill sites are to gather more information about: (1) the hydrological variability in Lake Ohrid ("CERAVA"-site, deepest hole: 90.48 meter below sediment depth (m blf)), (2) the biodiversity and mass wasting ("GRADISTE"-site, deepest hole: 123.41 m blf), and (3) the early development of the lake basin ("PESTANI"-site, deepest hole: 194.50 m blf). Due to the huge amount of sediment cores retrieved during the deep drilling, the cores from the marginal parts of Lake Ohrid have not been processed yet. The cores from the PESTANI site will be opened in the course of this summer at the University of Cologne, and a sampling party will be carried out for processing of the CERAVA and GRADISTE cores.

The cores from the main drill site, the DEEP site in the central part of Lake Ohrid have been opened, processed and subsampled at the University of Cologne since October 2013. In January 2016, we opened all cores for the establishment of a continuous composite profile down to the base of the sediment succession at 568.92 m blf. For this purpose, pre-selected core sections from the six drill holes retrieved at the DEEP site (more than 1500 m of sediments in total) were opened and processed. Processing of the cores includes high-resolution XRF scanning, MSCL-scanning, line-scan imaging, lithological core descriptions, core correlation, and core composition. After core composition, "meters below the sediment" (m blf) surface were replaced by "meter composite depth"(mcd). Sub-sampling is carried out at 8 cm resolution for proxy data analyses, and at 48 cm resolution for paleomagnetic studies. Macroscopic tephra layers are directly sampled after core opening and the major element composition of glass shards is analyzed at the University of Pisa and at IGAG-CNR in Rome, both in Italy. Presently, the laboratory work for the establishment of a multi-proxy data set down to the core base is ongoing and additional core sections, which have not been opened yet, are processed as described above.

The recovered sediment sequence from the DEEP site likely covers the entire history of Lake Ohrid, as a deeper penetration during the drilling operations was hampered by the occurrence of gravel and pebble-sized material. The coarse-grained basal deposits of the "DEEP"-site succession indicate that fluvial conditions prevailed when the graben structure of modern Lake Ohrid opened as a pull-apart basin. Fluvial and/or shallow lacustrine water conditions apparently persisted below ca. 420 m blf, where very heterogeneous deposits with clayey, silt-sized or gravelly sediments intersperse with several meter thick peat layers. First biogeochemical analyses on core catcher material and magnetic susceptibility measurements (MS) on the whole core yielded negligible total inorganic carbon (TIC) contents and high MS values below 420 m blf. Above 420 m sediment depth, the deposits appear homogenous and consist of silt-sized material with varying TIC and MS, which indicate more pelagic sedimentation in deeper waters. TIC and MS show cyclic oscillations on Milankovitch´s obliquity band (40 ka) until 270 m, and on Milankovitch´s eccentricity band (100 ka) above. This cyclic variability, likely connected to climatic change on glacial-interglacial time scales, imply that the DEEP site sediments are more than 1.2 Ma old (Wagner et al., 2014).

A more detailed core chronology for the upper part of the DEEP site sediments down to 247.8 mcd have been established by using tephrochronological information from 11 tephra layers (see Leicher et al., 2015 and associated contribution in this volume for more detailed information about tephrostratigraphic work) and by cross-correlation to orbital parameters (cf. Fig. 1). Geochemical and morphological analyses of glass shards from the tephra were used for correlation to well-known eruptions from Italian volcanoes, and the related radiocarbon and $^{40}Ar/^{39}Ar$ ages were transferred from the reference records to the DEEP site. For the OH-DP-0499 tephra at 49.947 mcd, correlated to the Tyrrhenian marker P-11, Zanchetta et al. (2015) suggest an age of 133±2 ka in consideration of its stratigraphic position and chronology in different records from the vicinity of Lake Ohrid. As the 11 tephra layers provide a robust basis for the age depth model of the DEEP site sequence, the tephrostratigraphic information was used as 1st order tie points.

The chronological information from the 11 tephra layers was also used to define cross correlation points to orbital parameters, which were included into the age depth model as 2nd order tie points. The tephra layers Y-5/CI, X-6, P-11, and A11/12 were deposited when there are minima in the TOC content and in the TOC/TN ratio and when there is an inflection point of increasing local summer insolation (21st June, 41°N) and an increasing winter season length (21st September to 21st March, cf. Fig. 1). Summer insolation and winter season length have a direct impact on the OM content and the TOC/TN ratio, as they trigger primary productivity during spring and summer and decomposition of OM during the mixing season. Low OM preservation and low TOC and TOC/TN in the sediments of Lake Ohrid may occur when summer insolation intensity and winter season length are balanced, i.e. when a long winter (mixing) season coincides with low summer insolation. In addition, the inflection points coincide with the perihelion passage in March. As the highest proportion of the annual radiation gets lost through surface albedo during spring (Berger et al., 1981), the period of the perihelion passage in March is characterized by cold and dry conditions in the central Mediterranean region (Magri and Tzedakis, 2000; Tzedakis et al., 2003; Tzedakis et al., 2006). Cold conditions at Lake Ohrid promote mixing during winter and restrict the primary productivity during summer. Thus, minima in TOC and TOC/TN are tuned to increasing insolation and winter season length.

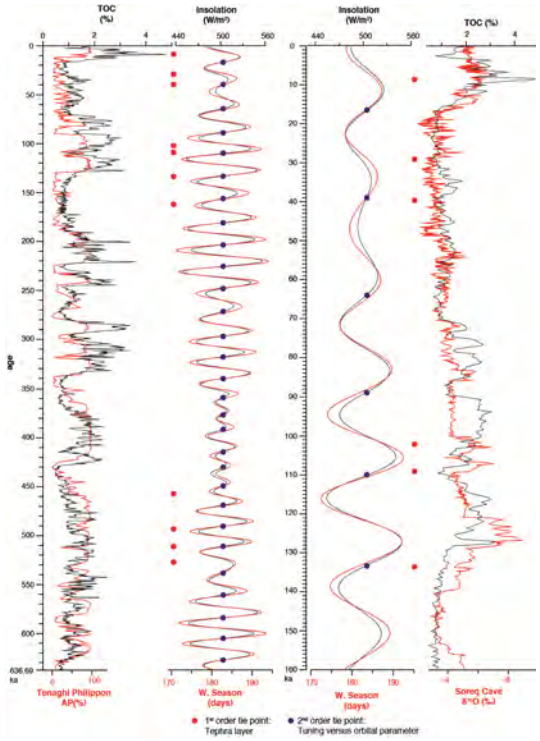

Figure 1. **Left:** Comparison between TOC (DEEP site) and arboreal pollen percentages (AP, Tenaghi Philippon, Tzedakis et al. (2006)) from 636.69 ka to the present. **Right:** Comparison between TOC (DEEP site) and $\delta^{18}O$ (Soreq Cave, Grant et al. (2012)) from 160 ka to the present. Red dots mark the tephrochonological age control points (1st order tie points), blue dots mark the TOC versus orbital parameter tuning points (2nd order tie points). The good correlation of the DEEP site TOC record with both Tenaghi Philippon and the Soreq Cave temporal series supports the age model of the DEEP site succession.

The 11 tephra layers and 31 cross correlation points of 2nd order were used for the establishment of an age-depth model. For the age depth modeling the Bacon 2.2 software package was used (Blaauw and Christen, 2011). The obtained age model yields that the sediment succession between 247.8 mcd and the sediment surface covers the time since 637 ka (corresponding to marine isotope stage (MIS) 16).

Based on the core chronology and on the lithological, sedimentological, and (bio-)geochemical data, the lake´s history including the development of the Lake Ohrid basin and the climatological variability on the Balkan Peninsula can be unraveled. The data imply that Lake Ohrid did not experience major catastrophic events such as extreme lake-level low stands or desiccation events during the last 637 kyrs. Hiatuses are absent and the DEEP site sequence provides an undisturbed and continuous archive of environmental and climatological change.

Overall, interglacial periods at Lake Ohrid are characterized by high primary productivity during summer,

restricted mixing during winter, and low erosion in the catchment. During glacial periods, the primary productivity is low and intense mixing of the water column promotes the decomposition of OM, which may have lowered the water pH and led to dissolution of calcite. Enhanced erosion of chemically altered siliciclastics and an overall higher clastic matter input into the lake during glacial periods can be a result of a less dense vegetation cover in the catchment and melt water run-off from local glacier on the surrounding mountains.

Following a strong primary productivity during spring and summer, the highest interglacial temperatures can be inferred for the first part of MIS11 and for MIS5. In contrast, somewhat lower spring and summer temperatures are observed for MIS15, 13, 9, and 7. The data also suggest that high ion and nutrient concentrations in the lake water promote calcite precipitation and diatom growth in the epilimnion during MIS15, 13, and 5, whereas less evaporated interglacial periods exhibit lower TIC and biogenic silica (bSi) contents (MIS9 and 7).

Most severe glacial conditions at Lake Ohrid occurred during MIS16, 12, 10, and 6, whereas somewhat warmer temperatures can be inferred for MIS14, 8, 4, and 2. Interglacial-like conditions occurred during parts of MIS14 and 8, respectively.

Once the severity and shaping of interglacial and glacial time periods at Lake Ohrid have been unraveled, future work will focus on more detailed high-resolution studies on shorter time periods. One period of particular interest is between 191 ka (MIS6) and 71 ka (MIS5). Previous studies based on hydro-acoustic and sediment core data from the northeastern part of the lake basin have shown that the lake level of Lake Ohrid was likely 60 m lower during MIS6. The 60 m lower lake level at Lake Ohrid during MIS6 can at least partly be explained by the ongoing subsidence, which persists in the basin until today. However, in the DEEP site sediments, the MIS6/MIS5 transition occurs at ca. 50 m sediment depth. This implies that climate-induced lake level fluctuation at Lake Ohrid are less severe compared for example to Lake Van (Turkey), were a 260 m lower lake level has been reported for the Younger Dryas, although Stockhecke et al. (2016) have shown that extensive dry conditions occur in the Mediterranean region during cold periods associated with a weakening of the Atlantic Meridional Overturning Circulation (AMOC).

The imprint of the environmental variations between 191 ka and 71 ka can also be seen in the catchment dynamics around the lake. Extraordinary high sedimentation rates, high clastic and negligible authigenic matter concentrations in DEEP site sediments during MIS6 imply enhanced erosion in the catchment despite relatively dry conditions. Thereby, elemental ratios (Zr/K) and environmental magnetic data (S-ratio) suggest that predominantly the products of chemical weathered, K-depleted old soils were transported into the lake. In contrast, a low sedimentation rate despite high authigenic matter concentrations during MIS5 implies less erosion in the catchment.

In order to obtain more information about the catchment dynamics at Lake Ohrid, future studies will encompass the analyses of uranium and lithium isotopes. U isotopes (^{234}U and ^{238}U) can be used to assess the balance between deep and shallow erosion, while Li isotopes (^{7}Li and ^{6}Li) can inform on the extent of chemical weathering in the sediment source area. The application of these tools on a Late Glacial to Holocene record from Lake Dojran (Macedonia, Greece) has recently shown that climatic perturbations (8.2 and 4.2 cooling event) and anthropogenic land use have a direct impact on the catchment dynamics.

References:

Berger, A., Guiot, J., Kukla, G., and Pestiaux, P.: Long-term variations of monthly insolation as related to climatic changes, Geol Rundsch, 70, 748-758, 10.1007/BF01822148, 1981.

Blaauw, M. and Christen, J. A.: Flexible paleoclimate age-depth models using an autoregressive gamma process, Bayesian Analysis, 6, 457-474, 10.1214/ba/1339616472, 2011.

Föller, K., Stelbrink, B., Hauffe, T., Albrecht, C., and Wilke, T.: Constant diversification rates of endemic gastropods in ancient Lake Ohrid: ecosystem resilience likely buffers environmental fluctuations, Biogeosciences, 12, 7209-7222, 10.5194/bg-12-7209-2015, 2015.

Grant, K. M., Rohling, E. J., Bar-Matthews, M., Ayalon, A., Medina-Elizalde, M., Ramsey, C. B., Satow, C., and Roberts, A. P.: Rapid coupling between ice volume and polar temperature over the past 150,000 years, Nature, 491, 744-747, 10.1038/nature11593, 2012.

Lacey, J. H., Francke, A., Leng, M. J., Vane, C. H., and Wagner, B.: A high-resolution Late Glacial to Holocene record of environmental change in the Mediterranean from Lake Ohrid (Macedonia/Albania), International Journal of Earth Sciences, 104, 1623-1638, 10.1007/s00531-014-1033-6, 2015.

Leicher, N., Zanchetta, G., Sulpizio, R., Giaccio, B., Wagner, B., Nomade, S., Francke, A., and Del Carlo, P.: First tephrostratigraphic results of the DEEP site record from Lake Ohrid, Macedonia, Biogeosciences Discuss., 12, 15411-15460, 10.5194/bgd-12-15411-2015, 2015.

Lindhorst, K., Krastel, S., Reicherter, K., Stipp, M., Wagner, B., and Schwenk, T.: Sedimentary and tectonic evolution of Lake Ohrid (Macedonia/Albania), Basin Research, 27, 84-101, 10.1111/bre.12063, 2015.

Magri, D. and Tzedakis, P. C.: Orbital signatures and long-term vegetation patterns in the Mediterranean, Quaternary International, 73–74, 69-78, 10.1016/S1040-6182(00)00065-3, 2000.

Stockhecke, M., Timmermann, A., Kipfer, R., Haug, G. H., Kwiecien, O., Friedrich, T., Menviel, L., Litt, T., Pickarski, N., and Anselmetti, F. S.: Millennial to orbital-scale variations of drought intensity in the Eastern Mediterranean, Quaternary Science Reviews, 133, 77-95, 10.1016/j.quascirev.2015.12.016, 2016.

Tzedakis, P. C., McManus, J. F., Hooghiemstra, H., Oppo, D. W., and Wijmstra, T. A.: Comparison of changes in vegetation in northeast Greece with records of climate variability on orbital and suborbital frequencies over the last 450 000 years, Earth and Planetary Science Letters, 212, 197-212, 10.1016/S0012-821X(03)00233-4, 2003.

Tzedakis, P. C., Hooghiemstra, H., and Pälike, H.: The last 1.35 million years at Tenaghi Philippon: revised chronostratigraphy and long-term vegetation trends, Quaternary Science Reviews, 25, 3416-3430, 10.1016/j.quascirev.2006.09.002, 2006.

Wagner, B. and Wilke, T.: Preface "Evolutionary and geological history of the Balkan lakes Ohrid and Prespa", Biogeosciences, 8, 995-998, 10.5194/bg-8-995-2011, 2011.

Wagner, B., Francke, A., Sulpizio, R., Zanchetta, G., Lindhorst, K., Krastel, S., Vogel, H., Rethemeyer, J., Daut, G., Grazhdani, A., Lushaj, B., and Trajanovski, S.: Possible earthquake trigger for 6th century mass wasting deposit at Lake Ohrid (Macedonia/Albania), Clim. Past, 8, 2069-2078, 10.5194/cp-8-2069-2012, 2012.

Wagner, B., Wilke, T., Krastel, S., Zanchetta, G., Sulpizio, R., Reicherter, K., Leng, M. J., Grazhdani, A., Trajanovski, S., Francke, A., Lindhorst, K., Levkov, Z., Cvetkoska, A., Reed, J. M., Zhang, X., Lacey, J. H., Wonik, T., Baumgarten, H., and Vogel, H.: The SCOPSCO drilling project recovers more than 1.2 million years of history from Lake Ohrid, Sci. Dril., 17, 19-29, 10.5194/sd-17-19-2014, 2014.

Zanchetta, G., Regattieri, E., Giaccio, B., Wagner, B., Sulpizio, R., Francke, A., Vogel, L. H., Sadori, L., Masi, A., Sinopoli, G., Lacey, J. H., Leng, M. L., and Leicher, N.: Aligning MIS5 proxy records from Lake Ohrid (FYROM) with independently dated Mediterranean archives: implications for core chronology, Biogeosciences Discuss., 12, 16979-17007, 10.5194/bgd-12-16979-2015, 2015.

IODP

The Climate History of the Mid-Depth Atlantic Deep Water Coral Reefs – Future needs for IODP?

N.FRANK[1,2], T. KRENGEL[2,] F. HEMSING[1], A. SCHRÖDER-RITZRAU[1], P. BLASER[1], M. LAUSECKER[1], J. FÖRSTEL[1], A.M. WEFING[1], L. BONNEAU[2,3], Q. DAUPHIN-DUBOIS[3], C. COLIN[3], E. DOUVILLE[4], D. BLAMART[4], D. VAN ROOIJ[5], J. LIPPOLD[6], M. GUTJAHR[7], P. MONTAGNA[8], C. WIENBERG[9], D. HEBBELN[9]

[1] Institute for Environmental Physics, University Heidelberg, INF229, 69120 Heidelberg, Germany
[2] Geosciences Institute, University Heidelberg, INF234, 69120 Heidelberg, Germany
[3] Laboratory of the Interactions and Dynamics of the Earth Surfaces Environments, University Paris-Sud, Bâtiment 504, 91405 Orsay, France
[4] Laboratory of Climate and Environmental Sciences, CEA, CNRS , USVQ, 91190 Gif-sur-Yvette, France
[5] Renard Center of Marine Geology, Department of Geology and Soil Science, Ghent University, Krijgslaan 281, Gent, Belgium
[6] Oeschger Center for Climate Change Research, University of Bern, Baltzerstrasse 1+3, CH-3012 Bern, Switzerland
[7] GEOMAR, Marine Biogeochemie, Wischhofstraße 1-3, D-24148 Kiel, Germany
[8] CNR - ISMAR - U.O.S. di Bologna –, Via Gobetti, 101 – 40129 Bologna, Italy
[9] MARUM, Centre for Marine Environmental Research, University Bremen, Leobener Str., D-28359 Bremen, Gemrnay

Framework forming cold-water corals are very unique archives of past ocean dynamics for the mid-depth eddy driven circulation at the upper part of the thermocline. For the past 800,000 years, corals can be dated by using U-series disequilibrium methods and beyond Sr-isotopes provide a valuable stratigraphic age tool. The hard parts of the coral skeletons store geochemical tracers, which permit assessing ambient seawater temperature, provenance of water masses and nutrient cycling (Robinson et al. 2013). During the past decades, numerous cold water coral reefs have been explored throughout the Atlantic from Brazil to Norway. One reef structure (Challenger Mound) was subject to a first IODP expedition (IODP 307), which retrieved 150m of coral bearing sediments spanning approximately 2.7 million years of time (Kano et al. 2007). Most recently, the seafloor drilling device MeBo (MARUM, Bremen) was successfully used during the Merian MSM36 cruise in 2014 to drill through coral mounds off Morocco and within the Alboran Sea. Corals as old as 1 million years can be expected on the seafloor based on first chronological studies.

The number of gravity cores collected on such coral mounds throughout the atlantic and Mediterranean Sea exceeds hundreds, but the time covered in 5 to 10m long cores is limited to the past few glacial cycles. Studies of those reefs reveal strongly discontinuous growth patterns on time scales of millennia, but also on time scales of hundreds of millennia. Often diagenesis of corals can be a major issue. The presence and absence of corals may be driven by numerous local factors, including bottom water current speed, fresh labile organic matter fluxes, temperature, availability of hardgrounds, and many others. However, the available data provides strong evidence that larger scale climate influences are key to the development of reefs. Since corals record environmental conditions during their short live spans (some years to decades) their remains provide punctuated but high resolution recordings of their environment. To constrain the environmental conditions during times of absent coral growth it is timely to envision coupled paleoceanographic studies from high resolution mid-depth pelagic sediments and coral bearing mounds. Here, we review the available evidences for links between climate driven coral growth throughout the Atlantic and large scale ocean dynamics according to previous studies (Frank et al. 2011; Wienberg et al. 2010; Matos et al. 2014; Henry et al. 2014). We will provide a first glance on what to expect if such studies would be coupled to conventional paleoceanographic recordings, to ultimately envision new IODP efforts answering pressing questions on the evolution of deep dwelling ecosystem hotspots near oceanographic gateways under climate stress.

References:

Robinson L. F, Adkins J. F, Frank N., Gagnon A. C, Prouty N. G, Brendan Roark E, van de Flierdt T., The geochemistry of deep-sea coral skeletons: A review of vital effects and applications for palaeoceanography, Deep Sea Research Part II: Topical Studies in Oceanography, 99, 184-198, (2013)

Kano, A.; Ferdelman, T. G; Williams, T.; Henriet, J. P.; Ishikawa, T.; Kawagoe, N.; Takashima, C.; Kakizaki, Y.; Abe, K.; Sakai, S.; Browning, E. L; Li, X. and IODP Expedition 307 scientific party, Age constraints on the origin and growth history of a deep-water coral mound in the northeast Atlantic drilled during Integrated Ocean Drilling Program Expedition 307. Geology, 35(11), 1051-1054, doi:10.1130/G23917A.1 (2007)

Matos L, Mienis F, Wienberg C, Frank N, Kwiatkowski C, Groeneveld J, Thil F., Abrantes F., Cunha M.R., Hebbeln D., Interglacial occurrence of col-water coral off Cape Lookout (NW Atlantic): First evidence of the Gulf stream influence, Deep Sea Research I, 105, 158-170, (2015)

Henry L.-A., Frank N., Hebbeln D., Wienberg C., Robinson L., van de Flierdt T., Dahl M., Douarin M., Morrison C. L, López Correa M., Rogers A.D, Ruckelshausen M., Roberts J. M., Global ocean conveyor lowers extinction risk in the deep sea, Deep Sea Research Part II, 99, 184-198, (2014)

Frank, N., Freiwald, A., Lopez Correa, M., Eisele, M., Hebbeln, D., Wienberg, C., van Rooij, D., Colin, C., van Weering, T., de Haas, H., Roberts, M., Buhl-Mortensen, P., B. de Mol, Douville, P., Blamart, D., and Hatte, C., North Atlantic cold-water coral reefs and climate, Geology, 39, 743-746 (2011)

Wienberg C., Frank N., Mertens K. N., Stuut J.-B., Mienis F., Marchant M., Hebbeln D., Glacial occurrence of cold-water corals in the Gulf of Cádiz - Implications of bottom current intensity and productivity, Earth and Planetary Science Letters 298, (3-4), 405-416 (2010)

ICDP

A simple and inexpensive technique for assessing microbial contamination during drilling operations

ANDRÉ FRIESE[1], DIRK WAGNER[1], JENS KALLMEYER[1]

[1]GFZ German Research Centre for Geosciences, Helmholtz Centre Potsdam, Section 5.3, Geomicrobiology, Telegrafenberg, 14473 Potsdam, Germany.

Exploration of the Deep Biosphere relies on drilling, which inevitably causes infiltration of drilling fluids, containing allochthonous microbes from the surface, into the core. Therefore it is absolutely necessary to trace contamination of the sediment core in order to identify uncontaminated samples for microbiological investigations.

Several techniques have been used in the past, including fluorescent dyes, perfluorocarbon tracers and fluorescent microspheres. Fluorescent dyes are inexpensive and easy to analyze on-site but are sensitive to light, pH and water chemistry. Furthermore, significant sorption to clays can decrease the fluorescence signal (Magal et al., 2008). Perfluorocarbon tracers are chemically inert hydrophobic compounds that can be detected with high sensitivity via gas chromatography (Smith et al., 2000),

which might be a problem for on-site analysis. Samples have to be taken immediately after core retrieval as otherwise the volatile tracer will have diffused out of the core. Microsphere tracers are small (0.2 - 0.5 µm diameter) fluorescent plastic particles that are mixed into the drilling fluid (Colwell et al., 1992). For analysis, these particles can be extracted from the sediment sample, transferred onto a filter and quantified via fluorescence microscopy. However, they are very expensive and therefore unsuitable for deep drilling operations that need large amounts of drilling fluids.

Here, we present an inexpensive contamination control approach using fluorescent pigments initially used for coloring plastics. The price of this tracer is nearly three orders of magnitude lower than conventional microsphere tracers. Its suitability for large drilling campaigns was tested at the ICDP Deep Drilling at Lake Towuti, Sulawesi, Indonesia. The tracer was diluted 1:1000 in lake water, which was used as the drilling fluid. Additionally, a plastic bag filled with 20 mL of undiluted tracer was attached to the core catcher to increase the amount of particles in the liner fluid right at the core. After core retrieval, the core was cut and the liner fluid collected. From each whole round core (WRC) that was taken for microbiological and biogeochemical analyses, small samples of 1 cm^3 were retrieved with sterile cutoff syringes from the rim, the center and an intermediate position. After dilution and homogenization in 9 mL MilliQ water, 10 µL of the sediment slurry was transferred onto a filter membrane and particles counted under fluorescence microscopy. Additionally, particles in the liner fluid were also quantified. This allows the quantification of the amount of drilling fluid that has entered the sediment sample during drilling. The minimum detectable volume of drilling fluid was in the order of single nanoliters per cm^3 of sediment, which is in the range of established techniques (Kallmeyer et al., 2006; Smith et al., 2000).

The presented method requires only a minimum of equipment and allows rapid determination of contamination in the sediment core and an easy to handle on-site analysis at low costs. The sensitivity is in the same range as perfluorocarbon and microsphere tracer applications. Thus, it offers an inexpensive but powerful technique for contamination assessment for future drilling campaigns.

References:

Colwell, F. S., Stormberg, G. J., Phelps, T. J., Birnbaum, S. A., McKinley, J., Rawson, S. A., . . . Grover, S. (1992). Innovative techniques for collection of saturated and unsaturated subsurface basalts and sediments for microbiological characterization. Journal of Microbiological Methods, 15(4), 279-292. doi: 10.1016/0167-7012(92)90047-8

Kallmeyer, J., Mangelsdorf, K., Cragg, B., & Horsfield, B. (2006). Techniques for contamination assessment during drilling for terrestrial subsurface sediments. Geomicrobiology Journal, 23(3-4), 227-239. doi: 10.1080/01490450600724258

Magal, E., Weisbrod, N., Yakirevich, A., & Yechieli, Y. (2008). The use of fluorescent dyes as tracers in highly saline groundwater. Journal of Hydrology, 358(1–2), 124-133. doi: 10.1016/j.jhydrol.2008.05.035

Smith, D. C., Spivack, A. J., Fisk, M. R., Haveman, S. A., Staudigel, H., & Party, L. (2000). Methods for quantifying potential microbial contamination during deep ocean coring. Ocean Drilling Program Technical Note. doi: 10.2973/odp.tn.28.2000

IODP

New insights on “elevated epifauna” as proxies for Mediterranean Outflow Water (MOW) reconstruction in the Gulf of Cadiz

ÁNGEL GARCÍA-GALLARDO[1], PATRICK GRUNERT[1], WERNER E. PILLER[1]

[1]Institute of Earth Sciences, University of Graz, NAWI-Graz, Heinrichstrasse 26, 8010 Graz, Austria.

The term “elevated epifauna” has been established for those benthic foraminifera adapted to inhabit elevated substrates (hard rocks, shells...) above the sediment surface to optimize food acquisition under the influence of strong bottom currents. In the Gulf of Cadiz, increased abundances of these taxa have been directly related to the presence of Mediterranean Outflow Water (MOW), providing a potentially powerful proxy for water mass reconstruction in the past. Quantitative analyses of Late Miocene to Early Pliocene benthic foraminifera from IODP Hole U1387C (IODP Expedition 339) was performed to reconstruct the onset of MOW. Multi-proxy records, including the elevated epifauna (represented by Planulina ariminensis, Cibicides lobatulus and C. refulgens) indicate the influence of Mediterranean waters only a few 100 kyrs after the opening of the Gibraltar Strait. However, our records show a clear correlation of peak abundances of C. lobatulus and C. refulgens with allochthonous shelf taxa and grain-size maxima, suggesting downslope transport to deeper settings. To clarify this issue, stable isotope analyses ($\delta^{18}O$, $\delta^{13}C$) have been performed on shells of shelf dwellers (Elphidium spp., Asterigerinata spp., Ammonia spp.), deep water epifauna (Cibicidoides pachyderma), infauna (Uvigerina peregrina), and elevated epifauna (C. lobatulus, P. ariminensis, C. refulgens) from the Pliocene sediments. Preliminary results show that C. lobatulus and C. refulgens are isotopically similar to the shelf dwellers. In contrast, shells of P. ariminensis show a signature close to the epifaunal C. pachyderma, suggesting their formation in deeper waters.

Our results suggest that in areas with unstable continental margins such as the Gulf of Cadiz the elevated epifauna is likely to be biased by downslope transport of taxa with a broad bathymetric range such as C. lobatulus and C. refulgens. Abundances of these taxa should be treated with caution when co-occurring with allochthonous shelf taxa. Other elements of the elevated epifauna such as P. ariminensis are restricted to slope environments and provide a more reliable indicator of bottom-current strength. In a next step, we will include foraminiferal shells of core-top samples in our analyses which will ultimately contribute to an improved understanding of the elevated epifauna as an indicator of MOW in the Gulf of Cadiz and bottom current strength in general.

IODP

The Arctic-Atlantic Gateway in the focus of continuing research and IODP initiatives

W. H. GEISSLER[1], A. C. GEBHARDT[1], J. MATTHIESSEN[1], J. KNIES[2]

[1]Alfred-Wegener-Institut Helmholtz-Zentrum für Polar- und Meeresforschung, Bremerhaven, Germany
[2]Geological Survey of Norway, Trondheim, Norway

The changing Arctic due to global warming became a hot topic over the last years. Therefore, it is of high interest to study the tectonic and climate history of the Arctic and its interrelations. One key region for the Arctic is the Arctic-Atlantic Gateway between Greenland to the west and the Svalbard/Barents Sea shelf to the east with the Fram Strait deep-water passage in its centre. This region encompassing several smaller ocean basins was the target of previous DSDP and ODP drilling campaigns (legs 38, 104, 151, 162), however, the last hole was drilled already two decades ago in 1996. Starting from these drilling campaigns and with the help of large geophysical datasets (bathymetry, seismic, gravity, and magnetic field data), knowledge on the tectonic evolution of the Northeast Atlantic Basins and continental margins increased. However, crucial issues are still the exact timing of tectonic phases and stratigraphic events and how these phases and events translate into seismic reflection stratigraphy.

In our contribution we want to document, why there is still continuing interest and need for research on the detailed timing of the Arctic-Atlantic Gateway opening phases and its consequences for ocean circulation, climate evolution in the Northern hemisphere and its influence on the glaciations both on Greenland and in the Svalbard-Barents Sea area.

IODP

Distinguishing detrital versus chemical remanent magnetization in marine sediments

S. GILDER[1], M. WACK[1], S. ROUD[1]

[1]Ludwig Maximilains Universität, Department of Earth and Environmental Sciences

Marine sediments from IODP cruises provide among the most detailed records of geomagnetic field behavior. Moreover, magnetic mineral concentrations from these archives often correlate with climate proxies, while relative paleointensity variations are used to calibrate nuclide production in the upper atmosphere. An overriding assumption when extracting and comparing geomagnetic field information from sediments is that the recording mechanism remained constant. The common hypothesis is that magnetic remanence is acquired via torque from the external field acting on a magnetic particle, which is termed a depositional or post-depositional remanent magnetization. However, chemical processes in the upper sediment layers can precipitate ferrimagnetic iron oxides and/or sulphides, thereby producing a chemical remanent magnetization. The physics behind the recording mechanisms between depositional and chemical remanences are fundamentally different, yet the potential influence of the latter is often ignored. Here, we show that sediments from ODP site 1063 in the Atlantic Ocean contain horizons of the chemical precipitate greigite, whereas previous studies from different working groups conclude magnetite is the sole remanence carrier. The identification was possible through experiments using an anhysteretic remanent magnetization, which is extremely time intensive, yet can be performed automatically with a homemade system, called the SushiBar, designed in Munich. We would like to further develop this technique and apply it to one other IODP core to better identify the presence of a chemical remanent magnetization.

IODP

Free and macromolecular-bound formate and acetate as potential substrates for the 2 km deep coalbed-biosphere offshore Shimokita, Japan (IODP Exp. 337)

C. GLOMBITZA[1], F. SCHWARZ[2], K. MANGELSDORF[3]

[1] Center for Geomicrobiology, Aarhus University, Aarhus, 8000, Denmark
[2] Helmholtz Centre Potsdam, German Research Centre for Geosciences GFZ, Potsdam, 14473, Germany

In summer 2012, the integrated Ocean Drilling Program (IODP) Expedition 337 retrieved the deepest core sample in the history of scientific ocean drilling from a depth of 2466 meters below sea floor and pioneered the riser drilling technique in scientific ocean drilling. Main target of the IODP Expedition 337 was a coal bearing horizon at approximately 2 km sediment depth with the aim to explore the deep biosphere associated to these organic matter rich layers (Inagaki et al., 2012). The primary objective was to explore the relationship of the deep subsurface biosphere and the subseafloor coalbeds. Some of the main scientific questions addressed by Expedition 337 were: Do deeply buried coalbeds act as geobiological reactors that sustain subsurface life by releasing nutrients and carbon substrates? What are the fluxes of both thermogenically and biologically produced organic compounds and what role do they play in subsurface carbon budgets? (Inagaki et al., 2012).

In subsurface environments, buried organic matter is the obvious carbon and energy source for microbial life (Arndt et al., 2013). With increasing burial depth sedimentary organic matter undergoes decomposition and structural alteration processes leading to complex macromolecular organic matter. Lignites and coals contain accumulated macromolecular organic matter of terrestrial origin with a total organic carbon content of usually more than 40%. During diagenesis structural alteration of the coal organic matter could result in the generation of smaller organic compounds that can serve as substrates for the metabolism of subsurface microbial communities. Important substrates for microbial metabolism (e.g. methanogenesis or sulfate reduction) are volatile fatty acids (VFAs) such as formate and acetate. In a previous study we have shown that lignites and sub-bituminous coals contain significant amounts of macromolecular–bound formate and acetate which are gradually released during diagenesis and early catagenesis in rates that are sufficient to sustain microbial metabolism (Glombitza et al., 2009). This shows that coals indeed can provide a substrate reservoir for the deep biosphere.

In the framework of the IODP Expedition 337 we have investigated the feedstock potential of the Shimokita coalbeds by quantifying the pool of macromolecular-bound

formate and acetate representing a substrate reservoir for future release during ongoing geological maturation. Additionally, we compared this pool to the water extractable pool of formate and acetate representing an VFA reservoir that is immediately available to the microbes without the breakdown of chemical bonds. For this purpose the freeze-dried and fine powdered coal samples were extracted with water during several days in a Soxhlet device. VFA concentrations were analysed by 2D IC-MS (Glombitza et al., 2014). The residue of the water extraction was additionally extracted by an organic solvent mixture to remove the bitumen from the sample. The residue containing the coal macromolecular organic material together with some inorganic matrix was subsequently subjected to an alkaline ester cleavage procedure to liberate the ester-bound VFAs. The cleaved acids were then analysed by ion chromatography (Glombitza et al., 2009).

The water extractable VFA pools in the coals were about 11 – 24 µmol g^{-1} sediment for formate and 8 – 18 µmol g^{-1} sediment for acetate. Extractable formate and acetate from the clayey siltstone and sandstone layers were significantly lower, 1.7 - 7 µmol g^{-1} sediment for both formate and acetate. The macromolecular-bound pools were higher for formate (coals: 42 – 130 µmol g^{-1} sediment, clayey siltstone and sandstone: 13 – 91 µmol g^{-1} sediment) and comparable for acetate (coals: 8 - 20 µmol g^{-1} sediment, clayey siltstone and sandstone: 1 – 8 µmol g^{-1} sediment). Based on estimated mean CO_2 respiration rates in the deep biosphere of 10^{-5} – 10^{-8} mg substrate g^{-1} sediment yr^{-1} (D'Hondt et al., 2002) we estimated a reservoir depletion time of 10^4 – 10^7 years representing a very rough estimate of the future time span during which the Shimokita coals beds could provide a sufficient supply of VFAs to the coalbed biosphere under the assumption of the published deep biosphere respiration rates. Generation rates for formate and acetate were previously calculated for a continuous maturation series from the New Zealand coal band with 6.1 x 10^{-7} mg g^{-1} sediment yr^{-1} for formate and 1.2 x 10^{-7} mg g^{-1} sediment yr^{-1} for acetate (Glombitza et al. 2009). On the basis of these numbers, we assume that microbial VFA turnover in the deep coalbed biosphere operates at rather low rates. Consequently, reservoir depletion times are most likely on the high side of the estimate and the substrate pools provided by formate and acetate alone have the potential to sustain the deep coalbed biosphere over geological times.

An interesting observation was made by comparison of the acetate to formate ratios from the macromolecular-bound pool to the water extractable, free VFA pool. Acetate to formate ratio is significantly lower in the bound pool (1:19 in the clayey siltstone and sandstone samples and 1:7 in the coal samples) than in the water extractable pool (1:0.75 in the clay and sandstone samples and 1:1.5 in coal samples). These differences might resemble microbial activity and could point either to a preferred removal or consumption of format from the free pool, a higher generation rate of acetate from macromolecular organic matter by hydrolysis or fermentation or an additional source of acetate to the extractable pool such as acetogenesis.

References:

Arndt, S., Jørgensen, B.B., LaRowe, D., Middelburg, J., Pancost, R., and Regnier, P. (2013). Quantifying the degradation of organic matter in marine sediments: A review and synthesis. Earth-Science Reviews.

D'Hondt, S., Rutherford, S., and Spivack, A.J. (2002). Metabolic Activity of Subsurface Life in Deep-Sea Sediments. Science 295, 2067-2070.

Glombitza, C., Mangelsdorf, K., and Horsfield, B. (2009). A novel procedure to detect low molecular weight compounds released by alkaline ester cleavage from low maturity coals to assess its feedstock potential for deep microbial life. Organic Geochemistry 40, 175-183.

Glombitza, C., Pedersen, J., Røy, H., and Jørgensen, B.B. (2014). Direct analysis of volatile fatty acids in marine sediment porewater by two-dimensional ion chromatography-mass spectrometry. Limnol. Oceanogr.: Methods 12, 455-468.

IODP

The tropical rain belt of western South America during early Pliocene

F. GRIMMER & L.M. DUPONT

MARUM – Center for Marine Environmental Sciences, Universität Bremen, Leobener Str., 28359 Bremen

A phenomenon of tropical climate that vividly displays the meeting point of the two hemispheres is the intertropical convergence zone (ITCZ). It is a region encircling the earth where the northeast and the southeast trade winds meet, characterized by low pressure, pronounced cloud formation and high levels of precipitation. The position of the ITCZ shifts seasonally following the sun's zenith point, but its average latitudinal position also shifts over longer timescales. While much is known about present annual ITCZ dynamics, also in relation to the El-Niño Southern Oscillation, major long-term shifts in the geological past, especially during the Pliocene are still controversially discussed. During the Pliocene, the progressive closure of the Central American Seaway (CAS) triggered a major reorganization of ocean and atmospheric circulation in the eastern Pacific and the Caribbean Sea, influencing also the latitudinal position of the ITCZ. The restriction of the surface water exchange between the Pacific Ocean and the Caribbean Sea is thought to have reached a critical threshold between 4.7 and 4.2 Ma. Both the eastern equatorial Pacific cold tongue and the pronounced sea surface salinity contrast between the Pacific and the Caribbean developed after the final closure of the CAS (Steph et al. 2010). While numeric modelling predicts a cooling of the eastern equatorial Pacific surface water directly after CAS closure resulting in a steeper east-west temperature gradient in the tropical Pacific and a northward shift of the ITCZ, paleoceanographic data from the Caribbean and the tropical Pacific indicate that the eastern equatorial Pacific cold tongue developed later and that the average position of the ITCZ moved southwards from a rather northern position during late Miocene and early Pliocene (Steph et al. 2006). The vegetation in Ecuador strongly depends on precipitation from the southernmost extension of the ITCZ, which is in turn influenced by sea surface temperatures and the east-west temperature gradient in the equatorial Pacific. A southern position of the ITCZ and a weak zonal temperature gradient (El-Niño like conditions) enhance precipitation over Ecuador.

Within the scope of this project, the aim is to determine the latitudinal position of the ITCZ over western South America during Pliocene. Thereby, the contradiction between numerical modelling results indicating a northward ITCZ shift and paleoceanographic data suggesting a southward ITCZ shift should be resolved. To tackle this, Pliocene vegetation changes in coastal Ecuador and the western Andean Cordillera are investigated using

marine palynological techniques. 25 samples from a marine sediment core drilled offshore Ecuador at ODP Site 1239 were analyzed focusing on the time window from 4.7 to 4.2 Ma. Pollen types were grouped according to ecosystem or habitat type for which they are most characteristic (Marchant et al. 2002). The applied chronology was developed by matching benthic isotope records with those from orbitally tuned nearby Site 1241, resulting in an indirectly orbitally tuned age model (Tiedemann et al. 2007).

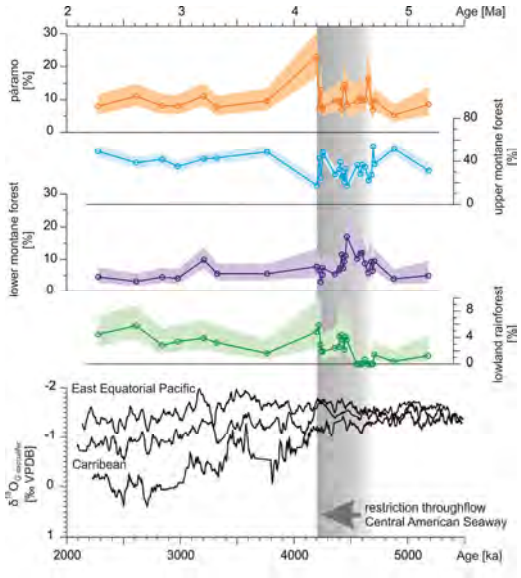

Vegetation change in Ecuador during the closure of the Central American Seaway. Pollen percentages of ODP Site 1239 offshore of Ecuador for four groups representing páramo, upper and lower montane forest, and lowland rain forest. Stable oxygen isotopes of the planktonic foraminifer G. *sacculifer* from ODP Sites 999 and 1000 in the Caribbean and ODP Site 1241 in the East Pacific after respectively Haug et al., Geology 29 (2001) 207, Steph et al. Proceedings ODP, Scientific results 202 (2006), and Steph et al. Paleoceanography 21 (2006) PA4221. During the throughflow restriction the representation of lowland rainforest increased indicating enhanced rainfall in northwestern Ecuador suggesting a southwand shift of the Intertropical Convergence Zone.

The pollen record comprises representatives from páramo, upper montane forest, lower montane forest and lowland rainforest. The latter group mainly includes spores of the Polypodiaceae. Pollen from upper montane forest are dominant in the marine sediments which is due to the better pollen production of some plants from this vegetation (for instance, Podocarpus or Hedyosmum). Also, the stronger winds at these high altitudes favor the aeolian seaward transport of pollen from páramo and upper montane forest. At 4.2 Ma, one sample indicates a strong increase in páramo vegetation. However, more samples need to be analyzed to confirm this observation. Between 4.7 and 4.2 Ma the relative abundance of lowland rainforest pollen and spores increases while that from the lower montane forest decreases. The number of spores compared to the number of pollen is generally high throughout this period. Grass pollen is low in abundance which indicates the lack of open habitats and substantiates a broad rainforest coverage.

In our preliminary interpretation the increase of lowland rainforest on the expense of the lower montane forest, as well as the high abundance of spores and the lack of open habitats, are an effect of more rainfall. We, therefore, corroborate the hypothesis of a southward shift of the ITCZ in line with paleoceanographic results.

References:

Marchant, R., Almeida, L., Behling, H., Berrio, J.C., Bush, M., Cleef, A., Duivenvoorden, J., Kappelle, M., De Oliveira, P., Teixeira de Oliveira-Filho, A., Lozano-Garcia, S., Hooghiemstra, H., Ledru, M.-P., Ludlow-Wiechers, B., Markgraf, V., Mancini, V., Paez, M., Prieto, A., Rangel, O. & Salgado-Labouriau, M.L., 2002. Distribution and ecology of parent taxa of pollen lodged within the Latin American Pollen Database. Review of Palaeobotany and Palynology, 121, 1-75.

Steph, S., Tiedemann, R., Prange, M., Groeneveld, J., Nürnberg, D., Reuning, L., Schulz, M. & Haug, G., 2006. Changes in Caribbean surface hydrography during the Pliocene shoaling of the Central American Seaway. Paleoceanography, 21, PA4221: 1-25.

Steph, S., Tiedemann, R., Prange, M., Groeneveld, J., Schulz, M., Timmermann, A., Nürnberg, D., Rühlemann, C., Saukel, S. & Haug, G., 2010. Early Pliocene increase in thermohaline overturning: A precondition for the development of the modern equatorial Pacific cold tongue. Paleoceanography, 25, PA2202: 1-17.

Tiedemann, R., Sturm, A., Steph, S., Lund, S.P. & Stoner, J., 2007. Astronomically calibrated timescales from 6 to 2.5 Ma and benthic isotope stratigraphies, Sites 1236, 1237, 1239, and 1241. Tiedemann, R., Mix, A.C., Richter, C. & Ruddiman, W.F. (eds.). Proceedings Ocean Drilling Program, Scientific Results, 202. ODP, College Station (TX).

IODP

Impact of the Indonesian Throughflow on northwestern Australian biochronology (5-1.8 Ma)

J. GROENEVELD[1], AND EXP. 356 SCIENTISTS

[1]Center for Marine Environmental Sciences (MARUM), University Bremen, Klagenfurterstrasse, D-28359 Bremen, Germany

International Ocean Discovery Program (IODP) Expedition 356 (August-September 2015) drilled a transect across 10° latitude of seven shelf and upper slope sites (Sites U1458-U1464) off Western Australia from the Perth Basin, through the Northern Carnarvon Basin, to the Roebuck Basin with the RV Joides Resolution. One of the main objectives was documenting the evolution of the Indonesian Throughflow (IT) since the Early Pliocene, a critical component of global thermohaline circulation and a driver of the southward-flowing Leeuwin Current (Gallagher et al., 2014). This in turn has influenced the development of aridity in Australia and the onset of the Australian monsoon.

Despite the modern shallow water depth of the sites, significant subsidence during the Late Miocene created an upper-bathyal setting, so that open-marine conditions prevailed during the Pliocene. This setting, which is located directly in the outflow of the IT, allowed accumulation of a unique sequence of sediments constituting a high-resolution record of IT changes since the Early Pliocene. Previous studies from the Maritime Continent (Molnar and Cronin, 2015) and from further offshore western Australia (Karas et al., 2011) have shown that significant changes in the IT occurred during the Pliocene. However, high-resolution records from directly within the outflow, which have the potential to directly link these changes to development of aridity and the monsoon across Australia, were lacking prior to Expedition 356.

Based on shipboard data, Site U1463 in the Northern Carnarvon Basin has the potential to become a reference site, not only for the Northwest Shelf, but also for the entire Indian Ocean for the Early Pleistocene-Pliocene time interval (1.8-5 Ma). Paleo-water depth at the site was

500-1000 m, and the site was far enough offshore to deposit mainly homogeneous mudstones with abundant foraminifera.

Creating a reliable reference requires a well-constrained age model. It is therefore planned to create a benthic foraminiferal stable oxygen isotope record with orbital-scale resolution that will be tuned to the benthic $\delta^{18}O$ stack of Lisiecki and Raymo (2005). This age model will then be used to calibrate the planktonic foraminiferal biostratigraphy. Biochronology is an essential part of paleoceanographic research as again proven by the Expedition 356 shipboard results (Fig. 1).

Indian Ocean planktonic foraminiferal biochronology and its calibration to the Geological Time Scale (Gradstein et al., 2012), however, is still largely unknown. Typically Pliocene bio-datums are either from the Atlantic or the Pacific and often have large differences between them, which may have been caused by tectonically driven changes in the IT. The objective of this project is calibrate Indian Ocean biochronology, based on Site U1463 analyses, on an orbitally-tuned benthic 18O time scale. This will allow major changes in the Indian Ocean to be linked to other oceanic basins and to changes in the IT.

References:

Gallagher, S.J., Fulthorpe, C.S., Bogus, K.A., (2014). Reefs, oceans, and climate: a 5 million year history of the Indonesian Throughflow, Australian monsoon,
and subsidence on the northwest shelf of Australia. International Ocean Discovery Program Scientific Prospectus, 356. http://dx.doi.org/10.14379/iodp.sp.356.2014.

Gallagher, S.J., Fulthorpe, C.S., Bogus, K., and the Expedition 356 Scientists, (2016). *Expedition 356 Preliminary Report: Indonesian Throughflow*. International Ocean Discovery Program. http://dx.doi.org/10.14379/iodp.pr.356.2015.

Gradstein, F.M., Ogg, J.G., Schmitz, M.D., and Ogg, G.M. (Eds.), 2012. The Geological Time Scale 2012: Amsterdam (Elsevier).

Karas, C., Nürnberg, D., Tiedemann, R., and Garbe-Schönberg, D., (2011). Pliocene Indonesian Throughflow and Leeuwin Current dynamics: implications for
Indian Ocean polar heat flux. Paleoceanography, 26(2):PA2217.

Lisiecki, L. E., and M. E. Raymo (2005), A Pliocene-Pleistocene stack of 57 globally distributed benthic $\delta^{18}O$ records, Paleoceanography, 20, PA1003,
doi:10.1029/2004PA001071.

Molnar, P., and T. W. Cronin (2015). Growth of theMaritime Continent and its possible contribution to recurring Ice Ages. Paleoceanography 30. doi:10.1002/
2014PA002752.

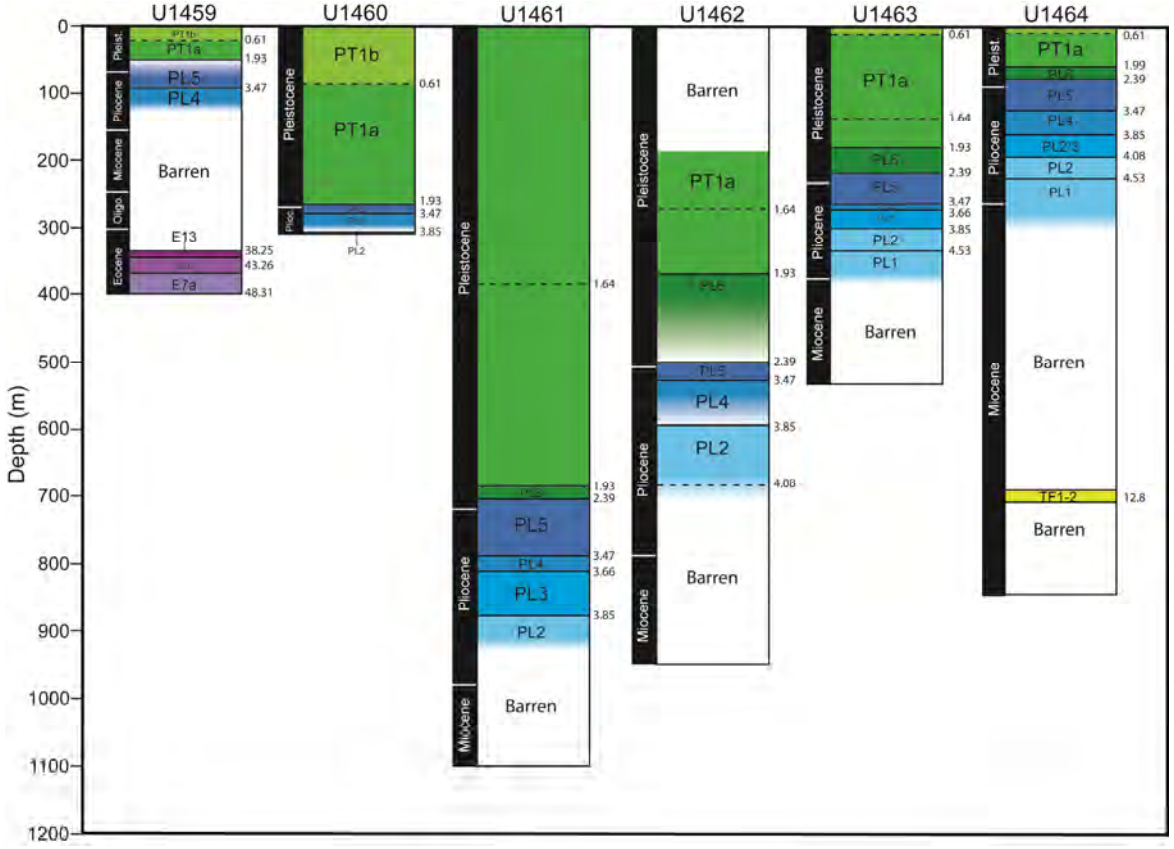

Figure 1) Biostratigraphic biozones for planktonic foraminifera recovered during IODP Expedition 356 (Gallagher et al., 2016). Site U1463 has the most complete and best preserved open-marine classifying it as possible reference site for paleoceanographic records of the Northwest Shelf and the Indian Ocean. Proposed samples cover biozones PL1-PL6 of Site U1463; additionally samples of biozones PL1-PL2 of Site U1464 will be included.

IODP

Early history of Mediterranean-Atlantic exchange – new insights from IODP Expedition 339

PATRICK GRUNERT[1], ÁNGELA GARCÍA-GALLARDO[1], MARLIES VAN DER SCHEE[2], GERALD AUER[1], BARBARA BALESTRA[3], FRANCISCO JIMÉNEZ-ESPEJO[4], CARL RICHTER[5], CARLOS ALVAREZ ZARIKIAN[6], ULLA RÖHL[7], JOSÉ-ABEL FLORES[2], FRANCISCO J. SIERRO[2], WERNER E. PILLER[1]

[1] Institute of Earth Sciences, University of Graz, NAWI Graz, Heinrichstrasse 26, 8010 Graz, Austria
[2] Department of Geology, University of Salamanca, Spain
[3] Institute of Marine Sciences, University of California Santa Cruz, United States of America
[4] Department of Biogeochemistry, Japan Agency for Marine-Earth Science and Technology (JAMSTEC), Yokosuka, Japan
[5] School of Geosciences, University of Louisiana at Lafayette, United States of America
[6] International Ocean Discovery Program, Texas A&M University, College Station, TX 77845, United States of America
[7] MARUM – Center for Marine Environmental Sciences, University of Bremen, Germany

Mediterranean Outflow Water (MOW) is a considerable source of heat and salt for today's North Atlantic and contributes to maintaining the Atlantic meridional overturning circulation (AMOC). There is evidence that MOW intensity varied on glacial/interglacial and stadial/interstadial timescales in the past, and that phases of MOW intensification potentially preconditioned the thermohaline circulation for its interglacial mode in the late Pleistocene (Rogerson et al., 2012; Bahr et al, 2014). Until recently, however, efforts towards a better understanding of MOW behavior through time and potential climatic feedback mechanisms between MOW, the African Monsoon, AMOC, and eustatic sea-level fluctuations have been impeded by the limitation of available sample material largely to the uppermost Pleistocene and Holocene. In 2011/12, IODP Expedition 339 drilled several sites in the Gulf of Cadiz and off the western Iberian Margin, recovering a total of 4.5 km of Pliocene to Holocene contouritic deposits of MOW (Hernández-Molina et al., 2014).

In this paper, we present new findings on early MOW history from IODP Sites U1387 and U1389, specifically its onset after the Messinian Salinity Crisis and its behavior at the transition from the late Pliocene warmhouse to early Pleistocene icehouse climate. New micropalaeontological and geochemical records suggest that IODP Site U1387 is affected by Mediterranean water shortly after the opening of the Gibraltar Strait and before the onset of contourite drift deposition, representing the first signs of the Mediterranean-Atlantic exchange. At IODP Site U1389, cyclic patterns are recognized in the $CaCO_3$ and TOC contents as well as Ca/Ti- and Zr/Al-ratios of upper Pliocene and lower Pleistocene sediments. A preliminary cyclostratigraphic analysis of these records in well-recovered intervals suggests an interplay of obliquity and precessional forcing on the depositional environment. A significant change from deposits strongly influenced by terrestrial input to deposits strongly affected by MOW occurs at ~2.8-2.6 Myrs, coinciding with the onset of Northern Hemisphere Glaciation.

This study contributes to project P25831-N29 of the Austrian Science Fund (FWF) and is financially supported by grants of ECORD and the Max Kade Foundation.

References:

Bahr, A., Jiménez-Espejo, F.J., Kolasinac, N., Grunert, P., Hernández-Molina, F.J., Röhl, U., Voelker, A.H.L., Escutia, C., Stow, D.A.V., Hodell, D., Alvarez-Zarikian, C.A., 2014. Deciphering bottom current velocity and paleoclimate signals from contourite deposits in the Gulf of Cádiz during the last 140 kyrs: An inorganic geochemical approach. Geochemistry, Geophysics, Geosystems 15, doi:10.1002/2014GC005356.

Hernández-Molina, F.J., Stow, D.A.V., Alvarez Zarikian, C.A., Acton, G., Bahr, A., Balestra, B., Ducassou, E., Flood, R.D., Flores, J.-A., Furota, S., Grunert, P., Hodell, D., Jimenez-Espejo, F., Kim, J.K., Krissek, L., Kuroda, J., Li, B., Llave, E., Lofi, J., Lourens, L., Miller, M., Nanayama, F., Nishida, N., Richter, C., Roque, A.C., Sanchez Goñi, M.F., Sierro, F.J., Singh, A.D., Sloss, C., Takashimizu, Y., Tzanova, A., Voelker, A., Williams, T., Xuan, C., 2014. Onset of Mediterranean outflow into the North Atlantic. Science 344, 1244–1250.

Rogerson, M., Rohling, E.J., Bigg, G.R., Ramirez, J., 2012. Palecoeanography of the Atlantic-Mediterranean exchange: overview and first quantitative assessment of climatic forcing. Reviews of Geophysics 50, RG2003.

IODP

Drake Passage and proximal-Antarctic Weddell Sea bottom water Pb isotopic records trace ice sheet dynamics and regional circulation patterns during the past 38 ka

M. GUTJAHR[1], F. KIRSCH[1], G. KUHN[2]

[1] GEOMAR Helmholtz Centre for Ocean Research Kiel, Wischhofstrasse 1-3, 24148 Kiel, Germany, mgutjahr@geomar.de;
[2] Alfred-Wegener-Institut, Helmholtz-Zentrum für Polar- und Meeresforschung, Am Alten Hafen 26, 27568 Bremerhaven, Germany, gerhard.kuhn@awi.de

Dissolved lead (Pb) is dominantly supplied to the oceans via the interplay of physical and chemical weathering on the continents. Because of its short residence time in seawater on the order of only a few decades, most Pb in near-Antarctic Southern Ocean settings will be derived from Antarctica. In contrast to other isotope systems such as neodymium (Nd), under glacial weathering regimes Pb is not supplied congruently to the ocean. As a consequence the Pb isotopic runoff flux can be significantly more radiogenic (higher $^{206,207,208}Pb/^{204}Pb$) than the average continental source catchment composition. The degree to which the bulk runoff Pb isotope signal is altered towards radiogenic Pb isotope compositions is a function of source lithology, the rate of both physical (e.g., glacial) and sub-glacial chemical weathering partially dissolving accessory mineral phases. Recently deglaciated landscapes in northeast North America for instance released a highly radiogenic Pb isotope signal into continental runoff during the last deglaciation (*1-3*).

In order to trace glacial-interglacial Antarctic ice sheet dynamics in the Drake Passage and the Weddell Sea, we analysed two sediment cores for their authigenic Fe-Mn oxyhydroxide-derived Pb isotopic evolution (*4*). While the sediment core in the southeastern Drake Passage was always exposed to open seawater conditions, the near Antarctic sediment core was situated under or near the sea-ice edge during the Last Glacial Maximum (*5*). Both sediment cores show distinct authigenic Pb isotope trends. In the Drake Passage, least radiogenic Pb isotopic compositions were recorded at 32 ka, while most radiogenic Pb isotope ratios were recovered during the deglacial interval (16-10 ka). The signal appears less radiogenic during the early Holocene yet changes to intermediate compositions during the latter part of the Holocene. We note that the average composition of this Drake Passage sediment core location is in excellent agreement with surface compositions recorded from nearby Southern Ocean Fe-Mn nodules (*6*).

The second core recovered from the east Antarctic continental rise provided significantly more extreme compositions during the glacial interval. The glacial section is generally highly radiogenic, however with a clearly resolvable unradiogenic excursion between 25 to 23 ka. The Pb isotopic signal changed to less extreme compositions during the early deglaciation yet remained elevated until the early Holocene, when compositions dropped to rather indistinct open ocean Pb isotopic values reported for Fe-Mn nodules further north from the sediment site (*6*).

Importantly, elemental Al/Pb ratios, measured alongside the Pb isotopic compositions from these samples are consistently below 100 for all but the youngest sample, providing evidence that no significant fraction of the terrigenous fraction was dissolved during reductive extraction of the authigenic Pb isotope signal (*2, 4*). The glacial radiogenic sections of both cores were not accompanied by elevated Al/Pb.

In this presentation we will discuss the implications of our findings with regard to Antarctic ice sheet dynamics and sub-glacial weathering input in response to deglacial warming.

References:

M. Gutjahr, M. Frank, A. N. Halliday, L. D. Keigwin, Retreat of the Laurentide ice sheet tracked by the isotopic composition of Pb in western North Atlantic seawater during termination 1. Earth and Planetary Science Letters 286, 546-555 (2009).

F. Kurzweil, M. Gutjahr, D. Vance, L. Keigwin, Authigenic Pb isotopes from the Laurentian Fan: Changes in chemical weathering and patterns of North American freshwater runoff during the last deglaciation. Earth and Planetary Science Letters 299, 458-465 (2010).

K. C. Crocket, D. Vance, G. L. Foster, D. A. Richards, M. Tranter, Continental weathering fluxes during the last glacial/interglacial cycle: insights from the marine sedimentary Pb isotope record at Orphan Knoll, NW Atlantic. Quaternary Science Reviews 38, 89-99 (2012).

M. Gutjahr et al., Reliable extraction of a deepwater trace metal isotope signal from Fe-Mn oxyhydroxide coatings of marine sediments. Chemical Geology 242, 351-370 (2007).

C.-D. Hillenbrand et al., Reconstruction of changes in the Weddell Sea sector of the Antarctic Ice Sheet since the Last Glacial Maximum. Quaternary Science Reviews 100, 111-136 (2014).

W. Abouchami, S. L. Goldstein, A lead isotopic study of circum-Antarctic manganese nodules. Geochimica et Cosmochimica Acta 59, 1809-1820 (1995).

IODP

Drake Passage and proximal-Antarctic Weddell Sea bottom water Pb isotopic records trace ice sheet dynamics and regional circulation patterns during the past 38 ka

M. GUTJAHR[1], F. KIRSCH[1], G. KUHN[2]

[1] GEOMAR Helmholtz Centre for Ocean Research Kiel, Wischhofstrasse 1-3, 24148 Kiel, Germany, mgutjahr@geomar.de;

[2] Alfred-Wegener-Institut, Helmholtz-Zentrum für Polar- und Meeresforschung, Am Alten Hafen 26, 27568 Bremerhaven, Germany, gerhard.kuhn@awi.de

Dissolved lead (Pb) is dominantly supplied to the oceans via the interplay of physical and chemical weathering on the continents. Because of its short residence time in seawater on the order of only a few decades, most Pb in near-Antarctic Southern Ocean settings will be derived from Antarctica. In contrast to other isotope systems such as neodymium (Nd), under glacial weathering regimes Pb is not supplied congruently to the ocean. As a consequence the Pb isotopic runoff flux can be significantly more radiogenic (higher $^{206,207,208}Pb/^{204}Pb$) than the average continental source catchment composition. The degree to which the bulk runoff Pb isotope signal is altered towards radiogenic Pb isotope compositions is a function of source lithology, the rate of both physical (e.g., glacial) and sub-glacial chemical weathering partially dissolving accessory mineral phases. Recently deglaciated landscapes in northeast North America for instance released a highly radiogenic Pb isotope signal into continental runoff during the last deglaciation (*1-3*).

In order to trace glacial-interglacial Antarctic ice sheet dynamics in the Drake Passage and the Weddell Sea, we analysed two sediment cores for their authigenic Fe-Mn oxyhydroxide-derived Pb isotopic evolution (*4*). While the sediment core in the southeastern Drake Passage was always exposed to open seawater conditions, the near Antarctic sediment core was situated under or near the sea-ice edge during the Last Glacial Maximum (*5*).

Both sediment cores show distinct authigenic Pb isotope trends. In the Drake Passage, least radiogenic Pb isotopic compositions were recorded at 32 ka, while most radiogenic Pb isotope ratios were recovered during the deglacial interval (16-10 ka). The signal appears less radiogenic during the early Holocene yet changes to intermediate compositions during the latter part of the Holocene. We note that the average composition of this Drake Passage sediment core location is in excellent agreement with surface compositions recorded from nearby Southern Ocean Fe-Mn nodules (*6*).

The second core recovered from the east Antarctic continental rise provided significantly more extreme compositions during the glacial interval. The glacial section is generally highly radiogenic, however with a clearly resolvable unradiogenic excursion between 25 to 23 ka. The Pb isotopic signal changed to less extreme compositions during the early deglaciation yet remained elevated until the early Holocene, when compositions dropped to rather indistinct open ocean Pb isotopic values reported for Fe-Mn nodules further north from the sediment site (*6*). Importantly, elemental Al/Pb ratios, measured alongside the Pb isotopic compositions from these samples are consistently below 100 for all but the youngest sample, providing evidence that no significant fraction of the terrigenous fraction was dissolved during reductive extraction of the authigenic Pb isotope signal (*2, 4*). The glacial radiogenic sections of both cores were not accompanied by elevated Al/Pb.

In this presentation we will discuss the implications of our findings with regard to Antarctic ice sheet dynamics and sub-glacial weathering input in response to deglacial warming.

References:

M. Gutjahr, M. Frank, A. N. Halliday, L. D. Keigwin, Retreat of the Laurentide ice sheet tracked by the isotopic composition of Pb in western North Atlantic seawater during termination 1. Earth and Planetary Science Letters 286, 546-555 (2009).

F. Kurzweil, M. Gutjahr, D. Vance, L. Keigwin, Authigenic Pb isotopes from the Laurentian Fan: Changes in chemical weathering and patterns of North American freshwater runoff during the last deglaciation. Earth and Planetary Science Letters 299, 458-465 (2010).

K. C. Crocket, D. Vance, G. L. Foster, D. A. Richards, M. Tranter, Continental weathering fluxes during the last glacial/interglacial cycle: insights from the marine sedimentary Pb isotope record at Orphan Knoll, NW Atlantic. Quaternary Science Reviews 38, 89-99 (2012).

M. Gutjahr et al., Reliable extraction of a deepwater trace metal isotope signal from Fe-Mn oxyhydroxide coatings of marine sediments. Chemical Geology 242, 351-370 (2007).
C.-D. Hillenbrand et al., Reconstruction of changes in the Weddell Sea sector of the Antarctic Ice Sheet since the Last Glacial Maximum. Quaternary Science Reviews 100, 111-136 (2014).
W. Abouchami, S. L. Goldstein, A lead isotopic study of circum-Antarctic manganese nodules. Geochimica et Cosmochimica Acta 59, 1809-1820 (1995).

IODP

High resolution variability in the Quaternary Indian monsoon inferred from records of clastic input and paleo-production recovered during IODP Expedition 355

A.HAHN[1], M.W. LYLE[2], D.K. KULHANEK[3], S. ANDÒ[4] P.D. CLIFT[5], AND EXPEDITION 355 SCIENTISTS

[1] MARUM, University of Bremen, Bremen, Germany
[2] College of Earth, Ocean and Atmospheric Sciences, Oregon State University, Corvallis, OR, USA
[3] International Ocean Discovery Program, Texas A&M University, College Station, TX, USA
[4] Department of Earth and Environmental Sciences, University of Milano-Bicocca, Milano, Italy
[5] Louisiana State University, Baton Rouge, LA, USA

The sediment cores obtained from the Indus fan at Site U1457 during Expedition 355 of the International Ocean Discovery Program (IODP) contain a ca. 100m spliced section covering the past ca. 1Ma. We aim to make use of this unique long, mostly continuous climate archive to unravel the millennial scale atmospheric and oceanic processes linked to changes in the Indian monsoon climate over the Quaternary glacial-interglacial cycles. Our aim is to fill this gap using fast, cost-efficient methods (Fourier Transform Infrared Spectroscopy [FTIRS] and X-ray Fluorescence [XRF] scanning) which allow us to study this sequence at a millennial scale resolution (2-3cm sampling interval). An important methodological aspect of this study is developing FTIRS as a method for the simultaneous estimation of the sediment total inorganic carbon and organic carbon content by using the specific fingerprint absorption spectra of minerals (e.g. calcite) and organic sediment components. The resulting paleo-production proxies give indications of oceanic circulation patterns and serve as a direct comparison to the XRF scanning data. Initial results show that variability in paleo-production is accompanied by changes in the quantity and composition of clastic input to the site. Phases of increased deposition of terrigenous material are enriched in K, Al, Fe and Si. Both changes in the weathering and erosion focus areas affect the mineralogy and elemental composition of the clastic input as grain size and mineralogical changes are reflected in the ratios of lighter to heavier elements. Furthermore, trace element compositions (Zn, Cu, Mn) give indications of diagenetic processes and contribute to the understanding of the depositional environment. The resulting datasets will lead to a more comprehensive understanding of the interplay of the local atmospheric and oceanic circulation processes over glacial-interglacial cycles; an essential prerequisite for regional predictions of global climate change impacts.

ICDP

The ICDP-TDP drilling at Lake Towuti, Indonesia, in 2015: first results of surface sampling, drilling and core processing

A. HASBERG[1], M. MELLES[1], M. MORLOCK[2], H. VOGEL[2], J.M. RUSSELL[3], S. BIJAKSANA[4] & TDP SCIENCE PARTY

[1] Institute of Geology and Mineralogy, University of Cologne, Zülpicher Str. 49a, 50674 Cologne, Germany, email: hasberg.ascelina@uni-koeln.de
[2] Institute of Geological Sciences and Oeschger Centre for Climate Change Research, University of Bern, 3012 Bern, Switzerland
[3] Department of Geological Sciences, Brown University, Providence, RI 02912, USA
[4] Faculty of Mining and Petroleum Engineering, Institute Teknologi Bandung, Bandung 40132, Indonesia

This contribution summarises first results of the DFG project ‘Decadal- to orbital-scale climate variability in the Indo-Pacific Warm Pool during the past ca. 650,000 years’ (grant no. ME 1169/26) that has commenced in January 2015. The project is part of the SPP 1006 ‘Towuti Bundle’, in which three other projects focus on the evolutionary biology (T. von Rintelen, Museum für Naturkunde Berlin), the geomicrobiology (J. Kallmeyer, GFZ German Research Centre for Geosciences Potsdam), and the downhole logging (T. Wonik, LIAG Hannover) within the scope of the Towuti Drilling Project (TDP).

The TDP concerns the sediment record in Lake Towuti, the largest tectonically formed lake of the Republic Indonesia (surface area: 561 km², maximum water depth: 203 m). Lake Towuti is located on Sulawesi Island, in the center of the Indo-Pacific Warm Pool (IPWP; fig. 1).

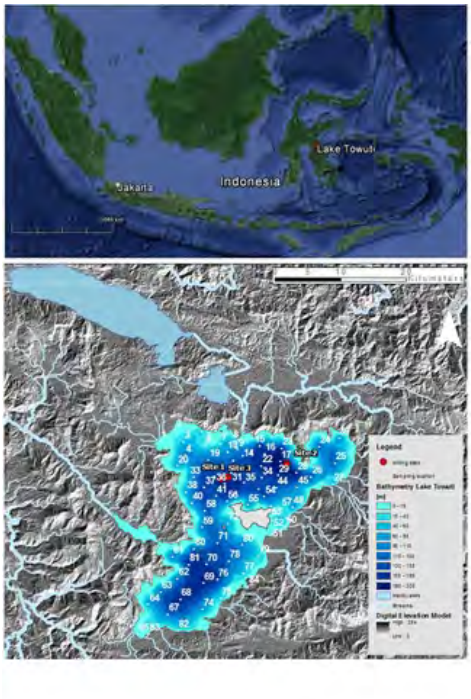

Fig. 1: Regional overview of Indonesia, Sulawesi Island with Lake Towuti. Beneath a digital elevation model of the Malili lake region with the bathymetry of Lake Towuti shows the drilling sites as well as the surface sample locations.

The IPWP is one of the major zones of deep atmospheric convection, in which the Earth's atmospheric moisture and heat budgets are energized. Hence, a better understanding of the tropical Indo-Pacific climate under different climate boundary conditions than today would strongly enhance our ability to make accurate predictions about future climate, and in particular future precipitation. The high potential of the sedimentary record in Lake Towuti for paleoclimatic research has been confimed by geophysical and geological results from the TDP site survey (Russel et al. 2014, Vogel et al. 2015).

DFG project participated both in the drilling campaign and in core processing activities.

The analytical work within the scope of the DFG project will focus on TDP site 2, which was drilled in front of the Mahalona River Delta (fig. 1). There, fluvial/deltaic sediments in the upper ca. 73 m overlay about 61 m of lacustrine sediments widely comparable to those found in the lower parts of sites 1 and 3 further to the west. Analyses will comprise XRF scanning (ITRAX Scanner, Cox), microstructural analyses (microscopy of thin sections), smear-slide analyses (polarization microscopy), radiocarbon dating (inhouse at Cologne AMS), grain-shape

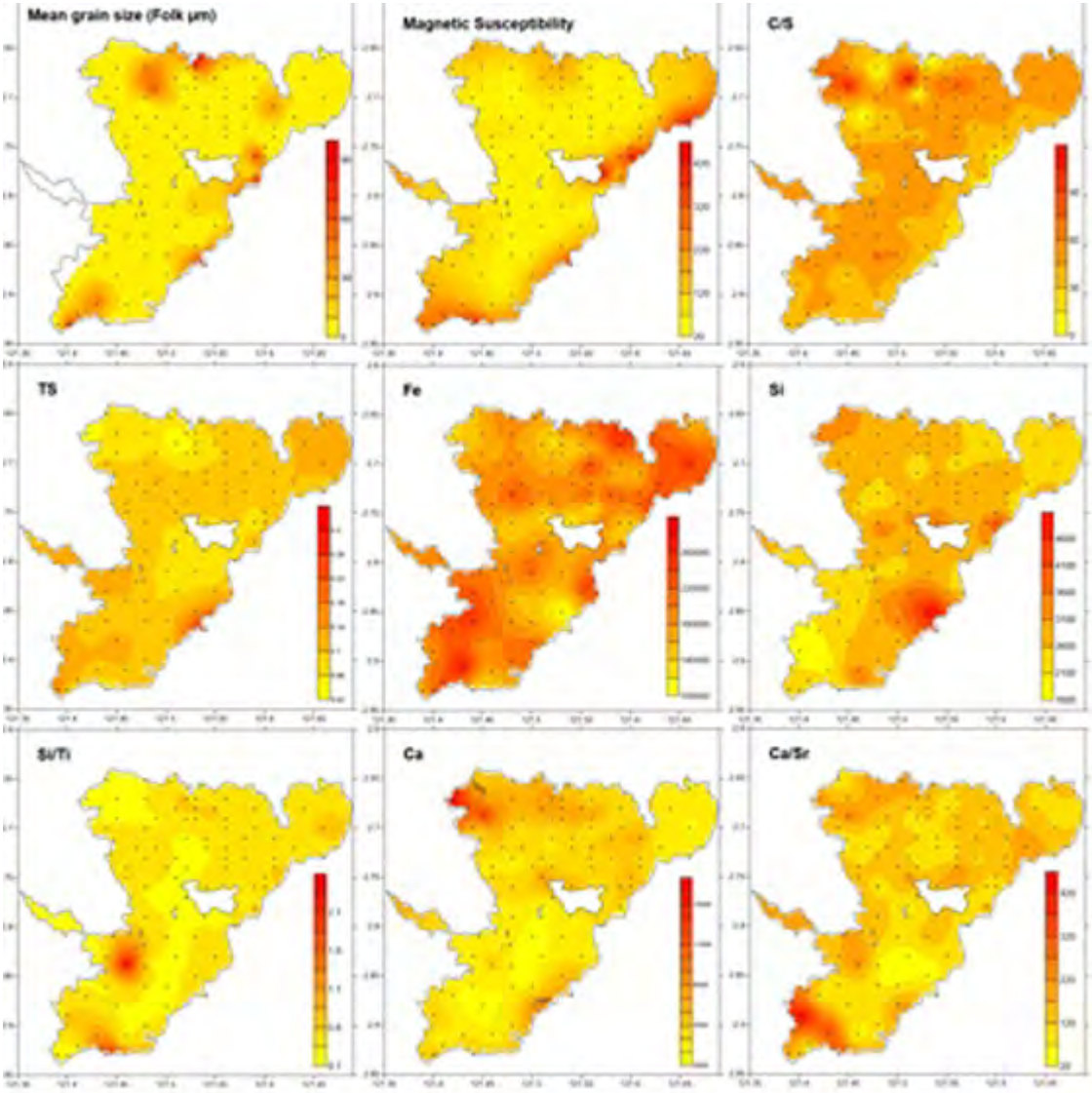

Fig. 2: Composition of Lake Towutis surface sample results from sedimentological, geochemical and paleaomagnetic analyses.

In spring 2015 (May - June), the TDP recovered more than 1000 meters of sediment core from three sites (table 1). At all three sites replicate cores down to 133, 154, and 174 m below lake floor have penetrated the entire lake sediment record, which is expected to comprise the past ca. 650.000 years almost continuously. Core processing (MSCL logging, core opening, and subsampling) took place by the TDP science party at LacCore, the U.S. core repository at the University of Minneapolis, Minnesota, in November 2015 and January 2016. The PhD student in the

analyses (FlowCAM, Fluid Imaging Technol.), grain-size analyses (saturn DigiSizer^{TM} 5200, micromeritics), coarse-fraction analyses (binocular microscopy), and analyses of the TOC, TN, TS, and carbonate contents (Dimatoc 100, Dimatec Co. and vario microcube, Elementar Co.) as well as bulk mineralogy (X'Pert Powder diffractometer, PANalytical Co.).

The results from the analytical work are expected to provide important information that (i) contributes to the dating of the sediment record, (ii) helps to decipher the

long-term development of Lake Towuti, with its formation and the onset of riverine input from other Malili lakes, (iii) contributes to the reconstruction of the precipitation-controlled riverine inflow from the Mahalano River during the past ~80,000 years with up to decadal resolution, (iv) helps to identify the dimension and potential reasons for lake-level fluctuations in Towuti, (v) supports the understanding of the variability in mixing and stratification of Towuti, and (vi) contributes to the reconstruction of weathering conditions and soil erosion in the lake´s catchment. The project thus will generate partly unique paleoenvironmental and paleoclimatological data that will not only complement respective research by other international projects on Lake Towuti but also provide important background information for the associated biological projects.

This reflects higher energies due to wave action and fluvial sediment supply, as well as the occurrence of magnetic minerals particularly in the sand and gravel fractions of the sediments. In regions of deeper waters and more distal to the shore the grain size and magnetic susceptibility decrease, but the organic carbon vs. total sulfur (C/S) ratio and redox-sensitive elements such as U, Cd, Mo, and V increase. This suggests that sulfur accumulation in Lake Towuti is controlled by autochthoneous pyrite formation, in dependence on differences in redox conditions, rather than gypsum accumulation. Highest silicon (Si) concentrations appear in front of the four major inlets of Lake Towuti, however, a distinct maximum also occurs close to the southeastern shore, where larger river inlets are missing. Consequently, the silicon distribution is partly controlled by fluvial input

site	hole	top – bottom [m]	cored sediment [m]	recovery [%]
1	A	0 – 113,58	105,83	93,18
	B	0 – 161,70	137,87	85,26
	C	0 – 5,64	4,46	78,90
	D	1,11 – 54,43	53,21	97,76
	E	45,00 – 128,72	76,19	91,01
	F	2,21 – 154,06	145,97	96,13
total site 1			523,52	91,87
2	A	0 – 137,58	134,52	97,78
	B	0,72 – 105,15	103,92	99,51
	C	49,44 – 52,44 + 79,43 – 82,43 + 98,00 – 133,21	34,18	82,94
total site 2			272,61	96,45
3	A	0 – 174,09	166,08	95,40
	B	0 – 60,88	55,30	90,83
total site 3			221,38	94,22
Total recovery			1017,51	93,57

Tab 1: The TDP-TOW 2015 total sediment core recovery – splitted due to the different holes of one site – of all three ICDP drilling sites.

For a better understanding of the palaeoenvironmental proxies to be analyzed on the drill cores, the modern processes of sediment formation in the lake and in its catchment - under known environmental conditions - were investigated on a set of 84 lake sediment surface samples. Sampling was conducted during the drilling campaign by grab sampler (UWITEC Corp., Austria) in a grid of 1 to 4 km resolution that covers the entire lake. The samples were analysed for inorganic geochemical composition (XRF powder scans and ICP-MS), magnetic susceptibility (Kappabridge), grain-size distribution (laser scanner), biogenic components (smear-slide analyses), biogenic silica contents (leaching), and carbonate, total organic carbon (TOC), nitrogen (TN), and sulfur (TS) concentrations (elemental analyzer).The sediments close to the lake shores and in front of the major river inlets are characterized by mean grain sizes coarser than average and high magnetic susceptibilities presented by high ratios of Cr, Ni, Co, and Zr (Fig. 2).

and partly by biogenic silica deposition; the latter is confirmed by high concentrations of pelagic and benthic diatoms as well as sponge spiculae in smear slides from the sediments at the southeastern shore. In summary, the data thus far obtained on the surface sediments of Lake Towuti show a strong influence of fluvial sediment supply and water-depth dependent redox conditions on the sediment composition. No indication, in contrast, was found for a significant influence of lake currents on the distribution of the sediments supplied by riverine input.

References:

Russell J.M., Vogel H., Konecky B.L., Bijaksana S., Huang Y., Melles M., Wattrus N., Costa K. & King J.W. (2014): Glacial forcing of central Indonesian hydroclimate since 60,000 y B.P. - PNAS, 111 (14): 5100-5105.

Vogel H., James M. Russell J. M., Cahyarini S. Y., Bijaksana S., Wattrus N., Rethemeyer J., and Melles M. (2015): Depositional modes and lake-level variability at Lake Towuti, Indonesia, during the past ~29 kyr BP. - Journal of Paleolimnology, December 2015, Volume 54, Issue 4, pp 359-377.

IODP

Indian monsoon development and variability from the radiogenic isotope and clay mineral composition of Bay of Bengal and Andaman Sea sediments

E. HATHORNE[1], S. ALI[2], D. GEBREGIORGIS[1], A. ASMUS[1], AND M. FRANK[1]

[1]GEOMAR Helmholtz.Centre for Ocean Research Kiel, Germany, [2]Physical Research Laboratory, Ahmedabad, India

Over 3 billion people live in the area influenced by the Asian monsoon and this population is estimated to be over 4 billion by 2050. The monsoon provides vital water resources while at the same time posing a risk to human life through flooding but is difficult to predict. Even the most advanced coupled ocean-atmosphere general circulation models find monsoon simulation a “severe test” although great improvements have been made (Meehl et al., 2012). Understanding how the monsoon behaves under different boundary conditions such as a warmer world with less continental ice cover is vital for these models. We need to understand how and when the monsoon first intensified, how it subsequently developed and how it has varied in relation to various potential influences including global climate change and analogue future warm periods, mountain building and opening of oceanic gateways. The timing of the intensification of the modern East Asian and Indian monsoon systems is controversial, with some proxy records indicating that initial intensification occurred ~7–8 Ma, whereas others suggest a considerably earlier onset, perhaps as early as ~22 Ma (e.g. Clift et al., 2008). Modelling studies have suggested that the intensification of the monsoon was directly related to the uplift of Tibet (e.g. Prell and Kutzbach, 1992), directly linking global climate and tectonics. Monsoon rainfall feeds the major Ganges-Brahmaputra and Irrawaddy rivers that discharge vast amounts of sediment to the Bay of Bengal and Andaman Sea. Positioned in the southern BoB on the topographic high of the Ninety East ridge, ODP Site 758 (redrilled by IODP Exp. 353 as U1443) is in a prime location to receive continuous sedimentation and thus record the history of these monsoonal river systems.

Delivery of terrigenous material to ODP Site 758 increased dramatically in the middle to late Miocene with two subsequent pulses at ~7.0 to 5.6 Ma and ~3.9 to 2.0 Ma, interpreted to represent variations in the fluvial sediment flux resulting from the uplift and erosion of the Himalaya (Hovan and Rea, 1992). These erosional pulses are broadly coincident with increases in the magnetic susceptibility of Chinese loess-red clay deposits (e.g. Quade et al., 1989) suggesting an Asia wide shift in climate. However, new clay mineral data from ODP Site 758 for the last 28 Myrs and mineralogical changes of ODP Site 1148 in the South China Sea (Clift et al., 2008) suggest the Asian climate already became wetter in the earliest Miocene. Although the general trends of these mineral proxies are similar, the data hint at significant differences in the timing of the development of the sub-monsoon systems in East and South Asia. For example, the data from the South China Sea suggest a relatively arid period around the Middle Miocene climatic optimum centred at 16 Ma. This is followed by peak monsoon (wet) conditions from 14 Ma to 10 Ma while in the BoB the clay minerals suggest a steady increase in continental wetness that peaked at 10 Ma and remained high thereafter. To ascertain variations in the source regions of the clay minerals transported to the southern BoB we measured the radiogenic Sr, Nd and Pb isotope composition of the clay fraction at ODP Site 758 for the last 28 Myrs at a coarse time resolution. The results clearly indicate a Himalayan source with more radiogenic excursions occurring between 24 to 20 Ma, and 12 to 10 Ma, most likely reflecting changes in the balance between Tethyan Sedimentary Series (TSS) and High Himalayan Crystalline (HHC) sources. These changes either resulted from tectonic changes preferentially exposing different sources to weathering or reorganisations of the transport pathways of detrital material to the BoB.

While the Miocene evolution of the East Asian monsoon has been studied at orbital resolution in the South China Sea (e.g. Holbourn et al., 2010), the proxy records of Indian Monsoon evolution are presently of insufficient time resolution to investigate the relationship between global climate and the Indian monsoon throughout the Miocene (Gourlan et al., 2008). The new continuous high quality cores from IODP Site U1443 now make it possible to obtain such records. To provide an example of the work we propose to conduct for the Miocene section of Site U1443, we present clay fraction (detrital) and mixed planktonic foraminifera (authigenic) Nd isotopes along with planktonic and benthic foraminiferal stable isotopes for the last 60 kyrs obtained from National Gas Hydrate Program Site 17 in the Andaman Sea. The data reveal a remarkably stable Irrawaddy source of detrital clays considering the marked climate changes of the last glacial cycle (Ali et al. 2015). The authigenic Nd isotope signal of bottom water is completely dominated by the terrigenous input of Nd, and therefore the flux of other trace metals and nutrients was also significant, until 8 ka when the waters at 1300m depth became more unradiogenic. This remote acquisition of the Nd isotope signature likely reflects increased supply from the Ganges-Brahmaputra source related to the early to mid Holocene peak in monsoon intensity.

References:

Ali, S., E.C. Hathorne, M. Frank, D. Gebregiorgis, K. Stattegger, R. Stumpf, S. Kutterolf, J.E. Johnson, and L. Giosan (2015), South Asian monsoon history over the past 60 kyr recorded by radiogenic isotopes and clay mineral assemblages in the Andaman Sea. Geochemistry, Geophysics, Geosystems 16, 505–521, doi:10.1002/2014GC005586.

Clift, P. D., K. V. Hodges, D. Heslop, R. Hannigan, H. Van Long, and G. Calves (2008), Correlation of Himalayan exhumation rates and Asian monsoon intensity, Nature Geosci, 1(12), 875-880.

Gourlan AT, Meynadier L, Allégre CJ (2008) Tectonically driven changes in the Indian Ocean circulation over the last 25 Ma: Neodymium isotope evidence. Earth and Planetary Science Letters 267 (1-2):353-364

Holbourn, A., W. Kuhnt, M. Regenberg, M. Schulz, A. Mix, and N. Andersen (2010), Does Antarctic glaciation force migration of the tropical rain belt?, Geology, 38(9), 783-786.

Hovan SA, Rea DK (1992) The Cenozoic Record of Continental Mineral Deposition on Broken and Ninetyeast Ridges, Indian Ocean: Southern African Aridity and Sediment Delivery from the Himalayas. Paleoceanography 7 (6):833-860. doi:10.1029/92pa02176

Meehl, G. a., J. M. Arblaster, J. M. Caron, H. Annamalai, M. Jochum, A. Chakraborty, and R. Murtugudde (2012), Monsoon regimes and processes in CCSM4, Part 1: The Asian-Australian monsoon, Journal of Climate, 25, 2583–2608.

Prell, W.L., and J.E. Kutzbach (1992), Sensitivity of the Indian monsoon to forcing parameters and implications for its evolution, Nature 360, 647-652.

Quade J, Cerling TE, Bowman JR (1989) Development of Asian monsoon revealed by marked ecological shift during the latest Miocene in northern Pakistan. Nature 342:163-166.

IODP

Deducing triggering mechanism of volcaniclastic mass flows: Late Pleistocene turbidites examined grain by grain (IODP 340; site U1397; Lesser Antilles)

F. HEUER[1], C. BREITKREUZ[1] AND THE IODP 340 SHIP PARTY[2]

[1]Institute for Geology, TU Bergakademie Freiberg, Bernhard-von-Cotta-Straße 2, D-09599 Freiberg
[2]http://iodp.tamu.edu/scienceops/expeditions/antilles_volcanism_landslides.html

Marine mass flows are among the most important sedimentary processes on Earth Depending on their flow properties, submarine mass flows can be distinguished into laminar debris flows and turbulent turbidity currents.

Here we present detailed investigation from an island arc system where volcaniclastic turbidites are directly associated with volcanic eruptions or their formation is related to other processes such as landslide, strong precipitation or sea level change.

The present paper deals with Late Pleistocene unconsolidated volcaniclastic and bioclastic turbidites, drilled during the IODP 340 cruise of the JOIDES Resolution west of Martinique (Lesser Antilles Arc, Le Friant et al. 2012).

The main task of this presentation is: Can data on depositional facies, grain shape and surface texture and on composition be used to identify the triggering mechanisms of submarine volcaniclastic mass flows? In U1397A, B (2,480 mbsl, 30 km offshore Martinique) different turbidite types have been distinguished based on their pumice content and their ratio between volcaniclastic and bioclastic material. Preliminary maximum age of deposits recovered from U 1397 is ≤ 400 ka.

We applied SEM imaging, modal analysis, mineral and glass chemistry (mineral liberation analyses, MLA). The main mineral phase in all 46 samples is plagioclase associated with pyroxene, amphibole and biotite. Volcanic glass has rhyolitic composition, with variation in Fe, Al and Ca content. Altered lithics contain rutile pointing to hydrothermal overprint in the volcanic edifice.

Mean grain size ranges between 0.3 – 3.0 Φ, poorly to moderately sorted. Most of the turbidite grains show medium to high relief with abundant mechanical textures associated with breakage. Most frequently are conchoidal fractures, microcracks, V-shaped depressions, as well as etching due to weathering and dissolution.

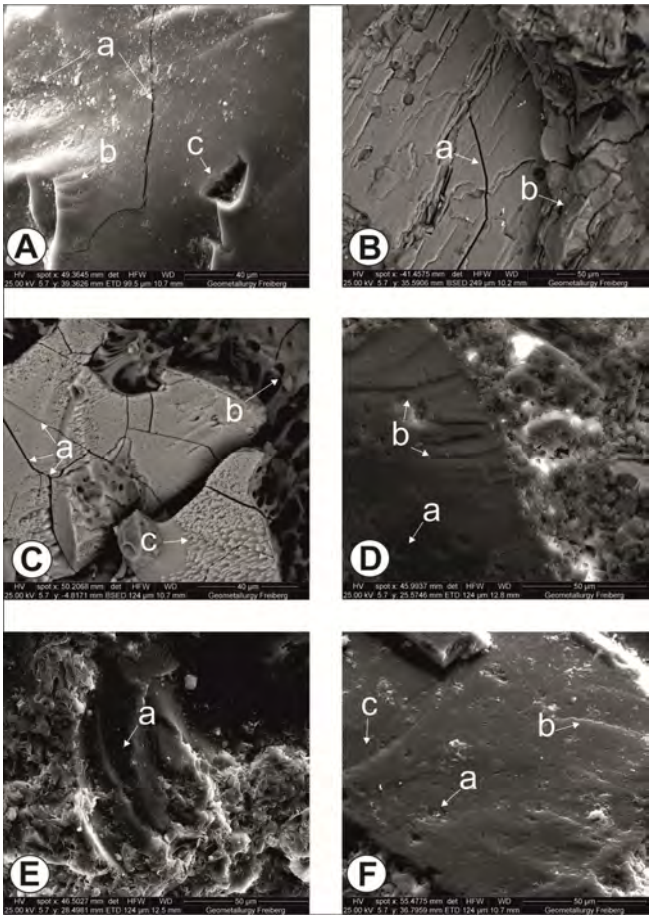

Fig. 1: SE images at high magnification of different microtextures on sand size crystals. A: Quartz crystal with medium relief, microcracks (a), conchoidal fractures (b) and a triangular deep groove (c); sample A-1 B: Feldspar crystal with deep microcrack (a) as part of a lithic with high relief (b). C: Intersecting microcracks (a) in perthite as part of glassy pumice grain (b); sample A-22. Typical overgrowth of metasomatic replacement is shown (c); sample A-11. D: Weathering and dissolution etching (a) of quartz with deep conchoidal fractures (b); sample A-1. E: Deeply inscribed conchoidal fractures (a) on a crystal with high relief; sample A-1. F: Weathering and dissolution etching (a) of quartz with conchoidal fractures (b) and mechanically formed V-shaped depressions (c); sample A-1.

Additionally deep grooves, deep gouges, slight crescentic gouges and shallow subparallel fractures occur (Fig. 1). Many of these features form during the submarine transport of the turbidity currents. Our data suggest that most analysed turbidites were associated with lavadome-failure, subordinately with open-vent eruptions. Furthermore, land slide, a common process in the Lesser Antilles, was an important trigger.

References:
Expedition 340 Scientists, 2012. Lesser Antilles volcanism and landslides: implications for hazard assessment and long-term magmatic evolution of the arc. IODP Prel. Rept., 340. doi:10.2204/ iodp.pr.340.2012

IODP

Deciphering the impact of the Indonesian Throughflow on the Australian climate during the Pliocene: A proposed Nd and Sr isotopic study

T. HIMMLER[1], AND EXP. 356 SCIENTISTS

[1]MARUM–Center for Marine and Environmental Sciences and Department of Geosciences, University of Bremen, 28334 Bremen, Germany

International Ocean Discovery Program (IODP) Expedition 356 (August to September 2015) aboard *RV JOIDES Resolution* cored seven shelf and upper slope sites (Fig. 1) off Western Australia. Two objectives of Exp. 356 are (1) to document the evolution of the Indonesian Throughflow (IT) - a seaway that transports warm water from the western Pacific through Indonesian seas into the eastern Indian Ocean (Gordon, 2005), and (2) to document the development of aridity in Australia and the variability of the Australian monsoon (Gallagher et al., 2014). Nd and Sr isotopic records off Western Australia are promising tracers to examine for achieving these objectives.

In particlar, analyses of the carbonate fraction and the detrital components of the same sample will reveal changes in oceanic currents as well as the provenance of the terrigenous material (Ehlert et al., 2011; Le Houedec et al., 2012). However, existing Nd and Sr isotopic data are restricted in time to the LGM to Holocene period (Ehlert et al., 2011), and to only two data points from the Pliocene (ODP Site 762; 1360 m water depth; Le Houedec et al., 2012).

Site U1463 was drilled on the Australian Northwest Shelf in the Northern Carnarvon Basin (Fig. 1) at a water depth of ~145 m (Gallagher et al., 2016). It yielded a complete stratigraphic succession, from the early Pleistocene to late Miocene (89% total recovery), of mainly homogeneous mudstone and wackestone with abundant foraminifera, that revealed a relatively high sedimentation rate (5–7 cm/ka). Consequently, Site U1463 provides an excellent sedimentary archive for examining carbonate and terrigenous Nd and Sr isotope systematics and for improving our knowledge of late Miocene to early Pleistocene climate history off Western Australia. In addition to Nd and Sr isotopic compositions, rare earth element concentrations will be measured on both, the carbonate and terrigeneous fractions. The analyses of the clay mineral assemblages will provide an independent proxy for climate and provenance, further constraining the mechanisms behind the paleoclimatic transition from the late Miocene to the early Pliocene.

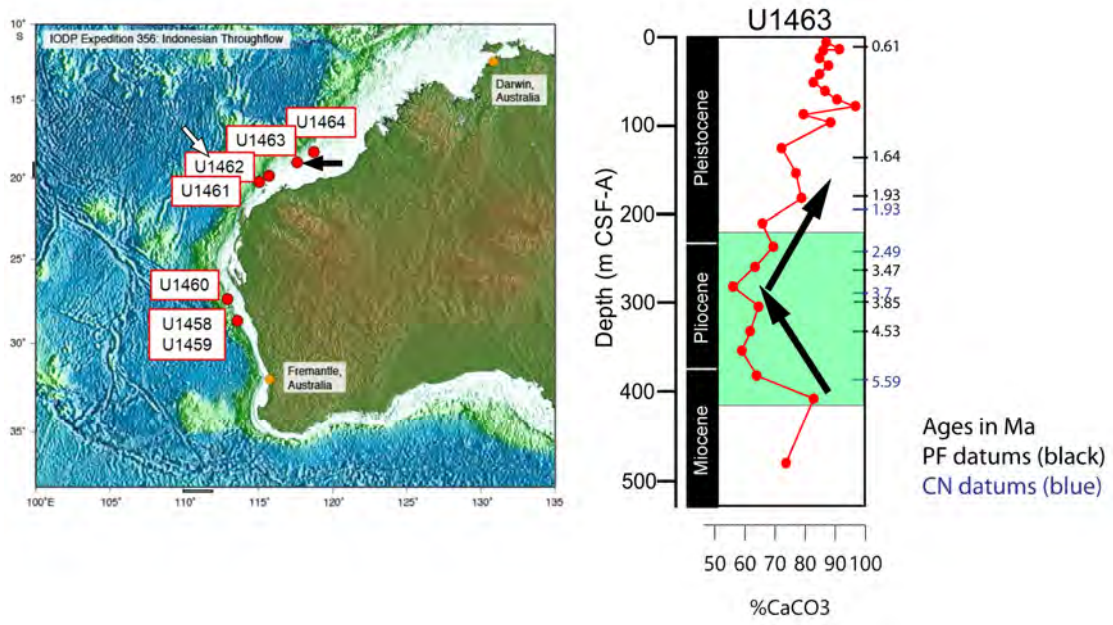

Figure 1: Left panel shows Exp. 356 drill site locations and indicates the proposed study site U1463 (black arrow), together with the location of ODP site 762 (white arrow). Right panel displays the carbonate content (weight-%) at Site U1463, indicating that significant environmental change occurred on the Australian Northwest Shelf during the late Miocene and throughout the Pliocene. The green band indicates the proposed sampling interval; arrows indicate the general trends. PF = planktic foraminifers; CN = calcareous nannofossils. Modified after Gallagher et al. (2016).

References:
Gordon, A.L., (2005). Oceanography of the Indonesian Seas and their throughflow. Oceanography 18, 14–27.
Gallagher, S.J., Fulthorpe, C.S., Bogus, K.A., (2014). Reefs, oceans, and climate: a 5 million year history of the Indonesian Throughflow, Australian monsoon, and subsidence on the northwest shelf of Australia. International Ocean Discovery Program Scientific Prospectus, 356. http://dx.doi.org/ 10.14379/iodp.sp.356.2014.
Gallagher, S.J., Fulthorpe, C.S., Bogus, K., and the Expedition 356 Scientists, (2016). Expedition 356 Preliminary Report: Indonesian Throughflow. International Ocean Discovery Program.
Ehlert, C., Frank, M., Haley, B.A., Böniger, U., De Deckker, P., Gingele, F., (2011). Current transport versus continental inputs in the eastern Indian Ocean: radiogenic isotope signatures of clay size sediments. Geochem. Geophys. Geosyst. 12.
Le Houedec, S., Meynadier, L., Allègre, C.J., (2012). Nd isotope systematics on ODP Sites 756 and 762 sediments reveal major volcanic, oceanic and climatic changes in South Indian Ocean over the last 35 Ma. Earth and Planetary Science Letters 327-328, 29–38.

IODP

Towards untangling the changing tectonic and climatic influence on deposition on the Surveyor Fan, Gulf of Alaska: A single grain geochemical and geochronological study

B. HUBER, H. BAHLBURG, C. DREWER

Institut für Geologie und Paläontologie, Westfälische Wilhelms-Universität Münster, Germany; barbara.huber@uni-muenster.

The Surveyor Fan depositional system, Gulf of Alaska, serves as a recorder of onshore processes in the evolving St. Elias orogen, the highest coastal mountain range on earth. Here, the relative contribution of tectonics and climate to clast production and denudation are controversial and need to be determined in detail. Absence of major onshore sediment traps allows fast transport of orogenic sediment to the ocean, minimising modifications of the sediment during transport. Exhumation and climatically controlled variations in glacier type and extent influence denudation rates and the characteristics of the sediments. We apply diverse tools of single grain geochemical provenance analysis to Neogene sediments from IODP 341 expedition sites U1417 (distal Surveyor Fan), U1418 (proximal Surveyor Fan) U1419 (continental slope) and U1420 (continental shelf). This will allow for deriving information about the relative contributions of tectonics and climate on rates and locations of exhumation and denudation as well as their temporal and spatial interplay in the evolving St. Elias orogen.

Target of the sampling were sands and silts, covering the Miocene to Pleistocene stratigraphy of the four sites. We apply microprobe analysis for main element geochemistry on different heavy minerals; cathodoluminescence imaging, U/Pb dating and REE and trace element measuring on zircons as well as $^{40}Ar/^{39}Ar$ dating of hornblende and mica.

First analyses point towards dominant sediment sources in the area of the Chugach Metamorphic Complex (CMC). U/Pb dating of zircons of samples in different stratigraphic positions from sites U1417 and U1418 shows peaks in age spectra between ca. 50 and 60 Ma, the youngest being 25.3 Ma ± 0.6 Ma, the oldest 1305.8 ± 38.1 Ma of age. Additional analyses of REE and trace elements from the same zircons imply granitoid sources, mainly granodiorites and tonalites, for most zircons measured. REE and trace element spectra of the 50 to 60 Ma zircons strongly resemble published REE patterns of zircons from the Sanak-Baranof plutonic belt in the CMC. Microprobe analyses of 450 hornblende grains of the same samples and additional analyses of samples from sites U1419 and U1420 show an overall dominance of magnesiohornblende and varying amounts of actinolite, kaersutite and tschermakite. Similar hornblende compositions have been published for a belt of metamafic rocks in the CMC. Microprobe data of garnets from these samples indicate derivation from granites or gneisses and amphibolites of metamorphic conditions transitional between amphibolite and granulite facies. This also matches with published information about lithologies in the area of the CMC.

The Chugach Metamorphic Complex, via the Bering glacier, seems to be one of the main long time sources of the Surveyor Fan sediments. Shipboard clast and other data indicate input also from the eastward lying Seward glacier and longshore transfer into the Surveyor Fan system. Changing amphibole compositions with time of deposition and zircons with ages older than ca. 50 Ma point to changes in source terranes which will be constrained by future analysis.

IODP

Friction properties of rocks in forearcs of accretionary convergent margins

A. HÜPERS[1], S. TRÜTNER[1], M.J.IKARI[1], A.J. KOPF[1]

[1] MARUM - Center for Marine Environmental Sciences, University of Bremen, P.O. Box 330440, 28334 Bremen, Germany.

The largest earthquakes in the world with moment magnitudes M_W>9 occur along the plate interface where an oceanic plate is subducting beneath a continental or another oceanic plate. The exact cause for the updip limit of earthquake nucleaction along the plate interface remains unknown, because the seismogenic zone of an active megathrust zone has not been sampled so far. Sediments in accretionary convergent margins experience major compositional changes from early diagenesis in the shallow subseafloor to metamorphism at greater depth in the forearc as they experience progressive burial through accretion or subduction. One assumption is that the prograde lithification in the subduction zone forearc causes the changes in mechanical and hydrogeological properties necessary for seismic behavior. To test this hypothesis we compare published friction properties of samples from the Nankai Trough subduction zone, obtained via the Integrated Ocean Drilling Program (IODP), with onshore samples we collected from the Shimanto Belt (Japan), a fossil accretionary prism in the hinterland of the active Nankai subduction zone. The Shimanto Belt samples have experienced paleo-temperatures as high as those appropriate for the seismogenic zone, and have undergone substantial lithification during diagenesis and low-T metamorphism.

The Shimanto Belt samples comprise the entire former oceanic-plate stratigraphy, which were identified as red shales, black shales and sandstones and reflect a coarsening and thickening of the incoming strata. Cylindrical samples of 63mm diameter were drilled from the specimens and cut to a height of at least 30 mm for the experiments. The shear behavior of the samples was tested under water-saturated conditions in a single-direct shear apparatus. In each experiment, we first broke the intact samples by shearing at

applied normal stress of $\sigma_n = 0$. Samples were then loaded to applied normal stresses σ_n of 81 to 117 MPa, which correspond to the depth range of the paleo-temperatures, and then sheared along the created fracture surfaces at a constant velocity of 10 µm/s until steady state shear strength (τ) was reached. For comparison, each sample was also crushed and sieved to a grain size of ≤125 µm and sheared under the same effective normal stress conditions to represent unlithified samples of the same composition. In order to calculate the velocity dependence of friction, as quantified by the parameter a-b, we increased the velocity (V) in one-order of magnitude steps within the range 0.1-100 µm/s. Velocity-strengthening materials (a-b>0) are expected to exhibit stable slip, whereas velocity-weakening behavior (a-b<0) is required for slip instability that results in earthquake nucleation.

For intact samples we measured during the shearing a rapid increase in the friction coefficient μ ($= \tau/\sigma_n$) until reaching a maxima (μ_{max}), ranging from 0.42 to 0.93, followed by a drop in μ to a residual value μ_{res} (0.79-0.42). Both velocity-strengthening and velocity-weakening is observed for all tested lithologies, with values of a-b ranging from -0.025 to 0.015. Powdered specimen have smaller coefficients of friction ranging from 0.35 to 0.7 with almost identical values between peak and residual shear strength. Differences in (a-b) values between intact and powdered samples are most dominant in the black shales which are consistently positive for powdered samples within a narrow range of 0.001 to 0.012. Despite the great variety in frictional parameter, we observed for both intact and powdered samples several lithologically independent trends. For example, a-b is mainly positive, with values ranging from 0 to 0.015 for weaker samples having residual friction coefficients of $\mu_{res}<0.5$. For stronger samples with friction coefficients $\mu_{res}>0.7$, the a-b parameter decreases and becomes mainly negative.

Previous friction studies on unlithified sediments entering the Nankai Trough subduction zone by Brown et al showed that the sediments are frictional weak because of abundant clay minerals with friction coefficients ranging from 0.15 to 0.5. Our powdered samples have higher friction coeffcients which correlates with an increased quartz content from diagenesis and low temperature metamorphism. In addition to compositional changes the elevated friction coefficients of intact samples seem also be related to the preserved fabric.

In conclusion we provided firsthand evidence that lithification can transform unlithfied sediment into frictionally stronger rock which has a tendency for unstable slip behavior. These results will be complemented by additional experiments using IODP samples, which experienced lower temperature conditions to better constrain the effects of incipient lithification. In addition, detailed X-ray diffraction, secondary electron microscopy and nuclear magnetic resonance analyses will be conducted to investigate the evolution of underlying key diagenetic to low-T metamorphic processes and their spatio-temporal occurance in the active Nankai Trough subduction zone forearc.

ICDP

Insights on Fault Slip Behavior from Long-term Laboratory Studies of ICDP/IODP Drilling Samples

M. IKARI[1*], A. KOPF[1]

[1] MARUM, Universität Bremen, Leobener Str., D-28359 Bremen, Germany
*mikari@marum.de

The primary goal of scientific drilling projects targeting plate-boundary faults is understanding how major faults slip, in order to understand how and why large and damaging earthquakes occur. Recent observations indicate that faults do not slip bimodally as either earthquakes or stable creep, but exhibit a range of transient slip behavior such as slow slip events or low frequency earthquakes. Moreover, portions of faults thought to be creeping or aseismic may still slip coseismically if they are induced by an earthquake propagating from an adjacement segment. In order to effectively analyze which fault conditions and rock properties are associated with the various aspects of fault slip, shearing on faults must be simulated in laboratory friction experiments. International Continental Scientific Drilling Program (ICDP) and Integrated Ocean Drilling Program (IODP) samples are essential for providing the exact material that deforms in plate-boundary faults zones to be tested in laboratory experiments.

For repeated earthquake rupture, two conditions are required: (1) a reduction in frictional strength upon an increase in slip rate (known as velocity-weakening behavior), and (2) the ability to regain the shear strength lost during earthquake stress drops (known as frictional healing). Both of these behaviors are directly measurable, in velocity-stepping tests usually carried out at slip velocities of ~10^{-7} to 10^{-4} m/s and slide-hold-slide tests in which the quiescent period (hold times) is usually up to ~1 hour. However, longer-term tests conducted at very slow velocities and very long hold times may be more relevant for natural faults because the more closely match the timescales of both fast and slow.earthquakes.

We discuss here laboratory friction data obtained from experiments performed on core samples from ICDP and IODP projects targeting major fault zones. These include the Alpine Fault in New Zealand, the San Andreas Fault, the Nankai Trough (Japan), the Tohoku region of the Japan Trench, and the Costa Rica subduction zone. We compare the behavior of these materials at typical intermediate timescale laboratory experiments and integrate new data from longer-term tests. For conventional laboratory experiments at intermediate timescales we observe a tendency for fault weakness (coefficient of friction < 0.5), mostly velocity-strengthening frictional behavior, and low rates of frictional healing (with some exceptions). For long-term tests, we observe similar friction coefficients but more prevalent velocity-weakening friction.

At very low slip rates, slow stick-slip instabilities analagous to slow slip events appear in samples from the Japan Trench, Costa Rica, and Alpine Fault. Long-term slide-hold-slide experiments using San Andreas Fault material reveal that enhanced healing rates occur for long hold times. Our results indicate that slower driving velocities and longer „interseismic“ hold times are more conducive to frictionally unstable behavior and repeated earthquake rupture, suggesting that intermediate time-scale experiments likely underestimate the risk of seismic behavior.

IODP

Assessing the roles of coral-algal symbiosis in coral calcification

M. INOUE[1,2], N. GUSSONE[1], T. NAKAMURA[3] Y. YOKOYAMA[4], A. SUZUKI[5], K. SAKAI[6], H. KAWAHATA[4]

[1]Institute für Mineralogie, Universität Münster, Corrensst. 24, D-48149 Münster, Germany
[2]Graduate School of Natural Science and Technology, Okayama University, 3-1-1 Tsushima-naka, Okayama 700-8530, Japan
[3]Faculty of Science, University of the Ryukyus, Nishihara, Okinawa 903-0213, Japan
[4]Atmosphere and Ocean Research Institute, The University of Tokyo, 5-1-5 Kashiwanoha, Kashiwa, Chiba 277-8564, Japan
[5]Geological Survey of Japan, National Institute of Advanced Industrial Science and Technology (AIST), 1-1-1 Higashi Tsukuba, AIST Tsukuba Central 7, Ibaraki 305-8567, Japan
[6]Sesoko Station, Tropical Biosphere Research Center, University of the Ryukyus, 3422 Sesoko, Motobu, Okinawa 905-0227, Japan

Geochemical tracers such as $\delta^{18}O$ and Sr/Ca ratios in the coral skeleton have been well known as environmental proxies for sea surface temperature and/or salinity changes though time. For instance, paleoclimate has been reconstructed using fossil *Porites* and *Isopora* corals collected from Tahiti and Great Barrier Reef by IODP Exp. 310 and 325, respectively (e.g., Felis et al., 2012; 2014). Especially, coral skeleton can reconstruct past climate or environmental change with higher time resolution because of their vigorous calcification which is enabled by their symbiotic relationship with photosynthesizing zooxanthellae. Although there is little evidence of a direct link between the presence of symbionts and the enhancement of calcification, mainly two hypotheses have been proposed to explain this stimulation of calcification (reviewed in Davy et al., 2012). First, that alteration of the dissolved inorganic carbon concentration (DIC) or pH at the calcification site changes the saturation state of aragonite, and second, that production of the organic matrix (OM) that serves as an essential precursor of aragonite crystal precipitation is promoted. In this study, we reared symbiotic and aposymbiotic primary polyps from the same coral colony (*Acropora digitifera*) in order to examine the role of symbionts for coral calcification. Especially to examine the two hypotheses raised above, U/Ca and Mg/Ca ratios were analyzed in polyp skeletons as a proxy for pH and organic matrix, respectively, reared under seawater temperature and salinity controlled treatments in which symbiotic primary polyps calcified much more than the aposymbiotic ones. In addition, calcium isotope ratios ($\delta^{44}Ca$) which may have information on variation of trans cellular Ca^{2+} transport were also measured to evaluate photosymbiont impact on activity of Ca^{2+} channel.

We cultured the polyps for 10 days at four temperatures (27, 29, 31 and 33˚C) and five salinities (34, 32, 30, 28, 26), and measured Mg/Ca, U/Ca ratios and $\delta^{44}Ca$ in their skeletons. We compared these data with their previously reported skeletal growth (polyp weight) responses to temperature and salinity changes. Five polyp samples were randomly chosen from each treatment and their concentrations of Mg, Ca, and U were measured with an inductively coupled plasma mass spectrometer (Thermo ELEMENT) following the previously described protocol. For $\delta^{44}Ca$ analyses, two polyps from every temperature settings and selected salinity settings (26, 30 and 34) were used. Calcium isotope analyses were conducted at the **'**Münster Isotope Research Center - MIRC**'** (University of Münster), using a Thermo-Fisher Triton T1 thermal ionization mass spectrometer based on the method described in Inoue et al. (2015). The isotope values are expressed relative to NIST SRM 915a as $\delta^{44}Ca = (((^{44}Ca/^{40}Ca)_{sample}/(^{44}Ca/^{40}Ca)_{SRM915a} - 1) \times 1000$.

It has been suggested that Mg^{2+} concentrations are likely related to OM secretion, as Mg is probably incorporated into the organic phase of the coral skeleton rather than into the crystal lattice. Therefore, Mg/Ca of polyp skeletons can be regarded as a proxy for OM secretion. On the other hand, since skeletal U/Ca has negative correlation against seawater pH, it can be used as a pH proxy. In our experiment, we observed a clear decrease of skeletal U/Ca, but not Mg/Ca, in symbiotic compared with aposymbiotic polyps in both the culture expetiments. These results suggest that OM secretion, the precursor step to $CaCO_3$ precipitation, is controlled mainly by the coral host, without any contribution from zooxanthellae. In contrast, our results imply a higher pH of the calcifying fluid in symbiotic versus aposymbiotic polyps. Isotope fractionations of Ca show no systematic differences between symbiotic and aposymbiotic polyps and environmental settings, suggesting activities of Ca^{2+} channel is not mainly controlled by the presense of zooxanthellae. Thus, our results demonstrate that the role of coral-algal symbiosis on coral calcification is predominantly to enhance the pH of the calcifying fluid rather than to promote OM secretion and/or activate Ca^{2+} channel.

References:

Felis, T., Merkel, U., Asami, R., et al. (2012) Pronounced interannual variability in tropical South Pacific temperatures during Heinrich Stadial 1. Nat. Commun. 3:965, doi: 10.1038/ncomms1973.

Felis, T., McGregor, H. V., Linsley, B. K., et al. (2014) Intensification of the meridional temperature gradient in the Great Barrier Reef following the Last Glacial Maximum. Nat. Commun. 5:4102, doi: 10.1038/ncomms5102.

Davy, S. K., Denis, A., and Weis, V. M. (2012) Cell Biology of Cnidarian-Dinoflagellate Symbiosis. Microbiol. Molecul. Biol. Rev. *76*, 229–261.

Inoue, M., Gussone, N. Koga, Y., et al. (2015) Controlling factors of Ca isotope fractionation in scleractinian corals evaluated by temperature, pH and light controlled culture experiments. Geochim. Cosmochim. Acta, 167, 80–92.

ICDP

The Campi Flegrei volcano (Napoli, southern Italy): $^{87}Sr/^{86}Sr$- $\delta^{18}O$ systematics and magma residence times

RAFFAELLA SILVIA IOVINE [1], GERHARD WÖRNER [1], FABIO CARMINE MAZZEO [2], ILENIA ARIENZO [3], LUCIA CIVETTA [4,2], MASSIMO D'ANTONIO[2], GIOVANNI ORSI [2]

(1) Geowissenschaftliches Zentrum, Georg-August-Universität, Göttingen, Germany
(2) Department of Earth, Environmental and Resources Science, University Federico II of Naples, Italy
(3) Istituto Nazionale di Geofisica e Vulcanologia – sezione di Napoli Osservatorio Vesuviano, Naples, Italy
(4) Istituto Nazionale di Geofisica e Vulcanologia – sezione di Palermo, Italy

We present a new and comprehensive Sr-O isotope data set on mineral separates (feldspar, Fe-cpx, Mg-cpx, magnetite, olivine) from 37 samples covering the entire stratigraphy of Campi Flegrei Volcano (Italy). Sr isotopic compositions were determined by TIMS after standard cation-exchange methods on separated hand-picked feldspar, clinopyroxene and olivine phenocrysts (~300mg), and on whole rocks, in case of insufficient sample size to separate crystals. Oxygen isotope ratios were measured by infrared laser fluorination on ~0.3 mg of hand-picked phenocrysts.

Although advance in laser fluorination mass spectrometry allows to directly link Sr- and O-isotope measurements at a sample size of individual crystals, isotopic heterogeneity within crystals remains a problem that we cannot not resolve by our method. O isotope ratios measured on phenocrysts were recalculated to magmatic values to account for mass-dependent fractionation during crystallization in magmas for given SiO_2 contents (Bindeman et al., 2004). Sr-isotopes range from 0.7069 to 0.7082 exceeding the variations in the bulk rock samples (0.7071-0.7081).

However, ranges in Sr-isotope compositions vary significantly between eruptive periods, with some eruptions showing larger scatter than others. Recalculated $\delta^{18}O$-melt values also show a large range mostly between 8 and 10 ‰ VSMOW, maximum and minimum values vary from ~12 to ~7.5 ‰ VSMOW. Our data obtained so far (Fig.1), show compositions that are very different from typical mantle values, from the other Italian Peninsula magmatic compositions (Alban Hills, Mts. Ernici, Ischia, Mt. Vesuvius, Aeolian Islands, Tuscany and Sardinia) and from typical trends of magmatic rocks in subduction zones worldwide (Kamchatka, Lesser Antilles, Indonesia and Central Andes). These results suggest that magmas are derived from (a) a mantle source variably modified by pelagic sediments (as for Vesuvius) that were later (b) assimilated by high $\delta^{18}O$ crustal material that did not significantly affect the Sr-isotope composition. Limestone assimilation is a possibility but can be ruled out by the absence of a correlation between $\delta^{18}O$ and CaO. Assimilation of altered high- $\delta^{18}O$ older volcanic deposits of similar Sr-isotope composition is more likely but needs to be tested.

In order to constrain the residence time of one large Campi Flegrei magma batch from the Agnano Monte Spina eruption (A-MS; 4.7 ka; VEI = 4; 0.85 km^3 D.R.E) we measured Ba zonation profiles of alkali feldspar phenocrysts by combined energy-dispersive and wavelength-dispersive electron microprobe analyses. We focused on distinct compositional breaks near the rim of the crystals that likely represent the last mixing event prior to eruption, following two different approaches (Fig.2): (1) quantitative Ba compositional profiles by point analyses across the crystals and (2) grey-scale profiles taken along a short transect crossing growth discontinuities parallel to the point profiles.

Our preliminary estimates gave diffusion times from quantitative point analyses between 100's up to 4000 years

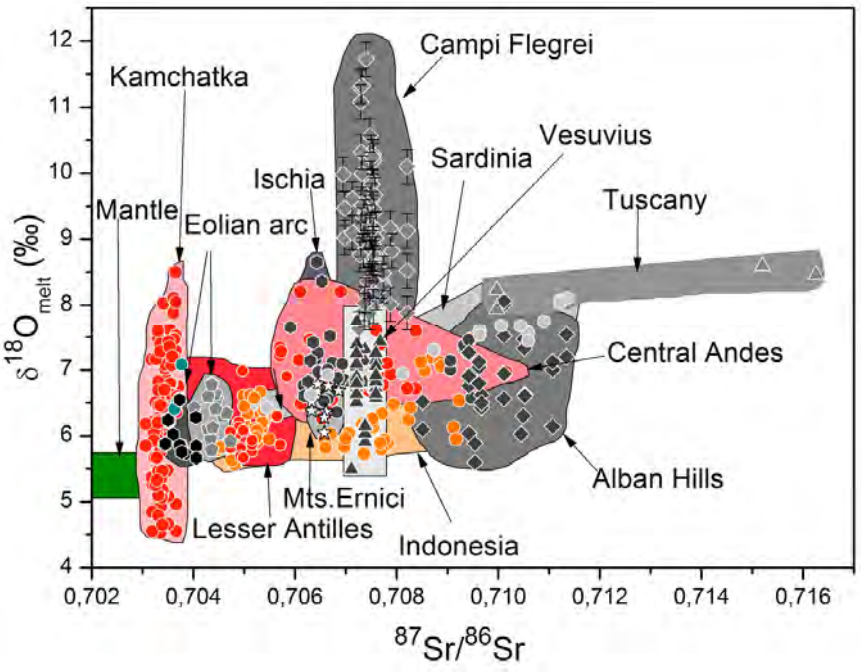

Fig. 1: $^{87}Sr/^{86}Sr$- $\delta^{18}O$ systematics in the Campi Flegrei magma system compared to to several subduction settings.

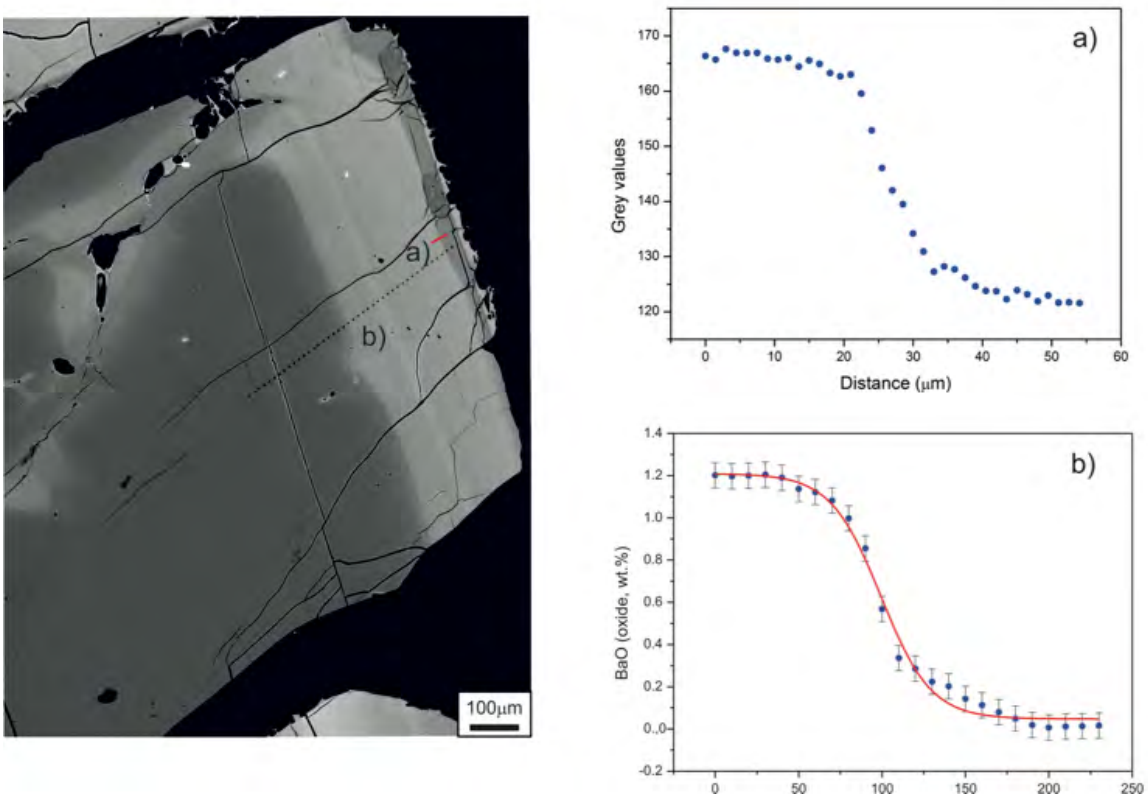

Fig. 2: A comparison between interpolated BaO profile and grey- scale profile in an alkali feldspar phenocryst in A-MS.

at 900°C. At higher T (950°C) these values reduce to from a few years to 600 yrs. Grey-scale profiles give times of 400 yrs (900°C) and 60 to 70 yrs (950°C). From a volcanological and geochronological point of view, a centuries to decades timescale is in reasonable agreement with the reconstructed volcanic history preceding the A-MS eruption.

References:
Bindeman IN, Ponomareva VV, Bailey JC, Valley JW (2004) Volcanic arc of Kamchatka: a province with high-$\delta^{18}O$ magma sources and large-scale $^{18}O/^{16}O$ depletion of the upper crust. Geochim Cosmochim Acta 68: 841-865.

IODP

Glacial-interglacial productivity changes in the eastern equatorial Pacific upwelling system and its response to Plio-Pleistocene ice-sheet dynamics

KIM A. JAKOB[1], PAUL A. WILSON[2], ANDRÉ BAHR[1], CLARA T. BOLTON[3], JÖRG PROSS[1], JENS FIEBIG[4], OLIVER FRIEDRICH[1]

[1]Institute of Earth Sciences, Heidelberg University, Im Neuenheimer Feld 234–236, 69120 Heidelberg, Germany
[2]National Oceanography Centre Southampton, University of Southampton, European Way, Southampton SO14 3ZH, UK
[3]Aix-Marseille Université, CNRS, IRD, CEREGE UM34, 13545 Aix en Provence, France
[4]Institute of Geosciences, Goethe-University Frankfurt, Altenhöferallee 1, 60438 Frankfurt am Main, Germany

Oceanic upwelling regions play a key role in controlling Earth's climate [e.g., *Pennington et al.*, 2006]. An ideal natural laboratory for studying the dynamics of an upwelling system is the eastern equatorial Pacific Ocean (EEP). There, both equatorial and coastal upwelling contribute to conditions that support more than 10% of the global biological production in the present-day oceans [*Pennington et al.*, 2006], making it an important component in Earth's atmospheric and marine carbon budget.

During the late Pliocene, large ice sheets were established on North America and Eurasia [e.g., *Shackleton et al.*, 1984; *Bailey et al.*, 2013]. This so-called "intensification of Northern Hemisphere glaciation" (iNHG) resulted in large productivity changes in the oceans on both secular and glacial-interglacial (G-IG) timescales. At the global scale proxy records for export productivity demonstrate high-latitude productivity shifts that are broadly coincident with but opposite in sign to (sub)tropical productivity patterns in upwelling regions

[e.g., *Lawrence et al.*, 2006]. The mechanisms driving these low-latitude productivity fluctuations are a subject of ongoing debate with hypotheses including changes in trade-wind strength/upwelling intensity ("upwelling hypothesis"; e.g., *Cleaveland and Herbert* [2007]) and/or changes in the nutrient content of the upwelled water masses ("nutrient delivery hypothesis"; e.g., *Lawrence et al.* [2006]).

In this study we test the competing hypotheses for G-IG productivity change in the EEP during the latest Pliocene to earliest Pleistocene. To shed new light on the dynamics and the origin of G-IG productivity changes in the EEP, we present new suborbital resolution proxy records for the latest Pliocene/early Pleistocene from Ocean Drilling Program (ODP) Site 849 (0°11'N, 110°31'W; 3851 m water depth [*Mayer et al.*, 1992]). This site is located within the equatorial divergence system in the heart of the EEP upwelling regime. We analyzed the time interval from 2.65 to 2.4 Ma (marine isotope stages (MIS) G1 to 94), including the first three consecutive large-amplitude (~1‰ in benthic $\delta^{18}O$) G-IG cycles (MIS 100 to 96) representing the culmination of late Pliocene iNHG. Marine isotope stage 100 has particular significance because it was the first glacial during which (i) the Laurentide Ice Sheet (LIS) advanced into the mid-latitudes [e.g., *Bailey et al.*, 2010] and (ii) ice rafting first became widespread across the North Atlantic Ocean [*Shackleton et al.*, 1984] with ice-rafted debris flux and provenance in the sub-polar North Atlantic comparable to that of the last glacial maximum [*Bailey et al.*, 2013]. Advance of the LIS into the mid-latitudes has important implications for atmospheric circulation and hydroclimate regionally [e.g., *Bailey et al.*, 2010] and therefore may also have significantly influenced the behavior and dynamics of upwelling in the EEP. Here, we use suborbitally resolved sand accumulation rates as a productivity proxy to compare with an alkenone-based paleoproductivity record from ODP Site 846 [*Lawrence et al.*, 2006]. We also generated $\delta^{13}C$ records in three foraminiferal species (shallow-dwelling planktic, thermocline-dwelling planktic, and benthic) to investigate the potential influence of different water masses at the study site and to evaluate $\delta^{13}C$ gradients between the sea-surface and thermocline, shedding new light on changes in thermocline depth and thus upwelling intensity.

Our results suggest that latest Pliocene/early Pleistocene primary productivity changes in the low-latitude Pacific Ocean follow the obliquity dominated G-IG cyclicity, but lag peak glacials by ~8 kyr at Site 849. Export productivity increased during early Pleistocene glacials and reached maximum values towards the glacial terminations of MIS 100, 98 and 96. We identify two processes that regulate the observed G-IG variability in primary productivity at Site 849. These processes are i) nutrient delivery from the Southern Ocean to the EEP, which was a regulating factor from MIS G1 to 94 and was presumably controlled by sea-ice extent in the Southern Ocean and ii) the intensity of trade-wind induced upwelling in the EEP, which started to play a major role in regulating EEP export productivity from MIS 100 onwards and which we hypothesize to be controlled by the influence of a large LIS. We conclude that enhanced nutrient delivery from high southern latitudes during peak glacials, superimposed by regional upwelling intensification towards glacial terminations strongly regulated primary productivity rates in the EEP from MIS 100 onwards.

References:
Bailey et al. (2010), A low threshold for North Atlantic ice rafting from "low-slung slippery" late Pliocene ice sheets, *Paleoceanography*, *25*, PA1212, doi:1210.1029/2009PA001736.
Bailey et al. (2013), An alternative suggestion for the Pliocene onset of major northern hemisphere glaciation based on the geochemical provenance of North Atlantic Ocean ice-rafted debris, *Quaternary Science Reviews*, *75*, 181–194.
Cleaveland & Herbert (2007), Coherent obliquity band and heterogeneous precession band responses in early Pleistocene tropical sea surface temperatures, *Paleoceanography*, *22*, PA2216, doi:2210.1029/2006PA001370.
Lawrence et al. (2006), Evolution of the eastern tropical Pacific through Plio-Pleistocene glaciation, *Science*, *312*, 79–83.
Mayer et al. (1992), *Proceedings of the Ocean Drilling Program, Initial Reports*, *138*, Ocean Drilling Program, College Station, Texas.
Pennington et al. (2006), Primary production in the eastern tropical Pacific: A review, *Progress in Oceanography*, *69*(2–4), 285–317.
Shackleton et al. (1984), Oxygen isotope calibration of the onset of ice-rafting and history of glaciation in the North Atlantic region, *Nature*, *307*, 620–623.

IODP

Late Pliocene to Holocene spatio-temporal variation in the flowpath of the Kuroshio Current (NW Pacific)

A.-S. JONAS[1], L. SCHWARK[1,2], T. BAUERSACHS[1]

[1]Christian-Albrechts-Universität, Institut für Geowissenschaften, Abteilung für Organische Geochemie, Ludewig-Meyn-Str. 10, 24118 Kiel
[2]WA-OIGC, Department of Chemistry, Curtin University, Perth, Australia

The Kuroshio Current (KC) is an important western boundary current of the Northwest (NW) Pacific Ocean, which transports warm and saline water masses from the Western Pacific Warm Pool to northern mid-latitudes. Therefore, its strength and flow pattern play an important role in the meridional advection of moisture and heat to northern latitudes and exert a major control on the climate evolution of the NW Pacific and the East Asian continent.

Several paleoceanographic studies (Chinzei et al. 1987, COHMAP members 1988) have demonstrated that the subtropical KC front shifted southward to 33°N during the last glacial period, allowing the Oyashio Current (OC) to transport polar waters to more southerly latitudes. At present, both ocean currents converge at 36°N east off Japan, where they are deflected eastward and form the KC-OC interfrontal zone. SE off Japan, the KC shows a bimodal stationary flow pattern with a large meander path and a path strictly following the coastline off Japan. The meander paths vary on short time scales and are mainly depending on changes in volume transport and current velocity of the KC (Kawabe 1995, 2005). During phases characterized by large meander paths, the warm waters of the KC are found further offshore and cold surface water masses establish off central Japan (Sawada and Handa 1998), resulting in a drop in sea surface temperatures (SST) in this area. By contrast, during phases of the short meander path, SSTs off central Japan are considerably higher compared to areas located upstream of the KC.

Although a number of studies have investigated the most recent history (~the last 25 ka) of climate evolution in the NW Pacific Ocean (e.g. Thompson 1981, Chinzei et al. 1987, Sawada and Handa 1998, Yamamoto et al., 2013), only little information on climate and paleoceanographic change over geological time scales is available. Our study

focuses on the long-term climate evolution of the NW Pacific Ocean off Japan from Late Pliocene to present, for which we have analyzed deep-sea sediments obtained from site U1437 (Izu-Bonin-Mariana rear-arc), which was drilled during IODP Expedition 350 “Izu-Bonin-Mariana Rear-arc: The missing half of the subduction factory” and which is located beneath the large meander of the KC. Site U1437 is located at a water depth of 2117 mbsl and yielded excellent core recovery in Holes U1437 B, D, and E, yielding a total thickness of 1806.5 m. Shipboard and postcruise biostratigraphy and magnetostratigraphy measurements indicate that the upper 1303 m of the sediment succession cover a time period from the Holocene to upper Miocene. The age model has not been fully extended to deeper depths yet but nannofossil assemblages and preliminary U-Pb zircon dates suggest an age ranging from ca. 11–15 Ma for the depth interval from 1389–1403 mbsf. A total of 327 samples has been collected over the entire sediment succession, of which 60 samples covering the last 3 Ma have been analyzed for their bulk geochemical inventory and their biomarker distributions, including the lipid paleothermometers $U^{K'}_{37}$ and TEX^{H}_{86}. Here, we compare our U1437 data to SST data from IODP Site C0011 from the Nankai Trough area, which was drilled during IODP Expedition 333 (“NanTroSEIZE Stage 2: Subduction Inputs 2 and Heat Flow”). The site is located beneath the short meander path of the KC allowing to infer information on the variation of the flow path of the KC over time and its impact on the paleoclimate evolution of the NW Pacific.

TOC values at Site U1437 decline with depth and range from 0.13 to 0.68 wt% (average 0.4 wt%), which is well in line with values previously reported from other deep-sea sediments (Müller et al. 1977) and also similar to values observed at Site C0011. BIT values are generally low (<0.14), showing that TEX^{H}_{86}–based SST can reliably be reconstructed from Site U1437. Results from our preliminary SST investigations at Site U1437 show the same overall decreasing trend both in $U^{K'}_{37}$- and TEX^{H}_{86}-inferred SSTs over the last 3 Ma; similar to what is seen in SSTs records from Site C0011 and the global $\delta^{18}O$ stack of benthic foraminifera by Lisiecki and Raymo (2005). This is likely associated with the onsetting northern hemisphere glaciation and the establishment of northern polar ice caps during the late Pliocene. TEX^{H}_{86}-SSTs ranged between 21.5°C at 180 ka and 25.7°C at 2 ka, while $U^{K'}_{37}$-inferred temperatures were at a maximum of 26.8°C in the oldest studied sample (2.98 Ma) and lowest (13.1°C) at 0.305 Ma (Fig. 1). Interestingly, $U^{K'}_{37}$-SSTs at Site U1437 are always lower than TEX^{H}_{86}-inferred SSTs, except for the time interval older than 2.2 Ma. This may be related to a shift in the production season of the biological sources of the lipid proxies (i.e., haptophyte algae and Thaumarchaeota). Prior to 2.2 Ma, the TEX^{H}_{86} signal rather represents SSTs of the colder months, while the $U^{K'}_{37}$ proxy likely reflects the SSTs of the warmer season. A subsequent shift of the TEX^{H}_{86} to warmer months compared to the $U^{K'}_{37}$ occurred after 2.2 Ma. Nonetheless, $U^{K'}_{37}$- and TEX^{H}_{86}-based SST records show a very similar pattern and seem to reflect the glacial-interglacial see-saw pattern of the mid- to late Pleistocene within the last 1 Ma.

The comparison of $U^{K'}_{37}$- and TEX^{H}_{86}- inferred SST records from Site U1437 and C0011 indicates that $U^{K'}_{37}$-

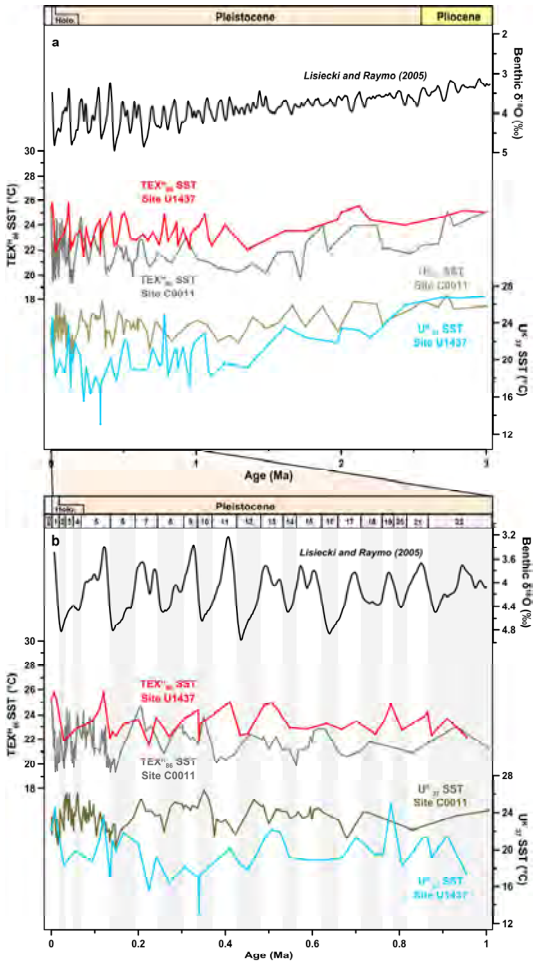

Fig.1: TEX^{H}_{86}- and $U^{K'}_{37}$-inferred SST evolution at IODP Sites U1437 and C0011 in the NW Pacific Ocean over the last 3 Ma (a) and 1 Ma (b) in comparison to the global $\delta^{18}O$-stack of benthic foraminifera by Lisiecki and Raymo (2005). Cold marine isotope stages (MIS) are indicated as grey-shaded bars.

SSTs at Site U1437 were always lower than those at Site C0011, while TEX^{H}_{86}-SSTs at Site U1437 were generally higher than those at Site C0011, except for a few periods during the mid to late Pleistocene. Since the two IODP sites are only ~230 km apart, changes in growth seasons of the two groups of source organisms can not account for the observed temperature offsets between the two sites.The alkenones used for the $U^{K'}_{37}$ calculation are synthesized by photosynthetic haptophyte algae, which dwell exclusively in the photic zone. Therefore, the inferred $U^{K'}_{37}$-SSTs represent the temperature evolution at the ocean´s surface, whereas TEX^{H}_{86}-SST may represent an integrated temperature signal of surface and subsurface water masses. Indeed, maximum isoprenoid GDGT production has been reported at the thermocline in the East China Sea (Nakanishi et al. 2012). Higher $U^{K'}_{37}$-SSTs at Site C0011 indicate that the short meander path of the KC was the dominant modification throughout the last 3 Ma. A shallower thermocline at Site U1437 due to a lower vertical expansion of warm surface water masses compared to Site C0011 may thus explain the higher observed TEX^{H}_{86}-SSTs at the site compared to those at site C0011.

References:

Chinzei, K., K. Fujioka, H. Kitazato, I. Koizumi, T. Oba, M. Oda, H. Okada, T. Sakai, and Y. Tanimura (1987). Postglacial environmental change of the Pacific Ocean off the coasts of central Japan. Mar. Micropaleontol. 11, 273-291.

COHMAP Members (1988). Climatic changes of the last 18,000 years: observations and model simulations. Science 241, 1043–1052.
Kawabe, M. (1995). Variations of Current Path, Velocity, and Volume Transport of the Kuroshio in Relation with the Large Meander. Journal of Physical Oceanography 25, 3103-3117.
Kawabe, M. (2005). Variations of the Kuroshio in the Southern Region of Japan: Conditions for Large Meander of the Kuroshio. Journal of Oceanography 61, 529-537.
Lisiecki, L. E., and M. E. A. Raymo (2005). Pliocene-Pleistocene stack of 57 globally distributed benthic delta δ18O records. Paleoceanography 20, PA1003.
Müller, P.J., (1977). C/N ratios in Pacific deep-sea sediments: effect of inorganic ammonium and organic nitrogen compounds sorbed by clays. Geochim. Cosmochim. Acta 41(6), 765–776.
Nakanishi, T., M. Yamamoto, T. Irino, and R. Tada (2012). Distribution of glycerol dialkyl glycerol tetraethers, alkenones and polyunsaturated fatty acids in suspended particulate organic matter in the East China Sea. J. Oceanogr. 69, 959-970.
Sawada, K., and N. Handa (1998). Variability of the path of the Kuroshio ocean current over the past 25,000 years. Nature 392, 592-595.
Thompson, P. R, (1981). Planktonic foraminifera in the western North Pacific during the past 150000 years: comparison of modern and fossil assemblages. Palaeogeogr. Palaeoclimatol. Palaeoecol. 35, 241-279.
Yamamoto, M., Kishizaki, M., Oba, T., and Kawahata, H. (2013). Intense winter cooling of the surface water in the northern Okinawa Trough during the last glacial period. Journal of Asian Earth Sciences 69, 86-92.

ICDP

Report on the ICDP Lake Towuti Drilling Campaign 2015 in Indonesia

JENS KALLMEYER[1], HENRIKE BAUMGARTEN[3], ANDRÉ FRIESE[1], ASCELINA HASBERG[2], MARTIN MELLES[2)], THOMAS VON RINTELEN[4], AURÈLE VUILLEMIN[1], THOMAS WONIK[3], THE TDP SCIENCE TEAM[5]

[1]GFZ Potsdam, Section 5.3 Geomicrobiology, Telegrafenberg, 14473 Potsdam
[2]University of Cologne, Institute of Geology and Mineralogy
[3]Leibniz Institute for Applied Geophysics (LIAG)
[4]Museum für Naturkunde, Leibniz-Institut für Evolutions- und Biodiversitätsforschung
[5]Brown University, Dept. of Earth, Environmental, and Planetary Sciences

Lake Towuti is a tropical 200 m deep tectonic lake seated in ophiolitic rocks and surrounded by lateritic soils. Its location on Sulawesi, Indonesia, renders Lake Towuti's sediments prime recorders of paleoclimatic changes in the tropical Indo-Pacific Warm Pool. The tropical climate and the lateritic weathering of the (ultra)mafic catchment of the Malili Lakes system cause a strong flux of iron to the lake, leading to ferruginous sediments that likely support microbial communities, which can utilize a range of metalliferous substrates. Iron oxides are effectively trapping all available phosphorus in the water column, thereby driving Lake Towuti's water column towards severely nutrient-limited conditions. However, due to anoxia in the deepest parts of the stratified water column and the sediment, metal reduction processes lead to a release of adsorbed phosphate, allowing for increasing biological activity.

From May to July 2015, the Towuti Drilling Project (TDP) carried out a drilling campaign at Lake Towuti that was mainly funded by the ICDP, the U.S. NSF, the Swiss NSF and the German DFG. Despite severe technical problems the project was able to recover over 1000 m of sediment drill cores from three sites. At all three sites, replicate cores down to 133, 154, and 174 m below lake floor penetrated the entire lake sediment record. Initial sedimentological data indicate that at least 800 ky of sedimentation history were recovered.

For the first time in the history of ICDP a dedicated core for destructive biogeochemical and geomicrobiological analyses was drilled, using a novel particulate tracer to check for contamination through infiltration of drilling fluid. GFZ's mobile geomicrobiology laboratory (BugLab) was deployed to provide a suitable environment for processing the geomicrobiological samples. Further geomicrobiological and biogeochemical analyses (porewater chemistry, turnover rates, microbial abundance and diversity, cultivation) are currently being carried out at GFZ.

Downhole logging data were acquired by LIAG at sites 1 and 2. The following tools were applied: spectral gamma ray, magnetic susceptibility, resistivity, dipmeter, borehole televiewer and sonic. Spectral gamma ray was run through the drillpipe and thereafter, pipes were pulled gradually to maintain the borehole stability. Some pipes were kept in hole to allow other probes to enter. Initial processing of the data at site 1 indicates a remarkable change in spectral gamma ray values from the bottom of the hole towards a depth of 103 m below lake floor (mblf). First lithological interpretation shows the transition from an initial state to lacustrine conditions at according depth. In addition, sharp spikes in the magnetic susceptibility data (e.g. at 70 mblf) are interpreted to indicate tephra layers.

Immediately after retrieval all cores were logged on site for magnetic susceptibility and p-wave velocity/amplitude. Except for the geomicrobiology core all other cores remained unopened on site and were shipped to the U.S. lacustrine core repository, LacCore, at the University of Minnesota, USA. There, core processing (MSCL logging, opening, core description, core correlation and subsampling) took place in late 2015 and early 2016. The archive core halves of site 2 in the northern part of Lake Towuti, close to the Mahalona River Delta, were shipped to the University of Cologne in Feb. 2016 for high-resolution XRF scanning, along with subsamples for sedimentological, granulometric, and geochemical analyses. The analytical work on these samples over the next months shall provide information on (i) the dating of the sediment record, (ii) the long-term development of Lake Towuti, with its formation and the onset of riverine input from other Malili lakes, (iii) the precipitation-controlled riverine inflow from the Mahalano River during the past ~80,000 years, (iv) the dimension and potential reasons for lake-level fluctuations, (v) the understanding of the variability in lake mixing and stratification, and (vi) the reconstruction of weathering conditions and soil erosion in the lake´s catchment. At Museum für Naturkunde, comprehensive comparative molecular clock analyses based on the major evolutionary radiations in the Malili Lakes and Lake Towuti in particular have shown a diverse range of ages (0.7-4 My) for the various species groups that can be linked to the timing of environmental events that drive organismic diversification, e.g. changes in lake connectivity, lake level fluctuations etc., which were recorded in the recovered sediment cores.

IODP

Geochemical Evolution of Mantle Plume Magmas in the Pacific

F. KEMNER, C. BEIER, K. HAASE

GeoZentrum Nordbayern, Universität Erlangen-Nürnberg, Schlossgarten 5, D-91054 Erlangen, Germany

Numerous volcanic island and seamount chains cross the Pacific Ocean floor, most of which are associated with the presence of mantle hotspots. These hotspots appear to be stationary and some have been active for at least 80 million years (e.g. Louisville and Hawaii) implying ascent of hot deep mantle material. Many volcanic chains are age-progressive and the magmatic activity of single volcanoes ranges from <1 to 8 Ma. Most Pacific intraplate volcanoes show changes in magma composition during their active life time where major element, trace element, and isotopic compositions vary considerably within time scales of 1-2 Ma. Hawaiian volcanoes apparently evolve through four magmatic stages, that are characterized by distinct magma compositions, duration of volcanism and volume of magmatic output. It is unclear whether all intraplate volcanoes follow these patterns, as many other intraplate volcanoes show only one or two magmatic stages. Variations of major elements of intraplate volcanoes with time have been suggested to reflect variations in degree and depth of melting as a function of the relative position of the moving lithospheric plate above the mantle plume. More recent publications proposed that the mantle may be heterogeneous in terms of major elements so that - at least to a certain extent - observed variations in intraplate volcanoes can be explained by melting of a heterogenous source.

Large data sets exist for volcanoes of the Hawaii-Emperor chain but also for other Pacific chains like those of the Marquesas and Societies. However, due to the scarcity of subaerial available rocks much less data is available from the Louisville seamount chain, whose time scale of magmatic activity is comparable to that of Hawaii. Prior to the RV Sonne expedition SO167 in 2002, where 8 volcanoes were dredged, only a hand full of rock samples were available. Additional samples were dredged during the AMAT expedition of the RV Revelle in 2006. From December 2010 to February 2011 6 guyots were drilled during IODP leg 330 and core material was recovered down to a maximum depth of 522 m.

The combined data set of major and trace elements of glasses from IODP 330 together with a compilation of whole rock data (major elements, trace elements, isotopes, and age-determinations) of the Louisville seamount chain from IODP 330 and older cruises together with data sets from the GEOROC data base for Hawaii, Society Islands and Marquesas allow us to compare geochemical variations on small scale within single volcanoes as well as on larger scales within and between these four plume trails. A combination of several factors may control the geochemical heterogeneity observed in plumes, such as source heterogeneity and variations in melting dynamics and thus determining the temporal magmatic evolution of single volcanoes along different hotspot trails can provide important insights into the origin of oceanic intraplate magmatism.

Hawaiian islands show a large variation in major elements with SiO_2 ranging from 35 to 67.6 wt% and large amounts of tholeiitic as well as alkaline samples with total alkalis up to 14 wt.%. Isotopic compositions range from 0.7029 to 0.7045 for $^{87}Sr/^{86}Sr$, from 0.5125 to 0.5133 for $^{143}Nd/^{144}Nd$ and from 17.587 to 18.859 for $^{206}Pb/^{204}Pb$. Incompatible trace element ratios range from 1.5 to 4.6 and from 4 to 60 for Dy/Yb and Ce/Yb, respectively. Single volcanoes show a linear trend with increasing Dy/Yb and Ce/Yb ratios that is in agree with an increasing garnet component in the mantle source at constant melting degrees during magma genesis.

The Society Islands also show a large variation in major elements with SiO_2 ranging from 36 to 65 wt.% with a majority of samples in the range of 42 to 50 wt.%. Only a minor part of the samples is tholeiitic and the vast majority of the samples is strongly alkaline with overall higher proportion of alkalis at given SiO_2 compared to Hawaii. There is a very strong negative linear correlation between $^{143}Nd/^{144}Nd$ and $^{87}Sr/^{86}Sr$. The isotopic variations of $^{143}Nd/^{144}Nd$ and $^{206}Pb/^{204}Pb$ of the Society Islands are significantly lower than those of Hawaii (by a factor of ~2 lower) and are the lowest of all four island chains, the variations in $^{87}Sr/^{86}Sr$ are by a factor of ~2 higher than in Hawaii. Compared to Hawaii the Ce/Yb ratios are generally higher at a given Dy/Yb ratio.

Variations in SiO_2 content of Marquesas samples is comparable to those of Hawaii and Society islands, the maximum alkali content (~17.5 wt.%) is higher than that of the other island and seamount chains. The Fatu Hiva group (south-western islands) have generally higher total alkalis at a given SiO_2 than the Ua Huka group (north-eastern islands). Isotopic variations in $^{87}Sr/^{86}Sr$ are similar to Society Islands, $^{143}Nd/^{144}Nd$ variations are significantly higher than those of the other island and seamount chains and $^{206}Pb/^{204}Pb$ variations are similar to that of Hawaii. The Ua Huka and Fatu Hiva groups show parallel linear trends of increasing $^{87}Sr/^{86}Sr$ with decreasing $^{143}Nd/^{144}Nd$ with the Fatu Hiva group indicating generally lower isotopic values. While Hawaii and Societies show increasing Zr/Nb ratios with decreasing $^{143}Nd/^{144}Nd$, samples of Marquesas show an opposite trend with increasing Zr/Nb and increasing $^{143}Nd/^{144}Nd$. Compared to Hawaii and Societies the Marquesas islands show higher Ce/Yb at given Dy/Yb ratios. The Fatu Hiva group samples have generally higher Ce/Yb than the Hiva Oa group samples.

Silica variations and the maximum total alkali content in Louisville samples are significantly lower than those of the other island chains ranging from 36 wt.% to 54 wt.% and 8 wt.%, respectively. The variations in $^{87}Sr/^{86}Sr$ are lower compared to the other island chains, the variation in $^{143}Nd/^{144}Nd$ is similar to that of the Societies and the variations in $^{206}Pb/^{204}Pb$ are lower compared to Hawaii and Marquesas but almost twice as high as in the Societies. In contrast to the other island chains there is no clear correlation between Zr/Nb and $^{143}Nd/^{144}Nd$. The variations of Ce/Yb and Dy/Yb of Louisville samples are similar to those of Hawaii.

IODP

Layered Gabbros from Hess Deep (EPR) drilled by IODP: The role of orthopyroxene

J. KOEPKE[1], C. ZHANG[1], O. NAMUR[1], R. MEYER[2]

[1] Institut fuer Mineralogie, Leibniz Universität Hannover; koepke@mineralogie.uni-hannover.de, o.namur@mineralogie.uni-hannover.de, c.zhang@mineralogie.uni-hannover.de
[2] GFZ Potsdam; romain.meyer@gfz-potsdam.de

At the Hess Deep Rift in the equatorial Pacific at the East Pacific Rise (EPR), IODP (International Ocean Discovery Program) Expedition 345 drilled, for the first time in the history of IODP, coherent cores of the deeper part of the lower, plutonic crust from a fast-spreading ridge (Gillis et al., 2014). The drilled cores show spectacular modal and/or grain size layering present in >50% of the recovered core, validating for the first time the use of the ophiolite model for interpreting EPR crust. Typical rocks recovered are primitive (Mg# 75-89) olivine gabbros and troctolites. A significant first-order observation from this expedition is that orthopyroxene was found as an abundant cumulus phase in many of the layered primitive gabbroic rocks. This was unexpected, since experiments on the liquid line of descent of MORB show that orthopyroxene always crystallizes late in the sequence of MORB-type systems, in a regime where the melt fraction is low, implying interstitial crystallization. Recovered rocks at Site U1415, however, show orthopyroxene as a prismatic phase in primitive gabbroic rocks and even as monomineralic bands in some primitive gabbronorites.

In the frame of the SPP IODP, a project was started which aimed to understand the exact mechanism of the magmatic evolution of the lower crust at Hess Deep. This projects follows a multimethodical approach: Theme (1) focusses on the petrology/geochemistry of the natural rocks by using microanalytical tools to be applied to the mineral phases of the gabbroic rocks drilled at Hess Deep, with focus on the role of orthopyroxene. Theme (2) is an experimental project with the approach to simulate both melt/rock interaction as well as equilibrium crystallization and near-perfect fractional crystallization in a system corresponding to Hess Deep bulk crust average, focusing to understand the role of orthopyroxene. Here, we present our first resultes with respect to theme (1): results of major (EPMA) and trace element (LA-ICP-MS) analysis of phases from natural gabbros from Hess Deep, with focus on the role of orthopyroxene.

The Mg#'s of ortho- and clinopyroxenes from 18 primitive gabbroic rocks from Hess Deep vary within a narrow range between 82-90 (clinopyroxene) and 80-86 (orthopyroxene). A good correlation between the Mg#'s of orthopyroxene and clinopyroxene implies a common evolution by co-crystallization/fractionation. Half of all analyses of orthopyroxene show Cr2O3 contents $\leq$ 0.1 wt%, indicating that these orthopyroxenes do not correspond to relics which survived from a melt in equilibrium with mantle. First results on trace element analysis of ortho-, clinopyroxene, and plagioclase in primitive olivine gabbros drilled by Expedition 345 and in more evolved gabbronorites from the top of the plutonic section of Hess Deep drilled by ODP Leg 147 reveal chondrite-normalized REE patterns which are very similar for the corresponding minerals. The patterns of the gabbronorite phases are always slightly enriched, compared to those of the primitive gabbro from the base of the crust, implying an origin by fractional crystallization from the same parental melt.

References:
Gillis, K.M., Snow, J.E., Klaus, A., Abe, N., Adriao, A.B., Akizawa, N., Ceuleneer, G., Cheadle, M.J., Faak, K., Falloon, T.J., Friedman, S.A., Godard, M., Guerin, G., Harigane, Y., Horst, A.J., Hoshide, T., Ildefonse, B., Jean, M.M., John, B.E., Koepke, J., Machi, S., Maeda, J., Marks, N.E., McCaig, A.M., Meyer, R., Morris, A., Nozaka, T., Python, M., Saha, A., Wintsch, R.P. (2014): Primitive layered gabbros from fast-spreading lower oceanic crust. Nature, 505, 204-207.

ICDP

Magnetic fabrics in shear zones of collisional orogens: a case study from the COSC-1 drilling, Sweden

A. KONTNY[1], M. SIEBERT[1], J.C. GRIMMER[1]

[1]Institut für Angewandte Geowissenschaften, Karlsruhe Institut für Technologie, Adenauerring 20a, 76131 Karlsruhe

The SPP-ICDP project "Collisional Orogeny in the Scandinavian Caledonides" (COSC) focuses on the transport and emplacement of far-travelled, metamorphic nappes in a major mid-Paleozoic orogen in western Scandinavia. Two, about 2.5 km deep drillings (COSC-1 and COSC-2) are proposed to core a composite profile of the high-grade metamorphic Seve nappes through the underlying lower grade metamorphic allochthons and Fennoscandian basement in order to understand the deformation history and fluid migration during metamorphism in space and time.

The COSC-1 drilling, which recovered oriented drill cores in summer 2014 comprising mainly garnet micaschists, gneisses, and minor amphibolites of the lower Seve nappe, has revealed significant magnetic anomalies, especially in its lower part (1900 - 2500 m) where mylonitic fabrics prevail. In this depth interval magnetic susceptibility varies from 0.1 to 100 x 10^{-3} SI units. These data indicate a strong variation from paramagnetic (dominated by Fe-bearing silicate minerals) to ferrimagnetic (dominated by magnetite) behaviour and allows to investigate different Fe-bearing silicate mineral and magnetite subfabrics. Degrees of magnetic anisotropy (P') range from 1.1 to about 3 (which means an anisotropy of 300%) with most samples grouping around 1.5. Samples with extremely high magnetic susceptibility and anisotropy show a field-dependence of the k_{max} direction of about 6% similar to earlier observations described in Kontny et al. (2012) for the Slipsiken shear zone about 150 km to the NNE of the COSC-1 drill site. Shape factors vary from prolate to oblate with a tendency towards more oblate shapes in the deeper, mylonite-dominated part of the profile.

The orientation of magnetic foliation is predominantly subhorizontal (Fig. 1) in agreement with the observed macroscopic foliation of the gneisses and mylonites in the drill cores. Magnetic lineation (k_1 axis in Fig. 1) shows different subhorizontal orientations, largely in agreement with the generally known tectonic transport directions (e.g. Grimmer et al., 2015).

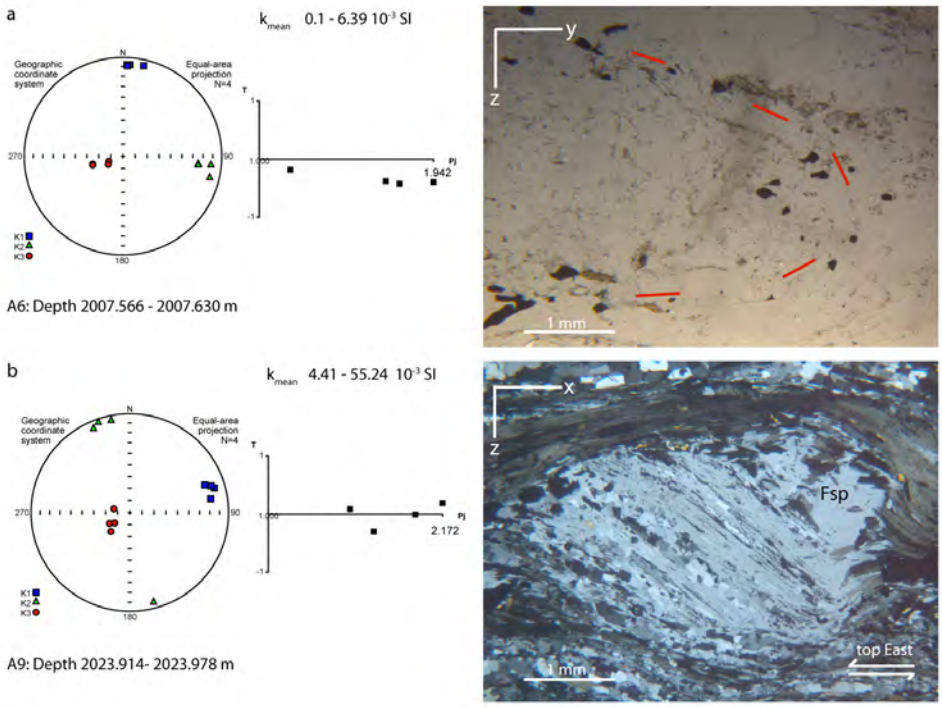

Figure 1: Stereographic projection (equal area, lower hemisphere) of principal magnetic susceptibility axis k_1, k_2 and k_{3x} for two representative samples of the amphibole gneiss with shape of AMS-ellipsoids presented in a Jelinek-diagram and microfabrics showing recumbent folds (in yz-section) and mineral stretching of Fe-Ti oxides (black) and feldspar porphyroblast with inclusion patterns interpreted as a syntectonic with respect to the main shearing deformation event (in xz-section).

Two main features are dominant: N to NNE oriented magnetic lineations suggest an intersection lineation (e.g. crenulation zonal axis, fold axis; Fig. 1a), and E-W to NW-SE oriented magnetic lineations indicate stretching lineations in agreement with top-to-E sense of shear (Fig. 1b). The main magnetic fabric forming deformation event observed in the COSC-1 drill cores is presumably related to a progressive post-peak metamorphic transport under lower amphibolite-facies conditions onto the lower nappe units of the Scandian orogen.

The drill core therefore provides the unique opportunity to study magnetic fabrics in relation to strain localization and deformation mechanism in different lithologies with varying mineralogical composition in a vertical crustal profile of several hundreds of meters and therefore our project will contribute significantly to the general questions i) how heterogeneously mylonitized nappe boundaries develop, ii) how strain intensity and deformation mechanisms are distributed across nappe boundaries, and iii) how deformation changes during nappe transport at changing PT-conditions. Our results will also contribute to a better understanding of the geology behind identified seismic reflectors and magnetic anomalies.

References:

Grimmer JC, Glodny J, Drüppel K, Greiling RO, Kontny AM (2015) Early- to mid-Silurian extrusion wedge tectonics in the central Scandinavian Caledonides. Geology 43/4, 347-350.

Kontny A, Engelmann R, Grimmer JC, Greiling RO, Hirt A (2012) Magnetic fabric development in a highly anisotropic magnetite-bearing ductile shear zone (Seve Nappe Complex, Scandinavian Caledonides). International Journal of Earth Sciences 101/3, 671-692

ICDP

Terrestrial ecosystem response to climate variability during MIS 12-11 in SE Europe based on high-resolution pollen analysis of `Lake Ohrid´ ICDP core sediments

I. KOUSIS[1], A. KOUTSODENDRIS[1], J. PROSS[1] AND THE SCOPSCO SCIENCE PARTY

Paleoenvironmental Dynamics Group, Institute of Earth Sciences, Heidelberg University, Im Neuenheimer Feld 234, D-69120 Heidelberg

To unravel the effects of short-term (centennial-scale) climate change during Marine Isotope Stages (MIS) 12 and 11 on terrestrial ecosystems in the Eastern Mediterranean region we here employ palynological analyses on Lake Ohrid sediment cores (DEEP site) that were recovered through an ICDP drilling campaign in 2013. The DEEP core represents a continuous archive spanning the past ~1.2 Ma (Wagner et al., 2014), thus allowing to investigate climate and ecosystem variability during the MIS 12 glacial, which was the most extreme glacial of the past 500 ka, and the MIS 11 interglacial, which represents one of the best orbital analogues for present and future climate. Specifically, this study aims at deciphering (i) the imprint of D–O- and Heinrich-like climate variability on vegetation in SE Europe during MIS 12; (ii) the ecosystem response to gradual climate warming during MIS 11; (iii) the response of SE European terrestrial and aquatic ecosystems to abrupt cooling events as they took place under full interglacial conditions during MIS 11 and are known to have affected ecosystem dynamics in Central Europe; and (iv) the development of temperature and precipitation gradients during MIS 12 and 11 on the Balkan Peninsula using

pollen-based climate reconstructions. Preliminary, low-resolution (~1.6 ka) pollen analysis of the DEEP core spanning the past 500 ka shows that MIS 12 is characterized by open vegetation with common presence of conifers and sporadically also of temperate trees, suggesting that the surroundings of Lake Ohrid served as a tree refugium during this glacial period (Sadori et al., 2015). Moreover, MIS 11 has a unique vegetation signature in contrast to more recent interglacials, i.e., a dominance of montane trees (*Abies* and *Picea*) and a weaker expansion of mesophilous trees (Sadori et al., 2015). To better understand the vegetation dynamics in SE Europe and tackle the main research questions of this study, ongoing palynological analysis will yield (i) centennial-scale resolution (~400 years) pollen records for MIS 12 and MIS 11 with high counting sums for pollen (>500 grains), algae and dinoflagellate cysts; and (ii) pollen-based climate reconstructions of the Lake Ohrid and Tenaghi Philippon (Pross et al., 2015) pollen records, which will be used for the establishment of temperature and precipitation gradients on the Balkans during MIS 12–11. The integration of the palynological data with sedimentological and geochemical data produced by collaborating working groups of the Lake Ohrid Science Party (SCOPSCO), as well as the pairing with regional and global climate records will ultimately allow deeper insight into the short-term climate and ecosystem variability during MIS 12 and 11.

References:

Pross, J., Koutsodendris, A., Christanis, K., Fischer, T., Fletcher, W.J., Hardiman, M., Kalaitzidis, S., Knipping, M., Kotthoff, U., Milner, A.M., Müller, U.C., Schmiedl, G., Siavalas, G., Tzedakis, P.C., Wulf, S., 2015. The 1.35-Ma-long terrestrial climate archive of Tenaghi Philippon, northeastern Greece: Evolution, exploration, and perspectives for future research. Newsletters on Stratigraphy 48, 253-276.

Sadori, L., Koutsodendris, A., Masi, A., Bertini, A., Combourieu-Nebout, N., Francke, A., Kouli, K., Joannin, S., Mercuri, A.M., Panagiotopoulos, K., Peyron, O., Torri, P., Wagner, B., Zanchetta, G., Donders, T. H. (2015). Pollen-based paleoenvironmental and paleoclimatic change at Lake Ohrid (SE Europe) during the past 500 ka. Biogeosciences Discussions, 12, 15461-15493.

Wagner, B., Wilke, T., Krastel, S., Zanchetta, G., Sulpizio, R., Reicherter, K., Leng, M.J., Grazhdani, A., Trajanovski, S., Francke, A., Lindhorst, K., Levkov, Z., Cvetkoska, A., Reed, J.M., Zhang, X., Lacey, J.H., Wonik, T., Baumgarten, H., Vogel, H., 2014. The SCOPSCO drilling project recovers more than 1.2 million years of history from Lake Ohrid. Scientific Drilling 17, 19-29.

ICDP

Borehole seismic in crystalline environment at the COSC-project in Central Sweden

F. Krauß[1], P. Hedin[2], B. Almqvist[2], H. Simon[3], R. Giese[1], S. Buske[3], C. Juhlin[2], H. Lorenz[2]

[1]Section 6.4, Centre for Scientific Drilling, GFZ German Research Centre for Geosciences, Helmholtz Centre Potsdam
[2]Dept. of Earth Sciences, Uppsala University
[3]Institute of Geophysics and Geoinformatics, TU Bergakademie Freiberg

As support for the COSC drilling project (Collisional Orogeny in the Scandinavian Caledonides; http://ssdp.se/projects/COSC), an extensive seismic survey took place during September and October 2014 in and around the newly drilled 2.5 km deep COSC-1 borehole. The main aim of the COSC project is to better understand orogenic processes in past and recently active mountain belts (Gee et al. 2010). For this, the Scandinavian Caledonides provide a well preserved case of Paleozoic collision of the Laurentia and Baltica continental plates. Surface geology and geophysical data provide knowledge about the geometry of the Caledonian structure. The COSC project will investigate the Scandinavian Caledonides with two approximately 2.5 km deep boreholes, located near Åre and Mörsil, in western Jämtland. The reflectivity geometry of the upper crust was imaged by regional seismic data and the resistivity structure by magnetotelluric methods. The crustal model was refined by seismic pre-site surveys in 2010 and 2011 to define the exact position of the first borehole, COSC-1 (Hedin et al. 2012).

The COSC-1 borehole was drilled close to the town of Åre during May to August 2014. The borehole was drilled through the Seve Nappe Complex, a part of the Middle Allochthon of the Scandinavian Caledonides that comprises units originating from the outer margin of Baltica. The upper 2350 m consist of alternating layers of highly strained felsic and calc-silicate gneisses and amphibolites. Below 1710 m the mylonite content increases successively and indicates a high strain zone of at least 800 m thickness (Hedin et al., 2015). At ca. 2350 m, the borehole leaves the Seve Nappe Complex and enters underlying mylonitised lower grade metasedimentary units of unknown tectonostratigraphic position. The borehole is completely open, except for the topmost 102 m for which a conductor casing with 102 mm inner diameter was installed. The diameters of the borehole are 96 mm from 102 m to 1616 m driller's depth and 76 mm below 1616 m driller's depth. The core recovery was nearly 100%.

The seismic survey consisted of three parts: a limited 3D-survey (Hedin et al. 2015), a high resolution zero-offset VSP (vertical seismic profile) and a multi-azimuthal walkaway VSP (MSP) experiment with sources and receivers along three surface profiles and receivers at seven different depth levels of the borehole. For the zero-offset VSP (ZVSP) a hydraulic hammer source (VIBSIST-3000) was used and activated over a period of 20 seconds as a sequence of impacts with increasing hit frequency, the so-called 'swept impact seismic technique' (SIST, Park et al. 1996). For each source point, 25 seconds of data were recorded. The wave field was recorded in the borehole by 15 three-component receivers using a Sercel SlimWave® geophone chain with an inter-tool spacing of 10 m. The ZVSP was designed to provide a geophone spacing of 2 m over the whole borehole length. The source was located about 30 m away from the wellhead of the borehole. Furthermore, a far-offset shot (FO-shot) was acquired to gain high-resolution 3C-data for the whole depth interval from wider angles of incidence. The FO-shot was approximately 1.9 km away from the borehole and was recorded with a receiver spacing of 5 m, but at some depths it ranged between 2 and 8 m due to survey issues. During the ZVSP and MSP experiments the wave field was also recorded on 429 1C-geophones with a 3D-geometry, covering an area of about 1.5 km^2 around the drill site (Hedin et al. 2015).

As a first pre-processing step, the VSP data from the hammer source were decoded, using a shift-and-stack algorithm (Park et al. 1996), and the repetitive shots were stacked together. Afterwards, the shots were merged to get two continuous shot gathers, containing the ZVSP-data and the FO-data, respectively. A horizontal rotation was performed, based on the S-wave arrivals to maximise the S-wave energy on one horizontal component.

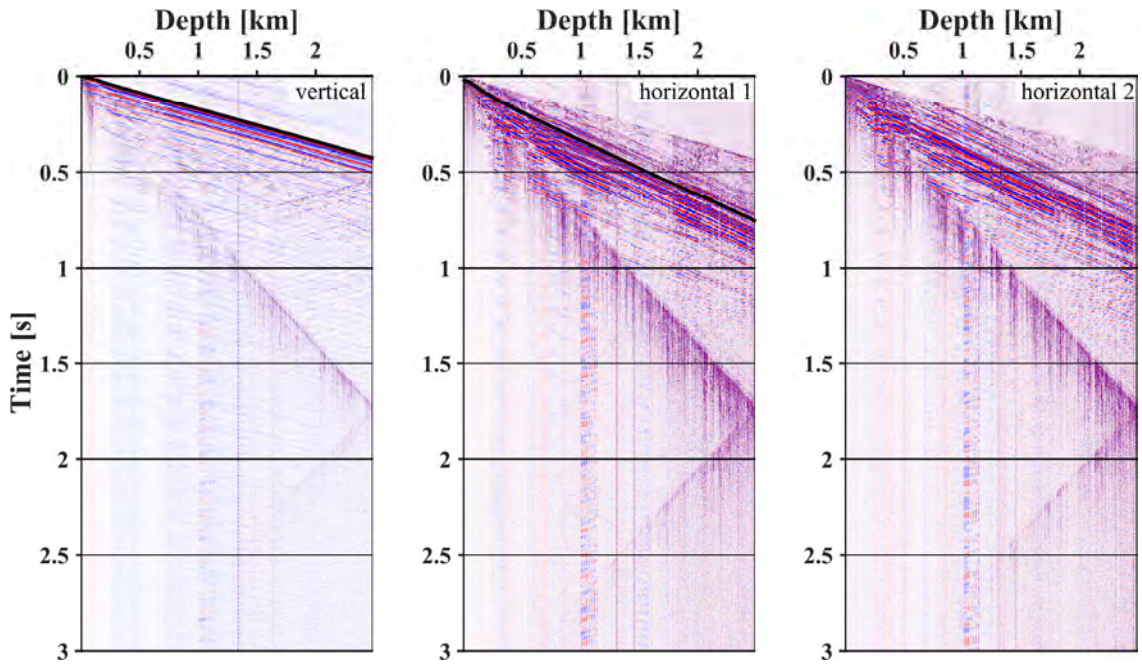

Figure 1: ZVSP-data sorted by component. Trace normalisation is applied and data are horizontally rotated. Black lines show picked first breaks of P- and S-waves.

The rotated ZVSP-data show a high signal-to-noise ratio and good data quality (Figure 1). Signal frequencies up to 150 Hz were recorded. On the vertical component, clear direct P-wave arrivals are visible. Several P-wave reflections occur below 1600 m logging depth. On both horizontal components, clear direct S-wave arrivals are visible. The observation that S-waves are visible on both horizontal components after rotation suggests that the penetrated rock is anisotropic. In addition, several PS-converted waves can be identified.

In order to integrate the borehole data into the 3D surface seismic data, further processing is concentrated only on the P-waves. As a first step, deconvolution was applied to sharpen the signal and to suppress multiple arrivals. Then the wave field was separated into upgoing and downgoing components by median filtering. Finally, a corridor stack was generated using the upgoing wave field in order to allow correlation with the borehole logging data and the surface seismic data.

References:
Gee, D.G. et al. (2010). Collisional Orogeny in the Scandinavian Caledonides (COSC). GFF, 132(1), 29-44
Hedin, P., Juhlin, C. & Gee, D.G., 2012. Seismic imaging of the Scandinavian Caledonides to define ICDP drilling sites. Tectonophysics, 554-557(0), 30–41
Hedin, P. et al (2015). 3D reflection seismic imaging at the 2.5 km deep COSC-1 scientific borehole, central Scandinavian Caledonides. Tectonophysics, accepted
Park C.B. et al. (1996). Swept impact seismic technique (SIST), Geophysics, 61(6), 1789-1803

IODP

Triaxial testing of marine sediments from offshore Costa Rica - Investigating forearc strength (IODP Expeditions 334 and 344)

R.M. KURZAWSKI[1], M. STIPP[1], RALF DOOSE[2], DETLEF SCHULTE-KORTNACK[2]

[1]Department of Geodynamics, GEOMAR Helmholtz Centre for Ocean Research Kiel, Wischhofstr. 1-3, 24148 Kiel, Germany, rkurzawski@geomar.de
[2]Institute of Geosciences, University of Kiel, Ludewig-Meyn-Str. 10, 24118 Kiel, Germany

There are two general types of ocean-continent subduction zones forming either accretionary or erosive continental margins. In the accretionary case, the overriding continental plate grows by the accretion of material tectonically detached from the downgoing oceanic plate. In the erosive case, however, the overriding continental plate shrinks due to tectonic erosion by the downgoing oceanic plate. Two major endeavors of the International Ocean Discovery Program (IODP), the Nankai Trough Seismogenic Zone Experiment (NanTroSEIZE) and the Costa Rica Seismogenesis Project (CRISP), investigate the processes and controlling factors of deformation and seismogenesis at accretionary and erosive margins including the incidence of large magnitude earthquakes and related tsunamis. Focussing here on the Costa Rica erosive margin, we study material properties of marine sediments promoting either distributed and continuous deformation or localized and discontinuous deformation in the forearc wedge. Our results will also be compared to similar investigations on sediments from the Nankai accretionary prism. Forearc stability and inherent tectonic failure processes at active continental margins very much depend on the strength of the composing sediments.

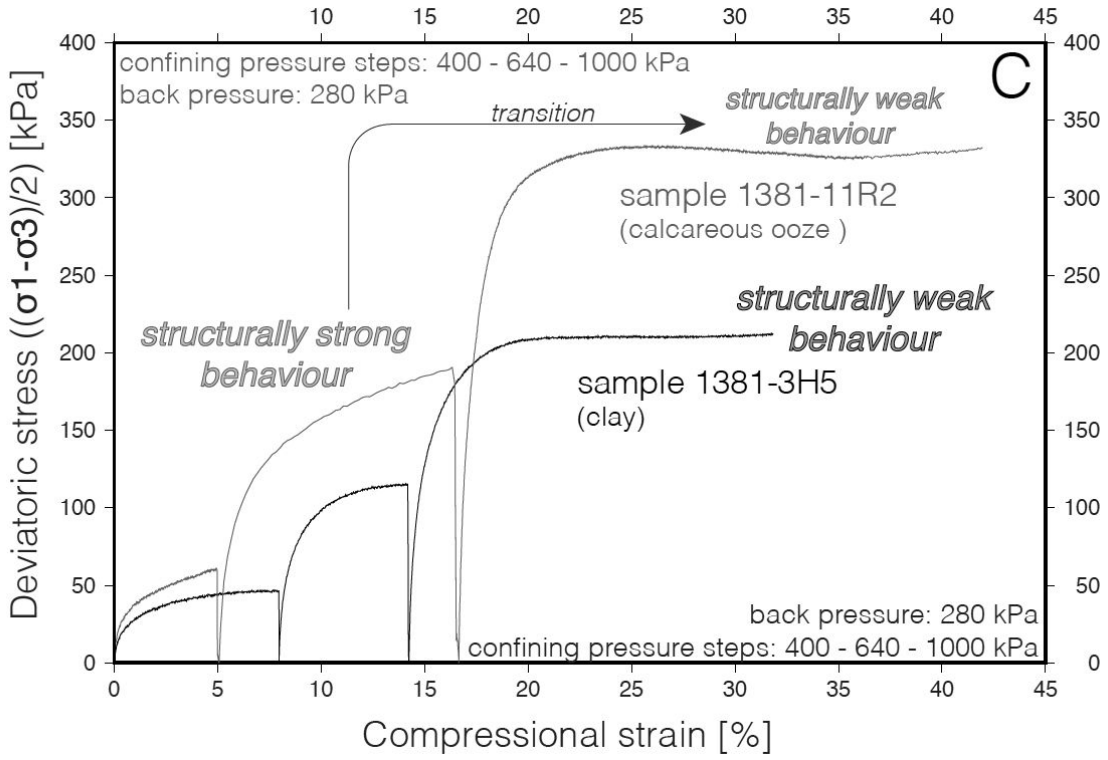

Fig.1 Stress-strain curves of pressure-stepping experiments. Note the transition from structurally strong to structurally weak behavior of calcareous ooze as response to elevated confining pressure.

Forearc sediments can either be prone to fracturing and more localized deformation or, alternatively, to creep and distributed deformation. Strength and deformation behavior can vary significantly depending on small differences in composition and fabric of the sediments as has been shown in a similar study on samples from the Nankai trench and forearc (Stipp et al., 2013). Whole-round core samples recovered during IODP Expeditions 334 and 344 from a depth range of 7–125 m below sea floor were experimentally deformed in a triaxial cell under consolidated and undrained conditions at confining pressures of 460–1000 kPa, room temperature, axial displacement rates of 0.01– 0.1 mm/min, and up to axial compressive strains of ~ 45%. First results show significant differences in the consolidation state and the mechanical behavior of between upper plate and incoming plate sediments (Fig. 1). Similar to previous findings from the Nankai trench, two "rheological groups" can be distinguished: structurally weak and structurally strong samples. One sample from the incoming plate shows a previously unrecognized transition from structurally strong to structurally weak behavior at elevated confining pressure of 1000 kPa. All samples, deformed and undeformed, are designated to texture analysis via synchrotron x-ray diffraction and anisotropy of magnetic susceptibility (AMS). The observed differences in mechanical behavior may hold a key for understanding strain localization and brittle faulting in forarc regions.

References:

Stipp, M., Rolfs, M., Kitamura, Y., Behrmann, J.H., Schumann, K., Schulte-Kortnack, D. and Feeser, V. (2013). – Geochemistry, Geophysics, Geosystems 14/11, doi: 10.1002/ggge.20290

ICDP

A detailed 3D-VSP experiment to image the Alpine Fault at the DFDP-2 drill site (Whataroa, New Zealand)

V. LAY[1], S. BUSKE[1], J. TOWNEND[2], R. KELLETT[3], J. ECCLES[4], A. GORMAN[5], D. SCHMITT[6], M. BERTRAM[7], D. LAWTON[7]

[1]Institute of Geophysics and Geoinformatics, TU Bergakademie Freiberg, 09596 Freiberg
[2]Victoria University Wellington, Wellington, Neuseeland
[3]GNS Science, Lower Hutt, Neuseeland
[4]University of Auckland, Auckland, Neuseeland
[5]University of Otago, Dunedin, Neuseeland
[6]University of Alberta, Edmonton, Kanada
[7]University of Calgary, Calgary, Kanada

The plate-bounding Alpine Fault in New Zealand is an 850 km long transpressive continental fault zone that is late in its earthquake cycle. The Deep Fault Drilling Project (DFDP) aims to deliver insight into the geological structure of this fault zone and its evolution by drilling and sampling the Alpine Fault at depth. Previously analysed 2D reflection seismic data image the main Alpine Fault reflector at a depth of 1.2-2.2 km with a dip of approximately 40° to the southeast below the DFDP-2 borehole. Additionally, there are indicators of a more complex 3D fault structure with several fault branches which have not yet been clearly imaged in detail.

For that reason we acquired a 3D-VSP seismic data set at the DFDP-2 drill site in January 2016. A zero-offset VSP and a walk-away VSP survey were conducted using a Vibroseis source. Within the borehole, a permanently installed "Distributed Acoustic Fibre Optic Cable" (down to 892 m) and a 3C Sercel slimwave tool (down to 400 m)

were used to record the seismic wavefield. In addition, an array of 160 3C receivers with a spacing of 10 m perpendicular and 20 m parallel to the main strike of the Alpine Fault was set up and moved successively along the valley to record reflections from the main Alpine Fault zone over a broad depth range and to derive a detailed 3D tomographic velocity model in the hanging wall.

We will show results from the acoustic forward modelling of the acquisition scenario as well as preliminary results from the data analysis. The data will be used to verify and improve the existing velocity model derived from the previously acquired 2D reflection line and processed by advanced seismic imaging methods to derive a structural image of the fault zone at depth. Finally, the results will provide a detailed basis for a seismic site characterization at the DFDP-2 drill site. Since the existing borehole did not intersect the Alpine Fault at depth, detailed seismic images will be of crucial importance for further structural and geological investigations of the architecture of the Alpine Fault in this area.

ICDP

Tephrostratigraphy of the last 637 ka of the DEEP site record, Lake Ohrid (Macedonia)

N. LEICHER[1], G. ZANCHETTA[2], R. SULPIZIO[3], B. GIACCIO[4,5], S. NOMADE[6], B. WAGNER[1], A. FRANCKE[1], AND P. DEL CARLO[7]

[1] Institute of Geology and Mineralogy, University of Cologne, Cologne, Germany
[2] Dipartimento di Scienze della Terra, University of Pisa, Pisa, Italy
[3] Dipartimento di Scienze della Terra e Geoambientali, University of Bari, Bari, Italy
[4] Istituto per la Dinamica dei Processi Ambientali (IDPA) CNR, Milan, Italy
[5] Istituto di Geologia Ambientale e Geoingegneria, CNR, Roma, Italy
[6] Laboratoire des sciences du climat et de l'environnement, CEA/CNRS/UVSQ, Gif-Sur-Yvette, France
[7] Istituto Nazionale di Geofisica e Vulcanologia, Sezione di Pisa, Pisa, Italy

Tephrochronology and tephrostratigraphy are becoming increasingly used techniques in many geological and archaeological studies in order to obtain temporal and stratigraphic control of a specific record (Lowe, 2011). The enormous amounts of pyroclasts (e.g. tephra), which are ejected by volcanic eruptions into the atmosphere and subsequently dispersed downwind of the volcanic source, can form widespread isochronous markers in different geological archives. Thus, tephra horizons form important chronostratigraphical event markers. The comparison and correlation of tephra layers from different archives among themselves and the exploration of their origin (volcanic province, specific eruption) is subject of tephrostratigraphy. If an absolute age can be assigned, the method is called tephrochronology. One field of application comprises various Quaternary fields, such as dating or interside-correlation/synchronisation of records from different regions. Another field of applications focusses on volcanological information obtained from distal tephra deposits is the another field of research, such as revealing the history and development of explosive volcanoes in terms of eruption frequency, distribution and strength of eruption. For both fields, distal tephrostratigraphy can be of great potential, being a frontier subject between volcanology and Quaternary sciences.

The Mediterranean region is a geodynamical active region, with numerous highly productive volcanic provinces, which are geochemically diverse due to their different tectonic settings. Their activity and geochemical diversity make this region favourable for tephrostratigraphic studies. Especially in the central Mediterranean region, tephrostratigraphy of the Italian volcanoes has been proofed to be a suitable tool for dating and correlating of marine and terrestrial records, often in the scope of paleoclimatic or archaeologic research. Pioneering work was done by Keller et al. (1978), who created the first marine tephrostratigraphy of the Mediterranean Sea. This tephrostratigraphy was spatially and temporally expanded to the central and eastern part of the Mediterranean Sea by numerous studies in the following years (cf. Paterne et al., 1988, 2008; Calanchi and Dinelli, 2008; Zanchetta et al., 2008, 2011; Bourne et al., 2010, 2015; Tamburrino et al., 2012; Insinga et al., 2014). The most extensive terrestrial studies were conducted at Lago Grande di Monticchio (Wulf et al., 2004, 2012) and cover the last 130 kyrs. As most of the tephrostratigraphic records are limited to the period < 200 ka, a well established tephrostratigraphy of the central Mediterranean is restricted to this period.

The knowledge of the older Middle Pleistocene tephrostratigraphy, when the Italian Quaternary explosive volcanism was in one of its most active periods, is relatively poor. However, in recent years new proximal and mid-distal records from various Italian continental basins significantly improved the knowledge of volcanic activity. Today's known active volcanic centres during the Middle-Pleistocene were i.e. the Roman Province (Sabatini, Vulsini, Alban Hills, Vico), the Ernici-Roccamonfina province, and the Vulture volcano. Promising information about this time is recorded e.g. in the Sulmona (Giaccio et al., 2009; Giaccio et al., 2013; Regattieri et al., 2016), the Acerno (Petrosino et al., 2014b), or the Mercure basin (Giaccio et al., 2014; Petrosino et al., 2014a), and other continental lacustrine successions in Italy. However, our knowledge about this period is still incomplete and continuous records downwind of the Italian volcanoes covering such an age range are rare.

To date, there are only two continuous records of the Mediterranean region covering the entire Middle and parts of the Early Pleistocene, which are the Calabrian Ridge core KC01B (Lourens, 2004; Insinga et al., 2014) and the peat record from Tenaghi Philippon, Greece (St. Seymour et al., 2004; Tzedakis et al., 2006; Pross et al., 2007). However, their published tephrostratigraphies are limited to the Holocene and to the late Middle Pleistocene.

One other very promising terrestrial archive to improve especially the older parts of central Mediterranean tephrostratigraphy is Lake Ohrid (Macedonia/Albania) in the eastern Mediterranean region, which is supposed to be the oldest continuously existing lake of Europe (Wagner et al., 2014). Previous tephrostratigraphic studies on relatively short sediment cores from Lake Ohrid are summarized in Sulpizio et al. (2010) and cover the last 135 kyrs. Over this period, eleven macroscopic and cryptotephra layers from Italian eruptions have been recognized and provide valuable information of tephra dispersal from Italian

volcanoes. They suppose that Lake Ohrid is an excellent tephra archive covering also the older periods.

In spring 2013, the ICDP deep-drilling campaign SCOPSCO (Scientific Collaboration on Past Speciation Conditions in Lake Ohrid) was conducted at Lake Ohrid. The SCOPSCO project comprised five drill sites with the master drill site, DEEP, in the centre of the lake. At this site, the maximum penetration depth was 569 m below the lake floor and initial data from borehole logging, core logging, and geochemical measurements indicated that this record continuously covers more than 1.2 Ma (Wagner et al., 2014). The recovered sediments are and will be analysed with different biological and geological methods and first results approve the preliminary age-estimation of the entire record. One of the main objectives is a detailed tephrostratigraphic study in order to provide more information on Italian volcanism and to obtain independent chronological tie points for the establishment of an age model of the DEEP site record.

Macroscopic tephra layers were identified during core-opening and description, but XRF down core data indicate also the occurrence of cryptotephra tephra horizons, which are not visible by naked eye. The uppermost 450 m composite depth (mcd) consist of pelagic sediments and represent more than 1 Myrs of Italian volcanism, as by now 53 tephra layers were identified in this section.

A first, detailed tephrostratigraphic record exists now for the uppermost 247.8 mcd (MIS 1–16, Leicher et al., 2015). Within this sequence, 34 tephra layers could be identified and major element analyses (SEM-EDS/WDS) were carried out on juvenile glass fragments. The geochemical analyses of the glass shards of all of these layers suggest an origin from the Italian volcanic provinces. 12 macroscopic tephra layers (OH-DP-0115 to OH-DP-2060) could clearly be identified and correlated with known and dated eruptions. They include: the Y-3 (OH-DP-0115, 26.68–29.42 cal ka BP), the Campanian Ignimbrite/Y-5 (OH-DP-0169, 39.6±0.1 ka), and the X-6 (OH-DP-0404, 109±2 ka) from the Campanian volcanoes, the P-11 of the Pantelleria Island (OH-DP-0499, 129±6 ka), the Vico B (OH-DP-0617, 162±6 ka) from the Vico volcano, the Pozzolane Rosse (OH-DP-1817, 457±2 ka) and the Tufo di Bagni Albule (OH-DP-2060, 527±2 ka) from the Colli Albani volcanic district, and the Fall A (OH-DP-2010, 496±3 ka) from the Sabatini volcanic field. Furthermore, a comparison of the Ohrid record with tephrostratigraphic records of mid-distal archives related to the Mediterranean area allowed the recognition of the equivalents of other less known tephra layers, such as the TM24-a/POP2 (OH-DP-0404, 101.8 ka) from the Lago Grande di Monticchio and the Sulmona basin, the CF-V5/PRAD3225 (OH-DP-0624, ca. 162 ka) from the Campo Felice basin/Adriatic Sea, the SC5 (OH-DP-1955, 493.1±10.9 ka) from the Mercure basin, and the A11/12 (OH-DP-2017, 511±6 ka) from the Acerno basin, whose specific volcanic sources are still poorly constrained. Additionally, one cryptotephra (OH-DP-0027) was identified by correlation of the potassium XRF intensities from the DEEP site with those from short cores of previous studies from Lake Ohrid. In these cores, a maximum in potassium is caused by glass shards, which were correlated with the Mercato tephra (8.43–8.63 cal ka BP) from Somma-Vesuvius. With the tephrostratigraphic work, a consistent part of the Middle Pleistocene tephrostratigraphic framework of Italian volcanoes was for the first time extended as far as to the Balkans.

Furthermore, the tephrostratigraphic work forms the backbone to correlate and interpret borehole logging and sediment core data in the light of environmental change over time. The obtained tephrochronological information was used to develop a robust chronology for the DEEP site sequence, for both the sediment core and the borehole sequence (cf. Baumgarten et al., 2015; Francke et al., 2015). Eleven radiocarbon and $^{40}Ar/^{39}Ar$ ages were transferred from the specific tephra equivalents to the DEEP site sequence, whereof the $^{40}Ar/^{39}Ar$ ages were re-calculated by using the same flux standard (1.194 Ma for ACs, which corresponds to FCs at 28.02 Ma) in order to obtain a homogenous set of ages. The obtained ages were included as first order tie points into the age depth model. Beside this second order tie points, obtained by tuning of biogeochemical proxy data to orbital parameters were additionally used to establish a Bayesian age-depth model (see Francke et al. 2015). The obtained age model imply that the upper 247.8 mcd of the DEEP site cover the last 637 kyrs.

This age-depth model will help to improve and re-evaluate the chronology of other, both undated and dated tephra layers from other records. The cross correlation with astronomical tuning, allows us to cross validate the proximal records and the reliability of ages obtained from these records. For example, the cross correlation of the Sabatini Fall A deposit in Lake Ohrid implies that the existing ages of more proximal Sabatini Fall A deposits in Italy are probably several thousand years too young. Even without tephrochronology, the tephra layers themselves provide a powerful, age-depth model independent tool to synchronize and correlate the DEEP site record with other records of the Mediterranean region, in which the same tephra equivalents can be found. This is of great interest especially for paleoclimatic studies focusing and comparing specific climatic intervals or addressing leads and lags between marine and terrestrial paleoclimate-records (cf. Zanchetta et al., 2015).

Between 248 and 450 mcd of the DEEP site sequence, another 18 tephra horizons were identified and are subject of ongoing work. These deposits, once correlated with their specific eruptive origin, will hopefully enable dating this part of the sequence. Even if the central Mediterranean tephrostratigraphy of these older periods is still restricted, there are at least some mid-distal archives covering some specific intervals. For instance, the Sulmona record provides valuable tephrochronological information, recording 31 tephra layers in MIS18-21 of which some are precisely $^{40}Ar/^{39}Ar$ dated (Giaccio et al., 2013; Giaccio et al., 2015; Regattieri et al., 2015).

Besides ongoing correlation of tephra layers in the deeper part, more analytical work will help to improve and establish proper correlations of tephras in the Ohrid core sequence with the relevant Italian volcanic provinces and their specific eruptions. The interval MIS 6-11 of the DEEP site record bears a number of tephra layers, which could not be correlated to a specific eruption so far.

New geochemical data (trace elements, isotopes) could help to succeed and greatly improve this part of the stratigraphy. In this way, the Lake Ohrid record is a unique continuous, distal record of Italian volcanic activity, which is candidate to become the template for the central Mediterranean tephrostratigraphy, especially for the hitherto poorly known and explored lower Middle Pleistocene period.

References:

Baumgarten, H., Wonik, T., Tanner, D. C., Francke, A., Wagner, B., Zanchetta, G., Sulpizio, R., Giaccio, B., and Nomade, S.: Age depth model for the past 630 ka in Lake Ohrid (Macedonia/Albania) based on cyclostratigraphic analysis of downhole gamma ray data, Biogeosciences Discussions, 12, 7671-7703, 2015.

Bourne, A. J., Lowe, J. J., Trincardi, F., Asioli, A., Blockley, S. P. E., Wulf, S., Matthews, I. P., Piva, A., and Vigliotti, L.: Distal tephra record for the last ca 105,000 years from core PRAD 1-2 in the central Adriatic Sea implications for marine tephrostratigraphy, Quaternary Science Reviews, 29, 3079-3094, 2010.

Bourne, A. J., Albert, P. G., Matthews, I. P., Trincardi, F., Wulf, S., Asioli, A., Blockley, S. P. E., Keller, J., and Lowe, J. J.: Tephrochronology of core PRAD 1-2 from the Adriatic Sea: insights into Italian explosive volcanism for the period 200-80 ka, Quaternary Science Reviews, 116, 28-43, 2015.

Calanchi, N. and Dinelli, E.: Tephrostratigraphy of the last 170 ka in sedimentary successions from the Adriatic Sea, Journal of Volcanology and Geothermal Research, 177, 81-95, 2008.

Francke, A., Wagner, B., Just, J., Leicher, N., Gromig, R., Baumgarten, H., Vogel, H., Lacey, J. H., Sadori, L., Wonik, T., Leng, M. J., Zanchetta, G., Sulpizio, R., and Giaccio, B.: Sedimentological processes and environmental variability at Lake Ohrid (Macedonia, Albania) between 640 ka and present day, Biogeosciences Discuss., 12, 15111-15156, 2015.

Giaccio, B., Messina, P., Sposato, A., Voltaggio, M., Zanchetta, G., Galadini, F., Gori, S., and Santacroce, R.: Tephra layers from Holocene lake sediments of the Sulmona Basin, Central Italy: implications for volcanic activity in Peninsular Italy and tephrostratigraphy in the Central Mediterranean area, Quaternary Science Reviews, 28, 2710-2733, 2009.

Giaccio, B., Castorina, F., Nomade, S., Scardia, G., Voltaggio, M., and Sagnotti, L.: Revised Chronology of the Sulmona Lacustrine Succession, Central Italy, Journal of Quaternary Science, 28, 545-551, 2013.

Giaccio, B., Galli, P., Peronace, E., Arienzo I., Nomade, S., Cavinato, G. P., Mancini, M., Messina, P., and Sottili, G.: A 560-440 ka tephra record from the Mercure Basin, Southern Italy: volcanological and tephrostratigraphic implications, Journal of Quaternary Science, 29, 232-248, 2014.

Giaccio, B., Regattieri, E., Zanchetta, G., Nomade, S., Renne, P. R., Sprain, C. J., Drysdale, R. N., Tzedakis, P. C., Messina, P., Scardia, G., Sposato, A., and Bassinot, F.: Duration and dynamics of the best orbital analogue to the present interglacial, Geology, 2015.

Insinga, D. D., Tamburrino, S., Lirer, F., Vezzoli, L., Barra, M., De Lange, G. J., Tiepolo, M., Vallefuoco, M., Mazzola, S., and Sprovieri, M.: Tephrochronology of the astronomically-tuned KC01B deep-sea core, Ionian Sea: insights into the explosive activity of the Central Mediterranean area during the last 200 ka, Quaternary Science Reviews, 85, 63-84, 2014.

Keller, J., Ryan, W. B. F., Ninkovich, D., and Altherr, R.: Explosive volcanic activity in the Mediterranean over the past 200,000 yr as recorded in deep-sea sediments, Geological Society of America Bulletin, 89, 591-604, 1978.

Leicher, N., Zanchetta, G., Sulpizio, R., Giaccio, B., Wagner, B., Nomade, S., Francke, A. and Del Carlo P.: First tephrostratigraphic results of the DEEP site record in Lake Ohrid, Macedonia, Biogeosciences, 2015. is the paper we submitted to BG?

Lourens, L. J.: Revised tuning of Ocean Drilling Program Site 964 and KC01B (Mediterranean) and implications for the δ18O, tephra, calcareous nannofossil, and geomagnetic reversal chronologies of the past 1.1 Myr, Paleoceanography, 19, PA3010, 2004.

Lowe, D. J.: Tephrochronology and its application: A review, Quaternary Geochronology, 6, 107-153, 2011.

Paterne, M., Guichard, F., and Labeyrie, J.: Explosive activity of the South Italian volcanoes during the past 80,000 years as determined by marine tephrochronology, Journal of Volcanology and Geothermal Research, 34, 153-172, 1988.

Paterne, M., Guichard, F., Duplessy, J. C., Siani, G., Sulpizio, R., and Labeyrie, J.: A 90,000–200,000 yrs marine tephra record of Italian volcanic activity in the Central Mediterranean Sea, Journal of Volcanology and Geothermal Research, 177, 187-196, 2008.

Petrosino, P., Ermolli, E. R., Donato, P., Jicha, B., Robustelli, G., and Sardella, R.: Using Tephrochronology and palynology to date the MIS 13 lacustrine sediments of the Mercure Basin (Southern Apennines – Italy), Italian Journal of Geosciences, 133, 169-186, 2014a.

Petrosino, P., Jicha, B. R., Mazzeo, F. C., and Russo Ermolli, E.: A high resolution tephrochronological record of MIS 14–12 in the Southern Apennines (Acerno Basin, Italy), Journal of Volcanology and Geothermal Research, 274, 34-50, 2014b.

Pross, J., Tzedakis, P. C., Schmiedl, G., Christanis, K., Hooghiemstra, H., Müller, C., Ulrich, K., Ulrich, K., and Stavros, M.: Tenaghi Philippon (Greece) Revisited: Drilling a Continuous Lower-Latitude Terrestirial Climate archive of the Last 250,000 Years, Scientific Drilling, 5, 44-46, 2007.

Regattieri, E., Giaccio, B., Zanchetta, G., Drysdale, R. N., Galli, P., Nomade, S., Peronace, E., and Wulf, S.: Hydrological variability over the Apennines during the Early Last Glacial precession minimum, as revealed by a stable isotope record from Sulmona basin, Central Italy, Journal of Quaternary Science, 30, 19-31, 2015.

Regattieri, E., Giaccio, B., Galli, P., Nomade, S., Peronace, E., Messina, P., Sposato, A., Boschi, C., and Gemelli, M.: A multi-proxy record of MIS 11–12 deglaciation and glacial MIS 12 instability from the Sulmona basin (central Italy), Quaternary Science Reviews, 132, 129-145, 2016.

St. Seymour, K., Christanis, K., Bouzinos, A., Papazisimou, S., Papatheodorou, G., Moran, E., and Denes, G.: Tephrostratigraphy and tephrochronology in the Philippi peat basin, Macedonia, Northern Hellas (Greece), Quaternary International, 121, 53-65, 2004.

Sulpizio, R., Zanchetta, G., D'Orazio, M., Vogel, H., and Wagner, B.: Tephrostratigraphy and tephrochronology of Lakes Ohrid and Prespa, Balkans, Biogeosciences, 7, 3273-3288, 2010.

Tamburrino, S., Insinga, D. D., Sprovieri, M., Petrosino, P., and Tiepolo, M.: Major and trace element characterization of tephra layers offshore Pantelleria Island: insights into the last 200 ka of volcanic activity and contribution to the Mediterranean tephrochronology, Journal of Quaternary Science, 27, 129-140, 2012.

Tzedakis, P. C., Hooghiemstra, H., and Palike, H.: The last 1.35 million years at Tenaghi Philippon: revised chronostratigraphy and long-term vegetation trends, Quaternary Science Reviews, 25, 3416-3430, 2006.

Wagner, B., Wilke, T., Krastel, S., Zanchetta, G., Sulpizio, R., Reicherter, K., Leng, M. J., Grazhdani, A., Trajanovski, S., Francke, A., Lindhorst, K., Levkov, Z., Cvetkoska, A., Reed, J. M., Zhang, X., Lacey, J. H., Wonik, T., Baumgarten, H., and Vogel, H.: The SCOPSCO drilling project recovers more than 1.2 million years of history from Lake Ohrid, Scientific Drilling, 17, 19-29, 2014.

Wulf, S., Kraml, M., Brauer, A., Keller, J., and Negendank, J. F. W.: Tephrochronology of the 100ka lacustrine sediment record of Lago Grande di Monticchio (Southern Italy), Quaternary International, 122, 7-30, 2004.

Wulf, S., Keller, J., Paterne, M., Mingram, J., Lauterbach, S., Opitz, S., Sottili, G., Giaccio, B., Albert, P. G., Satow, C., Tomlinson, E. L., Viccaro, M., and Brauer, A.: The 100–133 ka record of Italian explosive volcanism and revised tephrochronology of Lago Grande di Monticchio, Quaternary Science Reviews, 58, 104-123, 2012.

Zanchetta, G., Sulpizio, R., Giaccio, B., Siani, G., Paterne, M., Wulf, S., and D'Orazio, M.: The Y-3 tephra: A Last Glacial stratigraphic marker for the Central Mediterranean Basin, Journal of Volcanology and Geothermal Research, 177, 145-154, 2008.

Zanchetta, G., Sulpizio, R., Roberts, N., Cioni, R., Eastwood, W. J., Siani, G., Caron, B., Paterne, M., and Santacroce, R.: Tephrostratigraphy, chronology and climatic events of the Mediterranean basin during the Holocene: An overview, Holocene, 21, 33-52, 2011.

Zanchetta, G., Regattieri, E., Giaccio, B., Wagner, B., Sulpizio, R., Francke, A., Vogel, L. H., Sadori, L., Masi, A., Sinopoli, G., Lacey, J. H., Leng, M. L., and Leicher, N.: Aligning MIS5 proxy records from Lake Ohrid (FYROM) with independently dated Mediterranean archives: implications for core chronology, Biogeosciences Discuss., 12, 16979-17007, 2015.

ICDP

Detailed seismic interpretation integrating sedimentological and geophysical results of the of SCOPSCO ICDP campaign (Macedonia, Albania)

K.LINDHORST[1], S.KRASTEL[1], H. BAUMGARTEN[2], T. WONIK[2], A. FRANCKE[3], B. WAGNER[3]

[1]Christian-Albrechts-Universität zu Kiel, Institut für Geowissenschaften, Abteilung Geophysik, Otto-Hahn-Platz 1, 24118 Kiel, Germany, klindhorst@geophysik.uni-kiel.de
[2] Leibniz-Institute for Applied Geophysics (LIAG), Stilleweg 2, 30655 Hannover, Germany
[3] Institute für Geologie und Mineralogie, Universität Köln, Germany

Lake Ohrid is a transboundary lake shared by the Former Yougoslavia Republic Macedonia and Albania within the Dinaride-Helenide-Albanide mountain belt that has a remarkable sedimentary infill preserving a rich paleoenvionrmental record. It is the oldest lake in Europe (1-2 Ma) and is known for its high degree of endemism (more than 300 species described). High resolution hydroacoustic and seismic data revealed a thick and undisturbed sediment succession (>500m) in the central part of the basin. Lacustrine sediments contain valuable information on geological/environmental events over a long time period enabling scientists from different disciplines to study the links between climate, tectonics, paleoenvironmental conditions and biodiversity (Albrecht and Wilke, 2008).

The ICDP SCOPSCO project has been initiated with the following objectives: (1) to reveal a precise age and origin of Lake Ohrid, (2) to unravel the seismo-tectonic history of the lake area including effects of major earthquakes and associated mass wasting events, (3) to obtain a continuous record containing information on volcanic activities and climate changes in the central northern Mediterranean region, and (4) to better understand the impact of major geological/environmental events on general evolutionary patterns resulting in an extraordinary degree of endemic biodiversity (Wagner et al., 2014).

A successful deep drilling campaign took place in spring 2013 resulting in sediment cores with a total length of more than 2100 m (REF?). The work included measurment of Magnetic Susceptibility (MS) at all sections by using a Multi Sensor Core Logger (MSCL) device immediately after the 1m-long core sections were brought back from the drill barge. Down-hole logging was carried out at each site by the LIAG group from Hannover. A Vertical Seismic Profile (VSP) gathered at site DEEP in Hole 1C enables conversion of seismic Two-Way-Travel-Time into sediment depth and subsequen correlation of our seismic cross section for an revised interpretation. Cores from the main drill site (DEEP) have been opened, processed and undergone detailed sedimentological investigations summarized by (Francke et al., 2015).

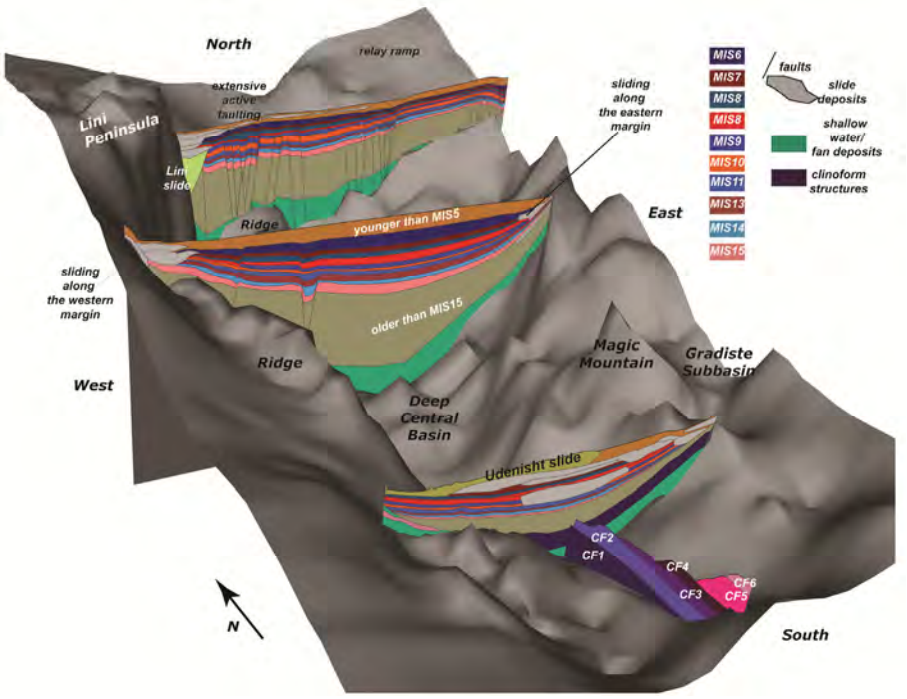

Fig.: Sedimentary infill distributed within Lake Ohrid Basin on top of the acoustic basement (grey) interpreted as the hard rock basement. Three interpreted seismic lines illustrate the differences of the northern area where active faulting is present, the central basin with thick undisturbed sediments, and the southern area where massive MTDs can be found. MTDs are can also be found along the margins. The colors represent the Marine Isotope Stages.

A correlation of sedimentological and sedimentphysical data with our seismic line crossing the drill site results in a revised and improved interpretation of seismic reflectors. So far, detailed interpretation of seismic lines in the last couple of years revealed a better understanding of the initial opening as well as the sedimentary and tectonic evolution of Lake Ohrid Basin (Lindhorst et al., 2015). A first seismo-chronological model already suggested that lacustrine sediments continuously deposited in the central basin at least over a time period of 1 Myrs but have been influenced by tectonic activities along the margins of fault bound Lake Ohrid. Offset seismic reflectors suggests active fault structures in the northern area (Fig.). Clinoform structures mainly in the southern area are good historical indicators for the subsidence of the basin. Unfortunately, the majority of these structures are older than MIS15 and hence have not been the target of a detailed study as they cannot yet be correlated with newly retrieved sediment cores (Fig.). Nevertheless, within the upper sediments Mass Transport Deposits (MTDs) are widespread and occur at different stratigraphic levels. No MTD has been detected older than the transition from MIS 9 to MIS 8 (~300ka, Fig.) and no sliding event is imaged within Interglacial MIS 7. During the MIS6 glacial period, several MTDs are found. Mass wasting in lake Ohrid has been continuously ongoing since the warm period MIS5. Several large and mid-sized sliding events have been detected, some of them are clearly visible on bathymetric data (Lindhorst et al., 2012).

Recent work correlating seismic reflectors to Marine Isotope Stages (MIS) based on the changes from Interglacial to Glacial time periods (and vice versa) allow further interpretation of the sediment cores (Francke et al., 2015). Within the very high resolution sediment echosounder data set of the uppermost 50 m we can identify tephra layers found in the cores (Leicher et al., 2015) and trace them throughout the basin. The most prominent reflectors are those associated with the change from MIS4 to MIS5, the change from MIS5 to MIS6, MIS7, a very strinking reflector within MIS9, a reflector package at the boundary of MIS11 to MIS12, and finally a seismic sequence interpreted to reflect the early MIS15 interval (Fig.). Interpretation and correlation of additional reflectors is not obvious, but by combining all available data sets we developed a 3D model of the sedimentary infill of Lake Ohrid Basin with the acoustic basement interpreted as the basement rock (Fig.). The model provides a summary of our basin infill interpretation by integrating sedimentological, geophysical and seismic data.

References

Albrecht, C., and Wilke, T., 2008, Ancient Lake Ohrid: biodiversity and evolution: Hydrobiologia, v. 615, p. 103-140.

Francke, A., Wagner, B., Just, J., Leicher, N., Gromig, R., Baumgarten, H., Vogel, H., Lacey, J., Sadori, L., and Wonik, T., 2015, Sedimentological processes and environmental variability at Lake Ohrid (Macedonia, Albania) between 640 ka and present day: Biogeosciences Discussions, v. 12, no. 17, p. 15111-15156.

Leicher, N., Zanchetta, G., Sulpizio, R., Giaccio, B., Wagner, B., Nomade, S., Francke, A., and Del Carlo, P., 2015, First tephrostratigraphic results of the DEEP site record from Lake Ohrid, Macedonia: Biogeosciences Discussions, v. 12, no. 18.

Lindhorst, K., Gruen, M., Krastel, S., and Schwenk, T., 2012, Hydroacoustic Analysis of Mass Wasting Deposits in Lake Ohrid (Former Yugoslavian Republic of Macedonia/Albania), *in* Yamada, Y., Kiichiro Kawamura, Ken Ikehara, Yujiro Ogawa, Roger Urgeles, David Mosher, Jason Chaytor, and Strasser, M., eds., Submarine Mass Movements and Their Consequences, Volume Advances in Natural and Technological Hazards Research 31, Springer Netherlands, p. 245-253.

Lindhorst, K., Krastel, S., Reicherter, K., Stipp, M., Wagner, B., and Schwenk, T., 2015, Tectonic and Sedimentary Evolution of Lake Ohrid (Albania/Macedonia): Basin Research, v. 27, no. 1, p. 84-101.

Wagner, B., Wilke, T., Krastel, S., Zanchetta, G., Sulpizio, R., Reicherter, K., Leng, M., Grazhdani, A., Trajanovski, S., Francke, A., Lindhorst, K., Levkov, Z., Cvetkoska, A., Reed, J., Zhang, X., Lacey , J., Wonik, T., Baumgarten, H., and Vogel, H., 2014, The SCOPSCO drilling project recovers more than 1.2 million years of history from Lake Ohrid: Scientific Drilling, v. 17, p. 19-29.

IODP

1 million years of North Atlantic deep water variability of ε_{Nd} at ODP Site 1063, a preliminary record of glacial – interglacial terminations

J. M. LINK [1,2], P. BLASER[1], J. LIPPOLD[3,] M. GUTJAHR[4], A. H. OSBORNE[4] , E. BÖHM[1,5], M. FRANK[4], O. FRIEDRICH[2], N. FRANK[1,2]

[1] Institut für Umweltphysik, Universität Heidelberg, INF 229, 69120 Heidelberg, Germany

[2] Institut für Geowissenschaften, Universität Heidelberg, INF 234, 69120 Heidelberg, Germany

[3] Institut für Geologie, Oeschger Center for Climate Change Research, University of Bern, Baltzerstrasse 1+3, CH-3012 Bern, Switzerland

[4] GEOMAR, Helmholtz-Zentrum für Ozeanforschung, Wischhofstraße 1-3, D-24148 Kiel, Germany

[5] Laboratory for Climate and Environmental Sciences, CEA – CNRS – UVSQ, Ave. de la Terrasse, 91190 Gif-sur-Yvette, France

The oceans play an important role in the Earth's climate system. In particular, the Atlantic and its Meridional Overturning Circulation (AMOC) are of great importance. During the Holocene deep-water formation in the North Atlantic has been active and North Atlantic Deep Water (NADW) has occupied most of the deep Atlantic basin. This circulation mode is often referred to as the 'warm', or 'interglacial' mode (RAHMSTORF 2002), However, the existence of different AMOC modes has been proposed for the past, mostly on the basis of stable carbon isotopes (BOYLE & KEIGWIN 1987; SARNTHEIN et al. 1994). In the 'cold', or 'glacial', mode, the glacial equivalent of NADW has been identified only at shallower depths than today, and is hence termed Glacial North Atlantic Intermediate Water. As a consequence, a large part of the deep North Atlantic was bathed in deep water advected from the Southern Ocean (LYNCH-STIEGLITZ et al. 2007; ROBERTS et al. 2010; BÖHM et al. 2015).

Recently, BÖHM et al. (2015) showed an unexpected stable deep water formation spanning the past 150 ka. Major perturbations solely occurred during periods of sluggish overturning resulting from major ice discharge events (Heinrich Events). This result was obtained using $^{231}Pa/^{230}Th$ as ocean interior advection tracer and ε_{Nd} was used to identify water mass provenance. Beyond 150 ka

$^{231}Pa/^{230}Th$ is no longer applicable, but ε_{Nd} can still be used to trace the provenance of deep water in the western North Atlantic. Depending on the Sm/Nd ratio and the age of the crust, ε_{Nd} (the deviation in parts per 10,000 of the measured $^{143}Nd/^{144}Nd$ ratio relative to the chondritic uniform reservoir) varies from light isotopic values for old continental crust to heavy isotopic composition for freshly formed volcanogenic material (GOLDSTEIN & HEMMING 2003). Today, North Atlantic Deep Water (NADW) is characterized by an ε_{Nd} signature of –13.5 (LACAN & JEANDEL 2005), while Antarctic Bottom Water (AABW) has more radiogenic values of -9 (STICHEL et al. 2012).

Here, we present the very first data regarding the provenance of water masses in the deep western North Atlantic spanning the last one million years of glacial-interglacial cycles. Sediment core ODP Site 1063 (Leg 172, 33°41' N, 57°37' W, water depth 4,584 m, Bermuda Rise) of the subtropical western North Atlantic was selected. This site bathes within NADW but was influenced by AABW in the past (KEIGWIN & JONES 1994), thus the sediment sensitively traces changes of the radiogenic neodymium isotope composition of seawater as demonstrated by BÖHM et al. (2015). The bottom water ε_{Nd} composition was reconstructed using the ferromanganese-oxyhydroxide coatings of the sediment. The neodymium isotopic composition across glacial terminations (T) IV, V and VII was investigated. Here, terminations are defined based on the foraminifera $\delta^{18}O$ record (POLI et al. 2000; BILLUPS et al. 2011; POIRIER & BILLUPS 2014) relative to the global stack LR04 (LISIECKI & RAYMO 2005).

During each glacial maximum, the site experiences ε_{Nd} values indicative of an advance of AABW. Thus the site was bathed by southern sourced water, which implies the cold-mode of the AMOC. In the course of the transition to full interglacial conditions, the AMOC switches back to its warm-mode and the deep Northern Atlantic was filled by NADW as reflected by ε_{Nd} values characteristic of NADW pointing at a recurring pattern in the re-organisation of the AMOC along with glacial-interglacial cycles. These findings are in agreement with the study of BÖHM et al. (2015) which covered the last glacial cycle. However, there is first evidence that the Marine Isotope Stage (MIS) 11c stands out with respect to the general north-south water mass competition. Significantly lighter ε_{Nd} values are recorded (as low as –17) and lasting over the full interglacial period. This observation was confirmed by studying ε_{Nd} composition of foraminifera. Since the Labrador Sea is an important source of unradiogenic Nd one may speculate on either intensified Labrador Sea deep water formation or enhanced continental weathering surrounding the Labrador Sea.

References:

BILLUPS, K., RABIDEAUX, N., & STOFFEL, J. (2011): Suborbital-scale surface and deep water records in the subtropical North Atlantic: implications on thermohaline overturn. - *Quaternary Science Reviews,* **30**, 2976-2987.

BÖHM, E., LIPPOLD, J., GUTJAHR, M., FRANK, M., BLASER, P., ANTZ, B., FOHLMEISTER, J., FRANK, N., ANDERSEN, M.B., & DEININGER, M. (2015): Strong and deep Atlantic meridional overturning circulation during the last glacial cycle. - *Nature*, **517**, 73-76.

BOYLE, E.A., & KEIGWIN, L. (1987): North Atlantic thermohaline circulation during the past 20,000 years linked to high-latitude surface temperature. - *Nature*, **330**, 35-40.

GOLDSTEIN, S.L., & HEMMING, S.R. (2003): 6.17 - Long-lived Isotopic Tracers in Oceanography, Paleoceanography, and Ice-sheet Dynamics. -In*:* TUREKIAN, K.K., & HOLLAND, H.D. (Eds.): Treatise on Geochemistry. Oxford: Pergamon, 453-489.

KEIGWIN, L., & JONES, G. (1994): Western North Atlantic evidence for millennial-scale changes in ocean circulation and climate. - *Journal of Geophysical Research: Oceans (1978–2012)*, **99**, 12397-12410.

LACAN, F., & JEANDEL, C. (2005): Acquisition of the neodymium isotopic composition of the North Atlantic Deep Water. - *Geochemistry, Geophysics, Geosystems,* **6**, 1-20.

LISIECKI, L.E., & RAYMO, M.E. (2005): A Pliocene-Pleistocene stack of 57 globally distributed benthic $\delta^{18}O$ records. - *Paleoceanography*, **20**.

LYNCH-STIEGLITZ, J., ADKINS, J.F., CURRY, W.B., DOKKEN, T., HALL, I.R., HERGUERA, J.C., HIRSCHI, J.J.-M., IVANOVA, E.V., KISSEL, C., MARCHAL, O., MARCHITTO, T.M., MCCAVE, I.N., MCMANUS, J.F., MULITZA, S., NINNEMANN, U., PEETERS, F., YU, E.-F., & ZAHN, R. (2007): Atlantic Meridional Overturning Circulation During the Last Glacial Maximum. - *Science*, **316**, 66-69.

POIRIER, R.K., & BILLUPS, K. (2014): The intensification of northern component deepwater formation during the mid-Pleistocene climate transition. - *Paleoceanography*, **29**, 1046-1061.

POLI, M.S., THUNELL, R.C., & RIO, D. (2000): Millennial-scale changes in North Atlantic Deep Water circulation during marine isotope stages 11 and 12: Linkage to Antarctic climate. - *Geology*, **28**, 807-810.

RAHMSTORF, S. (2002): Ocean circulation and climate during the past 120,000 years. - *Nature*, **419**, 207-214.

ROBERTS, N.L., PIOTROWSKI, A.M., MCMANUS, J.F., & KEIGWIN, L.D. (2010): Synchronous deglacial overturning and water mass source changes. - *Science*, **327**, 75-78.

SARNTHEIN, M., WINN, K., JUNG, S.J.A., DUPLESSY, J.-C., LABEYRIE, L., ERLENKEUSER, H., & GANSSEN, G. (1994): Changes in East Atlantic Deepwater Circulation over the last 30,000 years: Eight time slice reconstructions. - *Paleoceanography*, **9**, 209-267.

STICHEL, T., FRANK, M., RICKLI, J., & HALEY, B.A. (2012): The hafnium and neodymium isotope composition of seawater in the Atlantic sector of the Southern Ocean. - *Earth and Planetary Science Letters*, **317–318**, 282-294.

ICDP

Analysing the geothermal regime of the scientific COSC-1 well bore, west central Sweden

R. LÖWE[1], C. PASCAL[1], J. RENNER[1]

[1]Ruhr-University Bochum, Institute of Geology, Mineralogy and Geophysics, Endogenous Geology, Germany

In 2014 the first well of the Collisional Orogeny in the Scandinavian Caledonides (COSC) ICDP project was drilled near Åre in west central Sweden. The well penetrates the Seve Nappe complex, a result of subduction/ exhumation processes during the collision of Baltica and Laurentia ~ 400 Myrs ago (Gee et al. 2010). To gain a more detailed understanding of the geothermal state of fossil mountain belts and cratonic areas, it is necessary to study present-day heat transfer in the earth's crust in appropriate deep boreholes. Constraining the heat transfer requires temperature measurements in boreholes and determination of thermal properties of the rocks present. The specific object of our study is to derive a local thermal model providing the pristine thermal state and quantifying transient effects, i.e. paleoclimatic and convective effects, on the local geotherm.

The outstanding core recovery (~ 100%) of the 2495.8 m (MD) deep well in combination with extensive wireline logging campaigns provide an exceptional basis for a broad range of core measurements and well log correlations. A total of 105 core samples, representing all major lithologies, were carefully selected for laboratory investigations, such as determining heat capacity, thermal conductivity, and thermal diffusivity.

Density and thermal conductivity were determined for each of the 105 core samples under ambient pressure and unsaturated conditions. The thermal conductivity was measured using the optical scanning method (Popov et al. 1985) providing a first-order estimate of thermal properties along the cores' surfaces. Based on these preliminary measurements, a thermal conductivity profile was

constructed, showing a steep increase towards the lower section of the well. For the first ~ 2000 m the average thermal conductivity amounts to 2.5±0.6 W/(m.K) and increases to 4.1±1 W/(m.K) in the lower section of the well. In addition, spectral gamma ray logs were used to determine the amount of radiogenic heat production (Rybach, 1988). The integrated heat production within the well is merely low and amounts to ~3.3 mW/m2. Three temperature logs were measured about one week, one month, and one year after drilling. The observed gradual slowdown in temperature recovery suggests that the latest log was probably measured very close to thermal equilibrium. Furthermore, the latest temperature log appears to show a typical curvature reflecting sudden global warming at the Pleistocene-Holocene transition. Based on the latest temperature log an uncorrected average thermal gradient of ~21 C/km is tentatively proposed.

References:
Gee, D. G.; Juhlin, C.; Pascal, C.; Robinson, P. (2010): Collisional Orogeny in the Scandinavian Caledonides(COSC). In GFF 132 (1), pp. 29–44.
Rybach, L. (1988): Determination of Heat Production Rate. In R. Haenel, L. Rybach, L. Stegena (Eds.): Handbookof terrestrial heat-flow density determination. Guidelines and recommendations of the International Heat FlowCommission, pp. 125–142.
Popov, Y. A.; Berezin, V. V.; Semenov, V. G.; Korostelev V. M. (1985): Complex Detailed Investigations on theThermal Properties of Rocks on the Basis of a Moving Point Source. In Izvestiya, Earth Physics 21 (1), pp. 64–70.

IODP

Calcareous nannofossil biometry in Upper Aptian to Lower Cenomanian sediments from ODP Site 763B

N. LÜBKE [1], J. MUTTERLOSE [1]

[1] Institut für Geologie, Mineralogie und Geophysik, Ruhr-Universität Bochum, Universitätsstraße 150, 44801 Bochum, Deutschland

Introduction:Coccolith-bearing haptophyte algae, coccolithophores, have been one of the main marine primary producers and the main carbonate producers at least since their first fossil occurrence in Upper Triassic sediments. Assemblage analysis have been conducted intensely throughout the last decades and shed light on the relation of the abundance of several species and ecological parameters, such as for example sea-surface temperature, nutrient levels and salinity. Biometric analyses of coccoliths of single species give valuable insight into intra-specific adaptations to ecological parameters or environmental changes. This project studies nannofossil assemblages preserved in mid-Cretaceous marine sediments from various locations covering open-oceanic to coastal settings and different latitudes.

Material:ODP core 763B exposes an entire succession of Upper Aptian to Lower Cenomanian marine sediments, with high absolute abundances of calcareous nannofossils. The selected core displays good age control based on chemostratigraphy and nannofossil biostratigraphy. Nannofossil preservation and abundance are well suited for biometric studies and assemblage analyses. The studied species include *Watznaueria barnesiae, Biscutum constans, Tranolithus orionatus* and *Prediscosphaera columnata*.

Methods:Rock material is processed using the settling method by Geisen et al. (1999) resulting in plain-lying coccoliths, best suited for biometric measurements. Nannofossil assemblage analyses are based on counts of at least 300 individual specimens per sample using an Olympus BX51 transmitted light microscope mounted with a ColorView II camera. Nannofossil biometry was conducted on at least 50 plain-lying individual specimens per species per sample at a magnification of x2000. The resulting data set is evaluated statistically.

Results: The mean length of *W. barnesiae* varies between 6.3 µm and 7.1 µm, which is greater than coccoliths of comparable age (e.g., mean length 5.75 µm in Vocontian Basin, Late Albian, Bornemann and Mutterlose, 2006). With 3.3 µm to 4.2 µm, the mean length of *B. constans* is in the same range as shown in several biometric studies (mean length 3.8 µm in North Sea, Aptian, Lübke et al., 2015; mean length 3.4 µm in Vocontian Basin, Bornemann and Mutterlose, 2006). *T. orionatus* shows a mean length increase from 6.7 µm to 7.3 µm at the top of the section (at ~430 m). For all these three species, the data sets show a normal unimodal distribution for each sample.

P. columnata, the fourth studied species, is an exception. Nine of the 17 samples show a bimodal distribution, suggesting the presence of two morphotypes wihtin these samples. Therefore, additional 50 specimens were measured in these samples to improve statustic reliability. At the bottom of the core, the small morphotype ist more abundant than the large one; towards the top, this relation is reversed. Both morphotypes each show a slight increasing trend towards younger samples. However, the prominent size increase for the total of *P. columnata* is due to the increased abundance of the large morphotype. The size dicrepancy of the two morphotypes is not attributed to differences in, for example, shield width, but it reflects variations in total size with similar proportions of the coccoliths.

Outlook:SEM images will be used to determine potential variations in morphology of the two morphytypes of *P. columnata* other than their total size. Samples, that contain both the small and the large morphotype, and samples, that contain only one morphotype, will therefore be chosen.

References:
Bornemann, A., Mutterlose, J., 2006. Size analyses of the coccolith species Biscutum constans and Watznaueria barnesiae from the Late Albian “Niveau Breistroffer” (SE France): taxonomic and palaeoecological implications. Geobios, 39, 599-615.
Lübke, N., Mutterlose, J., Bottini, C., 2015. Size variations of coccoliths in Cretaceous oceans — A result of preservation, genetics and ecology? Marine Micorpaleontology, 117, 25-39.

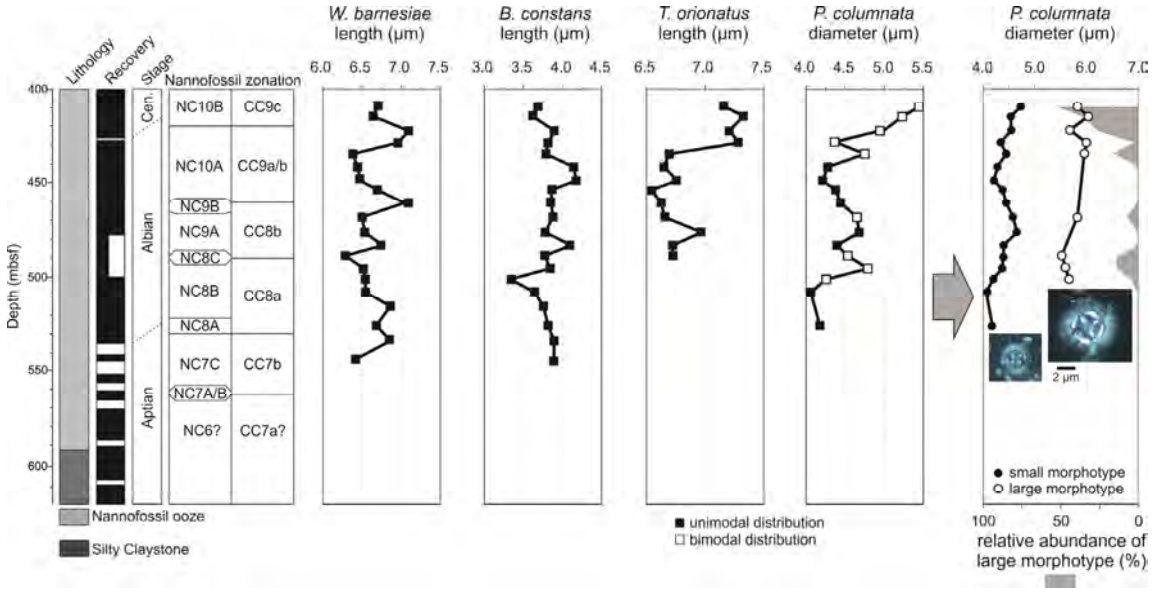

Figure 1: Summary of lithology, age, nannofossil zonation and biometric record of W. barnesiae, B. constans, T. orionatus and P. columnata at ODP Site 763B. Filled square indicates assemblages with normal unimodal distribution, open squares represent a bimodal distribution. Size data of P. columnata were splitted to show the individual size trend for the two morphotypes (filled circles = small morphotype; open circles = large morphotype). The grey shaded area indicates the increasing relative abundance of the large morphotype. Both microscope images derive from 408.9 m depth (top of the section).

ICDP

First evidences of neotropical glacial/interglacial (220-85 ka BP) climate change based on ostracodes and geochemical indicators from Lake Petén Itzá, northern Guatemala

L. MACARIO[1], S. COHUO[1], L. PÉREZ[2], S. KUTTEROLF[3], J. CURTIS[4], A. SCHWALB[1]

[1]Institut für Geosysteme und Bioindikation, Technische Universität Braunschweig, Langer Kamp 19c, 38106 Braunschweig, Germany
[2]Instituto de Geología, Universidad Nacional Autónoma de México, Ciudad Universitaria, 04510 México, D.F. Mexico
[3]GEOMAR Helmholtz-Zentrum für Ozeanfoschung, Kiel, Wischhofstr. 1-3, 24148 Kiel, Germany
[4] Department of Geological Sciences and Land Use and Environmental Change Institute, University of Florida, Gainesville, FL.USA.

The northern Neotropics is a key region for understanding past climatic changes and their role in shaping the actual environment. Lake sediments from this region are high-quality recorders of such climatic variations but only few lakes were capable to preserve continuous Pleistocene/Holocene-age deposits, because most of them were dry during the last glacial period, especially at the end of the deglaciation (Hodell et al. 2008). Seismic reflection surveys in Lake Petén Itzá revealed its potential for obtaining high quality sedimentary records in the lowlands of Guatemala (Anselmetti et al., 2006). Therefore, seven long cores (PI-1, PI-2, PI-3, PI-4, PI-6, PI-7 and PI-9) were retrieved under the auspices of the Lake Petén Itzá Scientific Drilling Project (PISDP) in 2006. The complete sedimentary record of all drill sites was believed to extend back to 200 ka BP (Mueller et al., 2010). The paleoclimatic history of the last 85 ka has been inferred by multiproxy analysis (magnetic susceptibility, density, stable isotopes, pollen and ostracodes) and revealed alternating environmental conditions, such as cold/dry Heinrich Stadials, cold/wet Last Glacial Maximum (LGM), warm/wetter conditions during the Bølling-Allerød, dry episodes during the Younger Dryas as well as warm and prevailing wetter conditions during the early Holocene. This highlights the high value of Lake Petén Itzá as climatic and environmental archive. This work focuses on cores PI-1 (65 m water depth) and PI-7 (46 m water depth) in which tephrochronology of lacustrine ash layers suggested that the stratigraphic sequence extends back to 84 – 225 ka and 146 - 405 ka BP, respectively.

The main scientific objectives of this study are: (1) to infer lake level and hydrological changes during the last 405 ka by expanding the original training set and further refining transfer functions based on freshwater ostracodes, (2) to reconstruct the ultrastructure of late Pleistocene climate extremes such as the transitions of glacial/interglacials and during the Holstein (MIS11), Purfleet (MIS 9), Aveley (MIS 7) and Eemian (MIS 5e) interglacials periods.

Quantification of paleoenvironmental variables: Ostracode training set and transfer functions. The original training set (50 aquatic ecosystem) and autoecological information of 29 ostracode species from southern Mexico, Belize and Guatemala was extended by sampling 70 additional systems in the Yucatán Peninsula and northern Central America (Guatemala, El Salvador, Honduras and Nicaragua) during the rainy season in summer/fall 2013. To refine the transfer functions for water temperature reconstructions, sampling took place through an elevation gradient ranging from 100 to 4000 m a.s.l. A total of 86 ostracode species were identified and their optima/tolerance ranges with respect to environmental

variables were calculated by applying a weighted averaging regression and calibration method (Birks, 1995). A preliminary transfer function for temperature was developed using the modern analog technique (MAT) and other methods such as partial-least-squares regression (PLS) and weighed averaging–partial least squares regression (WA-PLS).

about 85ka showed changes to low TOC (<2 %), high TIC (10 %) and C/N ratios up to 20. Ostracodes were only present during these periods, with *C. petenensis* dominant during the Eemian, and *C. ilosvayi* and *C. petenensis* prominent at around 85 ka BP. For the latter, abundance reached a maximum of up to 1000 valves per gram, suggesting a significant input of littoral ostracodes and thus decreasing lake levels by drier environments.

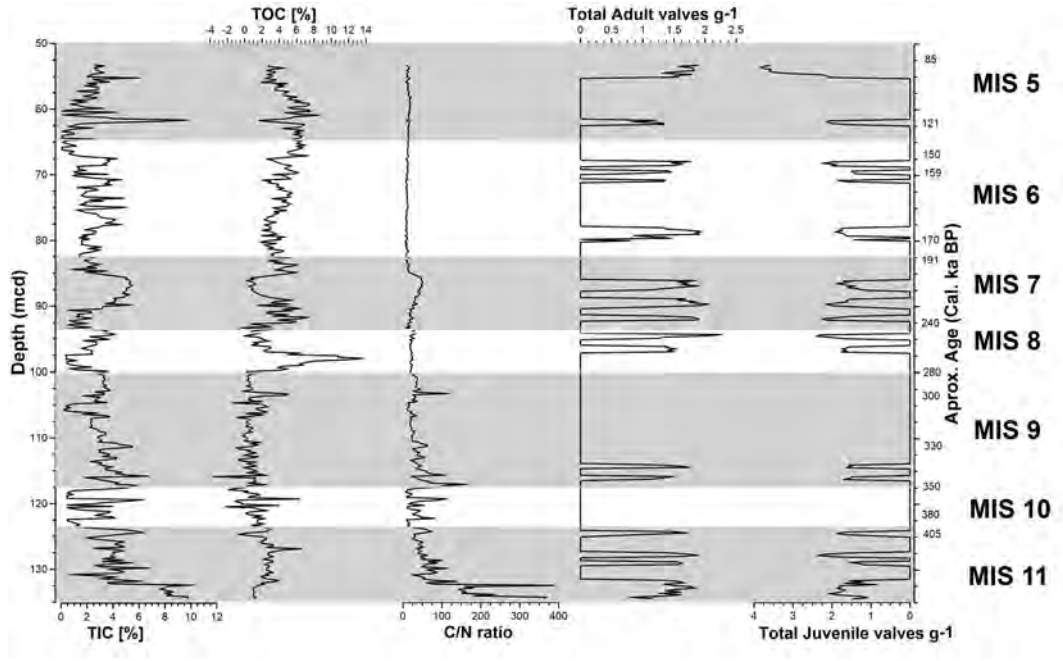

Fig 1. Geochemical parameters and ostracode abundance of cores PI-1 and PI-7 from Lake Petén Itzá, Guatemala, with preliminary age assignments.

Late Pleistocene climatic and environmental changes: glacial vs interglacial periods.

Interglacial periods:The interglacial periods recorded in our cores can be classified according to their general climate characteristics of warm/dry for MIS 11 and 9, and warm/wet for MIS 7 and 5. During MIS 11 estimated water temperatures ranged between 27-35°C. TIC (2-6%) and TOC (3-4%) values were relatively low and constant while C/N ratios were high (>30), particularly at around 400ka BP. Ostracode species composition was characterized by Paracythereis opesta, Darwinula stevensoni, Cytheridella ilosvayi and Cypria petenensis suggesting low water levels and extensive littoral zones. Similarly, MIS 9 displayed warm and dry conditions suggested by low TIC (1-5%) and TOC (0-5%) values and high C/N ratios (>30). Estimated temperatures ranged between 26- 34°C, and the ostracodes C. petenensis and P. opesta were the only species observed, also suggesting oligotrophic conditions.

In contrast to the previous interglacials, MIS 7 showed low values for TIC (0-6%), variable TOC (4-10%) and C/N ratio remained <24. Water temperatures ranged between 28-34°C, and the ostracode assemblage was composed of *C. petenensis* and *C. ilosvayi*. MIS 5 was characterized by low TIC (4 %), high TOC (6-8 %), and C/N ratio values ranging between 10 to 15. This suggests that warm and humid conditions prevailed during this period. Two particular periods corresponding to the Eemian and at

Observed hydrological changes during the interglacials in the Lake Petén Itzá agree with the estimated modeled global paleo-scenarios, lacustrine and speleothem records from the southern United States, suggesting relatively dry interglacial trends (Dahl-Jensen et al., 2013; Kleinen et al., 2014; Railsback et al., 2015). Temperature changes, however, are not in phase with ice volume variations. Although MIS 5 and 11 were considerably warm periods in northern latitudes (Coletti et al., 2015), our ostracode-derived temperatures suggest a minor warming in the northern Neotropics with temperatures ranging within the ranges of values observed today. This is consistent with Herold et al. (2012), who found small temperature variations in the Neotropics, using the Community Climate System Model 3, for modeling global temperatures during the interglacial periods.

Glacial periods: Glacial periods in the northern Neotropics were similar but not identical. For instance, temperature decreases were all small, as reflected by the presence of tropical species. The most important differences between these periods were precipitation rates which were highly variable during MIS 10 and constantly high during MIS 8 and 6. The geochemical characteristics of MIS 10 were low TIC (2-6%) and TOC (<5%) values, and variable C/N ratios (5-70). Ostracodes were absent during these periods. It is thus inferred that oligotrophic conditions predominated, with several drastic variations of

precipitation rates from humid to dry and vice versa. MIS 8 was characterized by temperatures ranging between 25-29°C and relatively constant TIC (0-2%) and TOC (8-12%) values. The C/N ratio was low (2-10) and ostracode assemblages consisted of benthic Pseudocandona sp. 1, D. stevensoni, and nektobentic species C. petenensis and H. putei. This suggests relatively wet conditions and moderate to high lake levels. MIS 6 showed a temperature decrease (23-30°C), and geochemical parameters were characterized by low TIC (2-4%), TOC (2-6%) and C/N ratios (7-15). The ostracode C. petenensis was the only species observed during the entire period, and littoral-related species D. stevensoni, Pseudocandona sp. 1, P. annae and H. putei showing up at the end of the period. It is thus inferred that wet conditions and high lake levels predominated in most of MIS 6, the presence of benthic and nektobenthic species at the end of the period, however, can be explained by a slight decrease of lake level or an increase in hydrodynamics which produced a transport of shells from littoral regions to deep lake areas. Similar wet glacial conditions were suggested by a consistent stalagmite growth in the Carlsbad Caverns and Valles Caldera, New Mexico (Railsback et al. 2015).

Conclusions: Our results suggest that glacial/interglacial cycles had small effects for the northern Neotropics. Thus the Neotropics may have acted as refugia of tropical aquatic taxa during the glacial periods. Our work highlights the importance of multiproxy analysis and especially underlines the complementarity of biological and geochemical records and provides the first high resolution evidence of climate variability in the northern Neotropics during the last 405 ka.

Acknowledgements: The project was funded by grants from the U.S. National Science Foundation, the International Continental Scientific Drilling Program, the Swiss Federal Institute of Technology, the Swiss National Science Foundation, the DFG-project SCHW 671/16-1 and CONACYT scholarships 218639, 213456 to the first two authors.

References:

Coletti, A. J., DeConto, R. M., Brigham-Grette, J., Melles, M., 2015. A GCM comparison of Pleistocene super-interglacial periods in relation to Lake El'gygytgyn, NE Arctic Russia. Clim. Past 11, 979-989.

Dahl-Jensen, D. & NEEM community members, 2013. Eemian interglacial reconstructed from a Greenland folded ice core. Nature 493, 489–494.

Anselmetti, F. S., Hodell D., Hillesheim M., Brenner M., Gilli A., McKenzie J, Mueller, A.D., 2006. Late Quaternary climate-induced lake level variations in Lake Petén Itzá, Guatemala, inferred from seismic stratigraphic analysis. Palaeogr., Palaeoclim., Palaeoecol. 230, 52-69.

Herold N., Yin Q., Karami M., Berger A., 2012. Corrigendum to "Modelling the climatic diversity of the warm interglacials". Quat. Sci. Rev. 56, 126–141.

Hodell, D.A., Anselmetti, F., Ariztegui, D., Brenner, M., Curtis, J.H., Gilli, A., Grzesik, D.A., Guilderson, T.J., Müller, A.D., Bush, M.B., Correa-Metrio, A., Escobar, J., Kutterolf, S., 2008. An 85-ka Record of Climate Change in Lowland Central America. Quat. Sci. Rev. 27, 1152-1165.

Kleinen, T., Hildebrandt, S., Prange, M., Rachmayani, R., Müller, S., Bezrukova, S., Brovkin, V., Tarasov, P., 2014.The climate and vegetation of Marine Isotope Stage 11 - model results 15 and proxy-based reconstructions at global and regional scale. Quat. Int., 348, 247–265.

Mueller, A., F. Anselmetti, D. Ariztegui, M. Brenner, D. Hodell, J. Curtis, J. Escobar, A. Gilli, D. Grzesik, T. Guilderson, S. Kutterolf, Plötze, M., 2010. Late Quaternary palaeoenvironment of northern Guatemala: evidence from deep drill cores and seismic stratigraphy of Lake Petén Itzá. Sedimentology 57, 1220-1245.

Railsback B., Brook G., Ellwood B., Liang F., Cheng Hai, Edwards L., 2015. A record of wet glacial stages and dry interglacial stages over the last 560 kyr from a standing massive stalagmite in Carlsbad Cavern, New Mexico, USA, Palaeogr., Palaeoclim., Palaeoecol., 438:256-266.

ICDP

ICDP Drilling Project in Wadi Gideah (Oman): crystallographic preferred orientations in the gabbro section

D. MOCK[1], B. ILDEFONSE[2], J. KOEPKE[1], T. MÜLLER[1], D. GARBE-SCHÖNBERG[3]

[1] Institut fuer Mineralogie, Leibniz Universität Hannover; dom.mock@web.de, koepke@mineralogie.uni-hannover.de, t.mueller@mineralogie.uni-hannover.de

[2] Géosciences Montpellier, Université de Montpellier 2, benoit.ildefonse@umontpellier.fr

[3] Institut für Geowissenschaften, Universität Kiel, dgs@gpi.uni-kiel.de

The Wadi Gideah in the Wadi Tayin Massif of the Oman ophiolite is one of the most promising sites for a section through intact fast-spread paleooceanic crust and was chosen as location for the ICDP Oman Drilling Project (http://www.omandrilling.ac.uk/). As preliminary work for this project, four field campaigns were undertaken, where samples of the lower crust, mid-crust and the dike/gabbro transition of the Oman paleocrust were collected, in order to provide a reference frame for the upcoming ICDP drillings. Our project within the SPP ICDP aims to provide constraints on the accretion and evolution of the Oman paleocrust with focus on depth logs with respect to (1) petrology, (2) major and trace element geochemistry on rocks and minerals, (3) crystallographic preferred orientations, (4) the evolution of hydrothermal alteration and (5) the sulfur cycle. To establish a coherent and comprehensive reference data set, more than 300 samples were taken along a section covering the whole crust from the mantle/crust boundary up to the dike/gabbro transition zone. The petrological and geochemical results obtained so far provide evidence for an upward differentiation trend within a hydrous tholeiitic system, and for a change in the mode of differentiation process between the layered and the foliated gabbro. Here, we present our results on crystallographic preferred orientations (CPO) obtained by EBSD.

The EBSD technique helps to quantify CPO of minerals in a rock, using the J-index of the Orientation Distribution Function (ODF J; e.g., Mainprice et al., 2014) and the BA-index to quantify the shape of the crystal fabric (e.g., Satsukawa et al., 2013; Mainprice et al., 2014). The BA index was primarily calculated for plagioclase and is classified in three types: Axial-B fabric with a point maximum in (010) and a girdle in [100] (BA-index ≈ 0); P-type fabric with point maxima in both (010) and [100] (BA-index ≈ 0.5); Axial-A fabric with a [100] point maximum and (010) girdle (BA-index ≈ 1; Satsukawa et al., 2013).

First analyses in the Montpellier EBSD lab were done on 48 samples from the lower crustal section (layered gabbro, foliated gabbro and varitextured gabbro). ODF J-index and BA-index of plagioclase versus depth plots provide evidence for a significant change in CPO and the crystal fabric of plagioclase, in the transition zone between layered and foliated gabbro. For a refinement of this trend, further 20 samples were recently analysed in the Montpellier EBSD lab. The so far evaluated microstructural change between foliated and layered gabbro was confirmed by the new data. The significant changes in both J- and BA-index is consistent with the geochemical evidence for a change in

formation/differentiation processes between the layered gabbros foliated gabbro sections. BA indices of almost all analysed samples scatter between 0.1 and 0.6, indicating a combination of Axial B- and Axial P-type providing evidence for magmatic deformation (Satsukawa et al., 2013). The combined EBSD and geochemical data support the hypothesis of an hybrid model after Boudier et al. (1996) for crustal formation at fast-spreading mid-oceanic ridges, where both in-situ crystallization by sill intrusion as well as the transport of gabbroic mushes via a "gabbro glacier" play a role. The genesis of the upper foliated gabbro can be better explained by the gabbro glacier model (e. g., Henstock et al., 1993), while in-situ crystallization according to the sheeted sill model (e. g., Keleman et al., 1997) is plausible for sections below the upper foliated gabbro.

Another significant change of both J- and BA-index takes place within the layered gabbro at ~3200 meters above the crust mantle boundary (CMB): From the base of the crust, the BA-index progressively decreases up to 3200 m above CMB and then increases above. The curve of the J-index shows a mirrored trend: it increases up to 3200 m and decreases above. These significant changes imply, that there is some kind of change in crystal growth in that crustal horizon and support the idea of the hybrid model with different crystallization processes in the upper foliated gabbro and the regions below, respectively.

References:
Boudier, F., Nicolas, A., Ildefonse, B., 1996. Magma chambers in the Oman ophiolite: Fed from the top and the bottom. Earth and Planetary Science Letters, 144, 239-250.
Henstock, T.J., Woods, A.W., White, R.S., 1993. The accretion of oceanic-crust by episodic sill Intrusion. Journal of Geophysical Research-Solid Earth, 98, 4143-4161.
Kelemen, P.B., Koga, K., Shimizu, N., 1997. Geochemistry of gabbro sills in the crust-mantle transition zone of the Oman ophiolite: Implications for the origin of the oceanic lower crust. Earth and Planetary Science Letters, 146, 475-488.
Mainprice, D., Bachmann, F., Hielscher, R., Schaeben, H., 2014. Descriptive tools for the analysis of texture projects with large datasets using MTEX: strength, symmetry and components. Geological Society, London, Special Publications, 409, SP409-8.
Satsukawa, T., Ildefonse, B., Mainprice, D., Morales, L. F. G., Michibayashi, K., Barou, F., 2013. A database of plagioclase crystal preferred orientations (CPO) and microstructures-implications for CPO origin, strength, symmetry and seismic anisotropy in gabbroic rocks. Solid Earth, 4, 511-542.

IODP

Three component borehole magnetometer in the Amami Sankaku Basin during IODP Expedition 351

MARTIN NEUHAUS[1], LAUREEN DRAB[2], SANG-MOOK LEE[3], CHRISTOPHER VIRGIL[1], SEBASTIAN EHMANN[1], ANDREAS HÖRDT[1], MARTIN LEVEN[4] AND IODP EXPEDITION 351 SCIENTISTS

[1]Technical University of Braunschweig
[2]Lamont Doherty Earth Observatory
[3]Seoul National University
[4]University of Göttingen

The interpretation of magnetic borehole data aids in constraining the paleomagnetic subsurface history, as it allows us to determine the direction and strength of the natural remanent magnetization (NRM) of penetrated formations. The NRM provides important constraints for the analysis of tectonic processes. In most of today's analysis, solely the inclination of the NRM vector is interpeted, because the estimation of its azimuth requires oriented cores which are very rarely taken. However, it becomes more and more attractive to derive a reliable estimation of the three component magnetization vector, as with only the information of the azimuth can one calculate the paleopoleposition. Here, oriented three component borehole magnetometers like the Göttinger Borehole Magnetometer (GBM) constitute a valuable alternative.

In summer 2014, IODP Expedition 351 drilled 1611 m of sediment and basement in the Amami Sankaku Basin west of the Kyushu-Palau Ridge in order to contribute to the questions of when and how subduction processes are initiated. To provide supplementary information, like the rotational history of the host plate, the Philippine Sea Plate (PSP), we successfully investigated 600 m of sediment between 600 mbsf and 1200 mbsf with the GBM.

Up-to-date processing of the data comprised depth correction and separation of the horizontal and vertical component of the magnetic flux density by usage of the GBM's orentational sensors . An initial assessment of the data revealed small but spatially coherent magnetic structures clearly related to a remanent magnetization and excels an overall satisfying data quality based on the good correspondence of uplog and downlog. Nevertheless further seperation into full three component information proved to be difficult as the characteristics of the underlying positioning system changed over time. In addition, rapid rotations of the tool in combination with the magnetometer's low pass filter affected the data in a complicated fashion. To counteract this, we conducted an extensive calibration of the positioning system and developed a scheme to attenuate the influence of the low pass filter.

IODP

Gulf Stream hydrography during the Late Pliocene/Early Pleistocene: low versus high latitude forcing of the Atlantic Meridional Overturning Circulation

A. OSBORNE[1], M. FRANK[1]

[1] GEOMAR Helmholtz Centre for Ocean Research Kiel, Kiel, Germany

The goal of this project is to reconstruct the hydrography of the Gulf Stream during the final stages of the closure of the Central American Seaway (CAS) in the Late Pliocene/Early Pleistocene. Material from ODP Sites 1006 and 1000 in the Florida Straits and central Caribbean will be used to test the hypothesis that there was a direct link between CAS closure, warming and increased salinity of the Gulf Stream, and a major strengthening of the Atlantic Meridional Overturning Circulation (AMOC), which led to the present day Atlantic circulation and climate system. An age model for Site 1006 (658 m water depth), a key site positioned ideally at the start of the Gulf Stream, will be established based on the stable isotope composition of oxygen and carbon in benthic foraminifera and will be the basis for a whole range of paleoceanographic research efforts.

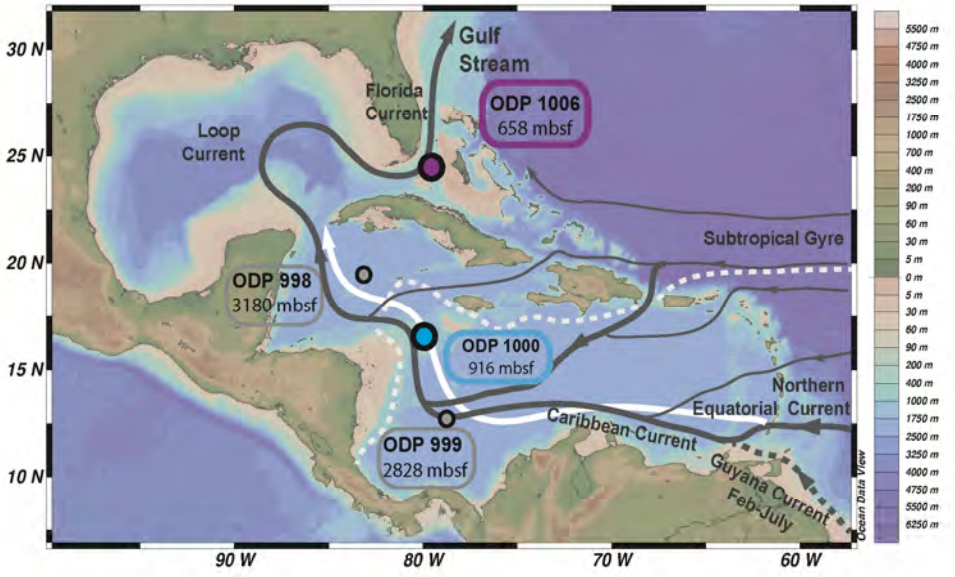

Figure 1 Location and water depth of ODP Sites to be used in this study (1000 and 1006) and other ODP Sites of interest in the Caribbean (998 and 999) serving for comparison. Depiction of major surface currents (grey lines) follows *Schott et al.* [2002] and *Steph et al.* [2006]. The white line with arrow represents the flow axis of the water mass at 800 m. South of the white dashed line, Antarctic Intermediate Water makes up more than 5 % of this water mass [after *Haddad and Droxler*, 1996 and *Wüst*, 1964]. Map produced using Ocean Data View [*Schlitzer*, 2001].

Building on previous successful application on the million year time scale [*Osborne et al.*, 2014] the radiogenic isotope composition of neodymium (Nd) in the Fe-Mn coatings of uncleaned foraminifera will be measured to trace intermediate water mass mixing and the strength of the AMOC during repeated millennial time scale episodes of CAS closure and re-opening caused by sea level changes. Upper water column hydrography will be reconstructed from the stable isotope composition of oxygen measured in mixed-layer and thermocline dwelling planktonic foraminifera. Together, these high resolution records will give us insight into the importance of low versus high latitude forcings of the strength of the AMOC. This will not only significantly improve our understanding of the mechanisms driving past changes in ocean circulation in response to major tectonic changes but will also provide information relevant to future climate perturbations as a consequence of changing sea surface salinity of the Gulf Stream influencing the functioning of the North Atlantic overturning circulation.

References:

Haddad, G.A., Droxler, A.W., 1996. *Paleoceanography 11*, 701-716.

Osborne, A.H., Newkirk, D.R., Groeneveld, J., Martin, E.E., Tiedemann, R., Frank, M., 2014b. The seawater neodymium and lead isotope record of the final stages of Central American Seaway closure. Paleoceanography 29, 715-729.

Schlitzer, R., 2011. Ocean Data View. http://odv.awi.de.

Schott, F.A., Brandt, P., Hamann, M., Fischer, R., Stramma, L., 2002. *Geophysical Research Letters 29.*

Steph, S., R. Tiedemann, M. Prange, J. Groeneveld, D. Nürnberg, L. Reuning, M. Schulz, and G. H. Haug (2006) *Paleoceanography*, *21*(4), doi:Pa4221/4210.1029/2004pa001092.

Wüst, G., 1964. Stratification and Circulation in the Antillean-Caribbean Basins, Part 1, Spreading and mixing of the water types with an oceanographic atlas. Columbia University Press, New York.

ICDP

New Project: Insights into the origin of a Mediterranean biodiversity hotspot based on palynological and biomarker analyses of Lake Ohrid sediments from Early Pleistocene (> 1.2 Ma)

K. PANAGIOTOPOULOS[1], J. HOLTVOETH[2], R. D. PANCOST[2], B. WAGNER[1], M. MELLES[1]

[1] Quaternary Geology Group, Institute for Geology and Mineralogy, University of Cologne, Germany

[2] Organic Geochemistry Unit, School of Chemistry, University of Bristol, UK

Mediterranean hotspots of plant diversity, such as the Ohrid region at present, are commonly associated with southern glacial tree refugia. Existing paleobotanical evidence suggests that SW Balkans have sheltered temperate tree populations over the last five climatic cycles. This project aims to use high-resolution palynological, charcoal and lipid biomarker analyses to study the origins of plant biodiversity at a southern refugium and to reconstruct the response of aquatic and terrestrial ecosystems to climate variability over the Early Pleistocene within the Ohrid Basin.

Our current knowledge about EarIy Pleistocene climate and flora in the Mediterranean region is based mostly on fragmentary terrestrial archives complemented by marine cores. In an effort to improve our understanding of the climate and flora evolution over this interval, a new 569m-long core was retrieved in 2013 within the ICDP drilling at Lake Ohrid. Preliminary geochemical, pollen and diatom

analyses show continuous sedimentation over the last ~1.2 million years and indicate major shifts in organic carbon, pollen and diatom assemblages corresponding to the characteristic marine isotope stage (MIS) stratigraphy (Wagner et al., 2014; Sadori et al., 2015).

Considering the reduced global ice volume and shorter climatic cycles paced by obliquity observed in marine cores during this period, the research objectives of this proposal are: (i) the determination of the floristic diversity in a southern refugium during the formation of Lake Ohrid and prior to the onset of the Mid-Pleistocene transition with a focus on relict subtropical species, (ii) the reconstruction of environmental and hydrological changes in the Ohrid Basin leading to the formation of the lake, (iii) the identification of the main drivers of terrestrial and aquatic ecosystem change in the Ohrid Basin since the formation of the lake until MIS 35 under an obliquity-controlled climate regime (41-kyr cycles), and (iv) the quantitative reconstruction and assessment of the nature and amplitude of climate variability during this interval in the Eastern Mediterranean region.

These objectives will be addressed in two work packages that will deliver the first highly-resolved pollen and non-pollen palynomorph and charcoal record, a lipid biomarker inventory of fluvial, peatland and lacustrine phases, as well as a biomarker-derived quantitative reconstruction of lake surface (TEX86) and air (MBT/CBT) temperatures for the Early-Pleistocene in the Mediterranean region. Complementary tephrochronological, sedimentological, geochemical and diatom analyses over the same interval (see bundle projects) will provide independent age control points and will refine our understanding of changes in lake hydrology driving aquatic organism community turnovers.

References:

Sadori, L., Koutsodendris, A., Masi A., Bertini, A., Combourieu-Nebout, N., Francke, A., Kouli, K., Joannin, S., Mercuri, A. M., Panagiotopoulos, K., Peyron, O., Torri, P., Wagner, B., Zanchetta, G., and Donders, T. H., (2015): Pollen-based paleoenvironmental and paleoclimatic change at Lake Ohrid (SE Europe) during the past 500 ka, Biogeosciences Discuss., 12, 15461-15493, doi:10.5194/bgd-12-15461-2015.

Wagner, B., Wilke, T., Krastel, S., Zanchetta, G., Sulpizio, R., Reicherter, K., Leng, M.J., Grazhdani, A., Trajanovski, S., Francke, A., Lindhorst, K., Levkov, Z., Cvetkoska, A., Reed, J.M., Zhang, X., Lacey, J.H., Wonik, T., Baumgarten, H., and Vogel, H., (2014): The SCOPSCO drilling project recovers more than 1.2 million years of history from Lake Ohrid, Sci. Dril., 17, 19-29.

IODP

Late Pliocene upwelling in the Southern Benguela region

BENJAMIN PETRICK[1], ERIN L. MCCLYMONT[2], SONJA FELDER[3], GEMMA RUEDA[4], MELANIE J. LENG[5,6], ANTONI ROSELL-MELÉ[4,7]

[1]Max Planck Institute for Chemistry, Climate Geochemistry Department, Hans-Meitner-Weg 1, 55128 Mainz Germany
[2]Department of Geography, Durham University, South Road, Durham, DH1 3LE, UK.
[3]School of Geography, Politics & Sociology, Newcastle University, Claremont Road, Newcastle upon Tyne, NE1 7RU, UK.
[4]Institut de Ciència i Tecnologia Ambientals (ICTA), Universitat Autònoma de Barcelona, Bellaterra, 08193, Spain
[5]School of Geography, Centre for Environmental Geochemistry, University of Nottingham, NG7 2RD, UK
[6]NERC Isotope Geosciences Facilities, British Geological Survey, Keyworth, Nottingham, NG12 5GG, UK.
[7]ICREA, Barcelona 08010, Spain

The Late-Pliocene has been proposed as a possible analogue for understanding future climate change and for testing climate models. Previous work has shown that during the Pliocene the major upwelling systems were relatively warm, and that this meant they were either inactive, contracted, or were upwelling warmer waters than present. Here, we examine evidence from a site located on the margins of the modern Benguela Upwelling system to test whether the upwelling cells had migrated or contracted relative to present during the Pliocene.

We applied several organic geochemistry proxies and foraminiferal analyses to reconstruct the Pliocene history of ODP Site 1087 (31º28'S, 15º19'E, 1374m water depth), including the U^{K}_{37}' and TEX_{86} indices (for reconstructing sea surface temperatures), chlorin and alkenone concentrations and carbon stable isotopes (for estimating export primary productivity), and planktonic foraminifera assemblages abundances (for inferring water mass changes). These proxies show that, between 3.5 and 3.0 Ma, the southern Benguela region was cooler than the northern Benguela region by 5 °C, the latter being where the main upwelling cells are found today. From the multiproxy data obtained, we infer that more extensive upwelling was present in the southern Benguela region during the Pliocene and that the Benguela Upwelling cells shifted northwards after the Pliocene epoch as a result of changes in the local wind field. We also find evidence that the Benguela Upwelling was sensitive to the pronounced cooling during the M2 and KM2 glacial stages, potentially associated with the expansion of sea ice and cooling in Antarctica in the late Pliocene.

ICDP

Vegetation changes in eastern Anatolia through the last two glacial-interglacial cycles

NADINE PICKARSKI[1], GEORG HEUMANN[1], OLA KWIECEIN[2], THOMAS LITT[1] AND THE PALEOVAN SCIENTIFIC TEAM

[1]University of Bonn, Steinmann-Institute for Geology, Mineralogy, and Paleontology, Nussallee 8, Bonn, Germany
[2]Ruhr University, Institute for Geology, Mineralogy & Geophysics, Universitätstr. 150, Bochum, Germany

Deep drilling cores recovered from a thick lacustrine sequence at Lake Van (Turkey), document multiple changes in vegetational communities through the last two

glacial-interglacial cycles. Long continuous terrestrial sedimentary archives, such as Lake Van, are rare in the eastern Mediterranean region. Therefore, Lake Van has the potential to add significantly to the picture of long-term glacial-intergalcial variability and high-frequency (millennial-to-centennial scale) oscillations representing changing vegetation history and climate conditions in the Near East. A unique multi-proxy study, derived from pollen and microscopic charcoal data, stable oxygen isotopes from bulk sediment samples and X-ray fluorescence (XRF) measurements, provides the opportunity to examine different paleoenvironmental indicators, e.g., melt water supply, evaporation rates and moisture availability in the catchment area. The robust chronological framework allows us to correlate the complete stratigraphical Lake Van record with other existing long-term southern European terrestrial sequences, marine and ice-core archives to evaluate regional response to gloabal climate changes such as ice volume changes, atmospheric greenhouse gas concentration, insolation forcing and the complex atmospheric-oceanic interaction of the Northern Hemisphere.

Here we present a new detailed high-resolution pollen and charcoal record (between ~100 and 1,000 years) from the 'Ahlat Ridge' composite profile. This sedimentary sequence down to a composite depth of 120.2 mcblf (meter composite below lake level) is considered to represent a record of approximately the past 257,000 years. The pollen profile shows alternation between open oak steppe-forest and semi desert-steppe vegetation communities, a reflection of major climatic shifts from interglacials to glacials. Superimposed on these oscillations, the sedimentary sequences shows short-term variablity associated with vegetation changes within interglacial (interstadial) and glacial periods (stadial).

During open oak steppe-forest periods (interglacials) a ecological succession is represented by (I) *Pistacia* cf. *atlantica* expanding early indicating summer dryness and mild winter conditions, followed by (II) deciduous *Quercus* and *Ulmus* indicating warm and humid climate condition with enhanced evaporation; (III) a *Carpinus betulus* phase suggesting increased wet and cool conditions with reduced evaporation rate, and finally (IV) a period of *Pinus*-dominated steppe-forest documenting the onset of colder/drier environment.

During open vegetation periods (glacials) a series of changes is observed from transitional steppe-forest vegetation, through grassland steppe communities (i.e., Poaceae), culminating in a discontinuous desert-steppe vegetation (e.g., *Artemisia*, Chenopodiaceae). Moisture deficiency and lower winter temperature would have led to significant reductions in the density and spatial extent of tree & shrub communities. Although individual periods may be characterized by dominance of one or more taxa, the underlying pattern of differential expansion is usually distinct and consistent.

A comparison between the penultimate interglacial complex (MIS 7, ~190.5 – 241.8 ka BP), the last interglacial complex (MIS 5, ~77.5 – 131.2 ka BP) and the current interglacial (MIS 1, ~11.7 ka BP – present) provides a vivid illustration of how different successive climatic cycles can be. Furthermore, it provides an improved insights into long-term vegetation dynamics. In particular during MIS 7, all three warm forested stages reach the level (esp. by deciduous *Quercus*) of MIS 5 and the Holocene, as a result of higher insolation rates along with subdued changes in global ice volume. Another interesting aspect in the Lake Van vegetation history is that the penultimate glacial (~131.2 – 190.5 ka BP), in contrast to the last glacial (~11.7 – 77.5 ka BP), can be divided into two parts: (I) an early period with pronounced temperate tree oscillations (Dansgaard-Oeschger like events) and (II) a later period with subdued AP (aboreal pollen) oscillations.

References:
Kwiecien, O., Stockhecke, M., Pickarski, N., Heumann, G., Litt, T., Sturm, M., Anselmetti, F., Kipfer, R., Haug, G.H., 2014. Dynamics of the last four glacial terminations recorded in Lake Van, Turkey. Quaternary Science Review 104, 42–52.

Litt, T., Pickarski, N., Heumann, G., Stockhecke, M., Tzedakis, P.C., 2014. A 600,000 years long continental pollen record from Lake Van, eastern Anatolia (Turkey). Quaternary Science Review 104, 30–41.

Pickarski, N., Kwiecien, O., Djamali, M., Litt, T., 2015a. Vegetation and environmental changes during the last interglacial in eastern Anatolia (Turkey): a new high-resolution pollen record from Lake Van. Palaeogeography, Palaeoclimatology, Palaeoecology 435, 145-158.

Pickarski, N., Kwiecien, O., Langgut, D., Litt, T., 2015b. Abrupt climate and vegetation variability of eastern Anatolia during the last glacial. Climate of the Past 11, 1491-1505.

Stockhecke, M., Kwiecien, O., Vigliotti, L., Anselmetti, F.S., Beer, J., Çağatay, M.N., Channell, J.E.T., Kipfer, R., Lachner, J., Litt, T., Pickarski, N., Sturm, M., 2014. Chronostratigraphy of the 600,000 year old continental record of Lake Van (Turkey). Quaternary Science Review 104, 8–17.

IODP

Vein structures in fore arc basalts and boninites related to post-magmatic tectonic deformation in the outer Izu-Bonin-Mariana fore arc system: preliminary results from IODP Expedition 352

D. QUANDT[1], P. MICHEUZ[1], W. KURZ[1]

[1]Institute of Earth Sciences, University of Graz, A-8010 Graz, Austria, dennis.quandt@uni-graz.at, peter.micheuz@uni-graz.at, walter.kurz@uni-graz.at

On the basis of four sites, the International Ocean Discovery Program (IODP) Expedition 352 aimed to drill through an entire volcanic sequence of the Izu-Bonin-Mariana fore arc. Thereby two sites at the upper trench slope penetrated a sequence of fore arc basalts (FAB) whereas the other two drilled through younger boninites at the outer fore arc. First results from IODP Expedition 352 and preliminary post-cruise data suggest that FAB were generated by decompression melting during near-trench sea-floor spreading and that fluids from the subducting slab were not involved in their genesis. Subduction zone fluids involved in boninite genesis appear to have been derived from progressively higher temperatures and pressures over time as the subducting slab thermally matured.

Structures within the drill cores combined with borehole and site survey seismic data indicate that tectonic deformation in the outer Izu-Bonin-Mariana fore arc is mainly post-magmatic associated with the development of syn-tectonic sedimentary basins. Faulting along west-dipping normal faults results in fore arc extension and is associated within halfgraben formation. Biostratigraphic analyses revealed that syntectonic sedimentation within the halfgrabens started at ca. 35 Ma. Within the magmatic basement deformation was accommodated by shear along cataclastic fault zones and the formation of tension

fractures, shear fractures and hybrid (tension and shear) fractures.

Veins form by mineral filling of tension or hybrid fractures and show no or limited observable macroscale displacement along the fracture plane. Major vein constituents are (Mg-) calcite and/or various types of zeolite determined by Raman spectra. The latter are considered to be alteration products of volcanic glass. Micrite contents vary significantly with depth and are related to neptunian dikes and/or cataclastic fault zones. In veins within FAB calcite forms consistently blocky crystals without any microscopic identifiable growth direction suggesting precipitation from a highly supersaturated fluid under dropping fluid pressure conditions. However, veins within boninites additionally develop fibrous and stretched crystals in places characterizing antitaxial as well as ataxial growth, respectively. Host rock fragments within veins indicate high fluid pressure before mineral precipitation. Cross-cutting relationships of veins point to multiple and probably chaotic fracturing and repeated mineral precipitation events. Hydrothermal fluids affected significantly the vein walls by forming selvages of asbestiform mineral bands and alteration halos along the vein-wall rock contact. Rock fragments show the same selvages as the vein walls. Moreover, volcanic glass can be completely altered to zeolite and/or palagonite. This hydrothermal activity took place shortly after magma cooling since vein frequency varies with depth but does not seem to correlate with the proximity to faults. With increasing depth, calcite grains in both sequences exhibit deformation microstructures more frequently than at shallower core intervals. These microstructures comprise thin twinning (type I twins), increasing in width with depth (type I and type II twins), slightly curved twins, and subgrain boundaries indicative of incipient plastic deformation. The differential stresses ($\geq$ 50 MPa) that triggered vein deformation were presumably related to IBM fore arc extension due to the retreat of the subducted Pacific plate.

IODP

Correlated global variations in abyssal peridotite - mid-ocean ridge basalt composition

MARCEL REGELOUS[1], KARSTEN HAASE[1], CHRISTOPH WEINZIERL[1]

[1]GeoZentrum Nordbayern, Universität Erlangen-Nürnberg, Schloßgarten 5, 91054 Erlangen

Abyssal peridotites represent the complex residues of partial melting beneath mid-ocean ridge spreading centres, and potentially can yield complementary information on the melting process to that obtained from geochemical studies of mid-ocean ridge basalts (MORB). Whereas crystal fractionation-corrected Na concentrations (Na_{90}) in MORB can be used to estimate the mean, or bulk degree of melting (F_B), the Cr content (Cr#) in spinel from abyssal peridotites can be used to calculate the maximum degree of melting (F_M). We carried out a detailed mineralogical and geochemical study of peridotites from spreading centres in the Indian, Atlantic, Arctic and Pacific Oceans, and combined our new data with literature data obtained from the PETDB online database. Abyssal peridotite samples showing the geochemical effects of extensive alteration or melt refertilisation were removed from the dataset. Our new database includes major and trace element data for whole-rock samples and for minerals for over 2200 samples. Systematic variations between spinel, orthopyroxene, clinopyroxene, and bulk rock compositions (e.g. Fig. 1) show that the samples preserve useful information on melting processes. Peridotite compositions were averaged over single spreading ridge segments, in order to be comparable with the global mid-ocean ridge basalt database of Gale et al. (2013).

We show for the first time, that abyssal peridotite and MORB compositions are correlated on a global scale (Fig. 2). Ridge segments exposing peridotites having undergone higher extents of melt extraction (high Cr# in spinel) erupt MORB representing large degrees of melting (low Na_{90}). Moreover, for ridge segments distant from hotspots, there is a clear dependence of ridge depth, MORB composition and peridotite composition with spreading rate. Very-slow spreading ridges are deeper, expose peridotite with low Cr#, and erupt MORB with high Na_{90}. We used a fractional melting model to calculate F_M and F_B for each ridge segment from Cr# and Na_{90}, respectively. For perfect passive decompression melting the ratio F_M/F_B will have a value of 2 (independent of mantle temperature), whereas for dynamic upwelling and decompression the F_M/F_B ratio is 1. The effects of thick lithosphere and incomplete melt extraction will yield intermediate values of F_M/F_B. Our calculated values of F_M/F_B vary from 0.78 to 2.94 (Fig. 2), with segments from slow-spreading ridges having the lowest F_M/F_B ratios. This large range in F_M/F_B can best be explained by melting of heterogeneous mantle beneath thicker lithosphere together with incomplete melt extraction beneath very-slow spreading ridges.

This relationship between the maximum and bulk degree of melting, reflected in the compositions of complementary melts and residues produced during decompression melting beneath spreading ridges provides a novel means to evaluate the role of decompression melting in other tectonic environments, for example at subduction zones. If decompression melting is the dominant process of melting in such tectonic settings, then the compositions of residual peridotites and associated lavas from supra-subduction zone ophiolites and fore-arcs melts should vary in a similar way as at spreading ridges. In contrast, if flux (fluid-addition) melting is important, melting will start deeper, melt productivity may be higher, and fluid addition of Na will result in higher Na_{90} for a given Cr# ($F_M/F_B > 2$) compared to the oceanic array. In order to test these hypotheses, we plan to carry out a geochemical study of fore-arc peridotites from the Tonga and Marianas Trenches (including samples drilled during ODP Legs 125, 195).

References:

Gale, A., Langmuir, C.H., Dalton, C.A. The global systematics of ocean ridge basalts and their origin. J. Petrol. 55 (2014) 1051-1082.

Weinzierl, C.G., Regelous, M., Haase, K.M. Controls on melting at spreading ridges from correlated abyssal peridotite – mid-ocean ridge basalt compositions. Earth Planet. Sci. Lett. (2016) submitted manuscript.

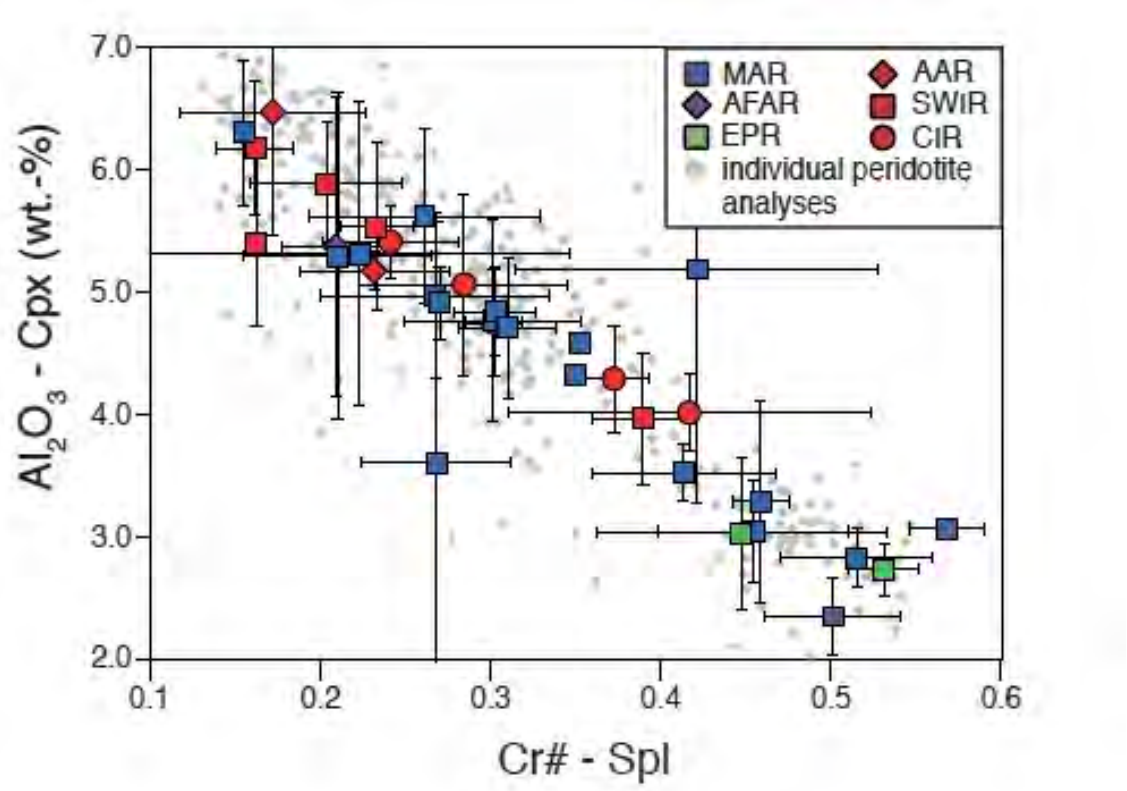

Figure 1. Systematic variation of Al in clinopyroxene and Cr in spinel from our new global abyssal peridotite database indicates that information on the melting process is preserved even in highly serpentinised peridotites. Grey symbols indicate individual peridotite samples, large coloured symbols are segment-averaged compositions.

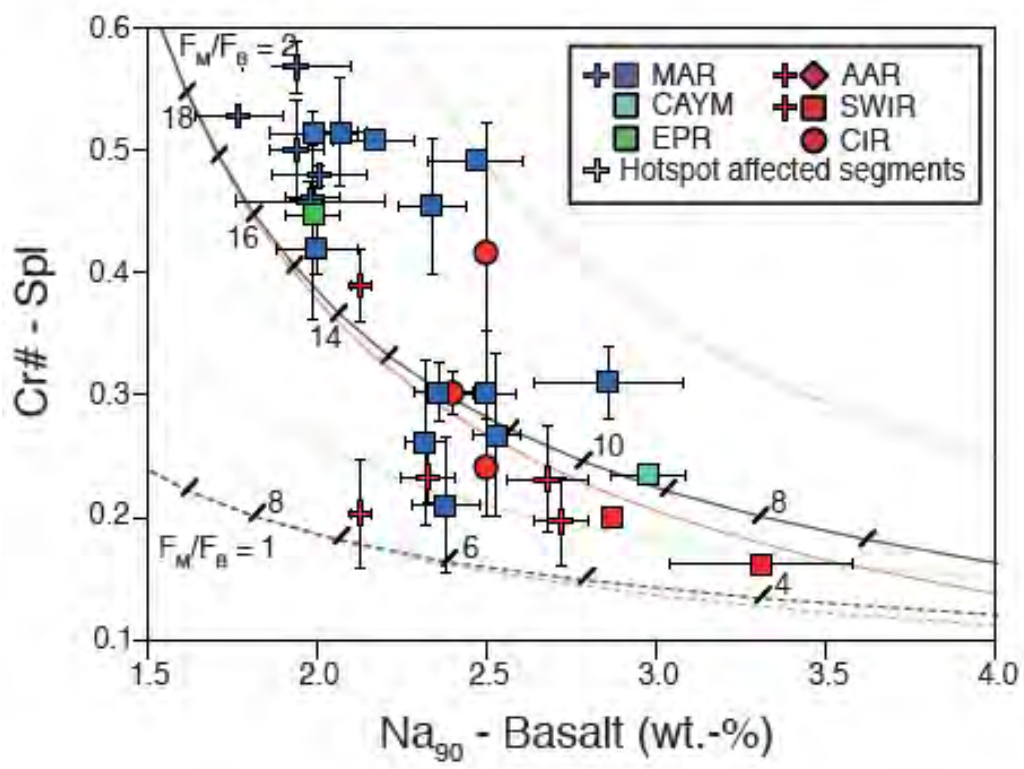

Figure 2. Melting indicators in abyssal peridotites (e.g. Cr in spinel) and mid-ocean ridge basalts from the same ridge segments (Na_{90}) are correlated on a global scale. Peridotites from which large volumes of melt have been extracted (high Cr#) are found on ridge segments which erupt mid-ocean ridge basalts produced by large degrees of mantle melting (low Na_{90}). Curves show expected relationships for passive ($F_M/F_B = 2$) and dynamic ($F_M/F_B = 1$) decompression melting.

IODP

Siliceous microfossils and the Cenozoic marine carbon and silicon cycles

J. RENAUDIE[1]

[1]Museum für Naturkunde, Leibniz-Institut für Evolutions- und Biodiversitätsforschung, Invalidenstraße 43, 10115 Berlin.

Modern marine planktonic diatoms have, as silicon biomineralizers and primary producers, a significant impact on both the Silicon and the Carbon cycle: there are at the same time the main silica and carbon exporter to the deep-sea. However, at the beginning of the Eocene, radiolarians were the main silica exporter and diatoms were only a rare, geographically-constrained group. Prior studies (Baldauf & Barron, 1990; Cortese et al., 2004; Lazarus et al., 2009, 2014; Renaudie, subm.) have highlighted two main events in the Cenozoic history of diatoms and radiolarians. The first one near the Eocene-Oligocene boundary is a diatom diversity and abundance peak during which they took over radiolarians for control of the marine silicon cycle. The second one occurred during the Middle Miocene and witnessed a complete spatial reorganization of the biogenic opal deposition pattern as well as a sustained rise in diatom diversity and abundance. Both events are coeval with known shifts in atmospheric pCO2 as well as shifts in strontium and osmium isotopes (indicative of changes in the silica weathering pattern).

In this new project (started in December 2015), I will be measuring the absolute abundance of each group of siliceous microfossils (with an emphasis on diatoms, radiolarians and silicoflagellates) in ca. 800 samples, spanning the last 55 Myr, from 27 DSDP-ODP-IODP sites covering the different biogeographical zones highlighted in the pilot study on Cenozoic diatom deposition patterns (Renaudie, subm.). In parallel to this sampling effort, a database of measured biogenic silica accumulation rates in DSDP-ODP-IODP sediments is being gathered from the literature as a backbone to the study. In order to calibrate correctly each time-series, an additional effort will be made to produce new age models for the sampled sites using the newly improved stratigraphic layer of the Neptune database (NSB; http://nsb-mfn-berlin.de).

With these time-series in hand, I intend to disentangle the causal relationships between diatoms and Cenozoic climate shifts, as well as to determine what made diatoms outcompete radiolarians and why diatom biogeography changed so drastically during the Cenozoic. Finally, biogenic opal being the only output of the marine silicon cycle and weathering its main input, I will be able to estimate from the measured time-series a global biogenic opal accumulation rate and, consequently, contrain the Cenozoic history of silica weathering intensity.

References:

Baldauf & Barron, 1990. Evolution of biosiliceous sedimentation patterns – Eocene through Quaternary: paleoceanographic response to polar cooling. Geologic history of the polar oceans: arctic vs antarctic, NATO ASI Series C, 308: 575-608.

Cortese, Gersonde, Hillenbrand & Kuhn, 2004. Opal sedimentation shifts in the World Ocean over the last 15 Myr. Earth and Planetary Science Letters, 224: 509-527.

Lazarus, Kotrc, Wulf & Schmidt, 2009. Radiolarians decreased silicification as an evolutionary response to reduced Cenozoic ocean silica availability. PNAS, 106(23): 9333-9338.

Lazarus, Barron, Renaudie, Diver & Türke, 2014. Cenozoic diatom diversity and correlation to climate change. PLoS ONE, 9(1):e84857.

Renaudie, subm. A quantitative review of the Cenozoic diatom deposition history.

IODP

NSB and ADP: a new, expanded and improved software system for marine planktonic microfossil and geochronologic data

J. RENAUDIE[1], P. DIVER[2] AND D. LAZARUS[1]

[1]Museum für Naturkunde, Invalidenstrasse 43, 10115 Berlin, Germany. johan.renaudie@mfn-berlin.de

[2]Divdat Consulting, 1392 Madison 6200, Wesley, AR 72773-8785 USA

Over 40 years of drilling has produced thousands of papers reporting the occurrences of thousands of species of planktonic microfossils in deep-sea sediments. These data are central to construction of age models for more than one thousand deep-sea sedimentary sections, as well as research in paleoceanography, biologic evolution and taxonomy/systematics. Because the majority of this research was published post-cruise, little of it has been captured in the official deep-sea drilling program databases. In the early 1990s the Neptune database was created at the ETH in Zürich to synthesize this data, making possible numerous published global studies of microfossil distributions through time, and, via the included age model library, global syntheses of other section data, e.g. sedimentologic and geochemical data for paleoceanography. The Neptune database was upgraded by the Chronos project (NSF, Ames, Iowa; Fils et al., 2009) and first brought online in the early 2000s but became orphaned and unstable soon after as funding ended. With funding support from CEES, Olso and the ESF/Earthime-EU a new version of Neptune has now been created: Neptune Sandbox Berlin (NSB). Data content has been upgraded from ca 500k to nearly 800k occurrence records, including most of the important newer ODP and IODP sections. The taxonomy has been thoroughly overhauled, based on IODP's recent Taxonomic Name List (TNL) project (e.g. Lazarus et al., 2015). Data has been scanned and flagged for errors and outliers. The ages have been updated to the Gradstein et al. 2012 scale. A website has been built to allow common data searches and downloads (www.nsb-mfn-berlin.de), while additional display functions are being developed in cooperation with the Geobiodiversity Database (Fan et al. 2013). The technology underlying NSB has also been simplified compared to the prior Chronos version (everything is in Python or PostgreSQL), making the system more sustainable for the future. NSB has been/is now being used in several paleobiologic studies (e.g. Hannisdal et al., 2012; Lazarus et al., 2014, several groups and studies in prep.). Access to NSB online requires only a free account which can be obtained from the authors.

Important new data types have been added, particularly the >27k stratigraphic events used to create age models for most holes, together with nearly 2k event definitions. In order to make effective use of these geochronologic extensions to NSB, a new open source implementation - NSB_ADP - of the ADP (Age Depth Plot) program (Lazarus, 1992; Bohling, 2005) has been created that rectifies several problems with these earlier software packages (see figure of sample output). For example, NSB_ADP includes all significant features of both prior implementations, including the ability (from the original ADP) to plot paleomagnetic polarity patterns and core

recovery vs depth, and (from the Chronos version) to download the event data directly from the NSB (previously Chronos Neptune) database, although NSB_ADP can also read data from local files. NSB_ADP uses the powerful 'matplotlib' Python data plotting library as its backend, which supports high quality graphic output in multiple standard formats. NSB_ADP is available in both a stand-alone clickable app version (easy to install, available for OS X [and soon Windows], but not modifiable by the end user) and as original, modifiable source code. The latter works on any OS and can be started from the command line, but requires careful installation of dependent Python packages prior to first use. Either version can be obtained from the authors, and an online repository version will soon be made available.

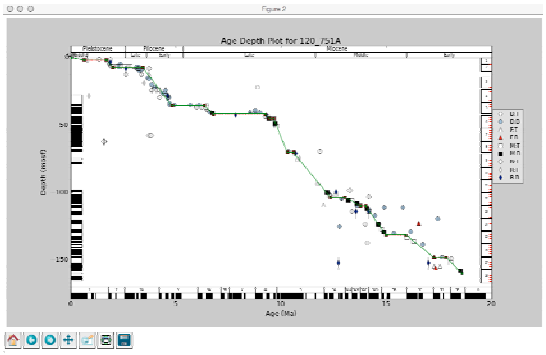

It is hoped that NSB and NSB_ADP will provide an improved platform for future research in marine micropaleontology and paleoceanography.

IODP

Reefs, drifts and carbonate slopes - Integrating seismic and core data on the North West Shelf of Australia

L. REUNING[1], S. BACK[1] AND EXP. 356 SCIENTISTS

[1]RWTH Aachen University, EMR-

The distally steepend carbonate ramp of the North West Shelf of Australia (NWS) equals in size the carbonate systems of the Bahamas or the Persian Gulf and forms an important template for the interpretation of ancient ramp systems. The NWS stretches between ~13° and 21°S and is situated at the transition between the tropical and sub-tropical realm. Carbonate sedimentation on this shelf is strongly controlled by regional oceanography, which is dominated by the south-flowing, warm, low salinity Leeuwin Current and the Indonesian Throughflow. The sediment distribution on the sea-floor is well documented, but information on the Neogene to Pleistocene sedimentary section of the NWS was until recently limited to cuttings from industry wells and geophysical data. A 2D/3D seismic interpretation tied to industry well data from the Browse Basin on the northern part of the NWS suggests that changes in the Indonesian throughflow, third-order eustatic variations and subsidence are important for reef and sediment drift development during the Neogene (Rosleff-Soerensen et al., 2012; 2016). Recently, IODP Expedition 356 (August-September 2015) cored the continental margin sequence of the southern and central part of the NWS to investigate its depositional history since the middle Miocene. The upcoming IODP Expedition 363 (September to November 2016) is planning to drill two sites in the northern part of the NWS. Data collected during these expeditions will allow for the first time to integrate core data with extensive 2D and 3D seismic-reflection surveys allowing regional and detailed geomorphological studies of the carbonate system on a basin scale.

References:

Rosleff-Soerensen, B., Reuning, L., Back, S. & Kukla, P. (2012): Seismic geomorphology and growth architecture of a Miocene barrier reef, Browse Basin, NW-Australia. Marine and Petroleum Geology, Vol. 29-1, pp.233-254; Elsevier, Amsterdam.

Rosleff-Soerensen, B., Reuning, L., Back, S. and Kukla, P. A. (2016), The response of a basin-scale Miocene barrier reef system to long-term, strong subsidence on a passive continental margin, Barcoo Sub-basin, Australian North West Shelf. Basin Res, 28: 103–123. doi:10.1111/bre.12100

ICDP

Long term tectonic and paleoclimatic history of Lake Issyk-Kul, Kyrgyzstan - preliminary results from an ICDP-related deep seismic pre-site survey campaign

REUSCH, A.[1,2], SPIEß, V.[2], KEIL, H.[2], SAUERMILCH, I.[4], MOLDOBAEV ASAT[5], OBERHÄNSLI, H.[3], GEBHARDT, C.[4], ABDRAKHMATOV, K.[5]

[1]ETH Zürich, Geological Institute, Sonneggstrasse 5, 8092 Zürich, Switzerland
[2]University of Bremen, Faculty of Geosciences, Klagenfurter Straße, 28359 Bremen, Germany
[3]Naturhistorisches Museum, Berlin, Germany
[4]Alfred-Wegener Institut für Polar- und Meeresforschung, 27568 Bremerhaven, Germany
[5]Institute of Seismology, NAS KR, Bishkek, Kyrgyztan

Lake Issyk-Kul in Kyrgyzstan became a potential target for ICDP drilling through a group of scientists who applied for and organized an ICDP workshop in 2011 in Baet/Kyrgyzstan (Oberhänsli and Molnar, 2012). Lake Issyk-Kul, located in the Kyrgyz Republic, is one of the deepest and largest lakes in the world. It occupies a deep basin within the Tien Shan mountain range in Central Asia, which is presently one of the Earth's tectonically most active intra-continental mountain belts. Up to 3500 m of terrestrial sediments have been deposited in the basin, including glacial, fluvioglacial, fluvial and lacustrine formations (Fortuna, 1993), of which the oldest are believed to date back to Oligocene – Miocene times (Abdrakhmatov et al., 1993; Chedia, 1986).

Lake sediments can act as important "recorders" of the regional processes active during and after their deposition. Lake Issyk-Kul's sediments likely comprise a promising record of tectonic events and past climate changes in the region, potentially ranging back to Miocene times. This sedimentary record is the base of a planned investigation of the International Continental Drilling Program (ICDP), with the aim to investigate the past climate conditions and the tectonic history of the region. In order to address these scientific objectives, ideal drilling sites are searched, with the aim to drill through a potentially complete, undisturbed sediment section representing the maximum amount of time. In 1997 and 2001, single-channel seismic sparker data were acquired by the Renard Centre of Marine Geology in Gent (RCMG) (DeBatist et al., 2002; Gebhardt et al., 2016). In order to gain a better understanding of the

deeper lake basin, a multichannel airgun seismic survey was organized in 2013, jointly funded by the Museum für Naturkunde Berlin, the University of Bremen, the AWI Bremerhaven, Centre of Seismology, Bishkek, Research Group Marine Technology/Environmental Research, Geosciences, Bremen and the ICDP coordination in May 2013. With these multichannel seismic data, it is possible to investigate the lake history further back in time, including reconstruction of the tectonic evolution, paleoseismic activity as well as climatic indications such as water level fluctuations.

First experiments of processing and interpreting of the multichannel seismic data (Fig. 1) were carried out as part of smaller projects at the University of Bremen, but further thorough and patially sophisiticated processing (multiple/noise suppression) and interpretation work is needed to identify deeper sediment packages and potentially the basal reflector of the deep lake basin. This is subject to a new project at the University of Bremen (Research Group Marine Technology – Environmental Research), presented at the IODP/ICDP Colloquium 2016.

References:
Abdrakhmatov, K. E., Turdukulov, A. T., and Khristov, E. B., 1993, Detailed seismic zoning of the Issyk-Kul basin.: Ilim Publications. Frunze.
De Batist, M., Y. Imbo, P. Vermeesch, J. Klerkx, S. Giralt, D. Delvaux, V. Lignier, C. Beck, I. Kalugin, and K. E. Abdrakhmatov (2002), Bathymetry and Sedimentary Environments of Lake Issyk-Kul, Kyrgyz Republic (Central Asia): A Large, High-Altitude, Tectonic Lake, in Lake Issyk-Kul: Its Natural Environment, edited by J. Klerkx and B. Imanackunov, pp. 101-123, Springer Netherlands.
Chedia, O. K., 1986, Morphology and neotectonics of the Tien Shan: Ilim Publications. Frunze, p. 313.
Fortuna, A. B., 1993, Detailed seismic profiling of the Issyk-Kul depression.: Ilim Publications.
Gebhardt, C.A., Naudts, L, De Mol, L., Klerkx, J., Abdrakhmatov, A., Sobel, E.R., De Batist, M., 2016, An extended history of high-amplitude lake-level changes in tectonically active Lake Issyk-Kul (Kyrgyzstan), as revealed by high-resolution seismic reflection data, Climat of the past, discussion, doi:10.5194/cp-2016-3
Oberhänsli, H., and Molnar, P., 2012, Climate Evolution in Central Asia during the Past Few Million Years: A Case Study from Issyk Kul: Sci. Dril., v. 13, p. 51-57.

IODP

Advanced seismic imaging for ground water modelling at the Near Jersey Shelf

M.RIEDEL[1], S. REICHE[2], S. BUSKE[1]

[1]TU Bergakademie Freiberg, Institut für Geophysik und Geoinformatik, Gustav-Zeuner-Straße 12, 09599 Freiberg
[2]RWTH Aachen, Institute for Applied Geophysics and Geothermal Energy, Mathieustraße 10, 52074 Aachen

Understanding the flow and distribution of submarine fresh water can be achieved by three-dimensional numerical simulations of seaward groundwater discharge. An important prerequisite for such an experiment is the construction of a realistic hydrogeological model by integrating various geophysical data. Structural and stratigraphic information of the subsurface can be obtained with high accuracy from reflection seismic images. In the work presented here, we therefore focus on deriving a structural image from the seismic profile Oc270 line 529 that was acquired prior to IODP Expedition 313. The line crosses three drilling locations (M27, M28, M29) at which pore water samples from the shelf area were recovered (Mountain et al., 2010). The images that are obtained from the seismic data will form the basis of a 3D hydrogeological model to be used in a later stage of the project for simulating groundwater flow.

In this context, we reprocessed the seismic line with particular emphasis on obtaining accurate depth information of dominant reflectors in the upper 1000 meters of the shelf. For this purpose, we iteratively built an accurate velocity model by utilizing different updating techniques ranging from one-dimensional RMS velocity inversion to layer-stripping tomography approaches. Furthermore, we applied and assessed various seismic imaging techniques, including conventional post- and pre-stack time migrations as well as more advanced focusing pre-stack depth migration techniques (Hlousek et al., 2015), which represent the most powerful tools among the imaging methods used in this study.

In this way, we were able to assess the accuracy of the different techniques and to examine the benefits of advanced imaging technology for obtaining reliable reflector depths in a marine environment. Finally, the resulting images provide the structural foundation that is required for subsequent groundwater flow simulations.

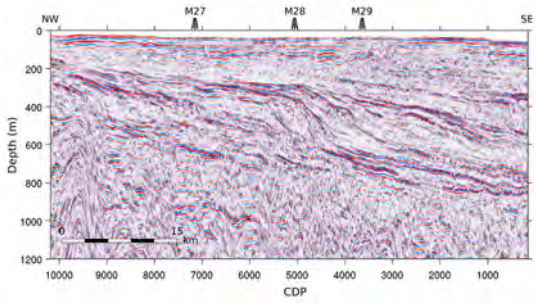

Figure 1: Seismic reflection image of profile Oc270 line529.

References:
Mountain, G., Proust, J-N., and the Expedition 313 Science Party (2010) The New Jersey Margin Scientific Drilling Project (IODP Expedition 313): Untangling the Record of Global and Local Sea-Level Changes. Scientific Drilling, No. 10, p. 26-34.
Hlousek, F., Hellwig, O., and Buske, S. (2015) Improved structural characterization of the Earth's crust at the German Continental Deep Drilling Site using advanced seismic imaging techniques, J. Geophys. Res. Solid Earth, 120, 6943-6959.

IODP

Mechanics of terrestrial peak-ring crater formation inferred from Expedition 364 (Chicxulub)

U. RILLER

Universität Hamburg, Institut für Geologie, Bundesstrasse 55, 20146 Hamburg (ulrich.riller@uni-hamburg.de)

Crater floors of large terrestrial impact structures, also known as impact basins, are largely flat and dissected by two or more morphological rings. Outstanding problems in our knowledge of large-meteorite impact cratering, and which are the prime structural geological objectives of Expedition 364 "Drilling the K-Pg Impact Crater" and this proposal, concern the mechanism of peak ring formation and causes for the existence of flat floors of large impact craters. These objectives will be addressed by the analysis of Expedition 364 drill core in terms of identifying (1) rock type and impact-induced deformation mechanisms, (2) kinematics of deformation and (3) identification of mechanisms resulting in mechanical weakening of target

rock. Moreover, Expedition 364 drill core will be investigated for (4) structural evidence of long-term relaxation of crust underlying the crater floor. To date, evidence for crustal relaxation of impact basins comes only from remote sensing analyses of respective basins from the Moon, Mercury and Mars and, thus, awaits ground truth from large impact craters on Earth.

Following macroscopic inspection, Expedition 364 drill core will be analysed with optical microscopy, notably quantitative image analysis applying an in-house image analysis work flow. The work flow uses an automated seeded region growing algorithm, which is based on variance analysis of five or more RGB images. The workflow is implemented in the open-source Geographic Information System (GIS) software SAGA (System for Automated Geoscientific Analyses). Image analysis will be complemented by X-ray micro-tomography (CT) scanning. 3D mineral fabric images of drill core segments will likely be analysed using the Petra III Synchrotron at the DESY (Hamburg) and a high-resolution micro CT facility at the Geological Survey (GTK) of Finland in Espoo. The facility includes a high acceleration voltage µ-CT scanner (>350 kV) and detectors that can be combined with µ-XRF imaging technology and high-performance data processing computing units. The facility can reveal structural details down to 10 µm resolution of a given rock sample. The high acceleration voltage of this instrument is able to image large samples (i.e., drill core segments of up 10 cm length) containing dense solids, such as metals.

Microstructural analysis of Expedition 364 drill core will be complemented by optical and acoustic televiewer data of the drill hole and by a microstructural analysis of the granite breccia of the Sudbury impact structure, Canada. This rock unit is lithologically akin to the basement rocks expected to be probed in Expedition 364 and occupies the equivalent position to the drilled rocks at Chicxulub, i.e., target rock below the peak ring. Comparison of microstructure in drill core from both impact structures promises to put the 1D structural information from Expedition 364 drill core into a more comprehensive framework of large impact cratering. Structural data gleaned from the proposed project promise to refine numerical models of impact cratering, petrophysical rock properties for seismic imaging and hydrothermal processes addressed by other working groups of Expedition 364.

IODP

Pleistocene seawater density reconstruction in the northeast Atlantic and its implication for cold-water coral carbonate mounds

ANDRES RÜGGEBERG[1,2,3,*], SASCHA FLÖGEL[2], WOLF-CHRISTIAN DULLO[2,**], JACEK RADDATZ[2,4], VOLKER LIEBETRAU[2]

[1] Unit of Earth Sciences, Dept. of Geosciences, University of Fribourg, Chemin du Musée 6, CH-1700 Fribourg, Switzerland.
[2] GEOMAR Helmholtz Centre for Ocean Research Kiel, Wischhofstr. 1-3, D-24148 Kiel, Germany.
[3] Renard Centre of Marine Geology, Ghent University, Krijgslaan 281, S8, B-9000 Gent, Belgium.
[4] Present address: Institute of Geosciences, Goethe University Frankfurt, Altenhöferallee 1, D-60438, Frankfurt am Main, Germany

[*] Corresponding author: andres.rueggeberg@unifr.ch
[**] Presenting author: cdullo@geomar.de

Carbonate build-ups and mounds are impressive biogenic structures throughout Earth history. In the recent NE Atlantic, cold-water coral (CWC) reefs form giant carbonate mounds of up to 300 meters of elevation. The expansion of these coral carbonate mounds is paced by climatic changes during the past 2.7 Million years. Environmental control on their development is directly linked to controls on its main constructors, the reef-building CWCs. Seawater density has been identified as one of the main controlling parameter of CWC growth in the NE Atlantic [Dullo et al., 2008]. One possibility is the formation of a pycnocline above the carbonate mounds, which is increasing the hydrodynamic regime, supporting elevated food supply and possibly facilitating the distribution of coral larvae.

The aim of this study is 1) to test regionally-calibrated equations to reconstruct seawater densities following the method of Lynch-Stieglitz et al. [1999a, b] and based on this 2) to test whether CWC mound growth during the past also occurred in similar seawater densities as today. To answer these questions, we analyzed sediment cores and reconstructed seawater densities from two different and well-studied carbonate mounds; Propeller Mound of the Hovland mound province, northern Porcupine Seabight and Challenger Mound of the Belgica mound province, eastern Porcupine Seabight.

The potential to reconstruct past seawater densities from stable oxygen isotopes of benthic foraminifera has been further developed: a regional equation gives reliable results for three different settings, *peak interglacials* (e.g., Holocene), *peak glacials* (e.g., Last Glacial Maximum), and *intermediate* setting (between the two extremes). Seawater densities are reconstructed for two different NE Atlantic CWC carbonate mounds in the Porcupine Seabight indicating that the development of carbonate mounds is predominantly found at a seawater density range between 27.27 and 27.67 kg m^{-3} (sigma-theta (σ_Θ) notation). Comparable to present-day conditions, we interpret the reconstructed density range as a pycnocline serving as boundary layer, on which currents develop, carrying nutrition and possibly distributing coral larvae. The close correlation of CWC reef growth with reconstructed seawater densities through the Pleistocene highlights the importance of pycnoclines and intermediate water mass dynamics.

Furthermore, CWC reef formation and carbonate mound development in the NE-Atlantic is triggered by processes and dynamics of ocean gateways: 1) Mediterranean Outflow at the Strait of Gibraltar intensified 3.3–3.5 Ma leading to a gradual increase of bottom water densities [Hernández-Molina et al., 2014], and 2) the closure of the Isthmus of Panama around 2.7 Ma [Haug and Tiedemann, 1998] or at least the onset of the meridional overturning circulation resulted in an enhanced subsurface water transport to higher latitudes in the Atlantic lowering the extinction risk of deep-sea ecosystems [Henry et al., 2014]. The consequences of the gateway-processes established the necessary density contrast in water masses enabling active CWC reef growth in the Porcupine Seabight around that time [Foubert and Henriet, 2009; Raddatz et al., 2011].

Overall, CWC carbonate mound growth portrays prolific marine benthic ecosystem development and is linked to small changes in ambient bottom water characteristics (i.e. density). These results show that marine benthic ecosystems occupy very narrow and specific ecological niches, which are very sensitive and even at risk to the actual global environmental changes, such as bottom water warming and acidification. As a consequence, our findings have lead to a robust diagnostic key-tool for the interpretation of basin-wide sudden onset or shutdown of carbonate mound growth during Earth history [e.g., Wood, 1999].

The study received funding from the Deutsche Forschungsgemeinschaft (DFG) projects TRISTAN, ISOLDE, and INWADE (Du 129/37, Du 129/45 and Du 129/48). AR additionally received funding from FWO International Coordination Action COCARDE-ICA (G.0852-09.N), which he greatly acknowledges. This study is part of ESF Research Network Programme COCARDE-ERN, a European Research Network on carbonate mound research.

References:

Dullo, W.-Chr. et al. (2008) Cold-water coral growth in relation to the hydrography of the Celtic and Nordic European Continental Margin. MEPS 371:165–176.

Foubert, A., and J.-P. Henriet (2009), Nature and Significance of the Recent Carbonate Mound Record, p. 298, Springer-Verlag, Berlin, Heidelberg.

Haug, G.H., and R. Tiedemann (1998), Effect of the formation of the Isthmus of Panama on Atlantic Ocean thermohaline circulation, Nature 393:673–676.

Henry, L.-A., et al. (2014), Global ocean conveyor lowers extinction risk in the deep sea, Deep-Sea Research I 88:8–16.

Hernández-Molina, F.J., et al. (2014), Onset of Mediterranean outflow into the North Atlantic, Science 344(6189):1244–1250.

Lynch-Stieglitz, J., et al. (1999a), Weaker Gulf Stream in the Florida Straits during the Last Glacial Maximum, Nature 402: 644-648.

Lynch-Stieglitz, J., et al. (1999b), A geostrophic transport estimate for the Florida Current from the oxygen isotope composition of benthic foraminifera, Paleoceanography 14(3):360–373.

Raddatz, J., et al. (2011), Paleoenvironmental reconstruction of Challenger Mound initiation in the Porcupine Seabight, NE Atlantic, Marine Geology 282:79–90.

Wood, R. (1999), Reef Evolution, 414 pp., Oxford University Press, Oxford, New York.

IODP

Izu-Bonin Tephras – Preliminary results from Expeditions 350 & 352

J.C. SCHINDLBECK[1], S. KUTTEROLF[1]

[1]GEOMAR Helmholtz Zentrum für Ozeanforschung Kiel, Wischhofstr. 1-3, 24148 Kiel

The Izu-Bonin-Mariana arc (IBM) ranges from Izu Peninsula (Japan) to Guam (USA) over a distance of 2800 km. It is the result of the subduction of the Pacific plate over the last 52 My (Stern et al., 2003). In the past it has been the target of several, individual, drilling projects complemented in 2014 by three closely related IODP Expeditions within the multiphased IBM drilling project.

Under the umbrella of the whole IBM project and the cross-cutting goals of IODP Expeditions 350 and 352 our own project focuses on the tephra layers from highly explosive eruptions that were sampled during these cruises.

Two sites were drilled during IODP Expedition 350: (1) Site U1436 was drilled in the forearc as a geotechnical hole in preparation for the proposed deep drilling at Site IBM-4. (2) Site U1437 lies about 160 km WSW of Site U1436 in a basin between two Izu reararc seamount chains (Manji and Enpo chains). At Site U1436 a nearly complete record of Late Pleistocene forearc sedimentation has been recovered that is strongly influenced by frontal arc explosive volcanism (Expedition 350 Scientists, 2015).

IODP Expedition 352 recovered 1.22 km of igneous basement and 0.46 km of overlying sediment at four sites (Expedition 352 Scientists, 2015). The cored volcanic rocks provide diverse, stratigraphically controlled suites of forearc basalts, related to decompression melting as mantle rose to fill the space created by the initial sinking of the Pacific Plate, and boninite generated slightly later during earliest arc development. The igneous basement is overlain by Late Eocene to Recent sediments. Three drill sites (Sites U1439-U1441) are located in small fault-controlled sediment basins up to several hundred meters thick, whereas one site (U1442) was positioned on thin sediments overlying a fault-controlled basement high. Three phases of highly explosive volcanism (latest Pliocene to Pleistocene; Late Miocene to earliest Pliocene; Oligocene) are represented by 132 observed, graded airfall tephra layers, which are correlative between the four drill sites. Felsic ash layers are abundant at Sites U1439 and U1440 (larger sediment ponds), compared to more mafic ash layers at Sites U1441 and U1442 (smaller basins).

It is our aim to establish a most complete arc-wide tephrostratigraphy that better classifies the origin, style and frequency of larger explosive eruptions from the Izu-Bonin arc, but we also want to decipher the influences by distal widespread tephras from other regions as for example Japan. This will extend the former, locally restricted, investigations of Izu-Bonin´s geochemical and volcanological evolution based on tephra layers to a widespread temporal and spatial provenance study of the explosive volcanism in that entire region incorporating also correlations between tephra layers from older DSDP/ODP and our recent IODP sites. Provenance analyses will identify tephra source regions at the arc, thus facilitating to constrain temporal variations in the tephra productivity along the arc. These objectives are complemented by studying the emplacement and origin of marine tephra layers that are deposited from flow rather than fall

processes. Finally, we want to study cyclicities that have been observed in marine ash records on a range of time scales, especially at the ring of fire.

The essential prerequisite for this work is the detailed chemical characterization of ~600 discrete tephra layers we have sampled during Expedition 350, covering an age range from Pliocene to Quaternary. These are complemented by ~150 tephra layers we recovered during Expedition 352 extending the investigated time interval to the Oligocene.

Here we present the first results of post-cruise work. We analysed ~650 tephra samples for their major and >350 samples for trace element compositions. The establishment of a compositional database is the prerequisit and the fundament for all further studies and the first step to achieve our project goals. First provenance analysis reveal a mixture of fallout tephras from, at least, the larger source areas of the Honshu and IBM arcs; the detailed regional origin will be determined in the next steps.

References:
Reagan, M.K., Pearce, J.A., Petronotis, K.E., and the Expedition 352 Scientists (2015) Proceedings of the International Ocean Discovery Program, Expedition 352: Izu-Bonin-Mariana Fore Arc: College Station, TX (International Ocean Discovery Program), http://dx.doi.org/10.14379/iodp.proc.352.2015

Stern, R.J., Fouch, M.J., and Klemperer, S., 2003. An overview of the Izu-Bonin-Mariana subduction factory. In Eiler, J. (Ed.), Inside the Subduction Factory. Geophysical Monograph, 138:175–222. http://dx.doi.org/10.1029/138GM10

Tamura Y., Busby C.J., Blum P., and the Expedition 350 Scientists (2015) Proceedings of the International Ocean Discovery Program, Expedition 350: Izu-Bonin-Mariana Rear Arc: College Station, TX (International Ocean Discovery Program), http://dx.doi.org/10.14379/iodp.proc.350.2015.

ICDP

The PALEX project - Paleohydrology and Extreme Floods from the Dead Sea ICDP Core

M. J. SCHWAB[1], M. AHLBORN[1], I. NEUGEBAUER[1], B. PLESSEN[1], R. TJALLINGII[1], Y. ENZEL[2], J. HASAN[3], A. BRAUER[1] AND PALEX SCIENTIFIC TEAM

[1]GFZ German Research Centre for Geosciences, Section 5.2 Climate Dynamics and Landscape Evolution, Telegrafenberg, Potsdam
[2]The Hebrew University of Jerusalem (HUJ), Institute of Earth Sciences, Edmond Safra Campus, Givat Ram, Jerusalem
[3]Al Quds University (AQU), Department of Earth and Environmental Sciences, Abu-Dies, P.O. Box: 20002, Jerusalem

Within the framework of the DFG Trilateral program / SPP1006 research project PALEX (Paleoclimate in the Eastern Mediterranean Region – Levante: Paleohydrology and Extreme Flood Events) sedimentologists, hydrologists and geochemists from Germany, Israel and Palestine are carrying out joint research including experts in the fields of sedimentology (e.g. varve micro-facies, lacustrine evaporitic and clastic sedimentology), geochemistry (fresh waters, brines), modern hydrology, and hydro-climatology of floods.

The reconstruction of the hydrological evolution of the Dead Sea watershed is crucial for anticipating possible future changes in this sensitive region for which models predict enhanced aridity associated with future global warming, which would impact millions of people inhabiting these regions. Long cores recovered by the ICDP DSDDP (Dead Sea Deep Drilling Program) drilling from the deep basin of the Dead Sea comprise an exceptional archive to reconstruct the natural hydro-climatic variability during the last 200 kyrs in this region Neugebauer et al. 2014, 2015 & 2016). For the first time, we have sediment archives at hand recording periods of rapid lake level falls like e.g. during the last deglaciation that are not represented in sediment outcrops.

PALEX will particularly focus on the role of extreme hydro-meteorological events like flash floods and their impact on the sedimentary regime (Fig.1). We will investigate changes in frequency and magnitude of floods and their possible relation of the occurrence of extremes to long and short-term climatic fluctuations in this region. A comparison of the new ICDP DSDDP sediment cores from the deep basin will result in a new level of interpreting sediment sections for comprehensive reconstructing of the late Quaternary climatic variability in the Levant. Analyses of several down-core sediment sequences from the lake center will be complemented by precise lake stage determination during the coeval deposition of specific sediments at the present day lake margins.

Fig.1 A sediment plume of silt with some clay floating and spreading over the Dead Sea during the first minutes of a fresh water flood entering the Dead Sea from the western tributary of Nahal Darga in December 1995 (photo: Y. Enzel, HUJ).

We will focus at first on intervals represented in cores and exposures during periods for which lake level reconstructions exist. Laminae thickness and their specific geochemistry during either lake level rising or falling will support data interpretation for older periods for which the deep lake sediment record core is the sole source of information. Parallel monitoring of modern hydroclimatology, floods, and sediment plumes will allow quantification and calibration of climatic and hydrological

processes that control sediment flux into the Dead Sea basin.

To achieve the targeted objectives we will:

(1) establish long, high-resolution time series of flood events at annual resolution,

(2) trace the sources and modes of transport and deposition as well as volumes of fine-detrital sediments,

(3) determine and compare sources and amounts of inflowing waters from the northern (Jordan River), eastern and western sources with those from the southern watershed of Nahal Arava drainage,

(4) link complementary flood monitoring and hydrological modeling with sediment proxy data. The monitoring systems will contribute to the hydrological regional cooperation and data-base.

References:

Neugebauer, I., Brauer, A., Schwab, M.J., Waldmann, N.D., Enzel, Y., Kitagawa, H., Torfstein, A., Frank, U., Dulski, P., Agnon, A., Ariztegui, D., Ben-Avraham, Z., Goldstein, S.L. and Stein, M., (2014): Lithology of the long sediment record recovered by the ICDP Dead Sea Deep Drilling Project (DSDDP). Quaternary Science Reviews 102, 149-165.

Neugebauer, I., Brauer, A., Schwab, M. J., Dulski, P., Frank, U., Hadzhiivanova, E., Kitagawa, H., Litt, T., Schiebel, V., Taha, N., Waldmann, N. D., DSDDP Scientific Party (2015): Evidences for centennial dry periods at ~ 3300 and ~ 2800 cal. yr BP from micro-facies analyses of the Dead Sea sediments. - Holocene, 25, 8, 1358-1371.

Neugebauer, I., Schwab, M. J., Waldmann, N. D., Tjallingii, R., Frank, U., Hadzhiivanova, E., Naumann, R., Taha, N., Agnon, A., Enzel, Y., Brauer, A. (2016): Hydroclimatic variability in the Levant during the early last glacial (~ 117–75 ka) derived from micro-facies analyses of deep Dead Sea sediments. - Climate of the Past, 12, 1, 75-90.

ICDP

Isotropic versus anisotropic velocity model around the COSC-1 borehole (Sweden), derived from a combined surface and borehole seismic survey

H. SIMON[1], F. KRAUß[2], S. BUSKE[1], R. GIESE[2], P. HEDIN[3], C. JUHLIN[3]

[1]Institute of Geophysics and Geoinformatics, TU Bergakademie Freiberg

[2]Centre for Scientific Drilling, Helmholtz Centre Potsdam GFZ German Research Centre for Geosciences

[3]Department of Earth Sciences, Uppsala University

The ICDP project COSC (Collisional Orogeny in the Scandinavian Caledonides) focuses on the mid Paleozoic Caledonide Orogen in Scandinavia in order to better understand orogenic processes, from the past and in recent active mountain belts (Gee et al., 2010). The Scandinavian Caledonides provide a well preserved example of a Paleozoic continent-continent collision. Surface geology in combination with geophysical data provide control of the geometry of parts of the Caledonian structure, including the lowermost allochthon, the underlying autochthon and the shallow W-dipping décollement surface that separates the two. This surface is closely associated with a thin layer of Cambrian black shales. The structure of the basement underneath the décollement is highly reflective and apparently dominated by mafic sheets intruded into either late Paleoproterozoic granites or Mesoproterozoic volcanic rocks and sandstones. The COSC project investigates the structure and physical conditions of these units, in particular the Seve Nappe Complex (SNC, "hot" allochthon), Lower Allochthon and the underlying basement with two approximately 2.5 km deep fully cored boreholes in western Jämtland (central Sweden).

In 2014 the COSC-1 borehole was successfully drilled (Lorenz et al., 2015) through the SNC and the underlying mylonites to ~2.5 km depth near the town of Åre (ICDP drill site 5054-1-A). The SNC (mainly gneisses) is part of the Middle Allochthon and has been ductilely deformed and transported during the collisional orogeny that formed the Scandinavian Caledonides. Right after drilling, a major seismic survey was conducted in and around the COSC-1 borehole which comprised both seismic reflection and transmission experiments. Combined with core analysis and downhole logging, the survey will allow extrapolation of structures away from the borehole. The survey consisted of three experiments: 1) a high-resolution zero-offset Vertical Seismic Profile (VSP) (Krauß et al., 2015), 2) a multi-azimuthal walkaway VSP in combination with three long offset surface receiver lines (this study), and 3) a limited 3D seismic survey (Hedin et al., 2015).

Data from the multi-azimuthal walkaway VSP experiment and the long offset surface lines have been used to derive a detailed velocity model around the borehole. The source points were distributed along three profile lines centered radially at the borehole. For the central part, up to 2.5 km away from the borehole, a hydraulic hammer source (Vibsist) was used, hitting the ground for about 20 s with a linear increasing hit rate. For the far offset shots, up to 5 km, explosive sources were used. The wavefield of both source types was recorded in the borehole using an array of 15 three-component receivers with a geophone spacing of 10 m. This array was deployed at seven different depth levels during the survey. At the same time the wavefield was also recorded at the surface by 180 standalone three-component receivers placed along each of the three up to 10 km long lines, as well as with a 3D array of single-component receivers in the central part of the survey area around the borehole.

The first arrival times for each line were inverted separately using a tomographic approach (Zhang and Toksöz, 1998) to obtain isotropic velocity models for different azimuths around the borehole COSC-1. The comparison of calculated first arrival times from these tomography results (mainly horizontally traveling rays) and from a 1D velocity function calculated from the zero-offset VSP (mainly vertically traveling rays) revealed clear differences in vertical (lower) and horizontal (higher) velocities. On the one hand, the tomography results provide a good fit of the first arrival times in the surface data and for far offset borehole data (due to the rays being closer to horizontal at far offsets), while the calculated first arrivals from the tomography model are too early for the zero-offset data (Fig. 1). On the other hand, the model derived from the zero-offset data provide a good fit of the first arrivals in the zero-offset data (as expected), while the calculated first arrivals from this model are too late for the surface data and far offset borehole data (Fig. 1).

Due to the observed differences between vertical and horizontal velocity a 1D VTI (transversely isotropic with vertical axis of symmetry) model was constructed using the P-wave velocity function from the zero-offset VSP (Fig. 2, top) and homogeneous Thomson parameters of $\delta = 0.3$ and $\varepsilon = 0.03$.

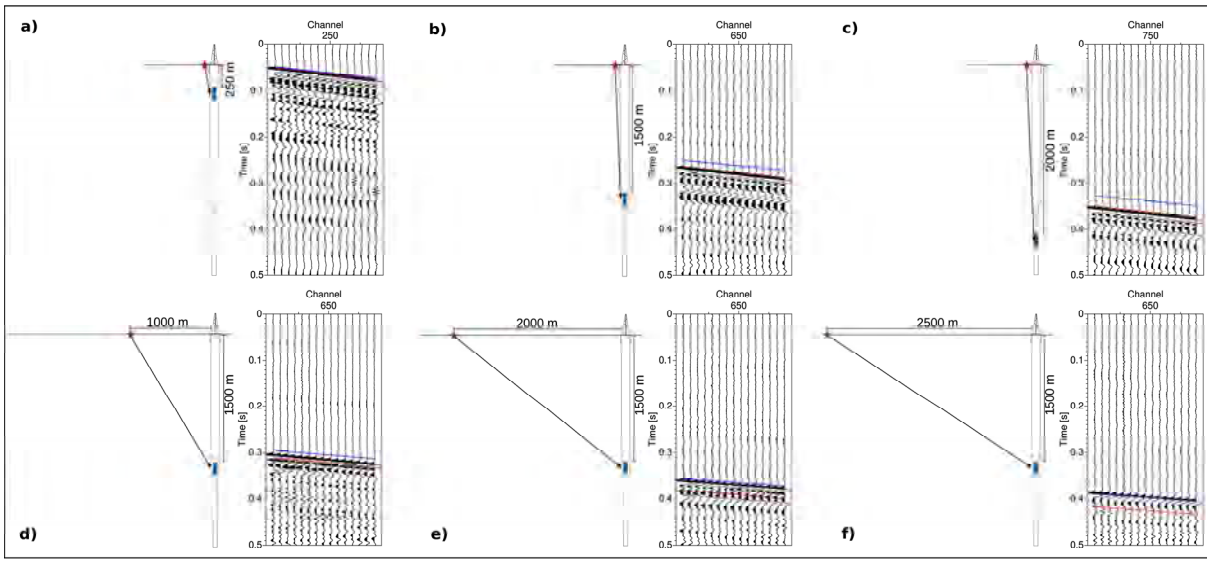

Fig. 1: Shot gathers from borehole data with calculated first arrival times for zero-offset velocity model (red) and from tomography using only surface recordings (blue). a)-c) Increasing vertical source-receiver offset. d)-f) Increasing horizontal source-receiver offset.

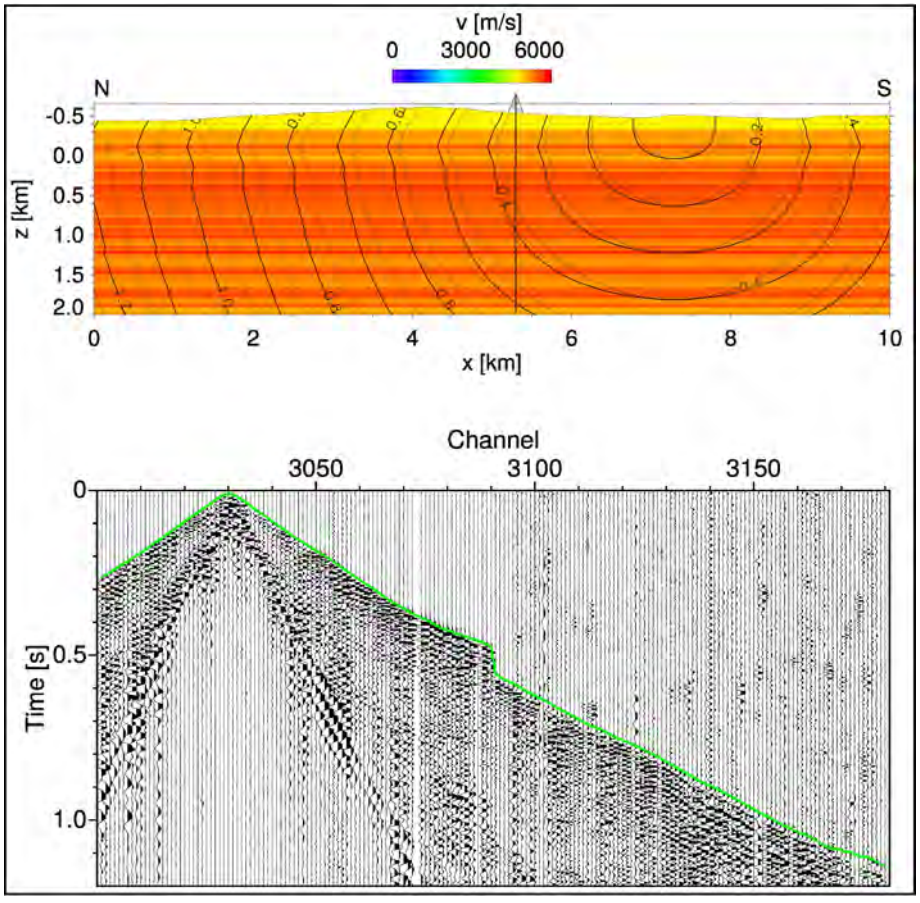

Fig. 2: Traveltimes calculated for VTI velocity model (ε = 0.03, δ = 0.3). Top: Velocity model from zero-offset VSP overlain by anisotropic (solid) and isotropic (dotted) traveltimes for one shot location. Bottom: Surface data shot gather with calculated first arrival times for the anisotropic velocity model (green).

The latter was derived from velocity measurements on a calc-silicate gneiss sample from the COSC-1 core (Wenning, 2015). The first arrival times from this model were calculated (Fig. 2, top) using an anisotropic eikonal solver (Riedel, 2015). With this relatively simple anisotropic velocity model a good fit for both the surface and borehole first arrival times (Fig. 2, bottom) could be achieved.

The calculated traveltimes from the obtained anisotropic model will serve as the basis for ongoing application of imaging approaches like pre-stack depth migration techniques. The results of our investigations will be high-resolution images of the fine-scale structures (including lithological boundaries, steeply dipping fault segments, fracture sets, etc.) around the borehole. This information is vital not only for a reliable spatial extrapolation of the structural and petrophysical properties observed in the borehole away from it, but also for a thorough understanding of the tectonic and geodynamic setting, including but not limited to, the past and present stress regime.

References:

Gee, D. G., Juhlin, C., Pascal, C., & Robinson, P. (2010). Collisional Orogeny in the Scandinavian Caledonides (COSC). GFF, 132(1), 29–44.

Hedin, P., Almqvist, B., Berthet, T., Juhlin, C., Buske, S., Simon, H., Giese, R., Krauß, F., Rosberg, J. E., Alm, P. G. (2015). 3D reflection seismic imaging at the 2.5 km deep COSC-1 scientific borehole, central Scandinavian Caledonides. Tectonophysics, accepted.

Krauß, F., Simon, H., Giese, R., Buske, S., Hedin, P., Juhlin, C., Lorenz, H. (2015). Zero-Offset VSP in the COSC-1 borehole. Geophysical Research Abstracts, 17, EGU2015-3255.

Lorenz, H., Rosberg, J.-E., Juhlin, C., Bjelm, L., Almqvist, B. S. G., Berthet, T., Conze, R., Gee, D. G., Klonowska, I., Pedersen, K., Roberts, N. M. W., Tsang, C.-F. 2015. COSC-1 – drilling of a subduction-related allochthon in the Palaeozoic Caledonide orogen of Scandinavia. Scientific Drilling, 19, 1–11.

Riedel, M. 2015. Efficient computation of seismic traveltimes in anisotropic media and the application in pre-stack depth migration. PhD Thesis, TU Bergakademie Freiberg.

Wenning, Q. 2015. Physical rock property and borehole stress measurements from the COSC-1 borehole, Åre, Sweden. MSc Thesis, ETH Zürich.

Zhang, J, and Toksöz, M. 1998. Nonlinear refraction traveltime tomography. Geophysics, 63(5), 1762-1737.

ICDP

Preliminary Results from a Lake Nam Co Reconnaissance Seismic Survey in 2014 Preparing a new ICDP-related Pre-Site Survey in Summer 2016

VOLKHARD SPIESS[1], F. GERNHARD[1], G. DAUT[2], T. HABERZETTL[2], R. MÄUSBACHER[2], J. WANG[3], L. ZHU[3]

[1]Marine Technology and Environmental Research, Department of Earth Sciences, Bremen University, Klagenfurter Str., 28359 Bremen, Germany

[2]Physical Geography, Institute of Geography, Friedrich Schiller University Jena, Löbdergraben 32, 07743 Jena, Germany

[3]Institute of Tibetan Plateau Research, Chinese Academy of Sciences, Beijing 100101, China

Lake Nam Co, located on the central Tibetan Plateau at the intersection of the Westerlies and the Indian Ocean Summer Monsoon, is well suited to study the monsoonal regime over different time scales. High-resolution and continuous sedimentary records from the Tibetan Plateau are still rare and only few reach back to the Last Glacial Maximum. For Nam Co, numerous multiproxy studies unravel the regional paleoclimate and paleoenvironmental history for the past 24,000 years. These promising results demonstrate the potential of Lake Nam Co as a geoarchive, but nature, thickness and geologic time of the sediment fill have not yet been determined.

Therefore the Institute of Tibetan Plateau Research (Chinese Academy of Sciences) and the Universities of Bremen and Jena jointly carried out an airgun multichannel seismic survey at Nam Co in June/July 2014. As main equipment, a micro GI Gun(2 x 0.1 L) was used in conjunction with a 64 m long seismic streamer (32 channels/2 m spacing) to achieve deep signal penetration, to confirm a thick sediment infill and to prove the suitability for deep coring of several hundred meters. Although only few lines could be shot due to technical and weather issues, several lines particularly from the deepest part of the lake provide new insight.

Preliminary data processing and interpretation had revealed a well layered sediment cover of potentially >700 m in the center of the lake. Seismic facies appears to vary in a cyclic manner, indicating a coupling to climatically-driven changes in lake level and sediment delivery. From a comparison with the Holocene/Late Glacial sedimentary and seismic record, several similar units could be imaged. Furthermore, rapid sedimentation is confirmed from the continuous cover of growth faults and doming, and continuous sedimentation throughout glacial/interglacial cycles appears likely due to the absence of erosional unconformities.

Based on these preliminary results, an ICDP workshop proposal had been submitted early 2015. While this had not yet been funded, resubmission was encouraged, and we intend to include new seismic data to be collected in June 2016 to improve the quality of seismic mapping and interpretation and to ensure an optimum choice of sites for a workshop discussion. Resubmission of the workshop proposal is planned for late 2016.

In the course of an ongoing master thesis (F. Gernhardt), thorough data processing had been carried out and improved with respect to earlier stages. A well-stratified unit of ~10 m thickness in contact with the seafloor represents Holocene and late Glacial sedimentation formed by suspension flow resulting in a flattened seafloor. The underlying unit has a distinct topography of up to 15 m, and internal reflections appear partially truncated, and partially indicating a postsedimentary deformation. This in turn may represent glacial conditions with lake level drop and glacier advances, resulting in ice margin setting at the flanks of the modern lake. Glacial deformation of previously formed lake floor deposits may be the result, reaching down ~20 m. The unit beneath resembles a similar seismic facies as the modern lake cover, thus originating likely from a phase of lake level rise and widespread deposition of suspended material. A likely assignment of this appx. 30 m thick unit may be to the long-lasting marine isotope stage 5, which in turn would indicate sedimentation rate on the order of 40-60 cm/kyr over the last 125 kyr. Deeper reflection have been identified but not yet assigned to environmental settings.

While the lake clearly provides a unique chance for recording pateau environmental conditions far back into the Quaternary, spatial variability due to local tectonics and sediment distribution patterns require a better data

coverage and mapping before identifying suitable drill sites. This is planned for another 4-week survey campaign in June 2016 as part of an ongoing DFG funded ICDP project..

IODP

Early Cretaceous climate and South Atlantic opening in the Kiel Climate Model (AOGCM)

S. STEINIG[1], S. FLÖGEL[1], W. PARK[1], W. DUMMANN[2], P. HOFMANN[2], T. WAGNER[3], J. O. HERRLE[4]

[1]GEOMAR, Helmholtz Centre for Ocean Research Kiel, Wischhofstrasse 1-3, D-24148 Kiel, Germany
[2]Insitute of Geology and Mineralogy, University of Cologne, Zülpicher Str. 49a, D-50674 Cologne, Germany
[3]Sir Charles Lyell Centre, School of Energy, Geoscience, Infrastructure and Society, Heriot-Watt University, Edinburgh, EH14 4AS, UK
[4]Institute of Geosciences, Goethe-University Frankfurt, Altenhöferallee 1, D-60438 Frankfurt am Main, Germany

Paleoceanographic data for the Early Cretaceous (i.e. Aptian-Albian) greenhouse show large scale perturbations of the global ocean-climate system linked to severe changes in the marine carbon cycle (e.g. Jenkyns, 2010). At the same time the ongoing break-up of Gondwana and the associated opening of the South Atlantic and Southern Ocean led to the emergence of young ocean basins, characterised by vast shelf areas and limited circulation. Several studies relate these evolving basins and their restricted environments to periods of increased black shale formation and carbon burial (Trabucho-Alexandre et al., 2012; McAnena et al., 2013). Model results underline the importance of the opening South Atlantic, indicating that up to 16% of global carbon burial was deposited in a region covering only 1% of the global ocean surface (McAnena et al., 2013).

Within this project we target the question whether carbon burial in the Cretaceous South Atlantic influenced or even triggered global climate perturbations. In order to asses the timing and magnitude of carbon burial we use a combined approach of physical and biogeochemical modelling which is constrained by a set of new multiproxy geochemical data provided by project partners at the University of Cologne (see abstract of Dummann et al.).

Oceanic gateways, such as the Falkland and Walvis Ridge Gateways in the Cretaceous South Atlantic, excert an important influence on carbon burial in young ocean basins. This is because progressive gateway opening enhances supply and recycling of nutrients to and within the ocean basin and the exchange of water masses across the gateways, thereby controlling the production and preservation of organic matter across the basin.

In order to simulate the evolution of the Falkland Gateway we will use the "Kiel Climate Model" (KCM), a coupled Atmosphere-Ocean General Circulation Model, with different sets of South Atlantic geometry and bathymetry to assess their influence on the oceanic circulation. A box model is then used to generate a transient response of key biogeochemical cycles from the KCM time slices and allow for quantification of carbon burial in the basin at different phases of the opening.

In a first step we use the KCM under Early Cretaecous boundary conditions, representing the Aptian period including a modified geography, a reduced solar constant and a pCO_2 of 1200 ppm (Hong & Lee, 2012). First results for the open South Atlantic set-up show a global mean surface temperature of 23.4 °C, an enhanced hydrological cycle and a significantly stronger horizontal atmospheric circulation. Driven by these atmospheric fields, an intensified oceanic surface circulation in the tropical and subtropical region developed that supported high surface temperatures and low salinities, and a stable stratification of the shallow water column, preventing any deep convection. Modelling suggests that the global meridional overturning circulation was restricted to the upper 2000 m.

References:

Hong, S. K. and Lee, Y. I. (2012), Evaluation of atmospheric carbon dioxide concentrations during the Cretaceous, Earth and Planetary Science Letters, Volumes 327–328, pp. 23-28, ISSN 0012-821X

Jenkyns, H. C. (2010), Geochemistry of oceanic anoxic events, Geochem. Geophys. Geosyst., 11, Q03004

McAnena, A., Flögel, S., Hofmann, P., Herrle, J., Griesand, A., Pross, J., Talbot, H., Rethemeyer, J., Wallmann, K. and Wagner, T. (2013): Atlantic cooling associated with a marine biotic crisis during the mid-Cretaceous period, Nature Geoscience, Vol. 6(7), pp. 558-561

Trabucho-Alexandre, J., Hay, W. and De Boer, P. (2012): Phanerozoic environments of black shale deposition and the Wilson Cycle, Solid Earth, Vol. 3(1), pp. 29-42

ICDP

Deep seismic imaging of the offshore sector of the Campi Flegrei caldera: preliminary IODP site survey results from a low-frequency multichannel seismic investigation

L. STEINMANN[1], V. SPIESS[1], M. SACCHI[2] AND THE CAFE_2016 SCIENTIFIC PARTY

[1] Department of Geosciences, University of Bremen, Klagenfurter Strasse, D-28359 Bremen, Germany
[2] Institute for Coastal Marine Environment (IAMC), Italian Research Council (CNR), Calata Porta di Massa, Porto di Napoli, 80133 - Napoli, Italy

Caldera-forming eruptions are regarded as one of the most catastrophic natural events to affect the Earth's surface and human society. The partly-submerged Campi Flegrei caldera, located in southern Italy, belongs to the world's most active calderas and, thus, has received particular attention in scientific communities and governmental institutions. Therefore, it has also become subject to a joint approach in the IODP and ICDP programs.

The Campi Flegrei caldera covers an area of ~120 km² defined by a quasi-circular depression, partly onshore, partly offshore. It is still under debate whether the caldera formation was related to only one ignimbritic eruption namely the Neapolitan Yellow Tuff eruption at 15 ka, or, in case it is a nested-caldera system, together by the NYT and the Campanian Ignimbrite eruption at 39 ka. In the last decades, the Campi Flegrei caldera has been characterized by short-term episodes of unrest involving considerable ground deformation (uplift and subsidence of several meters), seismicity and increased temperature at fumaroles. Furthermore, long-term deformation can be observed in the central part of the caldera with uplift rates of several tens of meters within a few thousand years. Recently, it has been proposed that the long-term deformation may be related to caldera resurgence, while short-term uplift episodes are probably triggered by the injection of magmatic fluids into a hypothesized shallow hydrothermal system at ~2 km depth. However, both long-term and short term uplift could

be interpreted as eruption precursor, thereby posing high-concern for a future eruption, which would expose more than 1.5 million people living in the surroundings of the volcanic district to extreme volcanic risks.

Structural information of the deep subsurface (>300 m) is still scarce and mainly limited to low-resolution seismic refraction tomography, gravity or magnetic measurements. Hence, the deeper-seated structure of the Campi Flegrei caldera is still to a large extent unknown. Filling this knowledge gap is essential in order to fully understand the caldera system, its formation and evolution. It also provides a unique chance to image a caldera system in much greater detail within a water-saturated marine depositional environment than would be anywhere possible on land.

On our poster, we will present preliminary results from a semi-3D (~50 m profile spacing) low-frequency (20–200 Hz) multichannel seismic survey collected in February 2016 during a joint Italian-German expedition, which will complement the 2008 high resolution survey with R/V Urania (see Abstract Steinmann, Spiess, Sacchi). This deep-penetrating dataset will provide not-yet existing information on the deep-seated caldera geometry (down to 2 km sub-bottom depth), thereby reaching down to the ICDP target depth and maximum IODP drilling depth. In particular, the low-frequency seismic data have the potential to provide conclusive evidence on the formation history of the Campi Flegrei caldera, supporting either the existence of a single caldera structure or a nested-caldera complex formed by two subsequent collapses. Also, the dataset may allow for an imaging of the maximum vertical extent of the caldera fill, which is yet completely unknown. As the caldera depression provides significant accommodation space, the caldera fill represents a unique and high-resolution sedimentary archive of regional volcanic activity and earlier large-scale eruptions. Furthermore, we expect to gain additional knowledge on the hypothesized existence of a shallow hydrothermal system by imaging deep-seated fluid pathways (e.g. faults, fractures) as well as amplitude anomalies, which may indicate trapped fluids/gases.

Together with the previously acquired high-frequency multichannel seismic dataset from 2008, these data represent a comprehensive seismic database, which shall eventually be utilized for a renewal of the IODP Proposal 671-pre. For the proper processing and interpretation of these seismic data, we intend to start a follow-up DFG project. In turn we will use these results for the development of a full IODP drilling proposal, for which we intend to apply for a Magellan workshop to integrate with a group of internationally renowned scientists working on similar caldera settings. The long-term goal of this project is to prepare an IODP drilling campaign complementary and directly linked to ICDP, dedicated to improve our understanding of the nature of caldera forming volcanic activity in rifted back-arc basins.

ICDP

The shallow structure of the Campi Flegrei caldera: Insights from a semi-3D high-frequency multichannel seismic survey for a combined IODP/ICDP drilling approach

L. STEINMANN[1], V. SPIESS[1], M. SACCHI[2]

[1] Department of Geosciences, University of Bremen, Klagenfurter Strasse, D-28359 Bremen, Germany
[2] Institute for Coastal Marine Environment (IAMC), Italian Research Council (CNR), Calata Porta di Massa, Porto di Napoli, 80133 - Napoli, Italy

The Campi Flegrei caldera has been considered as one of the world's most active calderas, proven by recent episodes of unrest. A future eruption could expose more than 1.5 million people living in the surroundings of the volcanic district to extreme volcanic risks. Hence, it has received major scientific and societal interest. In recent years, the Campi Flegrei volcanic system has also become subject to a joint approach in the IODP and ICDP programs.

The Campi Flegrei caldera is situated within the Campi Flegrei volcanic field at the western border of the city of Naples in southern Italy. It covers an area of~120 km² located partly onshore, partly offshore. Despite ample research, a scientific consensus regarding the formation history of the Campi Flegrei caldera has not yet been reached. To date, it is still under debate whether the Campi Flegrei caldera was formed by one single ignimbritic eruption, namely the Neapolitan Yellow Tuff (NYT) eruption at 15 ka, or, in case it is a nested-caldera system, together by the NYT and the Campanian Ignimbrite (CI) eruption at 39 ka. Comprehending the genesis of the Campi Flegrei caldera is still a missing link in the understanding of the overall caldera system and dynamics. In the post-collapse stage, a broad dome developed in the center of the caldera as result of long-term uplift related to caldera resurgence. Furthermore, particularly the onshore topography of the Campi Flegrei area was strongly modified by at least 60 post-collapse eruptions mainly clustered within three volcanic epochs, at 15 – 9.5 ka (epoch I), 8.6 – 8.2 ka (epoch II) and 4.8 – 3.8 ka (epoch III). Recently, since the 1960s, the Campi Flegrei caldera seems to have been reawakening as demonstrated by short-term episodes of uplift, accompanied by seismicity and increased fumarolic activity. While long-term uplift is likely related to an inflation of a deeper magma chamber, these recent uplift phases are assumed to be triggered by the injection of magmatic fluids into a hypothesized shallow hydrothermal system at ~2 km depth.

During a joint Italian-German research expedition in 2008, a semi-3D grid (100-150 m profile spacing) of high-frequency (up to 1000 Hz) multichannel seismic data were acquired to support both the ongoing onshore ICDP (*CFDDP*) and a proposed offshore IODP drilling campaign (*IODP Proposal 671-pre*). Due to the implementation of specialized multichannel seismic processing, the data provide a superb signal-to-noise ratio and high vertical resolution (~1 m). The 3D aspect in combination with high resolution allows for a detailed analysis of the shallow subsurface structure (<200 m) of the submerged part of the Campi Flegrei caldera.

Volcanoclastic deposits and volcanic edifices could clearly be distinguished from marine sediments based on

their seismoacoustic characteristics. While the volcanic units exhibit reflection-free facies, chaotic reflection pattern, irregular bounding surfaces and a mounded external morphology, the marine units are of laminated nature with continuous reflections and parallel to subparallel reflection configuration. Using a seismostratigraphic approach, the ages of the defined units could be constrained.

For the first time, reflection seismic data showed evidence for the existence of a nested-caldera system formed by (at least) two collapses related to the NYT and CI eruptions. Its formation and temporal evolution in response to sea-level variations and tectono-volcanic activity over the past 39 ka is presented in a comprehensive 2D model.

As the signal penetration limit was around 39 ka, interpretation was mainly focused on the timespan after the NYT eruption at 15 ka, which was investigated in 3D. Major structural features such as an arc-shaped shallow NYT caldera fault with a maximum vertical displacement of ~75 m and a resurgent dome could be mapped in great detail. The NYT caldera collapse at ~15 ka created significant accommodation space in the intra-caldera area. Our results show that the NYT caldera is filled with on average ~61 m of marine sediment deposited between 15 and 8.6 ka. In the timespan from 8.6 to 3.7 ka, the depositional environment in the offshore sector of the Campi Flegrei caldera was mainly influenced by the development of a post-collapse resurgent dome in the intra-caldera area. As result of resurgence-related uplift exceeding the rate of sea-level rise, major unconformities developed and the accommodation space on top of the resurgent dome was significantly limited. Between 3.7 and 2 ka, an infralittoral prograding wedge developed in the coastal shallow water. Furthermore, coastal erosion took place in water depth of ≤20 m, leading to the formation of a local erosional unconformity. Since 2 ka, the coastal area of the Gulf of Pozzuoli has undergone post-Roman subsidence of 3-25 m. Consequently, accommodation space was created and a coastal prograding wedge has deposited.

Furthermore, our results suggest that the NYT caldera fault has acted as pathway for the post-collapse ascent of gases/fluids, probably originating from a previously hypothesized shallow hydrothermal system. The presence of shallow gas/fluid-rich patches south of the NYT caldera fault indicates the existence of a deeper fracture zone probably related to the Campanian Ignimbrite caldera collapse at ~39 ka. Moreover, we found evidence that the ascent has occurred relatively recently (<3.7 ka).

ICDP

New insights into driving forces of evolution in ancient Lake Ohrid obtained from the SCOPSCO deep drilling program

B. STELBRINK, E. JOVANOVSKA, T. HAUFFE, C. ALBRECHT, T. WILKE

Department of Animal Ecology and Systematics, Justus Liebig University Giessen, Heinrich-Buff-Ring 26-32, 35392 Giessen, Germany

The Balkan Lake Ohrid is the most outstanding European ancient lake with an extraordinary species richness and a high degree of endemism in several groups of organisms. The processes governing this biodiversity, however, are only poorly understood. Preliminary molecular phylogenetic studies of selected benthic animal groups in Lake Ohrid suggested that most of the endemic taxa evolved intra-lacustrine, and probably without major changes in diversification rates over time. Such results may indicate the absence of major catastrophic events affecting Lake Ohrid during its long geological history, and have, among others, inspired the ICDP campaign “Scientific Collaboration on Past Speciation Conditions in Lake Ohrid” (SCOPSCO) in Lake Ohrid. Accordingly, we aim to identify drivers of evolutionary changes and community turnovers in ancient Lake Ohrid by using age estimates derived from molecular-clock analyses of several extant invertebrate species and information on gastropod community structures across the lake, complemented by micro- and macrofossil data, and palaeoenvironmental data from sediment cores.

In the first case study, we used the most speciose group of endemic animal taxa in Lake Ohrid, the non-pyrgulinid Hydrobiidae (microgastropods), to test for changes in diversification rates over time, which eventually determines endemic richness (Föller et al., 2015). Moreover, we attempted to assess the underlying geological, climatic and/or environmental drivers of potential rate change. We used DNA sequencing data, phylogenetic and molecular-clock analyses to infer the phylogenetic relationships, the age of this group, and rates of diversification over time. Our findings indicate that the group represents a species-rich monophyletic group (‘species flock’) and may have started to evolve prior to the origin of extant Lake Ohrid c. 1.2–2.0 million years (Ma) ago. However, the most important finding of this study is that the diversification-rate analyses suggest a constant rate over time (Fig. 1A). We propose that the constant diversification rate observed has been caused by a possible lack of catastrophic environmental events in Lake Ohrid and/or a high lake ecosystem resilience, buffering environmental disturbances. Parameters potentially contributing to Lake Ohrid’s ecosystem resilience are its distinct bathymetry, ongoing tectonic activities, and karst hydrology.

As our results on hydrobiid gastropods in Lake Ohrid did not indicate major changes of diversification rates over time, we were interested in the direct effect of major environmental events on diversification (specifically extinction) and community-assembly processes of diatoms. Therefore, in the second case study, we used diatom community data from the sediment records of Lake Ohrid and its 10 km distant sister lake Prespa as proxy to comparatively study the impact of the most severe ‘pulse disturbance event’ during the late Pleistocene (CI/Y-5 tephra influx, c. 39.6 ±0.1 ka ago) (Jovanovska et al., 2015). We analysed a total of 193 diatom samples, obtained from the DEEP core sequence of Lake Ohrid and from the Co1204 core sequence of Lake Prespa. After standard preparation of diatom samples, individuals were counted, converted to percentage values, and pair-wise community comparisons were conducted. We tested potential irreversible regime shifts, and if those were rejected, the time differences between same-group-membership before and after the tephra influx were used to define the recovery time.

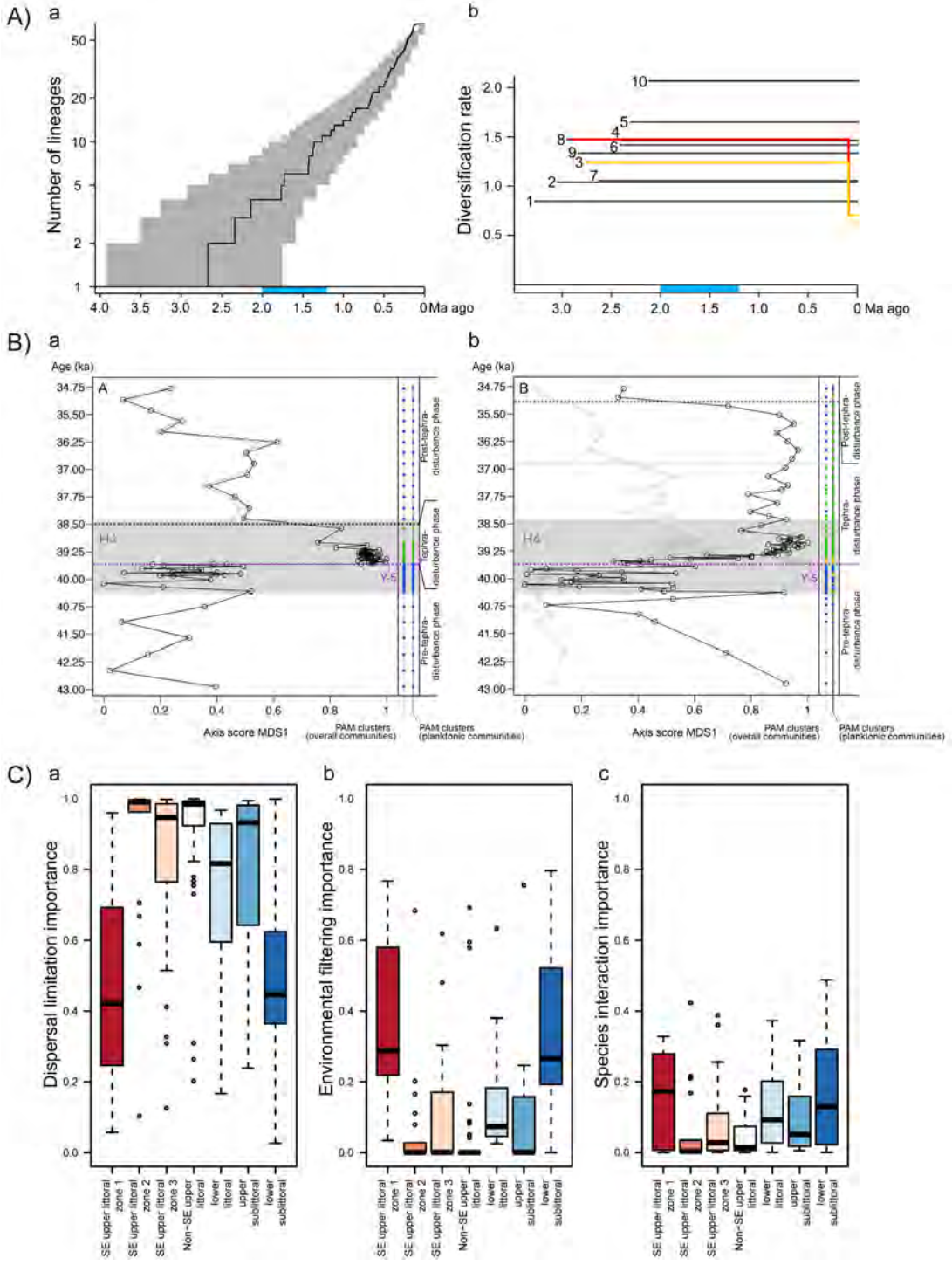

Figure 1. A) Lineage-through-time plot for the endemic non-pyrgulinid Hydrobiidae in Lake Ohrid (a). The plot is based on a molecular-clock analysis, with the black line showing the lineage accumulation according to the phylogeny with highest statistical support and the shaded area indicating the 95% confidence interval. The blue bar ranging from 1.2 to 2.0 My shows the assumed age of Lake Ohrid. Diversification rates obtained from the diversification-rate analyses (b). Trees with a single shift in diversification rates at 0.1 My (are highlighted in red and yellow). B) Diagrams showing the first axis of a metric multidimensional ordination, which displays major changes in diatom community compositions (black curves: planktonic communities; grey curves: overall communities) and respective cluster-analysis based community assignments (colored rectangles) for lakes Ohrid (a) and Prespa (b). Purple dashed lines: Y-5 eruption; light-brownish areas: timing of the H4 event; black and grey dashed lines: return of the respective planktonic and overall community compositions to quasi pre-disturbance state. C) Box plots showing the eco-zone dependent relative importance of (a) dispersal limitation, (b) environmental filtering, and (c) biotic interaction in structuring gastropod communities. These differences in process-importance due to eco-zones are statistically supported by a multivariate Bayesian generalized linear model.

Our results show that the Y-5 influx caused clear and rapid diatom community changes in both lakes, however, without evidences for extinction events. Intriguingly, both lakes subsequently returned to pre-disturbances conditions, indicating that neither lake underwent a regime shift (Fig. 1B). The combined evidence from these findings suggests that lakes Ohrid and Prespa have a high resilience to severe environmental disturbances. Yet, the estimated recovery times indicate that Lake Ohrid is more resilient than Lake Prespa (ca. 1,100 years vs. ca. 4,000 years, respectively), which can be attributed to differences in lake age, geology, and bathymetry.

The case studies above indicate that geological, climatic and/or environmental changes over time rather affected abundances of palaeo-species as well as species compositions than diversification rates. These results challenge the traditional view of a direct effect of these factors on evolutionary processes and the accumulation of endemic richness. They call for a holistic perspective involving evolutionary processes and ecological dynamics. The metacommunity speciation model considers how local communities linked by dispersal of multiple interacting species (i.e., the metacommunity) are affected by speciation and vice versa. In the third case study, we therefore focused on the question how extant gastropod communities are assembled by performing a novel process-based metacommunity analysis (Hauffe et al., 2015). We could show that dispersal limitations had the strongest influence on gastropod community structures. However, dispersal limitation was not the exclusive assembly process, but acted together with environmental filtering (i.e., the establishment of species whose ecological niche fits the local environmental conditions) and species interactions (e.g. competitive exclusion among resident and colonizing species) (Fig. 1C). According to this model, which proposes a link between community assembly processes on the short temporal scale and mode of speciation on longer evolutionary scale, our results suggest the presence of both geographical (due to physical barriers) and ecological speciation (due to divergent selection in different environments). Though the inferred high importance of dispersal limitations in structuring communities potentially implies a dominant role of geographical speciation in the lake, the inferred importance of environmental filtering and biotic interactions suggests a small but significant influence of ecological speciation, which is typically faster than geographic speciation.

The constant diversification rates in gastropods and the lack of regime shifts in the diatom communities suggest that Lake Ohrid has a high resilience to environmental disturbance and likely did not experience major catastrophic events throughout its geological history. As explanation for the high endemic biodiversity of Lake Ohrid we propose a continuous and uninterrupted species accumulation through intra-lacustrine speciation, driven by geographical distance/barriers and facilitated by fast acquisition of ecological differences among populations.

References:

Föller, K., Stelbrink, B., Hauffe, T., Albrecht, C., Wilke, T., 2015. Constant diversification rates of endemic gastropods in ancient Lake Ohrid: ecosystem resilience likely buffers environmental fluctuations. Biogeosciences 12, 7209–7222. doi:10.5194/bg-12-7209-2015

Jovanovska, E., Cvetkoska, A., Hauffe, T., Levkov, Z., Wagner, B., Sulpizio, R., Francke, A., Albrecht, C., Wilke, T., 2015. Differential resilience of ancient sister lakes Ohrid and Prespa to environmental disturbances during the Late Pleistocene. Biogeosciences Discuss. 12, 16049–16079. doi:10.5194/bgd-12-16049-2015

Hauffe, T., Albrecht, C., Wilke, T., 2015. Gastropod diversification and community structuring processes in ancient Lake Ohrid: a metacommunity speciation perspective. Biogeosciences Discuss. 12, 16081–16103. doi:10.5194/bgd-12-16081-2015

IODP

Greater depth samples show the same sediment strength variations across the Nankai forearc as originally found at shallow depth (IODP expeditions 315, 316, 333)

M. Stipp[1], B. Leiss[2], J.H. Behrmann[1]

[1]Marine Geodynamik, GEOMAR Helmholtz-Zentrum für Ozeanforschung Kiel, Wischhofstr. 1-3, 24148 Kiel, Germany, mstipp@geomar.de

[2]Geowissenschaftliches Zentrum, Universität Göttingen, Goldschmidtstr. 3, D-37077 Göttingen

For assessing the tsunamigenic potential, the mechanical strength, composition and fabric of forearc slope and accreted sediments from the Nankai Trough offshore SW-Japan have been investigated (NanTroSEIZE; IODP expeditions 315, 316, 333). Triaxial testing of shallow whole round samples (maximum depth of 130 mbsf) at confining pressures of 0.4-1.0 MPa, room temperature, strain rates of approx. 10^{-3} to 10^{-6} s^{-1}, and up to 64% axial strain (Stipp et al., 2013) revealed mechanically and structurally weak samples from the upper and middle forearc slope of the accretionary prism and strong samples from the accretionary prism toe (Stipp et al., 2013). In order to constrain these results, three additional experiments on samples from greater depth (211-221 mbsf) at confining pressures of 3.0-8.0 MPa, room temperature, strain rates of approx. 10^{-5} s^{-1}, and up to 54% axial strain were carried out. For these tests a digitally controlled servo-hydraulic triaxial appartus with a maximum load of 100 kN was used. Correspondingly to the shallow samples, these experiments show a deviatoric peak stress after only a few percent strain (< 10%) and a continuous stress decrease after this maximum combined with a continuous increase in pore pressure indicative of structurally weak behavior for the two forearc slope samples. The sample from the prism toe area, however, displays a continuous stress increase together with a decrease in pore pressure towards high strain indicative of structurally strong behavior.

Synchrotron texture and composition analysis of the experimentally deformed and undeformed samples using the Rietveld refinement program MAUD indicates an increasing strength of the illite and kaolinite textures with increasing depth down to 523 m below sea floor corresponding to a shape preferred mineral alignment due to compaction (Schumann et al., 2014). Experimentally deformed samples have generally stronger textures than related undeformed core samples, and they show increasing strength of the illite and kaolinite textures with increasing axial strain. Mechanically weak samples have a bulk clay plus calcite content of 31-65 vol.-% and most of their illite, kaolinite, smectite and calcite (001)-pole figures have maxima >1.5 mrd (multiples of a random distribution). Mechanically strong samples, which were deformed to approximately the same amount of strain (up to 40%) have no calcite and a bulk clay content of 24-36 vol.-%. Illite,

kaolinite and smectite (001)-pole figure maxima are predominantly <1.5 mrd.

The synchrotron textures indicate that the mineral fabric as a whole (clay and also calcite grains) becomes preferentially oriented in the mechanically weak samples. Reorientation of the mineral grains is an important cause of strain weakening and contraction, persisting to high compressive strains. In contrast, the strong samples from the accretionary prism toe keep their microfabric up to fairly high compressive strain, allowing for strain hardening and dilation. This soft sediment hardening tends to involve increasingly large volumes of sediment into the imposed deformation, permitting strain dissipation as long as the sediments are homogeneous. Deformation will tend to localize into structurally weak sediments if they occur within the lithological sequence. Such weak sediments, which soften further with increasing strain, predominate in the cover units of the forearc slope and around the existing megasplay fault. They may either provoke mechanical runaway situations allowing for earthquake rupture, surface breakage and tsunami generation, or slope destabilization and resulting submarine mass wasting.

Reference:
Schumann, K., Stipp, M., Leiss, B. and Behrmann, J.H. (2014). – Tectonophysics 636, 125-142, doi: 10.1016/j.tecto.2014.08.005.
Stipp, M., Rolfs, M., Kitamura, Y., Behrmann, J.H., Schumann, K., Schulte-Kortnack, D. and Feeser, V. (2013). – Geochemistry, Geophysics, Geosystems 14/11, doi: 10.1002/ggge.20290.

ICDP

DNA-Metabarcoding of phyto- and zooplankton in East African lake sediments as proxies for past environmental perturbation

R. TIEDEMANN[1], M.H. TRAUTH[2], M. HOFREITER[3]

[1]Unit of Evolutionary Biology/Systematic Zoology, Institute for Biochemistry and Biology, University of Potsdam
[2]Institute of Earth and Environmental Science, University of Potsdam
[3]Unit of Evolutionary Adaptive Genomics, Institute for Biochemistry and Biology, University of Potsdam

Lake-sediment cores provide natural archives of past environmental changes, traditionally analyzed with sedimentological, geochemical and paleontological methods. More recently, samples from sediment cores have also been subjected to molecular DNA analysis, targeting either the living community of soil microbes or remnants of organisms that inhabited the lake and/or its surface sediment in the past. Our project aims at evaluating the possibility for DNA metabarcoding in the up to 280 m long/ca. 500 kyr old Chew Bahir sediment cores, combining state-of-the-art techniques of environmental genomics and ancient DNA analysis. The principal research questions are: (1) How far back in time can DNA remnants in the Chew Bahir sediment cores be extracted and analyzed? (2) How congruent are the results of PCR-based vs. hybridization- capture-based metabarcoding? and (3) What are the long-term trends and shifts in the plankton communities in the Chew Bahir record? In our presentation, we will provide a short overview on the state-of-the-art of environmental DNA-metabarcoding and highlight the methodological advances in our project as well as its possible contribution to the understanding of interactions between the environment and the biosphere in the past, particularly in sediments, in which microscopically recognizable organic remains are scarce or absent.

ICDP

Advanced statistical analyses of XRF core scanner data from the Dead Sea record for an improved and rapid identification of extreme event deposits

RIK TJALLINGII[1], INA NEUGEBAUER[1], MARIEKE AHLBORN[1], MARKUS J. SCHWAB[1], ACHIM BRAUER[1]

[1] GFZ German Research Centre for Geosciences, Section 5.2 Climate Dynamics and Landscape Evolution, Telegrafenberg, D-14473 Potsdam, Germany

The longstanding cooperation between research groups from Israel and Germany resulted in the Dead Sea Deep Drilling Project (DSDDP) and the successful accomplishment of ICDP expedition 5017 (2010-2011). The cores recovered during this expedition provide the first continuous Dead Sea drilling record to study the Late Pleistocene climatic variability in the Levant region. The key record ICDP 5017-1 reveals a unique lacustrine sediment record of partly annually laminated lacustrine sediments (Neugebauer et al., 2014). Laminated sediments reveal an alternation of authigenic aragonite and detrital clay layers, with intercalated gypsum and coarse detrital layers. Furthermore, laminated halite-detritus sediments suggest frequent flood events even during driest conditions (Neugebauer et al., 2016). Earlier studies on the varved sediments of the Lisan formation revealed a remarkable accordance between drier periods and cold intervals in the Greenland ice core record during MIS2 (Prasad et al., 2009). Variations in the thickness and composition of the sediment lamina are directly linked with changes of evaporation and precipitation in the Levant region. Laminated Holocene sediments recovered from the western Dead Sea basin reflect long and short term climatic variations (Migowski et al., 2006, 2004; Neugebauer et al., 2015). Recent results on annually laminated sediments of the western margin of the Dead Sea (DSEn – Ein Gedi profile) reveal an increased frequency of flash floods during the overall dry periods between ~3300 and ~2800 cal. yr BP (Neugebauer et al., 2015). These flash floods are associated with changes in synoptic weather patterns over the southern Levant region.

Improving reconstructions of extreme events such as floods and dust storms requires better identification of detrital sediment sources, as perused by monitoring of fluvial sediment transport in the DFG-funded PALEX project. The origin of the Pleistocene and Holocene detrital sediments in the laminated deposits of ICDP 5017-1 is still ambiguous. To further constrain the origin and transport of these detrital sediments, we will apply a multivariate statistical clustering technique for micro X-ray fluorescence (XRF) element scanning in combination with petrographic thin section analyses. Preliminary results on the Holocene DSEn Ein Gedi profile (Neugebauer et al., 2015) reveal that this technique can greatly improve the geochemical characterization of the broad variety of laminated Dead Sea sediments (Fig. 1).

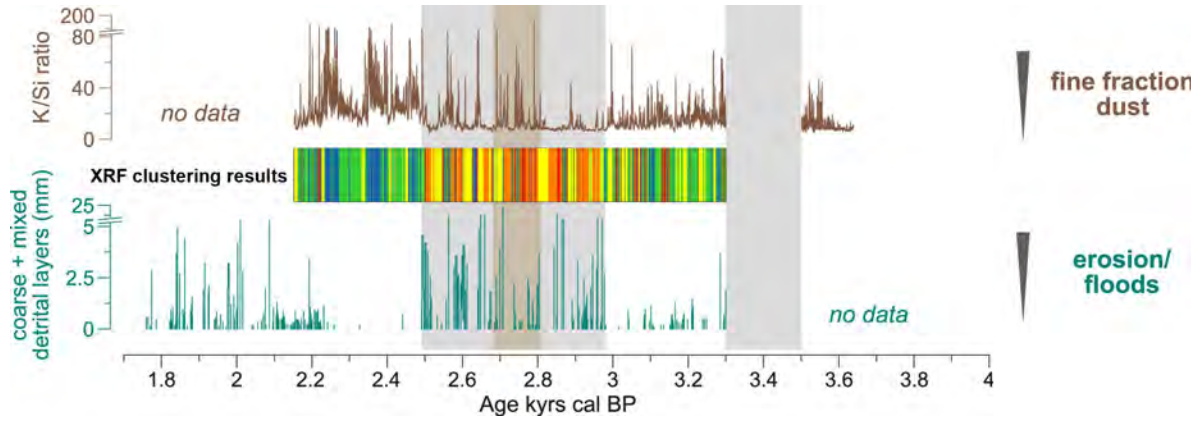

Figure 1. Reconstructions of flood events based on layer thickness as well as dust outbreaks and statistical clustering technique based on XRF core scanning from core DSEn (modified after Neugebauer et al., 2015). The statistical clustering technique reveals evaporitic gypsum layers dominated by the element S (yellow), aragonite and halite layers dominated by the elements Sr, Br, and Cl (green), and siliciclastic mineral layers dominated by the elements Si, Fe, and Ti (orange). Blue layers seem to correspond to layers with both evaporitic gypsum and siliciclastic minerals, whereas red layers seem to be associated with layers containing aragonite, halite and siliciclastic minerals.

Contrary to the common use of single geochemical elements or element ratios, this approach regards the simultaneous variation of all elements measured. These results (Fig. 1) reveal that there is a clear distinction between sediment layers dominated by the element S (yellow), the elements Sr, Br, and Cl (green), or the elements Si, Fe, and Ti (orange). Thin section analyses confirms that these sediment layers correspond with evaporitic gypsum, aragonite and halite, and siliciclastic minerals, respectively. This approach has great potential as a rapid geochemical identification technique for the laminated sediment sequences of ICDP core 5017-1 and to further constrain the origin detrital sediment layers related with flood events and dust deposits.

References:

Migowski, C., Agnon, A., Bookman, R., Negendank, J.F.W., Stein, M., 2004. Recurrence pattern of Holocene earthquakes along the Dead Sea transform revealed by varve-counting and radiocarbon dating of lacustrine sediments. Earth Planet. Sci. Lett. 222, 301–314. doi:10.1016/j.epsl.2004.02.015

Migowski, C., Stein, M., Prasad, S., Negendank, J.F.W., Agnon, A., 2006. Holocene climate variability and cultural evolution in the Near East from the Dead Sea sedimentary record. Quat. Res. 66, 421–431. doi:10.1016/j.yqres.2006.06.010

Neugebauer, I., Brauer, A., Schwab, M.J., Dulski, P., Frank, U., Hadzhiivanova, E., Kitagawa, H., Litt, T., Schiebel, V., Taha, N., Waldmann, N.D., Party, D.S., 2015. Evidences for centennial dry periods at ~ 3300 and ~ 2800 cal . yr BP from micro- facies analyses of the Dead Sea sediments. The Holocene 25, 1358–1371. doi:10.1177/0959683615584208

Neugebauer, I., Brauer, A., Schwab, M.J., Waldmann, N.D., Enzel, Y., Kitagawa, H., Torfstein, A., Frank, U., Dulski, P., Agnon, A., Ariztegui, D., Ben-Avraham, Z., Goldstein, S.L., Stein, M., 2014. Lithology of the long sediment record recovered by the ICDP Dead Sea Deep Drilling Project (DSDDP). Quat. Sci. Rev. 102, 149–165. doi:10.1016/j.quascirev.2014.08.013

Neugebauer, I., Schwab, M.J., Waldmann, N.D., Tjallingii, R., Frank, U., Hadzhiivanova, E., Naumann, R., Taha, N., Agnon, A., Enzel, Y., Brauer, A., 2016. Hydroclimatic variability in the Levant during the early last glacial (~117–75 ka) derived from micro-facies analyses of deep Dead Sea sediments. Clim. Past 12, 75–90. doi:doi:10.5194/cp-12-75-2016

Prasad, S., Negendank, J.F.W., Stein, M., 2009. Varve counting reveals high resolution radiocarbon reservoir age variations in palaeolake Lisan. J. Quat. Sci. 24, 690–696. doi:10.1002/jqs.1289

IODP

Comparing biosignatures from North Pond, Mid-Atlantic Ridge and the Louisville Seamount Chain, off New Zealand

ANDREAS TÜRKE[1], BÉNÉDICTE MÉNEZ[2], WOLFGANG BACH[1,3]

[1]University of Bremen, Department of Geosciences and MARUM, Germany
[2]Institut de Physique du Globe de Paris, France
[3]Centre for Geobiology, University of Bergen, Norway

The subseafloor ocean represents Earth's largest aquifer and the flow of seawater fluxed through these flanks is > 10^{16} L/yr, rivaling the rate of river discharge into the oceans. When volcanic basalt glass is exposed to oxygen-rich seawater, rims of palagonite form at the expense of glass. Within subseafloor basalt glass, a range of putative microbial biosignatures have been interpreted as traces of life in these basaltic aquifers, and these have been studied as a potential analogue for early life on Earth or extraterrestrial habitats for several years. However, little is known about the relationship of the physical and chemical nature of the habitat and the prevalent types of biosignatures. We report and compare biosignatures from two distinctly different study sites (North Pond; IODP Expedition 336 and Louisville; IODP Expedition 330) that vary strongly. We analyzed rock samples microscopically for their putative textural biosignatures and their associated organic molecules via Fourier transform infrared spectrometry. The biosignatures found in basalts from the North Pond Region, at the western flank of the Mid-Atlantic Ridge 23°N, which is young well-oxygenated crust, are characterized by a small textural diversity. However, the organic molecules associated, show evidence for the occurrence of complex molecules like proteins. In contrast, the biosignatures from the Louisville Seamount Chain, which are much older (50 – 80 Ma), are more diverse in terms of textures, while the organic molecules are more degraded and suggest an Archaeal origin.

We propose that microbial communities change significantly during crustal evolution and that microbes associated with older and severely altered crust may not be related to the textures commonly found within subseafloor basalt glass and often interpreted as trace fossils.

IODP

Changing sediment provenance in the Atlantic Ocean-Indian Ocean gateway during the Pliocene in relation to current dynamics and variations in continental climate

G. UENZELMANN-NEBEN[1]

[1] Alfred-Wegener-Institut, Bremerhaven, Germany, Gabriele.Uenzelmann-Neben@awi.de

As an integral inter-ocean link in the global thermohaline circulation (THC), understanding the Agulhas Current system is important for improving our knowledge of the global climate. We aim at the reconstruction of pathways and intensities of major deep water masses in Indian Ocean-Atlantic gateway during the Pliocene and early Pleistocene. Our investigation will be based on an integration of non-destructive physical and chemical core- and downhole-logging data to be obtained during IODP Exp. 361 ("Southern African Climates"). These records combined with already existing seismic reflection data will be used to map biogenic and terrigenous sediment accumulation rate changes and to deduce terrigenous sediment provenance variations during major climate transitions of the last 6 Ma, such as the mid Pliocene warm period and the onset of Northern hemisphere glaciation. Furthermore, we want to explore how changes in Antarctic ice volume influenced the ocean circulation patterns within the gateway. The high-resolution core scanning records will also allow investigating threshold behaviour of millennial scale climate variability in the area.

IODP

Drilling the Agulhas Plateau and Transkei Basin to reconstruct the Cretaceous - Paleocene Tectonic and Climatic evolution of the Southern Ocean Basin

G. UENZELMANN-NEBEN[1], B. HUBER[2], S. BOHATY[3], J. GELDMACHER[4], K.HOERNLE[4], K. MACLEOD[5], C.POULSEN[6], S.VOIGT[7], T.WAGNER[8],D. WATKINS[9], R.WERNER[4], T.WESTERHOLD[10]

[1] Alfred-Wegener-Institut, Bremerhaven, Germany, Gabriele.Uenzelmann-Neben@awi.de
[2]Smithsonian Institution, Washington, D.C., USA
[3]National Oceanography Institution, Southampton, UK
[4]GEOMAR, Kiel, Germany
[5]University of Missouri, USA
[6]University of Michigan, USA
[7]Universitat Frankfurt, Frankfurt, Germany
[8]University of Newcastle, Newcastle, UK
[9]University of Nebraska, USA
[10]MARUM, University of Bremen, Germany

The transition from the Cretaceous "Supergreenhouse" to the Oligocene icehouse provides an opportunity to study changes in Earth system dynamics from a time when climate models suggest CO_2 levels may have been as high as 3500 ppmv (parts per million by volume) and then declined to less than 560 ppmv. During the Supergreenhouse interval meridional temperature gradients were very low and oceanic deposition was punctuated by episodes of widespread anoxia, termed Oceanic Anoxic Events (OAEs) resulting in large scale burial of organic carbon reflected in positive delta 13C excursions. High CO2, greenhouse climate conditions are envisioned for the near future calling for action to get a better understanding of their potential impacts and dynamics.

Climate models have identified significant geography-related Cenozoic cooling arising from the opening of Southern Ocean gateways, pointing towards a progressive strengthening of the Antarctic Circumpolar Current as the major cause for cooler deep ocean temperatures. Analogous arguments point to an important role for deep circulation in explaining Late Cretaceous climate evolution. The Agulhas Plateau is located in a key area for retrieving high-quality geochemical records to test competing models, e.g. to what extent and exactly when the opening of Drake Passage contributed to cooling of the deep ocean. The proposed drill sites on Agulhas Plateau and Transkei Basin are at high latitudes (65°S-58°S from 100 to 65 Ma) and within a gateway between the newly opening South Atlantic, Southern Ocean and southern Indian Ocean basins. Recovery of expanded and stratigraphically complete pelagic carbonate sequences from this region, and comparison with drilling results from Naturaliste Plateau (760-Full), will provide a wealth of new data to significantly advance the understanding of how Cretaceous temperatures, ocean circulation, and sedimentation patterns evolved as CO_2 level rose and fell, and the breakup of Gondwana progressed.

ICDP

Characterization of diagenetic siderites formed in recent and ancient ferruginous sediments of Lake Towuti, Indonesia.

AURÈLE VUILLEMIN[1], JENS KALLMEYER[1], DIRK WAGNER[1], HELGA KEMNITZ[1], RICHARD WIRTH[1], ANDREAS LUECKE[2], CHRISTOPH MAYR[3,4], AND THE ICDP TOWUTI DRILLING PROJECT SCIENCE TEAM

[1]GFZ German Research Centre for Geosciences, Helmholtz Centre Potsdam, Sect. 5.3 Geomicrobiology, Sect. 4.1 Lithosphere Dynamics, Sect. 4.3 Chemistry & Physics of Earth Materials, Telegrafenberg, 14473 Potsdam, Germany
[2]Research Center Juelich, Institute of Bio- & Geosciences 3: Agrosphere, Wilhelm-Johnen-Straße, 52428 Jülich, Germany
[3]Institute of Geography, University of Erlangen-Nürnberg, Glückstrasse 5, 91054 Erlangen, Germany
[4]Institute of Paleontology & Geobiology, GeoBio-Center, University of Munich, Richard-Wagner-Strasse 10, 80333 Munich, Germany

Authigenic minerals in lacustrine settings can be formed in the water column and within the sediment, abiotically and/or triggered by biological activity. Such minerals have been used as paleosalinity and paleoproductivity proxies, reflecting trophic state, and/or early diagenetic conditions. They have also been considered as potential biosignatures of past and present microbial activity (Vuillemin et al., 2013).

Here we present a study from Lake Towuti, a deep tectonic basin in Sulawesi, Indonesia. Its geographic position makes it a prime location to record paleoclimatic changes in the tropical Western Pacific warm pool in its sedimentary sequence (Russell et al., 2014).

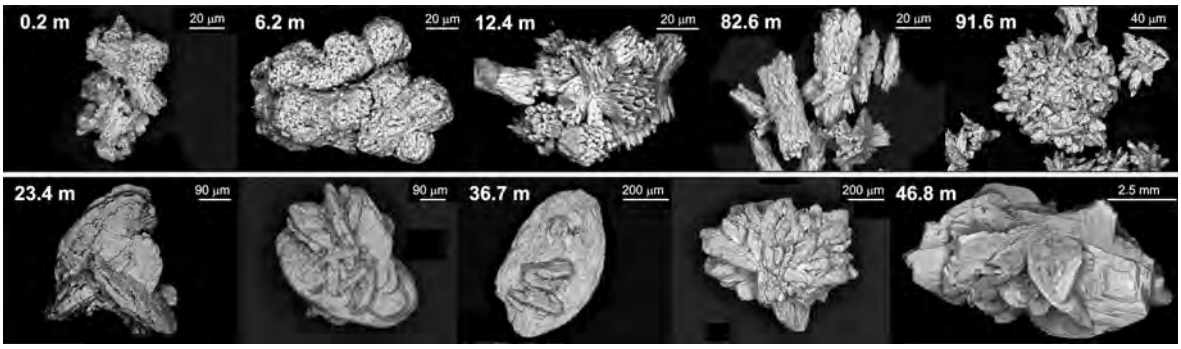

Figure 1: SEM images of siderite (top row) and vivanite (bottom row) crystals retrieved at increasing sediment depth

The ultramafic rocks and surrounding lateritic soils in the catchment area supply considerable amounts of iron and other metals to the lake. These elements further restrain primary productivity along with the development of specific microbial metabolic pathways involved in early diagenesis. Lake Towuti is stratified with anoxic conditions below 130 m, allowing metal reduction processes to take place in the hypolimnion. The extreme scarcity of sulphate and nitrate/nitrite make Lake Towuti's bottom waters a modern analogue for the Archaean Ocean (Crowe et al., 2014). It was therefore chosen as a drilling target by the International Continental Drilling Program (ICDP).

In May to July 2015, the Towuti Drilling Project recovered a total >1000 m of sediment core from three drilling sites, including a 114 m long core drilled with a contamination tracer dedicated to geomicrobiological studies. Heavy mineral fractions were extracted from core catcher samples and siderite crystals ($FeCO_3$) were selected from different depths. Characterization of their habitus was achieved via SEM and TEM imaging (Fig. 1). Preliminary results show that siderites grow from amorphous into nanocrystalline phases and form twinned aggregates developing into mosaic monocrystals with depth. Gradual filling of vugs and microporosity were observed along with inclusions of magnetite nanocrystals.

Work in progress includes parallel $\delta^{13}C$ measurements on bulk organic matter (OM) surrounding the minerals and on the siderites themselves to trace organic to inorganic carbon transfer associated with microbial respiration of OM and infer possible relationships to methane oxidation processes. Analysis of $\delta^{56}Fe$ compositions will complement this dataset to highlight the role of dissimilatory Fe (III) reduction in siderite formation. We hypothesize that sedimentary siderite is formed by precipitation from pore water due to saturation resulting from microbial OM and iron respiration processes. A similar approach will be applied to vivianite crystals ($Fe_3(PO_4)_3 \cdot 8H_2O$) that were found concomitantly with siderite in sedimentary horizons intercalated with tephra layers.

References:

Crowe S.A., Paris G., Katsev S., Jones C.A., Kim S.T., Zerkle A.L., Nomosatryo S., Fowle D.A., Adkins J.F., Sessions A.L., Farquhar J., Canfield D.E. (2014). Sulfate was a trace constituent of Archaean seawater. Science, 346: 735-739. doi: 10.1126/science.1258966

Russell, J.M., Vogel, H., Konecky, B.L., Bijaksana, S., Huang, Y., Melles, M., Wattrus, N., Costa, K., and King, J.W. (2014). Glacial forcing of central Indonesian hydroclimate since 60,000 y B.P. PNAS, 111: 5100-5105. doi: 10.1073/pnas.1402373111

Vuillemin, A., Ariztegui, D., De Coninck, A.S., Lücke, A., Mayr, C., Schubert, C.J., and the PASADO Science Team (2013). Origin and significance of diagenetic concretions in sediments of Laguna Potrok Aike, southern Argentina. Journal of Paleolimnology, 50: 275-291. doi:10.1007/s10933-013-9723-9

ICDP

Basalts from the Kimama core (Snake River Plain, Idaho) and experimental study on the link with associated rhyolites

M. WANG [1], O. NAMUR[1], R. ALMEEV[1], B. CHARLIER[1], F. HOLTZ[1]

[1]Institute of Mineralogy, Leibniz University of Hannover, Germany

The Snake River Plain-Yellowstone (SRPY) province preserves a unique volcanic activity linked to the interaction of mantle plume and is one of the best examples of bimodal tholeiitic basalt-rhyolite volcanism on Earth. Drilling by ICDP HOTSPOT project at Kimama was completed between September 2010 and January 2011 with a final depth of 1912 m The Kimama drill hole is dominated by basalt, with thin intercalations of sediment in the upper 200 m and lower 300 m. Detailed lithologic and geophysical logging has documented ~557 basalt flows, comprising at least 30 flow groups (13 to 170 m thick) representing distinct time periods, and magma batches, with the oldest lavas being dated at ~6 Ma (Bradshaw et al., 2012; Champion and Duncan, 2012; Potter et al., 2012).

190 natural samples from the Kimama drill core were collected for our research project. 105 samples were chosen for bulk-rock analysis and 25 representive samples were chosen for detailed microprobe analyses. Our preliminary results show that the basalts range from crystal-rich with more than 75% of phenocrysts to crystal-poor with less than 10% of phenocrysts. The typical mineral assemblage contains olivine (with Cr-spinel inclusions) and plagioclase as the dominant phenocrysts, clinopyroxene is abundant in the groundmass along with plagioclase, olivine, magnetite, ilmenite and apatite. Fe-Ti rich basalts with 17-19 wt% total FeO and 3.2-4.8 wt% TiO_2 occur in two stratigraphic intervals (1045-1047 m and 1731-1797 m). These rocks show a very fine-grained groundmass containing abundant Fe-Ti oxide. Harker diagrams and stratigraphic chemical trends demonstrate that fractionation is evident in the entire flow groups, with a progression from more primitive basalts at depth to evolved basalts upsection. The major and trace element variations are consistent with the fraction of the observed phenocrysts (olivine and plagioclase ± clinopyroxene). Decrease of MgO is consistent with olivine fractionation and decrease of Sr, CaO, Al_2O_3, and SiO_2 show the importance of plagioclase and clinopyroxene fractionation at low pressure. Comparison between the Fo number [Mg/(Mg+Fe)] of the olivines and the Mg# $Mg/(Mg+Fe_t)$] of the corresponding whole rock (Fig. 1)

suggests that most of the samples represent a mixture between liquid and accumulated phenocrysts.

Detailed microprobe profiles (with intervals of ~4-6µm) of major (Si, Fe, Mg, Mn) and minor (Ca, Ni) elements were measured in a total of 100 olivine crystals (composition vary from Fo 32 to Fo 82 in 25 samples). Olivine crystals are characterized by multiple zoning patterns ranging from 'normal' (decreasing Fo towards the rim) to 'reverse' (lower Fo core with higher rim), or more complex zoning, with reversely zoned interiors and normally zoned rims.

We interpret the various olivine core compositions and zoning patterns in all the studied samples as the result of open-system magmatic processes involving widespread magma mixing between compositionally distinct batches of magma that have emplaced in different sections of the plumbing system.Core and rim compositions of the plagioclase phenocrysts were obtained for 115 crystals. Core compositions can be classified into four groups by calcium contents, i.e., ~An80 , ~An75 ~An65, and ~An55. Analysis of calcic pyroxenes obtained for 290 crystals revealed augite and pigeonite compositions.

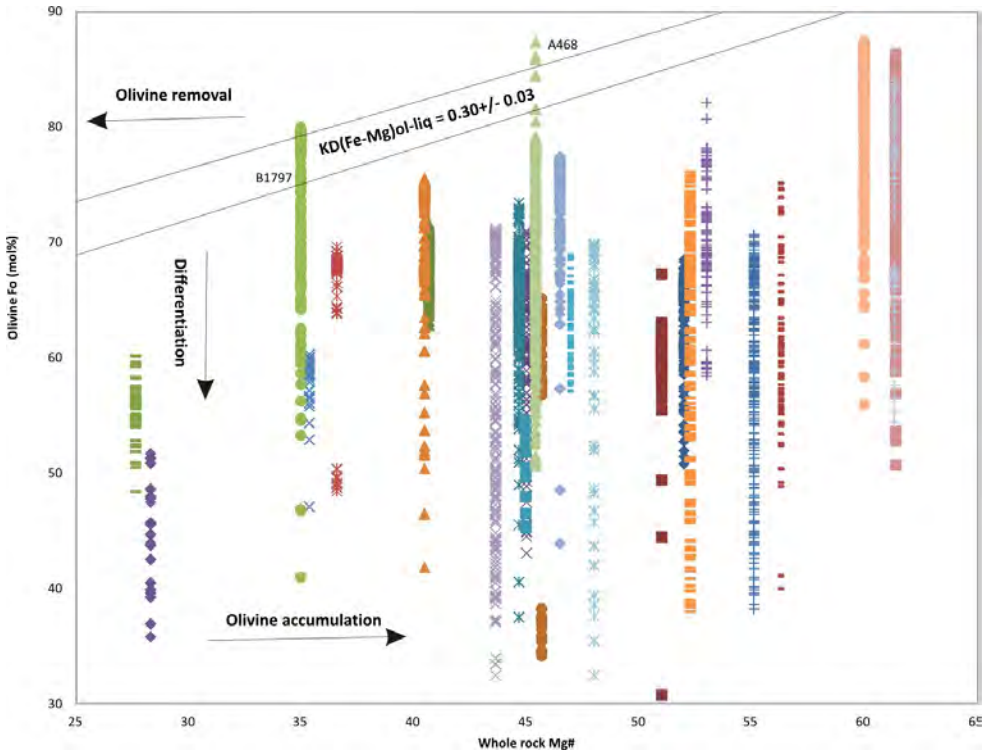

Fig. 1. Bulk-rock MgO vs Fo content of olivine in basalt samples. The curves indicate the relationship between equilibrium olivine Mg-number and bulk rock MgO content, assuming a Mg–Fe olivine–liquid partition coefficient of 0.30±0.03 (Roeder and Emslie, 1970).

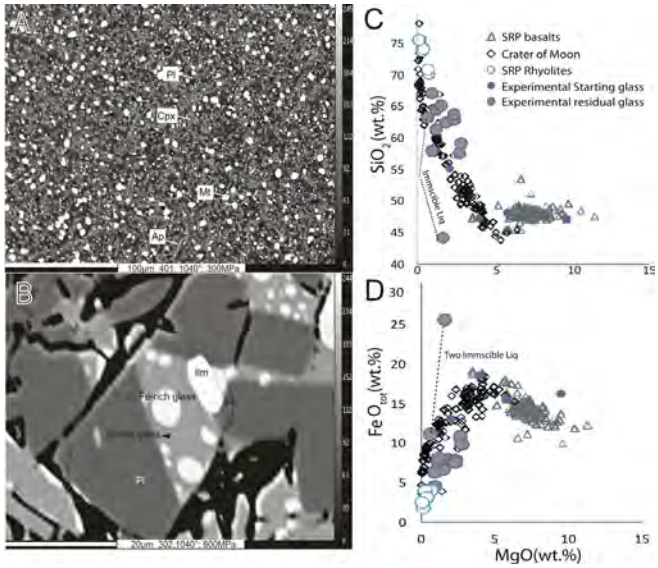

Fig. 2. BSE images of experimental products and the FeO vs SiO2 diagram of all natural and experimental data. Experimental Starting compositions: Compo4-1: average composition of glass from microprobe analyses of natural samples; IM-S1: average composition of basalts of Kimama core at 1045, 1046 and 3536m; IM-S2: average composition of basalts of Kimama core at 409, 860, 1147, 4056m; IM-S3: representative intermediate composition between evolved ferrobasalt and rhyolite as those found in Craters of the Moon (Leeman et al., 1976)

The complete range of the analysed clinopyroxene composition vary from Mg# 32 to Mg# 82, with a prominent peak at around Mg# 70.

In order to better understand the link between basalts and rhyolites and constrain the formation conditions of ferroan rhyolites from the SRPY, we conducted crystallization experiments using the most evolved ferrobasalts as starting compositions (47.12-55.08 wt% SiO_2 and 13.06-18.57 wt% FeO). Three series of experiments have been performed at 300 MPa and 600 MPa, at 1040 and 1020°C and run for 48 and 96 hours. Most of our samples are composed of glass and mineral phases. Clinopyroxene and plagioclase occur in all. Glass is absent in two samples (401 and 102) which are below the solidus. Apatite crystallized in all samples except sample 302. In this sample, silicate liquid immiscibility developed (Fig. 2b) producing an Fe-rich liquid with 44.13 wt% SiO_2 and 25.58 wt% FeO forming globules in a Si-rich liquid with with 63.13 wt% SiO_2 and 11.12 wt% FeO.

In Figure 2cd, compositions of the experimental residual liquids are plotted in Harker diagrams, together with the starting compositions and natural SRPY basalts and rhyolites. Experimental liquids produced at both pressures are generally approaching natural SRPY rhyolites, but degrees of crystallization (up to 82%) were not high enough to reproduce their compositions completely. This is a longstanding and challenging experimental problem to obtain reliable (equilibrium) and measureable experimental liquids under high degrees of crystallization. The use of thermocycling method in our experiments did help to produce relatively large melt pools, but it seems not yet sufficient to simulate and analytically characterize liquid phase after more than 90% of crystallization. To solve the problem we will experimentally simulate fractional crystallization process usinge an incremental approach. For each step of crystallization at lower temperature, we will synthesize a new glass based on the microprobe data of the glass composition obtained from the previous crystallization experiment at higher temperature. It should be noted, that in general, for the first time, formation of immisible Si-rich and Fe-rich liquids have been experimentally demonstarted at high pressure (600 MPa). Particularly, it is also remarkable that the Si-rich immisible liquid also approaching natural SRPY rhyolite compositions (Fig. 2cd), providing new evidences for the potential importance of liquid immiscibility in magma genesis of rhyolites from the SRPY and other bimodal volcanic provinces.

References:

Bradshaw, R.W., Christiansen, E.H., Dorais, M.J., Shervais, J.W., Potter, K.E., 2012. Source and crystallization characteristics of basalts in the Kimama core: Project Hotspot Snake River Scientific Drilling Project, Idaho. Eos Trans. AGU: V13B-2840

Champion, D., Duncan, R.A., 2012. Paleomagnetic and $^{40}Ar/^{39}Ar$ studies on tholeiite basalt samples from “HOTSPOT” corehole taken at Kimama, Idaho, central Snake River Plain. Eos Trans. AGU: V13B-2842.

Leeman, W. P., C. J. Vitaliano, et al. (1976). "Evolved Lavas from Snake-River Plain - Craters of Moon-National-Monument, Idaho." Contributions to Mineralogy and Petrology **56**(1): 35-60.

Potter, K.E., Shervais, J.W., Champion, D., Duncan, R.A., Christiansen, E.H., 2012. Project Hotspot: temporal compositional variation in basalts of the Kimama core and implications for magma source evolution, Snake River scientific drilling project, Idaho. Eos Trans. AGU: V13B-2839.

Roeder, P. L., and RFl Emslie.1970. "Olivine-liquid equilibrium." Contributions to mineralogy and petrology 29, 275-289.

IODP

Reconstructing the evolution of the Bengal Fan with the aid of physical and optical properties - IODP Expedition 354

M.E. WEBER[1], P.S. DEKENS[2], B.T. REILLY[3], T. WILLIAMS[4], S.K. ADHIKARI[5], P.A. SELKIN[6], H. LANTZSCH[7], L. MEYNADIER[8], J.F. SAVIAN[9], S.K. DAS[10], R.R. ADHIKARI[11], B.R. GYAWALI[12], G. JIA[13], L.R. FOX[14], J. GE[15], Y. MARTOS MARTIN[16], M.C. MANOJ[17], J. BAHK[18], K. YOSHIDA[19], C. PONTON[20], P. HUYGHE[21], V. SPIESS[11], C. FRANCE-LANORD[22], AND IODP EXPEDITION 354 SCIENTISTS

[1]University of Cologne, Cologne, Germany
[2]San Francisco State University, San Francisco, USA
[3]Oregon State University, Corvallis, USA
[4]IODP Texas A&M University, College Station, USA
[5]Shimane University, Matsue, Japan
[6]University of Washington, Tacoma, USA
[7]University of Bremen, Bremen, Germany
[8]Université Paris, Paris, France
[9] Universidade Federal do Rio Grande do Sul, Alegre, Brazil
[10]Presidency University, Kolkata, India
[11]University of Bremen, Bremen, Germany
[12]Tohoku University, Sendai, Japan
[13]Chinese Academy of Sciences, Guangzhou, China
[14]Natural History Museum, London, UK
[15]Chinese Academy of Sciences, Beijing, China
[16]British Antarctic Survey, Cambridge, UK
[17]Birbal Sahni Institute of Palaeobotany, Lucknow, India
[18]Korea Institute of Geoscience and Mineral Resources, Yuseong-gu Daejeon, Republic of Korea
[19]Shinshu University, Matsumoto, Japan
[20]University of Southern California, Los Angeles, USA
[21]University Joseph Fourier, Grenoble, France
[22]Centre National de la Recherche Scientifique, Vandoeuvre les Nancy Cedex, France

IODP Expedition 354 set out in February to March 2015 to drill seven sites along an east west oriented core transect of 320 km length at 8°N in the Bengal Fan (France-Lanord et al., 2015). Seven sites were recovered to reconstruct the Himalayan uplift since the Oligocene and to decipher the trubiditic depositional mechanisms on the lower Bengal Fan. The Bengal Fan accumulated the material from the erosional uplift of the Himalayan after the collision of India and Asia. The fan system, fed by turbidites coming from the Ganges and Brahmaputra river systems, contains the most complete flux since the continental collision. The majority of sediment bypasses the shelf via the "Swatch of No Ground", which connects to the only currently active channel-levee system that shows apparently no bifurcation over its 2500 km length on the fan. The new core transect crosses the active channel on the lower Bengal Fan. Six sites are located on the eastern side, one on the western side. Seismic imaging shows a complex pattern of levees and deeply incised channels, indicative of vertical aggradation and lateral migration. Data collection and discussion onboard led to ideas for follow-up studies that involve sediment physical properties, which will be the focus here.

First, the close correlation of lithology and sediment physics indicates that acoustic, physical, and optical properties such as *P*-wave velocity, wet and dry bulk density, magnetic susceptibility, natural gamma radiation, and sediment color are closely related to sediment composition. Moreover, it indicates that the grain size distribution of turbiditic sections can be derived adequately from measurements of wet bulk densities and *P*-wave velocities, an assignation that will be studied in detail. This concept should enable for quantitative calculation of

sediment budgets of clay, sand, and silt in combination with bio-, magneto- and seismostratigraphy.

Second, hemipelagic to pelagic sequences containing higher amounts of biogenic carbonate and opal are intercalated frequently. These sequences exhibit two end-members: relatively dark sediment rich in biogenic opal and/or clay, with low densities and velocities, and brighter sediment with higher densities and velocities and higher contents of biogenic carbonate. Here, we aim at providing quantitative estimates for biogenic opal and carbonate contents from measurements of sediment lightness (L*) and possibly from wet bulk density and *P*-wave velocity, in combination with ground-truth geochemical measurements (e.g., by Fourier transform infrared spectroscopy).

Third, investigation of the hemipelagic sequences younger than 300 ka, specifically the last glacial cycle, should provide the climate framework in which the terrestrial records are interpreted and to establish the link between the development and variability in monsoonal strength with global and regional climate conditions. Here, orbital tuning of sediment lightness, wet-bulk density, and *P*-wave velocity provides a first, robust age model. The tuning also reveals that sediment cycles in the hemipelagic sequences of the lower Bengal Fan vary almost exclusively on the 23-kyr insolation cycle, indicative for the close link to monsoonal development. This tuning strategy will be applied transect-wide for older hemipelagic sections in combination with ground-truth chronological control provided by bio- and magnetostratigraphy.

References:
France-Lanord, C., Spiess, V., Klaus, A., and the Expedition 354 Scientists, 2015. Bengal Fan: Neogene and late Paleogene record of Himalayan orogeny and climate: a transect across the Middle Bengal Fan. *International Ocean Discovery Program Preliminary Report*, 354. http://dx.doi.org/10.14379/iodp.pr.354.2015

IODP

New Eocene benthic stable isotope record in the Pacific: completing a 22 Ma single site high-resolution Paleogene section from Shatsky Rise

T. WESTERHOLD[1], U. RÖHL[1], B. DONNER[1], J.C. ZACHOS[2]

[1]MARUM – Center for Marine Environmental Sciences, University of Bremen, Bremen, Germany
[2]University of California, Santa Cruz, California, USA

The Paleocene/Eocene Thermal Maximum (PETM) is the most pronounced and well-studied global warming event of a series of warming events in the Late Paleocene to Middle Eocene. These warming events occurred in a dynamic climate regime with overall warm global temperatures and elevated atmospheric CO_2 levels unprecedented in the past 90 Myr (Zachos et al. 2008). They have been attributed to periodic carbon cycle perturbations of various magnitudes by rapid injection of greenhouse gases from a reduced carbon reservoir into the climate system. Characteristic for these rapid events of global warming is a paired negative excursion in $\delta^{13}C$ and $\delta^{18}O$ of bulk sediment and benthic foraminifera, and a clay rich layer in carbonate dominated deep-sea sediments indicating dissolution due to acidification (e.g., Zachos et al. 2005).

Up to now, the majority of the Eocene hyperthermal events found in deep sea drilling records is from Atlantic Ocean sediments. In the Ypresian Stage (56-47.8 Ma) the hyperthermal events PETM, ETM-2 and ETM-3 (Eocene Thermal Maxiumum) have been identified in Atlantic ODP Sites 550, 1051, 1262 and 1263 (e.g., Cramer et al. 2003, Zachos et al. 2005, Zachos et al. 2010, Lourens et al. 2005, Stap et al. 2010, Littler et al. 2014, Lauretano et al. 2015). These events together with several lower amplitude excursions in the Ypresian from the PETM to the top of Chron C24n are labeled from E to L and associated to short eccentricity cycle maxima (Cramer et al. 2003). More recently, not only the carbon isotope excursions H to L but 20 more carbon isotope excursions have been documented in the Ypresian to early Lutetian in equatorial Atlantic Site 1258 at Demerara Rise in bulk (Kirtland-Turner et al. 2014) or benthic data (Sexton et al. 2011). One event, the Chron C19r event, was initially described at Demerara Rise (Site 1260) in late Lutetian bulk isotope data (Edgar et al. 2007).

Records of Eocene hyperthermal events in Pacific deep sea drilling cores come from Site 577 and Leg 1209 sites from Shatsky Rise (e.g., Cramer et al. 2003, Zachos et al. 2003) as well as Site 1215 from the west-equatorial Pacific (Leon-Rodriguez and Dickens 2010). In contrast to the Atlantic record, multiple hyperthermal events in the Pacific have only been recorded in bulk stable isotopes from the Ypresian in New Zealand (e.g., Slotnik et al. 2015). There are almost no high-resolution deep-sea benthic stable isotope records from the Pacific showing signs of hyperthermal events in the Ypresian and Lutetian. For the Early to Middle Eocene in the Pacific section only a low-resolution stable isotope record from Site 1209 is available (Dutton et al. 2005) exhibiting that benthic foraminifers are moderately to well preserved. Although dissolution indexes suggest a relative shoaling of the lysocline in the late Eocene beginning at ~45 Ma (Hancock & Dickens 2005, Petrizzo et al. 2005), a more detailed record of benthic foraminifera from 37 to 45 Ma at Site 1209 suffers from the lack of a consistent correlation between Pacific records throughout the middle Eocene (Dawber & Tripati 2012). For deciphering details of the Early to Middle Eocene climate and carbon cycle variability it is crucial to acquire and investigate a high-resolution benthic stable isotope record from the Pacific and compare this with available Atlantic records.

We present a new 12 million year long high-resolution *Nuttallides truempyi* stable isotope record for ODP Site 1209 spanning the 56 to 44 Ma interval. Site 1209 is located on the southern high of Shatsky Rise (2387 m water depth) and contains an expanded Paleogene section (Bralower et al. 2002). This new benthic isotope record extended an existing record at the same site (Westerhold et al. 2011) to a now altogether unique 22 million year long, single site, benthic isotope section for the Pacific Ocean at 5 kyr resolution. The carbon isotope values reveals multiple carbon isotope excursions in the Ypresian and Lutetian that correspond in timing and magnitude to hyperthermal events previously observed elsewhere incl. for example New Zealand and the Atlantic section. These hyperthermals are also reflected by high XRF core scanning Fe intensities and pronounced minima in the wt% coarse fraction indicating carbonate dissolution. Furthermore, the benthic $\delta^{13}C$ data clearly exhibit the well-known Eocene trend in $\delta^{13}C$ from low-resolution benthic isotope compilations (Zachos et al. 2008), but in addition

now reveals previously unknown major shifts in $\delta^{13}C$ during Chron C23n and C21n. Interestingly, between the two shifts the $\delta^{13}C$ data do not show a trend indicating a time of relatively little influence of tectonic CO_2 degassing to the carbon cycle and /or stable climate conditions with balanced flux between carbon reservoirs. Physical properties, XRF core scanning, coarse fraction and benthic stable isotope data reveal eccentricity cycles that will be used for cyclostratigraphy. We are currently correlating Leg 198 (Sites 1209, 1210) and Leg 208 (Sites 1262, 1263) data based on a synchronized robust cyclostratigraphic framework to identify and label common hyperthermal events found in Site 1209. The new age model will allow reconstructing phase relationships between the Pacific and Atlantic paleoclimate in unprecedented detail. We aim to investigate these relationships - stable isotope data and terrigenous and carbonate records - at a resolution down to Milankovitch frequencies. These high-resolution investigations of the Eocene were not possible up to date and have the potential for providing completely new insights into greenhouse climate variability.

References:

Bralower, T. J., Premoli Silva, I., Malone, M. J., and et al.: Proc. ODP, Init. Repts., 198: College Station, TX (Ocean Drilling Program), 2002.

Cramer, B. S., Wright, J. D., Kent, D. V., and Aubry, M.-P.: Orbital climate forcing of $\delta^{13}C$ excursions in the late Paleocene - Eocene (chrons C24n-C25n), Paleoceanography, 18, 1097, 10.1029/2003PA000909, 2003.

Dawber, C. F., and Tripati, A. K.: Element/Calcium ratios in middle Eocene samples of Oridorsalis umbonatus from Ocean Drilling Program Site 1209, Clim. Past Discuss., 7, 3795-3821, 10.5194/cpd-7-3795-2011, 2011.

Dawber, C. F., and Tripati, A. K.: Exploring the controls on element ratios in middle Eocene samples of the benthic foraminifera Oridorsalis umbonatus, Clim. Past, 8, 1957-1971, 10.5194/cp-8-1957-2012, 2012.

Dutton, A., Lohmann, K. C., and Leckie, R. M.: Data report: Stable isotope and Mg/Ca of Paleocene and Eocene foraminifers, ODP Site 1209, Shatsky Rise, in: Proc. ODP, Sci. Results, 198, edited by: Bralower, T. J., Premoli-Silva, I., and Malone, M. J., 10.2973/odp.proc.sr.198.119.2005, 2005.

Edgar, K. M., Wilson, P. A., Sexton, P. F., and Suganuma, Y.: No extreme bipolar glaciation during the main Eocene calcite compensation shift, Nature, 448, 908-911, 10.1038/nature06053, 2007.

Hancock, H. J. L., and Dickens, G. R.: Carbonate dissolution episodes in Paleocene and Eocene sediment, Shatsky Rise, west-central Pacific, in: Proc. ODP, Sci. Results, 198: College Station, TX (Ocean Drilling Program), edited by: Bralower, T. J., Premoli Silva, I., and Malone, M. J., 1-24, 10.2973/odp.proc.sr.198.116.2005, 2005.

Kirtland Turner, S., Sexton, P. F., Charles, C. D., and Norris, R. D.: Persistence of carbon release events through the peak of early Eocene global warmth, Nature Geosci, 7, 10.1038/ngeo2240, 2014.

Lauretano, V., Littler, K., Polling, M., Zachos, J. C., and Lourens, L. J.: Frequency, magnitude and character of hyperthermal events at the onset of the Early Eocene Climatic Optimum, Clim. Past, 11, 1313-1324, 10.5194/cp-11-1313-2015, 2015.

Leon-Rodriguez, L., and Dickens, G. R.: Constraints on ocean acidification associated with rapid and massive carbon injections: The early Paleogene record at ocean drilling program site 1215, equatorial Pacific Ocean, Palaeogeography, Palaeoclimatology, Palaeoecology, 298, 409-420, 10.1016/j.palaeo.2010.10.029, 2010.

Littler, K., Röhl, U., Westerhold, T., and Zachos, J. C.: A high-resolution benthic stable-isotope record for the South Atlantic: Implications for orbital-scale changes in Late Paleocene–Early Eocene climate and carbon cycling, Earth and Planetary Science Letters, 401, 18-30, 10.1016/j.epsl.2014.05.054, 2014.

Lourens, L. J., Sluijs, A., Kroon, D., Zachos, J. C., Thomas, E., Röhl, U., Bowles, J., and Raffi, I.: Astronomical pacing of late Palaeocene to early Eocene global warming events, Nature, 435, 1083-1087, 10.1038/nature03814, 2005.

Pälike, H., Norris, R. D., Herrle, J. O., Wilson, P. A., Coxall, H. K., Lear, C. H., Shackleton, N. J., Tripati, A. K., Wade, B. S.: The Heartbeat of the Oligocene Climate System, Science, 314, 1894-1898, 2006.

Petrizzo, M. R., Premoli Silva, I., and Ferrari, P.: Data report: Paleogene plaktonic foraminifer biostratigraphy, ODP Leg 198 Holes 1209A, 1210A, and 1211A (Shatsky Rise, northwest Pacific Ocean), in: Proc. ODP, Sci. Results, 198: College Station, TX (Ocean Drilling Program), edited by: Bralower, T. J., Premoli Silva, I., and Malone, M. J., 1-56, 10.2973/odp.proc.sr.198.110.2005, 2005.

Sexton, P. F., Norris, R. D., Wilson, P. A., Pälike, H., Westerhold, T., Röhl, U., Bolton, C. T., and Gibbs, S.: Eocene global warming events driven by ventilation of oceanic dissolved organic carbon, Nature, 471, 349-352, 10.1038/nature09826, 2011.

Slotnick, B. S., Dickens, G. R., Hollis, C. J., Crampton, J. S., Percy Strong, C., and Phillips, A.: The onset of the Early Eocene Climatic Optimum at Branch Stream, Clarence River valley, New Zealand, New Zealand Journal of Geology and Geophysics, 58, 262-280, 10.1080/00288306.2015.1063514, 2015.

Stap, L., Lourens, L. J., Thomas, E., Sluijs, A., Bohaty, S., and Zachos, J. C.: High-resolution deep-sea carbon and oxygen isotope records of Eocene Thermal Maximum 2 and H2, Geology, 38, 607-610, 10.1130/g30777.1, 2010.

Tripati, A., Backman, J., Elderfield, H., Ferretti, P.: Eocene bipolar glaciation associated with global carbon cycle changes, Nature, 436, 341-346, 2005.

Westerhold, T., Röhl, U., Donner, B., McCarren, H. K., and Zachos, J. C.: A complete high-resolution Paleocene benthic stable isotope record for the central Pacific (ODP Site 1209), Paleoceanography, 26, PA2216, 10.1029/2010pa002092, 2011.

Zachos, J. C., Wara, M. W., Bohaty, S., Delaney, M. L., Petrizzo, M. R., Brill, A., Bralower, T. J., and Premoli-Silva, I.: A Transient Rise in Tropical Sea Surface Temperature During the Paleocene-Eocene Thermal Maximum, Science, 302, 1551-1554, 2003.

Zachos, J. C., Röhl, U., Schellenberg, S. A., Sluijs, A., Hodell, D. A., Kelly, D. C., Thomas, E., Nicolo, M., Raffi, I., Lourens, L. J., McCarren, H., and Kroon, D.: Rapid Acidification of the Ocean During the Paleocene-Eocene Thermal Maximum, Science, 308, 1611-1615, 10.1126/science.1109004, 2005.

Zachos, J. C., Dickens, G. R., and Zeebe, R. E.: An early Cenozoic perspective on greenhouse warming and carbon-cycle dynamics, Nature, 451, 279-283, 10.1038/nature06588, 2008.

Zachos, J. C., McCarren, H., Murphy, B., Röhl, U., and Westerhold, T.: Tempo and scale of late Paleocene and early Eocene carbon isotope cycles: Implications for the origin of hyperthermals, Earth and Planetary Science Letters, 299, 242-249, 10.1016/j.epsl.2010.09.004, 2010.

IODP

Can genera be used as proxies for species in studies of biodiversity-climate sensitivity? - A test using Cenozoic marine diatoms

R. WIESE[1], J. RENAUDIE[2], D. LAZARUS[2]

[1]Institut für Geologische Wissenschaften, Freie Universität Berlin, Melteserstraße 74-100, 12249 Berlin, Germany.
[2]Museum für Naturkunde, Leibniz-Institut für Evolutions- und Biodiversitätsforschung, Invalidenstraße 43, 10115 Berlin, Germany.

It is widely accepted within the field of paleodiversity studies in paleontology to use genera as a proxy for species diversity. In several studies, genus diversity has been compared to past environmental reconstructions. It has been argued that the correlations, or equally, lack of them, seen between diversity and climate in such studies are relevant to decisions on how much humanity should invest in protecting living biodiversity in response to future global climate change. Many researchers however have questioned the adequacy of genera as a proxy for species diversity in paleontology. For example, in studies of living diversity, genera have been shown to be only sporadically useful as proxies for species diversity. Further, the ratio of species to genera is known to be both correlated to absolute diversity, and to vary systematically with environmental conditions. Lastly, there are to our knowledge no explicit tests of the impact of using genus vs species level taxonomy in studies correlating paleodiversity to paleoenvironmental factors. This last is due to the rarity of good species level diversity data in the published fossil record.

We test the effect of using genera instead of species in paleodiversity-paleoenvironmental studies, based on such a dataset: a recently published species diversity analysis of Cenozoic marine planktonic diatoms (Lazarus et al.,

2014).This study had showed a strong correlation of species diversity to geochemical climate proxies, and had noted that future global warming may put many of the species most important for carbon cycling at risk of extinction. Using an updated version of the dataset used in Lazarus et al., we re-confirm the strong correlation of Cenozoic diatom species diversity to environment, and the risk of species extinction with warming. However, using the identical dataset, but substituting genera, results in loss of all significant correlations of diversity to environmental change, and thus as well the ability to detect risk of extinction with warming.

Paleodiversity data using genera cannot be simply assumed to be adequate for examining the correlation of diversity to climate. Such studies need to demonstrate the adequacy of their generic data as a proxy for species diversity, or use species-level data.

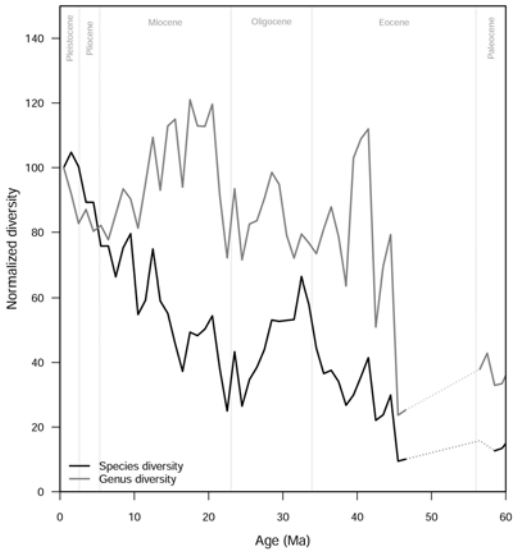

Figure 1:
Marine diatom paleodiversity patterns throughout the Cenozoic at species and genus levels in 1 Myr time bins. Both are subsampled using SQS subsampling (Alroy, 2010) and corrected using D(80) evenness metrics (Lazarus et al., 2014).

References:
Alroy, J., 2010. Fair sampling of taxonomic richness and unbiased estimation of origination and extinction rates. In: Alroy, J., Hunt, G. (Eds), Quantitative Methods in Paleobiology, The Paleontological Society: 55-80.
Lazarus, D., Barron, J., Renaudie, J., Driver, P., Türke, A., 2014. Cenozoic Planktonic Marine Diatom Diversity and Correlation to Climate Change. PLoS ONE 9(1): e84857.

ICDP

Magma storage depths of the Yellowstone Supervolcano: New insights from project HOTSPOT

S. WILKE[1], F. HOLTZ[1] T. BOLTE[1], P. NOWACZYK[1], R. ALMEEV[1], E.H. CHRISTIANSEN[2]

[1]Institute of Mineralogy, Leibniz University of Hannover, Callinstr. 3, 30167 Hannover, Germany
[2]Department of Geological Sciences, Brigham Young University, Provo, UT 84602, USA

General aim of the study:The scientific drilling project in the Snake River Plain. – Yellowstone (SRPY) volcanic province offers an opportunity to shed light on various magmatic processes such fractionation, assimilation and magma recharge which resulted in strong peculiarities, as well as on the influence of possible interactions of these magmas with lithosphere in space and time. As one of the worlds largest recent and still active silicic volcanic eruptive provinces (Hildreth *et al.*, 1991) the SRPY volcanic system bears an extraordinary opportunity to investigate the interactions of continental lithosphere with a mantle hotspot, currently located beneath the north-western edge of the US-state Wyoming.

Our project was aimed at understanding the evolution of magma storage depth with time in the SRPY. The core samples from the Kimberly drilling site, Twin Falls eruptive center, and of erupted rocks from other localities were used to determine the depths of magma storage prior to eruption. In our previous experimental project we have successfully demonstrated that the effect of pressure (P) on the silica content of cotectic rhyolitic melts (in equilibrium with quartz and feldspar) can be utilized as a geobarometer (Almeev *et al.,* 2012). In our current project we also demonstrate that the projection of rhyolitic glass compositions in the quartz (Qz, SiO_2) – albite (Ab, $NaAlSi_3O_8$) – orthoclase (Or, $KAlSi_3O_8$) ternary system can be used to discrimintate cotectic compositions produced under different P, which makes it a useful tool for geobarometry and for the determination of the depth of magma storage of water poor rhyolitic systems (Wilke *et al.*, 2015). The software rhyolite-MELTS is an alternative tool recently applied for this goal (Gualda & Ghiorso, 2014). However, rhyolite-MELTS is based on a calibration dataset that is mostly restricted to experiments conducted at high water activety, in FeO and more importantly CaO-free haplogranitic (Qz-Ab-Or only) systems. In natural rhyolites, however, the presence of several wt.% CaO (expressed hereafter as a normative melt anorthite - An, $CaAl_2Si_2O_8$) is a common feature which has strong effect on the P determination using rhyolite-MELTS. In our project a set of experiments was designed to investigate the effect of normative melt An on composition of the cotectic curves when projected on a ternary system Qz-Ab-Or. The results were used to construct a new geobarometer (Wilke *et al.,* in preparation).

Based on our experimental data, we developed a new geobarometer (DERP, Determining Eutectic Rhyolite Pressures) and demonstrated its reliability against a set of previously published geobarometers proposed for rhyolitic systems. We show that the applications of DERP for the ICDP samples from Kimberly core and for other related rhyolites from SRP provide some new insights on the evolution of magma storage P with time.

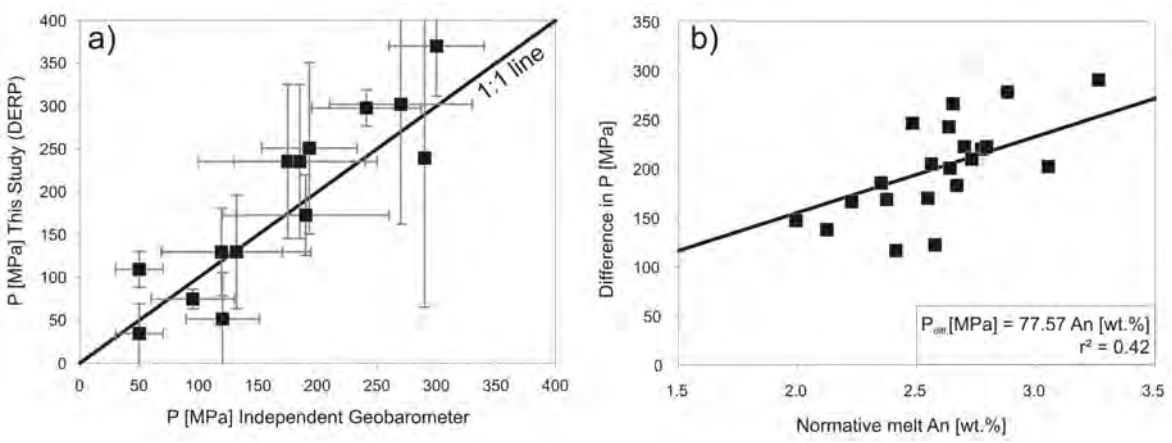

Figure 1a) P of rhyolitic melts from various locations calculated with DERP and an independent geobarometer (c.f. Wilke *et al.*, in preperation) 1b) difference in P between DERP and rhyolite-MELTS calculations at various normative melt An contents. Data from Pamukcu *et al*. (2015).

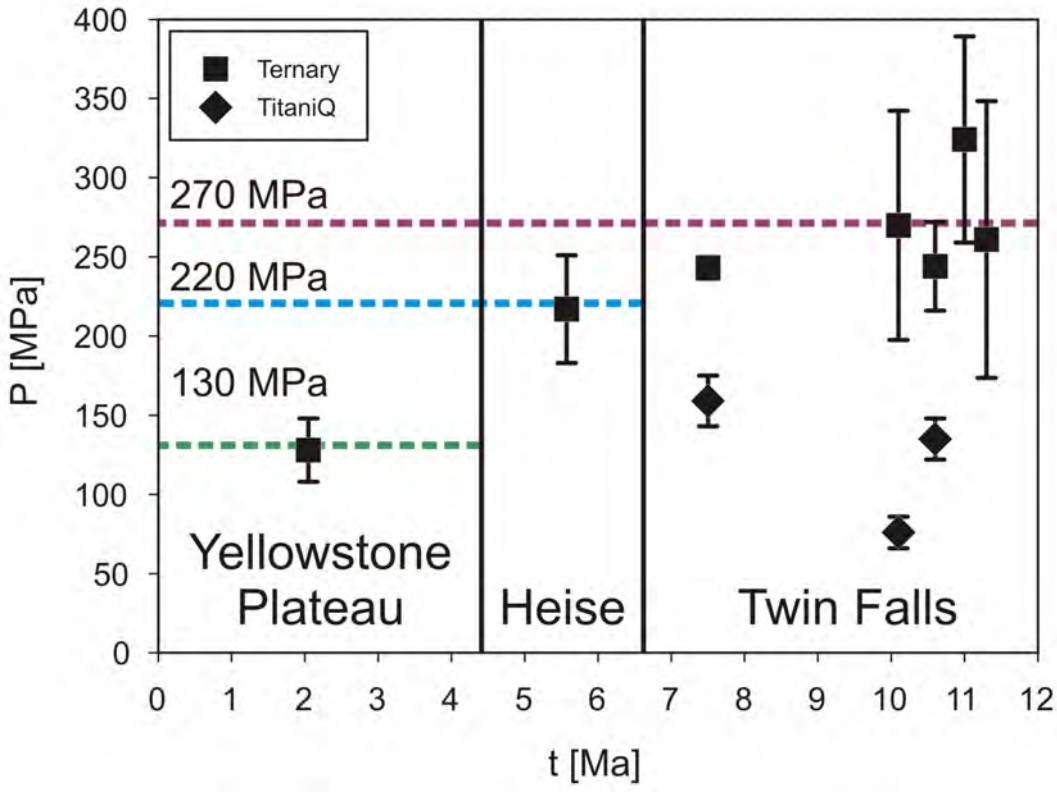

Figure 2: Evolution of P over time in the SRPY. Squares: P determined by ternary projection (DERP); diamonds: P determined by TitaniQ geobarometry using the model from Huang and Audétat (2012). The colourful lines illustrate the P steps between the three eruptive centers Twin Falls, Heise volcanic field and Yellowstone Plateau.

Experimental results and elaboration of a geobarometer based on cotectic glass compositions: We determined six new phase diagrams that enabled us to constrain the position of eutectic points and cotectic curves at various P and melt normative An contents. These data were derived by conducting crystallization experiments under following conditions: A) 200 MPa, 3 wt.% H_2O, 3.5 wt.% An (Wilke et al., 2015); B) 200 MPa, 1.4 wt.% H_2O, 3.5 wt.% An; C) 200 MPa, 1.3 wt.% H_2O, 7 wt.% An; D) 500 MPa, 3 wt.% H_2O, 3.5 wt.% An; E) 500 MPa, 1.4 wt.% H_2O, 3.5 wt.% An and F) 500 MPa, 1.3 wt.% H_2O, 7 wt.% An (all Wilke *et al.*, in preparation).This extended experimental database was used to develop a set of coupled linear equations linking P, melt water content and melt An content with cotectic compositions. This new "DERP geobarometer" was able to reproduce independent P

estimates obtained by various geobarometers within 50 MPa accuracy: figure 1a shows P estimates for 11 rhyolites derived from independent geobarometers in comparison to those calculated by DERP. When comparing pressures calculated with DERP and rhyolite-MELTS, an offset is observed that positively correlates with the melts normative An content (Figure 1b). DERP is calibrated to calculate the magma storage P from the compositions of cotectic glasses with up to 7 wt.% normative melt An and any melt H_2O content in the pressure range 50 – 500 MPa. Its application is restricted to high silica rhyolitic systems saturated with respect to quartz and feldspar(s).

Samples from the drill core:The Kimberly drill core was retrieved in the frame of project HOTSPOT, supported by ICDP, between January 2011 and June 2011 in the Twin Falls eruptive center which was active mostly between 10.5 and 8.5 Ma ago (Nash et al. 2006). It provides a continous record of almost 2 km rhyolitic ignimbrites seperated in three different units, labeled rhyolite units 1, 2 and 3 in the following description. Rhyolite unit 3 was recovered between 122 and 244 m depth. This rhyolitic lava flow contains plagioclase, K-Feldspar, pigeonite, augite, magnetite, sparse ilmenite and accessory apatite but no preserved glass matrix. It is tentatively correlated with the rhyolite of Shoshone Falls. Rhyolite unit 2 was recovered between 427 and 600 m depth. The high-silica rhyolite lava flow contains quartz, plagioclase, sanidine, augite, pigeonite, magnetite, sparse ilmenite and accessory apatite and zircon in a glassy matrix. It is tentatively correlatted with the Greys Landing ignimbrite. Beeing the only rhyolite unit in the drillcore to host quartz, feldspar and a glass phase, Rhyolite unit 2 is the only unit suitable for DERP geobarometry. Rhyolite unit 1 was recovered between 610m and the end of the borehole at 1958m depth with no indication of the actual thickness of that unit. Rhyolite 1 is a low-silica ignimbrite with plagioclase, pigeonite, augite, magnetite and accessory apatite, zircon, and pyrite. It is tentatively correltated with the tuff of McMullen Creek. In this study we provide evidence that this rhyolitic sequence complements rhyolitic field outcrops of the Cassia Mountains described by Ellis et al. (2010).

Application of DERP to natural sampels from Snake River Plain: Investigation of five different units of Twin Falls rhyolites (Magpie Basin Member, Big Bluff Member, Tuff of Steer Basin, Wooden Shoe Butte Member and Kimberly Rhyolite 2) provides evidence that the magma storage P over the volcanic fields eruption history was relatively constant within 250 to 300 MPa between at least ~11 to 9 Ma. In contrast, lower pressures are found for rhyolitic magmas from younger eruption centers, e.g. 220 MPa for the ~5.6 Ma old Wolverine Creek Tuff from the Heise volcanic field or 130 MPa for the ~2 Ma old Huckleberry Ridge Tuff from the Yellowstone Plateau (see Fig. 2). A possible interpretation is that every eruptive complex is fed by a magma chamber network of limited vertical extend located at a constant depth over a very long time. The chamber network for the next, younger eruption complex would then be established at shallower levels.

Wherever possible, we tried to verify the P information obtained from DERP for the investigated Twin Falls rhyolites using the Ti in quartz geothermobaromether from Huang and Audétat (2012). Ti measurements in quartz performed with a Cameca SX electron microprobe (detection limit 17 ppm Ti) however revealed heterogeneous contents ranging from ~170 to 240 ppm Ti in different units of the Twin Falls eruptive center translating into considerably lower P of 80 to 160 MPa. Whether this offset is a consequence of problems with one (or both) of the geobarometers or related to a complex formation history of the different quartz grains is yet the aim of ongoing investigations. Temperatures (T) calculated for rhyolites from Twin Falls by various geothermometers are constantly around ~900°C, with little changes in time. As the T of rhyolites along the SRPY hotspot track is known to generally decrease with time, this raises the question whether Twin Falls is an exception to this rule or if cooling happens stepwise between the different eruption centers rather than continuously.

Future work will focus on field samples of the rhyolites correlated with the units found in the Kimberly drill core to strengthen the verifiifaction of the correlation between depth and age observed in Fig.2. Age determination on the Kimberly rhyolites will help to link the units to the local eruption history. Furthermore it should be tested if Kimberly rhyolite units 2 and 3 are truly products of Twin Falls or if they have been derived from the next younger eruption center Picabo. The Picabo eruption center started its activity shortly after Twin falls and both centers were active simultaneously for at leat one million years (Nash et al., 2006).

References:

Almeev, R. R., Bolte, T., Nash, B. P., Holtz, F., Erdmann, M., & Cathey, H. E. (2012). High-temperature, low-H2O silicic magmas of the Yellowstone hotspot: an experimental study of rhyolite from the Bruneau–Jarbidge Eruptive Center, Central Snake River Plain, USA. Journal of Petrology, 53(9), 1837-1866.

Ellis, B. S., Barry, T., Branney, M. J., Wolff, J. A., Bindeman, I., Wilson, R., & Bonnichsen, B. (2010). Petrologic constraints on the development of a large-volume, high temperature, silicic magma system: The Twin Falls eruptive centre, central Snake River Plain. Lithos, 120(3), 475-489.

Gualda, G. A., & Ghiorso, M. S. (2014). Phase-equilibrium geobarometers for silicic rocks based on rhyolite-MELTS. Part 1: Principles, procedures, and evaluation of the method. Contributions to Mineralogy and Petrology, 168(1), 1-17.

Hildreth, W. E. S., Halliday, A. N., & Christiansen, R. L. (1991). Isotopic and chemical evidence concerning the genesis and contamination of basaltic and rhyolitic magma beneath the Yellowstone Plateau volcanic field. Journal of Petrology, 32(1), 63-138.

Huang, R., & Audétat, A. (2012). The titanium-in-quartz (TitaniQ) thermobarometer: a critical examination and re-calibration. Geochimica et Cosmochimica Acta, 84, 75-89.

Nash, B. P., Perkins, M. E., Christensen, J. N., Lee, D. C., & Halliday, A. N. (2006). The Yellowstone hotspot in space and time: Nd and Hf isotopes in silicic magmas. Earth and Planetary Science Letters, 247(1), 143-156.

Pamukcu, A. S., Gualda, G. A., Ghiorso, M. S., Miller, C. F., & McCracken, R. G. (2015). Phase-equilibrium geobarometers for silicic rocks based on rhyolite-MELTS—Part 3: Application to the Peach Spring Tuff (Arizona–California–Nevada, USA). Contributions to Mineralogy and Petrology, 169(3), 1-17.

Wilke, S., Klahn, C., Bolte, T., Almeev, R., & Holtz, F. (2015). Experimental investigation of the effect of Ca, Fe and Ti on cotectic compositions of the rhyolitic system. European Journal of Mineralogy, 27(2), 147-159.

Wilke, S., Neave, D., Almeev, R., Holtz, F (*in preparation*): The effect of normative anorthite on the mineral saturation surfaces of rhyolitic melts and its implications for geobarometry

IODP

Fractionation of Ca isotopes during transport and recrystallisation processes in marine deep sea sediments

A. WITTKE[1], N. GUSSONE[1], B.M.A.TEICHERT[2]

[1] Westfälische Wilhelms-Universität Münster, Institut für Mineralogie, Münster, Germany
[2] Westfälische Wilhelms-Universität Münster, Institut für Geologie und Paläontologie, Münster, Germany

Biogenic marine calcium carbonate shells are important archives for changes of the Earth system throughout Earth's history, as their element and isotopic composition is used for the reconstruction of many paleo-environmental parameters. The reliability of those proxies depends not only on factors during archive formation, but also on the preservation, which in turn depends on post depositional diagenetic processes such as partial dissolution and recrystallization.

Sediments retrieved during IODP Expeditions 320/321 provide well preserved high resolution archives throughout the Cenozoic; they are hence the basis for important paleoclimate reconstructions (cf. Pälike et al. 2012). Nevertheless, despite the overall good preservation, porewater concentrations revealed indications for carbonate recrystallization. A tool for the investigation of diagentic processes in marine sediments, including recrystallization (Fantle and DePaolo 2007), deep fluids and ion exchange (Teichert et al. 2009, Ockert et al. 2013, 2014) is the isotopic composition of Ca of sedimentary porewater.

So far, Ca isotope studies on marine porewaters focussed on continental margin sediments and carbonate plateaus (Fantle and DePaolo 2007, Teichert et al. 2009, Turchyn and DePaolo 2011), and little is known about Ca isotope cycling during diagenesis of deep-sea sediments. Here we present first Ca isotope data of porewater and associated deep-sea sediments from the Equatorial Eastern Pacific drilled during IODP Expeditions 320/321, namely Sites U1331, U1335, U1336, U1337 and U1338. Our initial results demonstrate differences in the Ca isotope porewater profiles between deep-sea sediments and continental margin and carbonate plateau sediments, but also differences between deep-sea sites.

Sites U1335, U1336 and U1338 show a decrease in $\delta^{44/40}Ca_{porewater}$ from seawater like values at the sediment - bottomwater interface towards increasing sediment depth. Porewater Ca isotope ratios converge with the low $\delta^{44/40}Ca$ values of the solid sediment between 100 and 200 m ccsf. In greater sediment depth (about 300 m ccsf) Sites U1335 and U1338 show again an increase in $\delta^{44/40}Ca$ towards greater depth, approaching seawater-like $\delta^{44/40}Ca$ values near the basaltic basement. This observation indicates a seawater source at the sediment basis, consistent with circulation of seawater through the basement and part of the sediment column, driven by hydrothermalism. The Ca isotope systematics of U1331 is unique as it shows seawater-like $\delta^{44/40}Ca$ of the porewater throughout the whole sediment cover. Thus, sediment and porewater are not in equilibrium, although Site U1331 represents the oldest sediments drilled during IODP Exp. 320/321.

References:

Fantle, M. S. and DePaolo, D. J., 2007. Ca isotopes in carbonate sediment and pore fluid from ODP Site 807A: The Ca^{2+}(aq)-calcite equilibrium fractionation factor and calcite recrystallization rates in Pleistocene sediments. Geochim. Cosmochim. Acta 71, 2524-2546.

Ockert, C., Gussone, N., Kaufhold, S., Teichert, B. M. A., 2013. Isotope fractionation during Ca exchange on clay minerals in a marine environment. Geochim. Cosmochim. Acta112, 374-388.

Ockert, C., Wehrmann, L.M., Kaufhold, S., Ferdelman, T.G., Teichert, B.M.A., Gussone, N. (2014) Calcium-ammonium exchange on standard clay minerals and natural marine sediments in seawater. Isotopes in Environmental and Health Studies 50, 1-17.

Pälike, H., Lyle, M. W., Nishi, H., Raffi, I., Ridgwell, A., Gamage, K., Klaus, A., et al., 2012. A Cenozoic record of the equatorial Pacific carbonate compensation depth. Nature 488, 609–614.

Teichert, B. M. A., Gussone, N., Torres, M. E., 2009. Controls on calcium isotope fractionation in sedimentary porewaters. Earth Planet. Sc. Lett. 279, 373-382.

Turchyn, A. V. and DePaolo, D. J., 2011. Calcium isotope evidence for suppression of carbonate dissolution in carbonate-bearing organic-rich sediments. Geochim. Cosmochim. Acta. 75, 7081-7098.

IODP

Bacterial endospores in the marine subsurface: assessment of their abundance and relevance through culture-independent, biomarker-based quantification

L. WÖRMER[1], R. ADHIKARI[1], N. GAJENDRA[1], B. STERN[1], B. VIEHWEGER[1], T. MEADOR[1], K.-U. HINRICHS[1]

[1]Organic Geochemistry Group, MARUM & Dept. of Geosciences, University of Bremen, 28334 Bremen

Scientific drilling in the last decades has evidenced the abundance of Earth's deep microbial biosphere, as well as its importance in driving carbon and nutrient cycles. A major question presented by the existence of these large and understudied microbial communities is how they deal with progressive burial and the associated gradual energy starvation. Morono et al. (2011) tested the capacity of deeply buried cells to assimilate isotope-labeled substrates and concluded that the vast majority of these microorganisms are not dead, but physiologically intact and capable of rapid metabolism. Assuming most cells are not only alive but also active, mean metabolic rates for deep subsurface bacteria have been calculated to be several orders of magnitude lower than those for surface ecosystems, resulting in hypothetical generation times of up to thousands of years (e.g. D'Hondt et al., 2002; Jørgensen, 2011). While such longevity is difficult to reconcile with our current understanding of microbial life, but may be biologically feasible, an alternative explanation could be the existence of a large fraction of dormant cells, with only a few truly active cells.

Bacterial endospores are metabolically inactive, dormant cells that are structurally different from vegetative cells and show increased resistance and the ability to monitor the conditions of their habitat in order to resume active growth once they become favorable. Sporulation can be triggered by a variety of stimuli, the main one being prolonged starvation. The ability to form endospores is unique to the phylum *Firmicutes* and widespread among the different physiological groups of the phylum, including those potentially relevant in the subseafloor microbial community. *Firmicutes* are considered major contributors to the deep biosphere given their abundance in culture-dependent biodiversity studies. Consequently, in these ecosystems exposed to progressive burial and energy starvation, endospores may constitute a critical survival strategy for *Firmicutes*.

Endospores have been poorly accounted for in previous subseafloor censuses, as it remains questionable to what

degree DNA stains are capable of penetrating into these cellular entities and cultivation-based approaches suffer considerable limitations due to the selectivity of employed growth media and conditions. A more robust quantification method relies on the specific biomarker molecule dipicolinic acid (DPA). DPA is exclusive to the endospore core, it is released in a few minutes when endospores initiate germination and it is extremely labile; being rapidly degraded even under anoxic conditions. Therefore DPA provides a highly specific link to intact endospores. While initial attempts to quantify DPA abundance in environmental samples were not successful, due to analytical limitations, Fichtel et al. (2007) pioneered the adaptation of a method based on the fluorescence of terbium dipicolinate (Tb-DPA) to sediment samples. This enabled the acquisition of data that have started to outline the importance of endospores in the deep biosphere (e.g. Fichtel et al. 2008; Lomstein et al., 2012).

We have recently implemented and further developed the Tb-DPA based method in our lab, and now have the accurate analytical tools to unravel the abundance and ecological relevance of endospores in the marine subsurface. For example, a selection of 48 rather shallow samples (max. depth = 6.3 mbsf) from eight sites in the Mediterranean, Black and Marmara Sea provided an ideal set to establish the factors driving endospore abundance. Retrieved during the DARCSEAS 1 and 2 cruises (M84-1 and POS450) these samples have been extensively studied by molecular, geochemical, and sedimentological methods. By placing DPA data in this framework, we were able to identify terrestrial input as a main driver of endospore abundance. A more detailed look on selected sites aditionally identified depositional and post-depositional singularities directly influencing endospore profiles.

Endospore abundance in deep drilling sites is currently being determined in several locations in order to complete and further define the picture outlined by Lomstein et al. (2012), i.e. the gradual increase of endospore abundance compared to vegetative cells with depth. In addition, we focus on samples from deep, microbial activity promoting layers. In such scenarios of transient cell stimulation, endospores may become a very important microbial survival strategy. By acting as an inoculum for microbial populations in hardly accessible, extreme environments, endospores may be contributing to push the limits of life in the marine subsurface.

References:

D'Hondt, S., Rutherford, S., Spivack, A.J. (2002). Metabolic activity of subsurface life in deep-sea sediments. Science 295, 2067-2070

Fichtel, J., Koester, J., Scholz-Boettcher, B., Sass, H., Rullkoetter, J. (2007b). A highly sensitive HPLC method for determination of nanomolar concentrations of dipicolinic acid, a characteristic constituent of bacterial endospores. J Microbiol Meth 70, 319-327.

Fichtel, J., Koester, J., Rullkoetter, J., Sass, H. (2008). High variations in endospore numbers within tidal flat sediments revealed by quantification of dipicolinic acid. Geomicrob J25, 371-380.

Jørgensen, B.B. (2011). Deep subseafloor microbial cells on physiological standby. Proc Nat Acad Sci USA 108, 18193-18194.

Lomstein, B.A., Langerhuus, A.T., D'Hondt, S., Jorgensen, B.B., Spivack, A.J. (2012). Endospore abundance, microbial growth and necromass turnover in deep sub-seafloor sediment. Nature 484, 101-104.

Morono, Y., Terada, T., Nishizawa, M., Ito, M., Hillion, F., Takahata, N., Sano, Y., Inagaki, F. (2011). Carbon and nitrogen assimilation in deep subseafloor microbial cells. Proc Nat Acad Sci USA 108, 18295-18300.

ICDP

Visco-elastic full waveform inversion of controlled seismic data from the San Andreas Fault Observatory at Depth

J. ZEIß[1], M. PASCHKE[2], F. BLEIBINHAUS[1]

[1]Chair of Applied Geophysics, University of Leoben, Peter-Tunner-Straße 25, Leoben, Austria

[2]Institute for Geosciences, Friedrich Schiller University, Burgweg 11, Jena, Germany[3]

We apply visco-elastic full waveform inversion (FWI) to a 50-km-long controlled-source refraction /reflection seismic survey at the San Andreas Fault (SAF) to obtain high resolution P-wave and S-wave velocity models for the SAF Observatory at Depth (SAFOD) drill site near Parkfield. The profile consists of 63 explosive sources and a fixed spread of 912 3-component receivers.

In a previous study, Beibinhaus et al. (2007) derived a high-resolution model for P-wave velocities using acoustic FWI. Despite significantly improved resolution, their final model fell short of imaging the small, but relevant low velocity zones representing damage zones due to faulting (Zoback et al., 2011).

By considering the topography with free surface and also considering mode conversions between P- and S-waves during modeling, improvements in the resolution are expected compared to this study.

Traveltime models from Ryberg et al. (2012) and Hole et al. (2006) are used to derive velocity starting models for FWI. Attenuation is estimated from Qp and Qs t*-tomography models after Bennington et al. (2008). Density is estimated from P-wave velocity using Gardner`s relation (Gardner et al., 1974).

Preprocessing includes the muting of noisy traces, the estimation of spatio-temporal weighting factors to exclude Rayleigh waves, which otherwise mask the comparatively low-amplitude body wave signals, and a 3D-to-2D-conversion, which is carried out separately for P- and S-waves and their coda. The separation of P- and S wave arrivals is based on travel-time and polarization analysis.

The forward-modeling is based on a time-domain visco-elastic FD-algorithm of Robertsson et al. (1996). Topography is considered using the image method. The inversion is performed in the frequency-domain using the multi-scale approach.

As a first step, we derived individual source wavelets for the different shots at the low frequencies (2-6 Hz). On the poster, we will show the preprocessing of the seismic data, the prepared starting models and the derivation of individual source wavelets.

References:

Bleibinhaus, F., J. A. Hole, T. Ryberg, and G. S. Fuis, 2007. Structure of the California Coast Ranges and San Andreas Fault at SAFOD from seismic waveform inversion and reflection imaging. J. Geophys. Res., 112, B06315, doi:10.1029/2006JB004611.

Gardner, G.H.F., L.W. Gardner, and A.R. Gregory, 1974. Formation velocity and density – the diagnostic basics for stratigraphic traps. Geophysics, 39, 770-780.

Hole, J., T. Ryberg, G. Fuis, F. Bleibinhaus and A. K. Sharma, 2006. Structure of the San Andreas fault zone at SAFOD from a seismic refraction survey. Geophys. Res. Lett., 33, L07312, doi:10.1029/2005GL025194.

Robertsson, J.O.A., J.O. Blanch and W. W. Symes, 1994. Viscoelastic finite-difference modelling. Geophysics, 59, 1444-1456.

Ryberg, Z., J. A. Hole, G. S. Fuis, M. J. Rymer, F. Bleibinhaus, D. Stromeyer and K. Bauer, 2012. Tomographic Vp and Vs structure of the California Central Coast Ranges, in the vicinity of SAFOD, from controlled-source seismic data. Geophysical Journal International, 190, 1341–1360, doi: 10.1111/j.1365-246X.2012.05585.x.

Zoback, M., S. Hickman, W. Ellsworth and the SAFOD Science Team, 2011. Scientific Drilling Into the San Andreas Fault Zone – An Overview of SAFOD's First Five Years. Sci. Dril., 11, 14-28, doi:10.5194/sd-11-14-2011.

Nach dem 15.02.2016 eingereichte Abstracts:

IODP

Calcium and Strontium Isotopes in Low Temperature Alteration Calcites of the Ocean Crust

F. BÖHM, A. EISENHAUER

GEOMAR Helmholtz Centre for Ocean Research Kiel, Germany

Calcite cements filling veins and vugs in ocean crust basalts in the deep sea form from mixtures of cold seawater and warm hydrothermal fluids (about 0-70°C). These low temperature alteration (LTA) calcites have recently gained new interest as proxy recorders of seawater composition (Coggon et al. 2010; Gillis & Coogan 2011; Rausch et al. 2013; Li et al. 2014, Coogan & Dosso 2015). Recent LTA calcite reconstructions of the Sr/Ca and Mg/Ca evolution in ocean waters point to considerably lower Sr/Ca and Mg/Ca ratios during the Cretaceous and Paleogene than in the modern ocean. The results are in agreement with ocean modelling studies (e.g. Hardie 1996, Hansen & Wallmann 2003, Higgins & Schrag 2012) and with halite-hosted fluid inclusion data (e.g. Horita et al. 2002), but show significant mismatches with some fossil-based reconstructions (e.g. Steuber & Veizer 2002, Creech et al. 2010, Sosdian et al. 2012) and are therefore controversially disputed (e.g. Broecker & Yu, 2011).

The composition of LTA calcites is controlled by several factors. Besides water temperature and chemistry, which control the element partitioning between fluid and calcite (Rausch et al. 2013), the seawater composition may be altered by reaction with the ocean crust. In addition, diagenetic alteration during burial in marine sediments may alter the composition of the calcite. All of these factors need to be known to reliably reconstruct seawater compositions from LTA calcites. This can be carried out using multi-proxy approaches: oxygen isotopes are used to reconstruct calcite precipitation temperatures; strontium isotopes indicate alteration of seawater (high $^{87}Sr/^{86}Sr$) by reactions with the ocean crust (low $^{87}Sr/^{86}Sr$), i.e. basement influence (Coggon et al. 2010).

Additional information about the basement influence during formation and diagenesis of LTA calcites can be derived from analyses of stable calcium and strontium isotopes ($\delta^{44/40}Ca$, $\delta^{88/86}Sr$). We find systematically low $\delta^{44/40}Ca_{SRM915a}$ values (0.6 to 1.2 ‰) for DSDP and ODP Sites where the $^{87}Sr/^{86}Sr$ ratios of LTA calcites indicate basement influence (Sites 418, 553, 801, 896), i.e. where measured $^{87}Sr/^{86}Sr$ ratios are lower than seawater composition at the time of formation. Sites 417 and 1149 lie within the $^{87}Sr/^{86}Sr$ range of Early Cretaceous seawater, however low $\delta^{44/40}Ca$ values indicate basement influence. All of these Sites are either older than 50 Myr or show precipitation temperatures of the calcites of >50°C.

Sites 335, 395, 396, 407, 597, 1224 are much younger (<25 Myr) and had formation temperatures <10°C. They show $\delta^{44/40}Ca_{SRM915a}$ values of about 1.4 to 1.7 ‰ and no indication of basement influences in the $^{87}Sr/^{86}Sr$ ratios. Average $\delta^{44/40}Ca$ values of these Sites are in good agreement with the Neogene seawater $\delta^{44/40}Ca$ evolution (Heuser et al. 2005).

Stable strontium isotopes show less variability between sites ($\delta^{88/86}Sr_{SRM987}$ between 0.30 and 0.35‰). Significantly higher $\delta^{88/86}Sr$ (0.4‰) were observed only at temperatures >50°C.

The calcium isotope results indicate basement influence on LTA calcite composition at temperatures >10°C. Radiogenic strontium isotopes, in contrast, can be used as unequivocal basement influence indicator only at temperatures above 30°C. At formation temperatures around 20°C (Cretaceous Sites 417 and 114) $^{87}Sr/^{86}Sr$ ratios are no reliable indicators of basement influence.

All LTA calcites of the Sites older than 50 Myr formed (or possibly recrystallized) at temperatures above 15°C. Therefore, as indicated by the low $\delta^{44/40}Ca$ values, the fluid from which the calcites formed was isotopically altered seawater. From the ~0.3‰ lowered $\delta^{44/40}Ca$ of the Cretaceous LTA calcites we estimate that about one third of the calcium in the LTA fluids was derived from leaching of basement rocks. From the difference in $^{87}Sr/^{86}Sr$ between Cretaceous seawater and the LTA calcites we estimate that between about 20 and 40% of the Sr in the LTA fluid were leached from the basement. Therefore, Sr/Ca ratios in the Cretaceous LTA fluids were probably only slightly altered compared to seawater. The Sr/Ca measurements of LTA calcites can consequently provide useful estimates about the seawater composition of the Cenozoic and Mesozoic oceans.

References:

Broecker, W. S., & Yu, J. (2011). What do we know about the evolution of Mg to Ca ratios in seawater? *Paleoceanography*, *26*(3), doi:10.1029/2011PA002120.

Coggon, R. M., Teagle, D. A. H., Smith-Duque, C. E., Alt, J. C., & Cooper, M. J. (2010). Reconstructing past seawater Mg/Ca and Sr/Ca from mid-ocean ridge flank calcium carbonate veins. *Science*, *327*, 1114–1117.

Coogan, L. A., & Dosso, S. E. (2015). Alteration of ocean crust provides a strong temperature dependent feedback on the geological carbon cycle and is a primary driver of the Sr-isotopic composition of seawater. *Earth and Planetary Science Letters*, *415*, 38–46.

Creech, J. B., Baker, J. A., Hollis, C. J., Morgans, H. E. G., & Smith, E. G. C. (2010). Eocene sea temperatures for the mid-latitude southwest Pacific from Mg/Ca ratios in planktonic and benthic foraminifera. *Earth and Planetary Science Letters*, *299*, 483–495.

Gillis, K. M., & Coogan, L. A. (2011). Secular variation in carbon uptake into the ocean crust. *Earth and Planetary Science Letters*, *302*, 385–392.

Hansen, K. W., & Wallmann, K. (2003). Cretaceous and Cenozoic evolution of seawater composition, atmospheric O_2 and CO_2: A model perspective. *American Journal of Science*, *303*(2), 94–148.

Hardie, L. A. (1996). Secular variation in seawater chemistry: An explanation for the coupled secular variation in the mineralogies of marine limestones and potash evaporites over the past 600 m.y. *Geology*, *24*(3), 279–283.

Heuser, A., Eisenhauer, A., Böhm, F., Wallmann, K., Gussone, N., Pearson, P. N., Nägler, T. F., Dullo, W.-C. (2005). Calcium isotope ($\delta^{44/40}Ca$) variations of Neogene planktonic foraminifera. *Paleoceanography*, *20*(2), doi:10.1029/2004PA001048.

Higgins, J. A., & Schrag, D. P. (2012). Records of Neogene seawater chemistry and diagenesis in deep-sea carbonate sediments and pore fluids. *Earth and Planetary Science Letters*, *357-358*, 386–396.

Horita, J., Zimmermann, H., & Holland, H. D. (2002). Chemical evolution of seawater during the Phanerozoic: Implications from the record of marine evaporites. *Geochimica et Cosmochimica Acta*, *66*(21), 3733–3756.

Li, S., Geldmacher, J., Hauff, F., Garbe-Schönberg, D., Yu, S., Zhao, S., & Rausch, S. (2014). Composition and timing of carbonate vein precipitation within the igneous basement of the Early Cretaceous Shatsky Rise, NW Pacific. *Marine Geology*, *357*, 321–333.

Rausch, S., Böhm, F., Bach, W., Klügel, A., & Eisenhauer, A. (2013). Calcium carbonate veins in ocean crust record a threefold increase of seawater Mg/Ca in the past 30 million years. *Earth and Planetary Science Letters*, *362*, 215–224.

Sosdian, S. M., Lear, C. H., Tao, K., Grossman, E. L., O'Dea, A., & Rosenthal, Y. (2012). Cenozoic seawater Sr/Ca evolution. *Geochemistry Geophysics Geosystems*, *13*(10), doi:10.1029/2012GC004240.

Steuber, T., & Veizer, J. (2002). Phanerozoic record of plate tectonic control of seawater chemistry and carbonate sedimentation. *Geology*, *30*(12), 1123–1126.

ICDP

Strain localization at a Plate Boundary: investigation of the Principal Slip Zone of the Alpine Fault, NZ, in borehole and outcrop samples

B. SCHUCK[1], C. JANSSEN[1], V. G. TOY[2], G. DRESEN[1,3]

[1]Helmholtz Zentrum Potsdam, Deutsches GeoForschungsZentrum, Sektion 4.2: Geomechanik und Rheologie; Telegrafenberg 14473, Potsdam (bernhard.schuck@gfz-potsdam.de)
[2]Department of Geology, University of Otago, P.O. Box 56, Dunedin 9054, New Zealand
[3]Institut für Erd- und Umweltwissenschaften, Universität Potsdam

The transpressive Alpine Fault is the main structure forming the Australian and the Pacific Plate boundary within New Zealand's South Island (Sutherland et al., 2006; Toy et al., 2015). Over the past 20 Ma about 470 km of cumulative dextral movement has been accommodated on its 800 km long onshore segment (Cande & Stock, 2004; Sutherland et al., 2006; Toy et al., 2015). Since at least 5 Ma 90 ± 20 km of shortening across the fault manifest at vertical uplift rates of up to 6 – 9 mm a^{-1}. They have resulted in the formation of the up to 3724 m high Southern Alps southeast of the fault trace (Beaven et al., 2002; Little et al., 2005; Toy et al., 2015). Nowadays, this shortening plus up to 27 ± 5 mm a^{-1} lateral motion accommodate about 70 % of the relative plate motion between the Australian and the Pacific Plate (Sutherland et al., 2007).

The moderately southeast dipping fault exhumes rocks from a décollement in 35 km depth (Little et al., 2005). The hanging wall is composed of the Alpine Schist. Within 1 km of the fault, this is transposed to mylonite which displays increasing evidence of ductile shear strain towards the SW. Within 50 m of the principal slip surface of the fault, there is cataclasite, which is considered as the fault's damage zone (Toy et al., 2015). The fault core is characterized by a 20 to 30 cm thick package of cataclasites and clay gouge (Toy et al., 2015). The footwall comprises Quaternary gravels, Devonian turbidites (Greenland Group) and Paleozoic and Cretaceous igneous intrusives (Boulton et al., 2012, Barth et al., 2013).

The Alpine Fault is capable of generating large (i.e. M_w > 8) earthquakes with up to 600 km rupture lengths (Sutherland et al., 2007) and a recurrence interval of 329 ± 68 a (Berryman et al., 2012). Since the last major earthquake was in 1717 (Sutherland et al., 2007), the fault is considered to be late in its earthquake cycle.

The fast uplift rates have bought the brittle-ductile transition and the overlying earthquake-generating zone to very shallow depths (5km?). This provides motivation to drill the Alpine Fault to investigate seismogenic and brittle-ductile transition processes (Townend et al., 2009; Toy et al., 2015). In 2011, the first phase of the Alpine Fault Deep Fault Drilling Project (DFDP-1) was carried out. During this, the Alpine Fault was penetrated by two shallow boreholes at 91 m and 128 m depth, respectively (Toy et al., 2015). A second phase (DFDP-2) was designed to encounter the fault at ~1 km depth, but drilling terminated in December 2015 at ~820 m vertical depth due to technical problems.

Compared to the mylonitic rocks associated with the Alpine Fault (i.e. the result of ductile creep at depth) and the brittle damage zone, which have been subject of various detailed investigations (e.g. Norris & Cooper, 2003; Toy, 2007; Cooper & Norris, 2011), the clay gouge has attracted less attention (e.g. Warr & Cox, 2001; Barth et al., 2013).

In the frame of this project we aim to analyze the fabric, texture and mineralogy of clay gouge samples from DFDP-1 cores and at least four different outcrops to understand how the mechanical behaviour of the fault has generated, and is recorded, in this unit. We will combine high-resolution microscopy (e.g. BIB-SEM and TEM) with mineralogical and geochemical analysis (e.g. XRD, XRF and EBSD) to describe microstructures that might explain strain localization in the fault core. We will dicuss our findings in the context of similar observations of other major crustal-scale faults, such as within the Gulf of Corinth and the San Andreas Fault.

References:

Barth, N. C., Boulton, C., Carpenter, B. M., Batt, G. E. & Toy, V. G. (2013): Slip localization on the southern Alpine Fault, New Zealand. – Tectonics **32**: pp. 620 – 640.

Beavan, J., Tregoning, P., Bevis, M., Kato, T. & Meertens, C. (2002): Motion and rigidity of the Pacific Plate and implications for plate boundary deformation. – Journal of Geophysical Research **107**: pp. 2261 – 2276.

Berryman, K. R., Cochran, U. A., Clark, K. J., Biasi, G. P., Langridge, R. M & Villamor, P. (2012): Major Earthquakes Occur Regularly on an Isolated Plate Boundary Fault. – Science **336**: pp. 1690 – 1693.

Boulton, C., Carpenter, B. M., Toy, V. G. & Marone, C. (2012): Physical properties of surface outcrop cataclastic fault rocks, Alpine Fault, New Zealand. – Geochemistry, Geophysics, Geosystems **13**: p. 13.

Cande, S. C. & Stock, J. M. (2004): Pacific-Antarctic-Australia motion and the formation oft the Macquarie Plate. – Geophys. J. Int. **157**: pp. 399 – 414.

Cooper, A. F. & Norris, R. J. (2011): Inverted metamorphic sequences in Alpine Fault mylonites produced by oblique shear within a plate boundary fault zone, New Zealand. – Geology **39**: pp. 1023 – 1026.

Little, T. A., Cox, S., Vry, J. K. & Batt, G. E. (2005): Variations in exhumation level and uplift rate along the oblique-slip Alpine Fault, central Southern Alps, New Zealand. – Geological Society of America Bulletin **117**: pp. 707 – 723.

Norris, R. J. & Cooper, A. F. (2003): Very high strains recorded in mylonites along the Alpine Fault, New Zealand: implications fort he deep structure of plate boundary faults. – Journal of Structural Geology **25**: pp. 2141 – 2157.

Sutherland, R., Berryman, K. R. & Norris, R. (2006): Quaternary slip rate and geomor- phology of the Alpine Fault: implications for kinematics and seismic hazard in southwest New Zealand. – Geological Society of America Bulletin **118**: pp. 464 – 474.

Sutherland, R., Eberhart-Phillips, D., Harris, R. A., Stern, T., Beavan, J., Ellis, S., Henrys S. Cox, S., Norris, R. J., Berryman K. R. Townend, J., Bannister, S., Pettinga, J., Leitner, B., Wallace, L., Little, T. A., Cooper, A. F., Yetton, M. & Stirling, M. (2007): Do great earthquakes occur on the Alpine Faulz in central South Island, New Zealand?. – A Continental Plate Boundary: Tectonics at South Island, New Zealand. Ed. by D. Okaya, T. Stern & F. Davey. American Geophysical Union: Geophysical Monograph **175**, pp. 235 – 251.

Townend, J., Sutherland, R., and Toy, V. G. (2009): Deep Fault Drilling Project – Scientific Drilling **8**: p. 75 – 82.

Toy, V. G. (2007): Rheology of the Alpine Fault Mylonite Zone: deformation processes at and below the base of the seismogenic zone in a major plate boundary structure. – PhD Thesis, University of Otago, Dunedin: p. 653.

Toy, V. G., Boulton, C., Sutherland, R., Townend, J., Norris, R. J., Little, T. A., Prior, D. J., Mariani, E., Faulkner D. Menzies, C. D., Scott, C. D., Scott, H. & Carpenter, B. M. (2015): Fault rock lithologies and architecture of the central Alpine Fault, New Zealand, revealed by DFDP-1 drilling. – Lithosphere **7**: pp. 155 – 173.

Warr, L. N. & Cox, S. (2001): Clay mineral transformations and weakening mechanisms along the Alpine Fault, New Zealand. – Geological Societiy London, Special Publications **186**: pp. 85 – 101.